ISOTOPIC RELATIONSHIPS IN THE CHILLAGOE - HERBERTON AREA, NORTH QUEENSLAND

by

LANCE PRESTON BLACK

A thesis submitted for the degree of

DOCTOR OF PHILOSOPHY

in the

AUSTRALIAN NATIONAL UNIVERSITY

July, 1969

STATEMENT

The data contained in this thesis were collected over the period January 17, 1966 to July 16, 1969. These, and the resultant interpretations, are the work of the author alone unless specific acknowledgement is otherwise made.

L. Black.

L. P. BLACK

ACKNOWLEDGEMENTS

I am deeply grateful to my supervisor, Dr J. R. Richards, for suggesting this project and providing considerable help and encouragement throughout. My 'trace lead' colleagues also provided helpful instruction. In particular, Dr P. H. Reynolds was always willing to advise on various practical and theoretical aspects. Mr J. A. Cooper was responsible for the calibration of the lead spike, Dr R. B. Farquharson the thorium spike, and Dr P. H. Reynolds the uranium spike.

Dr B. W. Chappell of the Geology Department of this university generously made available his X-ray spectrometer for trace element study. Mr J. M. Worden provided instruction and assistance with X.R.F. studies in this department.

I am grateful to Dr W. Compston for permitting the use of the Rb - Sr facilities, and performing several mineral analyses on my behalf in the later part of this study. Mr M. J. Vernon was very helpful in demonstrating the Rb - Sr procedures and providing general assistance throughout my course. Mr D. J. Millar also provided practical assistance with the Rb - Sr techniques.

Dr I. McDougall allowed the use of the K - Ar laboratory, and gave valuable instruction and help with the argon analyses. Mr I. H. Ingram and Miss S. Dinter kindly demonstrated the practical aspects of the method.

Mr J. M. Worden and J. E. Robertson, with the permission of Dr K. S. Heier, instructed in the use of the γ-ray spectrometer. Drs S. R. Taylor and A. J. Graham performed two analyses on my behalf using an MS-7 spark-source mass spectrograph. The computer programs used for data reduction were made available by others, both in and outside this department; Dr P. A. Arriens was chiefly responsible for the programming. I am also indebted to Dr Arriens and Mr E. Penikis for frequent servicing and upgrading of the twelve inch mass-spectrometer. Mr A. Powell and Mr E. H. Pedersen prepared the thin sections and messers H. Berry, R. Rudowski and Z. Wasik instructed in rock-crushing procedures.

Many other people provided helpful discussion, and in particular I wish to thank the following:- Drs C. D. Branch, F. de Keyser and J. M. Dickins from the B.M.R.; Dr D. H. Blake from C.S.I.R.O.; Professor D. A. Brown, Drs K. S. W. Campbell, K. L. Williams and A. J. R. White and Mr J. C. Bailey from the Geology Department; also Mr M. J. Dallwitz (Physics Department), Mrs M. E. White and Mr W. R. Morgan. I am deeply indebted to Professor Brown for practical assistance with the preparation of this thesis.

The Atherton 1 : 250,000 sheet which appears in the back of this thesis does not represent the work of the author.

I am extremely grateful to my wife for typing the various drafts and final copy of this thesis.

Finally I would like to thank the A.N.U. for awarding the generous scholarship which has made this study possible.

TABLE OF CONTENTS

LIST OF TABLES

LIST OF FIGURES

CHAPTER 1

INTRODUCTION

The rocks and mineral deposits of the Cairns hinterland, on the north-eastern edge of Queensland, Australia, have been investigated because of the widespread mineralisation which is thought to relate to the extensive igneous rocks. The area has been mapped by officers of the Bureau of Mineral Resources and Geological Survey of Queensland who have shown that two major geological elements are present. In the west is an inlier of Precambrian metamorphic and granitic rocks which is separated by a large fault from the northern end of a Palaeozoic geosyncline of continental dimension. The extensive Palaeozoic igneous rocks occur as high-level granite intrusions and associated comagmatic volcanics, usually occurring in huge cauldron subsidence areas.

A reconnaissance dating survey, using chiefly the K-Ar method, has shown that the majority of the igneous rocks are Upper Palaeozoic in age.

Economic interest centres on the diversity of mineral deposits, as the overall production of most ores has been relatively small. Tin has been the most economically important mineral almost throughout the entire life of the mining field. A mining boom at the turn of the century has gradually given way to a low present-day production.

The main purpose of this study is to evaluate the role of igneous activity in ore-body formation by means of comparative lead isotopic studies. Limited Rb-Sr analyses have also been undertaken to clarify the geochronology and provide useful geochemical information on the igneous rocks. Special problems arose during the rather cumbersome procedures of rock-lead extraction and purification, and these have resulted in modifications to the original method.

Six weeks was spent in the field during the initial phase of this work. This time was mostly confined to the collection of samples for analysis. The ore specimens were collected from mine dumps, as most of the workings are now inaccessible. Gelignite was routinely used to collect rocks which showed negligible signs of alteration. Only limited time was spent examining the field relations, and the discussion of this in the next section is drawn from the observations of other workers. The petrographical descriptions, however, are derived from the work of previous investigators combined with further observations by the author on 70 thin sections. In general the results are complementary, and I have only made specific reference to mine when they vary from the other observations. The mineralogy of each individual ore deposit on which isotopic work was performed is listed in the appendix. The minerals were identified microscopically from 43 thin sections and 70 polished sections of ore material. Mr E. H. Pedersen of this

department prepared the thin sections and mounted the ores in clear plastic; the latter were subsequently hand polished by the author. Previous mineralogical reports are also included where possible, since random mine dump sampling produces only a rather incomplete idea of the mineralisation.

Unless specifically qualified, the term 'granite' is used in this thesis in the broad sense as defined by Harker (1954) to include all medium to coarse-grained rocks composed of one or two feldspars, quartz and some ferromagnesian mineral, together with accessory constituents. The classification of Hatch, Wells and Wells (1961), in which subdivisions are made according to the alkali feldspar to plagioclase ratio, is used when the terms granite, adamellite and granodiorite are used in the strict sense (s.s.) as in the appendix. The fine-grained equivalents of these rocks, rhyolite, rhyodacite and dacite are always used in the specific sense.

CHAPTER 2

GEOLOGY

Geological Setting

The Precambrian Georgetown Inlier of north-east Queensland covers approximately 37,000 square miles (Branch, 1966), and is separated from the main Australian Shield 200 miles further west by Mesozoic sediments of the Great Artesian Basin. On its eastern flank is the Palaeozoic Tasman Geosyncline, a regional structure which extends the whole length of eastern Australia. In north-east Queensland this varies from 50 to 150 miles wide and contains about 40,000 feet of sediments.

Both the Precambrian inlier and the Palaeozoic geosyncline are covered by large areas of Palaeozoic acid igneous rocks. These rocks include both plutonic and volcanic members. Many of the intrusives were emplaced very close to the surface; the volcanics occur chiefly in huge cauldrons. Flat-lying, Lower Cretaceous quartz sandstone, continuous with the sediments of the vast Great Artesian Basin, unconformably transgresses older formations and forms the north- and south-western boundaries of the inlier. Cenozoic basalt provinces cover approximately 6,000 square miles both on the inlier and outside its eastern margin.

The area covered in this investigation occupies about 7,000 square miles and straddles the north-eastern margin of the Georgetown

Inlier; it is mainly depicted on the Atherton 1 : 250,000 series sheet which is enclosed in the back pocket to supplement the text.

Precambrian Rocks

Precambrian rocks of the Georgetown Inlier are abundant on the western side of the area covered by the Atherton sheet; small scattered inliers of gneissic rocks occur in the south-east. Rock types include micaceous schist, garnet-mica schist, andalusite schist, gneiss, migmatite, quartzite, augen gneiss, muscovite pegmatite, quartzite amphibolite and granitic rocks (de Keyser and Wolff, 1964). The metamorphics are faulted and folded and are thought to have been derived from aluminous and siliceous rocks rich in potassium. All rock types except the amphibolites grade into each other.

The amphibolites are dark grey and medium-grained. In thin section they are seen to consist dominantly of oriented rods of brown-green hornblende and highly altered plagioclase. Quartz is also present and garnet may or may not occur. The accessory minerals noted were sphene, apatite and iron oxide. L. J. Robinson (personal communication) considers that the colour of the hornblende is indicative of middle to upper amphibolite facies.

The migmatites and gneisses generally contain more muscovite than biotite. De Keyser and Wolff attribute the chloritisation of biotite to retrograde metamorphism. Oligoclase is twinned and occurs as roughly equidimensional grains which are only weakly zoned.

Microcline is interstitial, untwinned and subordinate to plagioclase. Quartz occurs as composite grains with sutured internal boundaries. Myrmekite is commonly present. Sillimanite is infrequent, occurring as both rods and masses of fibres surrounded by fine-grained muscovite. Accessory minerals include epidote, monazite, zircon, carbonate, and apatite occurring as rods and needles. The mineralogy of the metamorphic rocks is indicative of the almandine-amphibolite facies of metamorphism. This conclusion was also reached by de Keyser, Bayly and Wolff (1959).

Several bodies of gneissic granite outcropping in this region are considered to be members of the composite Forsayth batholith, which has its maximum development in the Georgetown area 80 miles further south-west. These granite bodies have ill-defined gradational contacts with the gneisses of the surrounding country rock. In hand specimen they appear grey, coarse-grained and massive to porphyritic. The mineralogy of the granite is similar to but not identical with that in the gneisses and migmatites examined. Biotite and muscovite are present in approximately equal proportions (about 10 per cent each). Basic oligoclase makes up about 40 per cent of the rock. It is again twinned according to the albite, Carlsbad-albite and pericline laws, but it shows strong oscillatory zoning around grain boundaries. Quartz (25 per cent) is present as composite grains, most of which possess highly undulose extinction. Microcline (about 15 per cent) is untwinned and generally

interstitial. Large grains may poikilitically enclose plagioclase grains. Myrmekite is present; zircon and apatite are accessories.

These oldest rocks in the area probably date in the uppermost third of the Precambrian; that is, are no older than the youngest tectonic period so far detected in the more westerly Mount Isa region (1540 m.y. - Richards, 1966). Thus the Croydon Volcanics, on the western margin, yielded an age of 1460 m.y. in a reconnaissance dating project by Richards et al (1966). Only one Precambrian rock from the Atherton sheet area was analysed, yielding a K-Ar age of 1040 m.y. on the mass of Forsayth Granite south-west of Chillagoe. Richards considers this value can only be interpreted as a minimum value for the true age.

Palaeozoic Sedimentary Formations

Palaeozoic sediments are separated from these Precambrian rocks by the Palmerville Fault, a major lineament which extends 600 miles from Princess Charlotte Bay in the north to Townsville in the south (de Keyser, 1963). The fault, however, is not readily apparent in the Almaden - Mt Garnet region and de Keyser has consequently postulated its degeneration into an intricate fracture zone in this area.

a) THE CHILLAGOE FORMATION

The Chillagoe Formation occurs (Amos & de Keyser, 1964) alongside the Palmerville Fault and extends from Ootann northwards into and beyond the area covered by the adjoining Mossman sheet.

Its major component is 5,000 to 10,000 feet of interbedded limestone and chert, with minor quartz greywacke, siltstone, conglomerate, sedimentary breccia and volcanics. The sediments indicate a near-shore, shallow-water mixed clastic and reef environment. The limestone is strongly folded and faulted, and most dips are nearly vertical. In contrast to the unaltered limestone which is massive and dark grey, that occurring near acid intrusions is bleached to light grey or white marble.

Maximum outcrop width of the Chillagoe Formation is six miles. Fossils are very common in the limestone, corals being particularly abundant. These fossils indicate an Upper Silurian to Lower Devonian age for these rocks.

b) THE HODGKINSON FORMATION

The Hodgkinson Formation is for the most part stratigraphically younger than the Chillagoe formation. Recently Blake (1968) has grouped together the Mt Garnet, Hodgkinson and Ringrose Formations, and the Montalbion Sandstone (as defined by Best, 1962, and Zimmerman, Yates and Amos, 1963) into a single formation for which the name Hodgkinson is again used. Similarity of rock type and apparent lack of basal discontinuities has compelled Blake to use this reclassification; it is used hereafter in this thesis.

The Hodgkinson Formation is confined to scattered outcrops in the north-eastern half of the Atherton sheet area but continues northward where it constitutes the Hodgkinson Basin, a major unit in

the Tasman Geosynclinal Zone. Similar rocks occur in the Georgetown-Clarke River area to the south (White, 1965). This unit is highly folded and is presumed to overlie the Precambrian unconformably. Evidence for its Silurian-Devonian-Lower Carboniferous age is given by the included corals, conodonts and plants.

The great thickness, the general uniformity of the sediment type, and the presence of turbidity current structures probably indicate that the Hodgkinson Formation was deposited in a flysch type of environment (Blake, 1968).

c) THE SILVER VALLEY CONGLOMERATE

The Hodgkinson Formation is unconformably overlain by the Silver Valley Conglomerate which crops out over three square miles, eight miles south-west of Herberton. This coarse polymictic conglomerate is massive and poorly sorted and contains megaclasts of Hodgkinson sediments and volcanic material. Thin, commonly cross-bedded arenite lenses are interbedded. Minor ash-fall tuffs and welded tuff sheets are associated. Blake suggests that the conglomerate was deposited in alluvial fans along a narrow valley.

Maximum thickness of the flat-lying (dipping generally less than ten degrees) Silver Valley conglomerate is 300 feet. Associated plant fossils which include Rhacopteris indicate a Carboniferous age.

Palaeozoic Igneous Rocks

a) DEVONIAN INTRUSIVES

Although the majority of Palaeozoic intrusive rocks are of Carboniferous-Permian age, a few small bodies of ultrabasic and basic

rocks which occur along strong faults in the east of the Atherton sheet area are thought to be possibly Devonian (Best, 1962). No other Devonian intrusives have yet been recognised. However, the dating survey by Richards et al revealed the presence of previously misidentified Devonian granites in the southerly corner of the Georgetown Inlier 70 miles further south. These include the biotite-granite (s.s.), adamellite and granodiorite of the Dumbano Granite and a biotite-hornblende trondjhemite which has been called the Dido Granodiorite (White, 1965). Thus unrecognised Devonian granites may crop out in the study area or alternatively occur at shallow depth.

b) 'PERMO-CARBONIFEROUS' IGNEOUS ROCKS

General

The majority of Upper Palaeozoic igneous rocks occurring on or to the east of the Georgetown Inlier have been interpreted by Branch (1966, 1967) as members of well-defined volcano-plutonic formation of this age-group. High-level plutons, ring complexes and large cauldrons filled with ash flows are extensively developed. Most of the rocks are of a rather uniform acidic composition. Total outcrop area is about 10,000 square miles.

Branch has subdivided the granites forming the plutons into two fundamental types, one of which includes the Elizabeth Creek and Esmeralda Granites and the other the Herbert River and Atherton Granites. The Elizabeth Creek Granite occurs on the north and central parts of the inlier. It covers an area of 2,000 square miles and the

predominant rock type is pink leucocratic adamellite. He regards this as being equivalent to the Esmeralda Granite, which crops out over an area of 250 square miles on the western edge of the inlier. Here the main rock type is grey biotite adamellite; the intrusions have the same form as those of the Elizabeth Creek Granite. Richards et al (1966), however, have presented evidence derived from radiometric dating that the Esmeralda Granite is probably at least as old as 1200 million years and does not belong in this Permo-Carboniferous igneous suite.

The volcanic rocks, which are also thought to be comagmatic with the Elizabeth Creek Granite, are dominantly composed of rhyodacite welded tuff. Other rock types which are also calcalkaline comprise rhyolite, trachyandesite, andesite and basalt. The volcanics are almost exclusively confined to cauldron subsidence areas which vary from eight to 75 miles long. Eleven of these have been recognised with an aggregate outcrop area of 4,000 square miles. Branch has estimated the volume of the volcanic rocks at 1,000 cubic miles. Each cauldron contains from two to eight ash flows which vary in thickness from 50 to 1,500 ft, and may cover the entire cauldron. As already stated Richards et al have obtained an age of about 1400 million years for the volcanics occupying the most westerly cauldron on the inlier (Croydon Volcanics), showing that they too are not members of this Upper Palaeozoic suite. Two cauldrons in the centre and north-east of the inlier yielded respectively Devonian to

Carboniferous and Carboniferous to Permian indicated ages. This suggests that there may either be a spectrum or distinct groups of ages for the Palaeozoic suite rather than a single brief episode of intrusion.

Seven ring complexes, which all contain both volcanic and plutonic members, occur over the inlier. The complexes range in size from 170 square miles to less than 20. The youngest stocks in the complexes are generally composed of Elizabeth Creek Granite of the same composition as that which commonly surrounds and intrudes the margins of the ring structures. Branch considers that the location of the ring complexes and cauldrons is controlled by pre-existing fractures in the Precambrian basement.

Intrusive rocks of the Herbert River Batholith crop out over 4,500 miles in and beyond the north-eastern quarter of the inlier. The main rock types are grey biotite adamellite with subordinate hornblende-biotite granodiorite. Branch (1966) states that the rocks of this batholith are distinct from the Elizabeth Creek Granite and have a completely different anatectic origin.

Volcanic Rocks

The Upper Palaeozoic volcanic rocks of the Atherton sheet area have been classified by previous workers (Best, 1962; Zimmerman et al, 1963; de Keyser and Wolff, 1964; Branch, 1966; Blake, 1968) into different formations according to location and mode of occurrence. Branch describes the state of preservation of the cauldron subsidence

areas by using the terms 'complete' and 'remnant'. The former term refers to a cauldron in which the general form of the original subsidence area is easily recognised; the latter refers to an area containing blocks of volcanics which are thought to be related. The Featherbed Cauldron Subsidence Area is an example of a 'complete' cauldron. All other cauldrons in the area are described as 'remnant'. These are the Scardons, Nanyeta, Glen Gordon, Kallon and Gingerella Cauldron Subsidence Areas. Two isolated volcanic vents occur at Crystal Brook and east of Ootann.

Detailed isotopic investigation has been restricted to only one of these structures, the Featherbed Volcanics. These Volcanics will therefore be described in most detail in the following text. The Nychum Volcanics which are not contained in a cauldron subsidence area (Branch, 1966), crop out chiefly to the north of the area. They will be discussed in a separate chapter because previous stratigraphical and palaeobotanical observations have been in apparent conflict, and all evidence must be considered together to determine the most probable relationship.

a) The Featherbed Volcanics. These occur just outside the north-eastern edge of the inlier. Branch suggests that they occupy a cauldron subsidence area 62 miles long and 20 miles wide; total outcrop area is 950 square miles, the maximum thickness is about 2,000 ft, and the volume of the volcanics is about 200 cubic miles.

In the central and northern sections of the cauldron (which extends northwards beyond the Atherton sheet area) the volcanics form the Featherbed Range, a mountainous area with 1,200 ft relief.

Most of the Featherbed Volcanics are massive and structureless; welded tuffs predominate, but normal lava flows and pyroclastic accumulates also occur.

In the area north-east of Chillagoe, and also north-west of Petford, a series of puys up to 600 feet high of flow-banded pink rhyolite crop out along the marginal fault. Evidence for an extrusive origin for the volcanics includes low bedding dips, the attitude of columnar jointing and the occurrence of a fossil volcanic vent five miles north-east of Petford (de Keyser and Wolff, 1964). Bedding dips increase in the vicinity of the marginal fault; dips immediately adjacent to the fault tend to be parallel to it. Branch (1966) interprets this as resulting from drag on the volcanics along the fault plane as the cauldron was forming.

The Featherbed Volcanics unconformably overlie the Almaden Granite (Best, 1962; Branch, 1966) and the Hodgkinson Formation. Blake (1968) lists several localities where breccia or conglomerate beds occurring at the base of the Featherbed Volcanics contain rock fragments identical in composition to components of the underlying steeply-dipping Hodgkinson Formation.

Branch (1966) and Blake (1968) cite examples where the Elizabeth Creek Granite intrudes the volcanics, and conclude that this is the

general case. From a single Rb-Sr analysis Richards et al (1966) have suggested an approximate age of 280 m.y. ($\lambda = 1.47 \times 10^{-11} yr^{-1}$).

The volcanics are predominantly of rhyodacitic composition; rhyolite is fairly common at the base of the sequence, dacite and intermediate rock types are rare.

Brief petrographic descriptions, based on the work of Branch (1966), Blake (1968) and the author, are included in the appendix.

b) The Tennyson Ring Dyke. The Tennyson Ring Dyke is a large composite ring dyke, three quarters of a mile wide and sixteen miles long, which forms the boundary of the Featherbed Cauldron between Almaden and Petford (Branch, 1966). Spilled-over flows are still preserved west of Lappa (de Keyser, 1964). The Tennyson Ring Dyke is probably the source of some of the Featherbed Volcanics. De Keyser considers that the dyke may continue unrecognised around most of the edge of the Featherbed Range. This would be in agreement with the theory of Branch that the volcanics filling the various cauldrons were derived from marginal ring fissures.

The ring dyke is mainly composed of light pink and grey fluidised porphyritic rhyodacite (Branch) cut by pipes filled with tuff and volcanic breccia-agglomerate. Mineralogy is very similar to the rhyodacite welded tuffs of the Featherbed Volcanics with which they are probably related.

c) Other Volcanic Rocks. As in the Featherbed Volcanics, rhyodacite welded tuff is the dominant rock type in the following volcanic

outcrops. Rhyodacite, rhyolite, dacite, trachyandesite and quartz andesite occur as minor flows. Volcanic agglomerate, airfall tuff, tuffaceous sandstones and siltstones are present in subordinate amount.

The Glen Gordon Volcanics occur in a cauldron subsidence area 65 miles long by 11 miles wide immediately outside the eastern extremity of the inlier (Branch, 1966). These volcanics unconformably overlie the Hodgkinson Formation and are intruded by the Elizabeth Creek Granite. Branch (1966) correlates these rocks with the Featherbed Volcanics.

The Walsh Bluff Volcanics occupy a 90 square mile triangular area to the north of the Glen Gordon Volcanics. Branch considers that the volcanics occur in the same cauldron as the Glen Gordon Volcanics. Blake, however, interprets the structure as a shallow basin completely separate from the Glen Gordon cauldron. The Walsh Bluff Volcanics unconformably overlie the Elizabeth Creek Granite (in contrast to all other volcanics but those at Slaughter Yard Creek) and are intruded by the Watsonville Granite (dated by Richards et al (1966) as Lower Permian), which has been subdivided from the Herbert River Granite type by Blake (1966).

The Slaughter Yard Creek Volcanics, previously grouped with the Glen Gordon Volcanics, are composed of acid lavas and intrusive rocks and crop out over six square miles between Herberton and Watsonville. The volcanics have intruded, sheared and recrystallised the Elizabeth Creek Granite with which they are in contact (Blake, 1968). The

groundmass of the volcanics also increases in grain-size away from the granite contact. Hence the volcanics post-date the Elizabeth Creek Granite. They are, however, intruded by the Watsonville Granite.

The Nanyeta Volcanics occur in a small cauldron to the north of Mt Garnet. They are intruded by the Elizabeth Creek Granite.

The Scardons Volcanics occur on the western margin of the Atherton Sheet area. The volcanics crop out over 250 square miles and are intruded by the Elizabeth Creek Granite.

The Kallon and Gingerella Volcanics occur in two separate deeply eroded cauldron subsidence areas on the southern margin of the study area. Both unconformably overlie the Precambrian and are intruded by the Elizabeth Creek Granite. The Barwidgi volcanic fissure, a complex vent filled with rhyodacite and volcanic breccia and extending seven miles, crops out in the Gingerella Cauldron.

d) Isolated Volcanic Vents. The Crystal Brook Volcanic Neck is three quarters of a mile in diameter. It occurs three miles south-west of Crystal Brook Homestead and is composed of biotite-hornblende granodiorite. No volcanic breccia is associated with the vent, which occurs in Elizabeth Creek Granite.

A fissure vent 15 ft wide and 600 ft long, containing flow banded rhyodacite and volcanic breccia, occurs in granite six miles east of Ootann. The breccia is composed of blocks of rhyodacite and Precambrian metamorphics in a tuffaceous matrix (Branch, 1966).

Ring Dyke Complexes and Dyke Swarms

The Warby Ring Complex (Branch, 1966) is centred in the south-western corner of the study area and consists of two overlapping ring structures. In the northerly complex, hornblende-biotite granite (s.s.), and adamellite, and hornblende-biotite-quartz trachyandesite ring-dykes enclose two blocks of downfaulted volcanics. The dominant volcanic member is rhyodacite welded tuff; subordinate rhyolite welded tuff, volcanic breccia and rhyolite occur. The northern member of the complex has axes of ten and a half miles and thirteen and a half miles. A circular granitic stock eight miles in diameter constitutes the southern member.

The Doolan Creek Ring Complex (de Keyser and Wolff, 1964; Branch, 1966) occurs ten miles north of Chillagoe and crops out over an oval area of about twenty square miles. A large downfaulted block of rhyodacitic volcanics (which may be correlated with the Nychum Volcanics) is intruded by a central stock of granite (s.s.), microgranite and adamellite. The complex is cut by rhyodacite dykes.

The Boxwood Ring Complex (de Keyser and Wolff, 1964; Branch, 1966) lies eight miles south-west of Petford and is a circular structure which covers 45 square miles. Downfaulted blocks of Hodgkinson sediments, Herbert River Granite and Boxwood Volcanics (dominantly massive grey rhyodacite welded tuff) are intruded by a stock of Elizabeth Creek Granite and rhyodacite dykes. The complex is almost completely surrounded by Elizabeth Creek Granite. Both

the Doolan Creek Ring Complex and the Boxwood Ring Complex are cut by the marginal fault of the Featherbed cauldron.

The Claret Creek Ring Complex (Branch, 1966) lies 13 miles west-north-west of Mt Garnet; it has a circular outcrop of 50 square miles. A crescentic block of downfaulted Hodgkinson Formation in the north of the complex is bounded on its southern margin by a long thin dyke of rhyodacite. A smaller crescentic block of Hodgkinson Formation sediments defines the southerly margin of the complex. Within this crescentic block and the arcuate rhyodacite dyke lies a block of downfaulted Claret Creek Volcanics (rhyodacite welded tuff and interbedded breccia). A crescentic dyke of microadamellite is the next innermost member of the complex. The final member is a plug of fine-grained basic granodiorite which occurs in the south-east corner. Branch considers that this predates the complex but detailed remapping by J. C. Bailey (personal communication) has revealed that this is the youngest member. A large volcanic vent containing volcanic breccia and grey rhyodacite occurs in the Hodgkinson Formation rocks in the north-west corner of the complex.

The Gurrumba Ring Complex (Blake, 1968) crops out over five square miles and is located six miles south-south-west of Emuford. It is essentially composed of three elements; an outer igneous ring ten yards to one mile wide completely surrounds an inner sedimentary member, which itself is intruded by a complex igneous core. The outer ring is made up of granophyre, olivine gabbro, and a variety of

intermediate hybrid rocks (mostly of quartz diorite composition). These rocks are often intimately associated, forming a net-veined complex with rounded inclusions of basic and intermediate rocks in a granophyre matrix. The olivine gabbro is an unusual representative of this Permo-Carboniferous suite; it is composed of bytownite-anorthite, augite, hypersthene, olivine, and iron oxide.

The second member of this complex consists of greywackes and siltstones of the Hodgkinson Formation. The third and innermost member is made up of two small bodies of acid lava (autobrecciated and flow-banded rhyolite named the Gurrumba Volcanics by Blake) and a small plug of quartz diorite.

The igneous rocks of the Gurrumba Ring Complex intrude the surrounding Elizabeth Creek Granite. Contacts between the outer ring dyke and the granite are vertical, and are irregular in detail.

Dykes and Dyke Swarms (Branch, 1966; Blake, 1968) are widespread and intrude the bulk of the pre-Mesozoic rocks. Most are rhyodacitic and porphyritic, but trachyandesite, andesite and dolerite dykes also occur. The dykes are thought to be related to the Upper Palaeozoic volcanic rocks. Branch distinguishes five major dyke-swarms. The Wireyard, Emu, and Graves Dyke Swarms strike approximately north-west and crop out between the Featherbed and Scardons Cauldron Subsidence Areas. The Parada and Collins Weir swarms also strike north-west. They intrude the Hodgkinson Formation in the north-east corner of the study area.

The Granites

Upper Palaeozoic granitic rocks crop out over a large proportion of the study area and probably underlie much of the remainder at shallows depths. During the regional mapping the granites were classed as two main units - the Herbert River and the Elizabeth Creek Granites (Best, 1962; Zimmerman et al, 1963). Branch (1966) continued this twofold classification in detail and concluded that the two were separable on genetic grounds.

De Keyser et al (1959), however, considered that the situation was in fact much more complex, and that the various rock-types represented numerous modifications of the one batholith. In 1964 de Keyser and Wolff divided the granites of the Chillagoe area into six or more groups. They point out that even these divisions are arbitrary, and the group boundaries are gradational or obscure. Blake (1968) agreed with de Keyser that the situation was more complex than originally thought. He has subdivided the granites of the Herberton - Mt Garnet area into at least ten units.

The Mareeba Granite, another Upper Palaeozoic variety, has a limited outcrop in the extreme north-east corner of the study area. It is, however, the dominant granite-type to the north.

The different classifications applied to separate parts of the Atherton Sheet area mentioned above considerably confuses any discussion of these rocks.

As one of the main purposes of this study is to investigate the two-magma theory of Branch, it is imperative that it be generally followed here. It is also the only classification which has been used over the entire area.

The Herbert River Granite. According to Branch, the Herbert River Granite was derived from an anatectic magma at the base of the geosynclinal pile in the Hodgkinson Trough, and is not genetically related to the volcanic rocks. He bases this argument on its distribution; it intrudes the north-eastern edge of the inlier and the adjacent sediments of the Hodgkinson Formation. As no evidence of forceful disruption of country rock can be seen, Branch considers that the igneous intrusion was by a block-stoping mechanism. The Herbert River Granite type (Almaden variety) intrudes the Nychum Volcanics but is overlain unconformably by the Featherbed and Glen Gordon Volcanics. It is intruded by the Elizabeth Creek Granite.

Four main exposures of the Herbert River Granite occur in the study area.

1) A belt five miles wide trends 40 miles in a north-westerly direction from Herberton to Wolfram Camp.

2) A 550 square mile northerly-striking outcrop bisects the study area.

3) Granite occurs south of Bulleringer Homestead in the south-west corner of the area.

4) A small outcrop in the south-east corner is continuous with granitic rock in the type area to the south.

The Herbert River Granite is predominantly a grey biotite adamellite which in places grades into a hornblende biotite granodiorite. In hand specimen it is seen to be a medium-grained rock with slightly porphyritic pink alkali feldspar. Aplite, pegmatites, xenoliths (generally basic and small), flow foliation and lineation are stated by Branch (1966) to be uncommon. In the Herberton - Mt Garnet area, however, Blake has found that xenoliths are common. No greisens have been found to be associated with this granite. Contacts are sharp; metamorphism in the country rocks is generally of low grade.

Petrographic descriptions drawn from the work of de Keyser (1964), Branch (1968) and from observations made by the author are summarised in the appendix.

The Almaden Granite. This is a basic modification of the Herbert River Granite and comprises most of the intrusives cropping out between Almaden and the Walsh River. In the Almaden area, contacts between these two granite types are gradational (Branch, 1966). There has been much controversy over the origin of the Almaden Granite, and various theories have been postulated. Initially Branch (1960) attributed its features to assimilation of limestone from the Chillagoe Formation by Herbert River Granite magma. Then in 1962 Branch appealed to assimilation of basic magma (such as the basalts of

the Nychum Volcanics) by the Herbert River Granite. De Keyser and Wolff (1964) suggested that magmatic differentiation may have been at least partly responsible for the formation of the different granite types.

The Almaden Granite is a medium grained, grey, biotite-bearing hornblende granodiorite which is sometimes porphyritic. J. C. Bailey (personal communication) estimates that basic xenoliths, which appear to be uniformly distributed, make up two to four per cent of the rock, and generally range in size from ten to 15 centimetres. A composite petrographical summary of this granite is presented in the appendix.

Intrusive rocks of still more basic aspect crop out in the area and according to Branch's classification are also called Almaden Granite. The orthoclase diorite from Petford is an example. The term 'Herbert River Granite', then, when used in the broad sense of Branch, covers the spectrum of rock types from adamellite through granodiorite to diorite. It thus encompasses rock types of quite widely varying compositions.

The Mareeba Granite. This granite occurs in one restricted outcrop in the north-eastern corner of the study area, but continues northwards along the Hodgkinson Trough as the dominant granite type. Branch (1966) records that the granite is similar in both hand specimen and major element chemistry to the Herbert River Granite, and invokes a common genesis. Blake (personal communication) also considers the Mareeba Granite to be very similar to the Herbert River Granite of the

type area and the unit around Watsonville which he has renamed the Watsonville Granite. The only noticeable petrological difference is that muscovite is common in the Mareeba Granite (but less abundant than biotite) while it is only rarely present in the Herbert River Granite.

The Mareeba Granite which has been dated by Richards et al at $264^{+}_{-}2$ million years (Lower Permian) is younger than the Elizabeth and Herbert River Granites (see next section), and was emplaced during a much shorter time interval.

The Elizabeth Creek Granite. The Elizabeth Creek Granite forms scattered outcrops over the area. It is typically a leucocratic biotite adamellite but grades into alkali granite (s.s.) in places. Salmon to pale pink, orange, white, and grey varieties occur. Grain-size is variable; both even-grained and porphyritic modifications are common. Quartz phenocrysts in the fine-grained porphyritic varieties are commonly rounded; pink and white feldspar phenocrysts also occur. Porphyritic coarse-grained rocks sometimes contain feldspar phenocrysts over six centimetres long. Associated veins of aplite are very common (Blake), but pegmatites are rare. Xenoliths are uncommon, even in contact zones. A noticeable feature of the Elizabeth Creek Granite is the widespread occurrence of associated greisens which are particularly abundant in mineralised areas. Greisenisation has affected most, if not all, of the varieties (Blake). The greisens, which occur as veins and massive bodies, were probably formed by pneumatolitic alteration of granite in situ.

Granite contacts are abrupt. Some are irregular in detail; others which are straight or gently curved are probably fault-controlled. Evidence of chilling is provided by the common presence of porphyritic microgranite near intrusive contacts (Blake). The gently-dipping contacts (commonly as low as 15° indicate that the outcrops now exposed frequently represent the roof zones of the intrusions. In the Herberton - Mt Garnet area roof pendants of country rock are common in the granite. Branch (1966, 1967) contends that emplacement has been controlled by ring fracturing and underground cauldron subsidence and that this has given rise to strongly-jointed intrusions with flat roofs. He estimates that the granite was intruded to within 500 to 2,000 feet of the surface.

Blake reports that sediments of the Hodgkinson Formation have been hornfelsed up to three miles away from the nearest granite exposure. The meaning of this is somewhat dubious, however, as the flat-dipping granite is conceivably present at shallow depth.

Branch (1961) found that in areas where the Elizabeth Creek and Herbert River Granites crop out together, the latter is always the older. On this basis he postulated two distinct periods of intrusion for these granite types. Later work by Blake (1968) has shown, however, that the Herbert River Granite sometimes intrudes the Elizabeth Creek. Moreover, K-Ar estimates of the times of intrusion of the two granites are statistically indistinguishable (Richards et al, 1966) even although both were intruded over a long time period

($\pm$27 million years). Hence Branch has now classed these granites as contemporaneous but of different origin.

In earlier studies, White (1961) and Best (1962) considered that the Elizabeth Creek Granite was of Upper Permian to Triassic age. This estimate was based on palaeobotanical and stratigraphical evidence from the Nychum and Agate Creek Volcanics (see Chapter 8) coupled with the none too secure grounds of lithological correlation. The K-Ar work of Richards et al, however, has since indicated that the Elizabeth Creek Granite (and the Herbert River) are about 285 million years old; that is, either uppermost Carboniferous or lowermost Permian. De Keyser (1964), Branch (1966) and Blake (1968) have all mentioned the possibility of two slightly different ages for Elizabeth Creek Granite, as stratigraphical relations are not always consistent. For example the Tennyson Ring Dyke (continuous at least with part of the Featherbed Volcanics) contains boulders of Elizabeth Creek Granite which must predate the volcanics. In the Bamford Hill and Wolfram Camp area, on the other hand, stocks of Elizabeth Creek Granite intrude the Featherbed Volcanics. The reconnaissance dating survey of Richards et al (1966) may also be interpreted as suggesting two distinct periods of intrusion.

The Elizabeth Creek Granite, although chemically a highly siliceous rock (see chemical section), is generally classed on petrographical grounds as an adamellite; some granitic variants do occur. A petrographical description of this granite appears in the appendix.

Economic Geology

GENERAL

The first economic discovery was made in 1874 when J. V. Mulligan found alluvial cassiterite in the Wild River. This sparked off a mining boom which reached its peak in the late nineteenth and early twentieth centuries. Since then production has dwindled to the low present-day level.

The prominent economic feature of the Atherton area is the diversity of mineral deposits: tin, tungsten, silver, lead, molybedenum and copper ores are the most important. Gold, fluorspar, iron, zinc, limestone, silica, antimony, bismuth, mica and cobalt have also been mined. Details of the mineral deposits can be found in Best (1962), Zimmerman et al (1963), de Keyser and Wolff (1964), Branch (1966) and Blake (1968).

The number (3000) of recorded lode mines and prospects gives a false impression of the economic importance of the area; a more realistic evaluation may be obtained from the following figures. The total lead production of approximately 70,000 tons is only one third of the 1960 production of Broken Hill. Only 40,000 tons of copper have been recovered; this corresponds to only two thirds of the 1960 production at Mt Isa. Wolfram has been more important economically; the 6,500 tons of ore recovered is equivalent to one third of the total production at King Island (Australia's main tungsten producer). Most economic interest has centred on tin virtually throughout the

entire life of the mining field; fifteen per cent of Australia's total tin production has come from the Atherton area. At present the bulk of the tin concentrates are obtained by bucket-dredging of alluvial deposits.

TIN MINERALISATION

Primary tin deposits generally occur in the following three environments in the study area.

1) Greisenised granite dykes, which usually vary from two to ten feet wide and 50 to 100 feet long, commonly contain two to 25 per cent cassiterite. These bodies are shallow, and generally cut out at 50 to 100 feet.

2) Granite and massive greisen sometimes contain sufficient disseminated fine-grained cassiterite to form a workable deposit. This disseminated tin is probably the main source of the alluvial deposits.

3) Chlorite-quartz lodes occur in granite and sedimentary rocks. The latter have yielded more than half the lode tin produced in the area. The lodes are generally pipe-like and appear to have formed at the intersection of fracture zones in competent beds of the Hodgkinson Formation, with vertical joints perpendicular to the granite contact (Branch). The Vulcan mine at Irvinebank, which occurs in one of these structures, is by far the biggest tin mine in the area. This mine, which produced nearly 1,400 tons of cassiterite, is the deepest tin mine in Australia (1,485 ft). Most tin mines, however, are less than 150 ft deep.

Tin is mainly present as the oxide, cassiterite, but stannite has also been found, and Blake considers it is probably more common than is currently accepted.

Tin mineralisation is almost exclusively confined to hypothermal deposits (Blake) in the Elizabeth Creek Granite (and associated greisens) and sediments of the Hodgkinson Formation which have been contact-metamorphosed (presumably by this granite). Virtually all tin production has come from the Herberton - Mt Garnet - Petford region. Because of this spacial association with the Elizabeth Creek Granite the most current widely-held belief is that this granite was the source of the tin mineralisation.

WOLFRAMITE - MOLYBDENITE MINERALISATION

Wolfram Camp and Bamford Hill (three and 17 miles north of Petford respectively) have been by far the most important wolframite - molybdenite mining centres in the area. Two major types of primary deposit have been distinguished.

1) Segregations and disseminations occur in greisenised granite cupolas.

2) Irregular, tortuous quartz pipes which are surrounded by sheaths of greisen have formed the richest deposits.

The Elizabeth Creek Granite is the host rock for the ore and is believed to be genetically related to it.

COPPER MINERALISATION

The Ruddygore copper mine (situated two miles north-east of Chillagoe) is a disseminated low grade 'porphyry-copper' type deposit in the Almaden Granite (de Keyser and Wolff, 1964; Bateman, 1950). All other important copper mines in the study area are associated with significant lead mineralisation.

SILVER - LEAD MINERALISATION

Most of the important silver - lead - zinc - copper deposits occur in a zone six miles wide which extends from Almaden 30 miles north-westwards to Mungana. The majority of these deposits are in limestone of the Chillagoe Formation. Other silver - lead deposits of the Atherton Sheet area occur in Precambrian metamorphics, Palaeozoic sediments of the Hodgkinson Formation, and the Featherbed Volcanics. Most lead ores carry increasing sphalerite with depth. The workings are generally small, disconnected and shallow.

As this study is particularly concerned with the isotopic composition and origin of the lead in the ore bodies, the prominent features of important mining centres are summarised below. The descriptions are drawn from de Keyser et al (1964), Blake (1968) and Zimmerman et al (1963), and are somewhat incomplete as most of the mine workings are now innaccessible. Complete mineralogical descriptions are given in the appendix.

A) Mungana area

Nearly half the silver - lead output of the study area and about one fifth of the copper have come from two mines one half mile apart in the Mungana area, the Girofla and the Lady Jane. The primary ore consists of pyrite, pyrrhotite, marcasite, galena, sphalerite, chalcopyrite, jamesonite, tetrahedrite, arsenopyrite and stannite. Oxidation and supergene enrichment have formed lead and copper carbonates, cuprite and native copper, and secondary copper sulphides.

The lodes occur in vertical pipe-like bodies filled with chert breccia and clay matrix, and capped by siliceous and ferruginous rocks. Chillagoe Formation limestone is the host rock for these lodes, which appear to have been localised in fracture zones. The brecciation is currently considered to be the product of hydrothermal-pneumatolitic corrosion and silicification (de Keyser and Wolff, 1964).

B) Redcap area

Workings in the Redcap area occur in a narrow 3,000 ft lode which strikes north-west (and dips 45° south-west) along a well-defined fault zone at the boundary of the Chillagoe Formation and a mass of undifferentiated Upper Palaeozoic acid volcanics. The lode material is commonly brecciated and consists of a dark-coloured massive siliceous, ferruginous and manganiferous rock. The prominent mineralisation changes from lead in the north-west to copper in the south-east. Most ore has been won from the zones of oxidation and

secondary enrichment. Outcrops of the Almaden Granite occur nearby. Little is known of the production figures but the area was far less important than the Mungana lodes. The important producers were the Redcap, Queenslander and Morrison mines.

C) Chillagoe - Ootann area

Scattered mines of reasonably similar aspect occur in limestone of the Chillagoe Formation between Chillagoe township and Ootann. This group includes the Chillagoe, Calcifer and Muldiva areas of de Keyser and Wolff (1964). The Calcifer mines and the small mine near Ootann occur in roof pendants. All deposits occur at or close to granite contacts, and are considered by de Keyser to be excellent examples of contact metasomatic and fissure lode deposits.

Metamorphism and/or metasomatism of the country rock has resulted in the formation of marble, skarn and calc-silicate rocks. Gangue minerals include quartz, jasper, garnet, wollastonite, actinolite, diopside, epidote and calcite. Silver, lead and copper have been obtained from those mines, which are characterised by lodes with north-west strike.

Six mines from this group were selected for investigation. These are (proceeding south-eastwards) the Christmas Gift, Upper and Lower Hensey, Maniopota, Paisley and Ootann mines.

D) Cardross area

The Cardross group of mines occurs in Precambrian schists and gneisses in the north-western corner of the study area. A zone of

north-north-easterly strike, two miles long and one third mile wide, encloses the major mines. The ore occurs in very irregular intersecting veins and shears which generally dip west. Although wall rocks are sometimes unaltered they are more commonly converted to muscovite and kaolinite. Quartz veining is frequent; gossans are rare. Much of the ore has been recovered from a rich zone of supergene enrichment. Pyrite, chalcopyrite, arsenopyrite and magnetite comprise the common primary minerals. The Cardross group produced economic quantities of copper, gold and silver. Galena and sphalerite occur in only a few mines. Two of these, the Caledonia and the Clansman, were sampled for isotopic work.

E) Dargalong area

The Dargalong mines occur in Precambrian schists and gneisses eight miles south-west of Chillagoe. The mines strike north-west along a two mile shear zone and dip steeply to the south-west. An intrusion of Forsayth Granite flanks the eastern side of the mines. They consist of small, disconnected shallow workings in a quartz-ironstone lode six inches to six feet wide. The low-grade siliceous, primary ore contains galena, pyrite, sphalerite and chalcopyrite. High-grade oxidised silver - lead ores (cerrusite, anglesite and massicot) occurred near the surface. Copper production was negligible.

Galena was collected from two mines - the Jubilee at the southern end of the lode and an unnamed mine to the immediate north (called Dargalong mine in this thesis).

F) Almaden area

Torpey's Crooked Creek mine lies four miles east of Almaden in the sediments of the Hodgkinson Formation. A little cerussite was exposed at the surface and rich galena ore was found at depth. Gangue minerals are pyrite, sphalerite and fluorite. An unusual feature of the ore is the complete lack of associated copper minerals.

G) Koorboora area

A group of tin mines in the Koorboora area contains minor associated galena. In general the galena content of the ore increases with depth, as do also sphalerite, pyrite and chalcopyrite. The ore occurs in tortuous pipe-like chlorite lodes in pneumatolytically-altered host rocks (de Keyser and Wolff).

Galena samples were obtained from the Tennyson, Proserpine, Shakespeare, Conroy and Mountain Maid mines.

H) Featherbed area

This rather artificial group has been formed to simplify data presentation. The mines, although scattered over a wide area, all occur in and close to the margin of the Featherbed Volcanics. They all appear to have been small mines which produced rather high-grade ore.

The Bamford group of mines (three miles north-west of Petford) includes the Comstock mine, a small unnamed show to the north-east (represented by Pb 108), and the Silver Bead mine, at which ore from

both shafts was sampled. These mines contained small, rather rich packets of ore in vertical veins which pinch and swell in width.

The Orient Camp group of mines on the eastern margin of the Featherbed cauldron consists of a few tens of shafts in shear zones which strike approximately east-north-east and dip steeply to the south. High-grade galena and lead carbonate ore was recovered. A galena sample was collected from the Silver Star group of shafts.

The Nightflower mine is situated near the northern boundary of the Featherbed Volcanics in the adjoining Mossman Sheet area. The lode (which may be up to 15 feet wide) occurs in a silicified northerly-striking fault zone. Galena, stibnite, pyrite, chalcopyrite and sphalerite have been recorded.

Two small unnamed mines occur six miles west of Irvinebank (from which galena number Pb 239 comes) and 2.5 miles north-east of Petford (Pb 255). No information is available on these mines.

I) Emuford - Irvinebank - Stannary Hills area

This area includes many hundreds of mines which occur outside the eastern and south-eastern borders of the Featherbed Volcanics. All deposits are in contact-metamorphosed sediments of the Hodgkinson Formation. Many of the lodes are chloritic and occupy shear zones which dip steeply and generally strike west-north-west to north. The ore minerals are concentrated in small irregular pipe-like bodies within the lode. Less than a hundred of these mines contain lead mineralisation. Of these only the Victoria Amalgamated produced as

much lead as the smaller mines in the Mungana - Almaden area. Lead mineralisation in this area is very much subordinate to that of tin. Many of the lead mines were more important as tin producers. Economic copper deposits also occur in some of the lead mines.

Eleven deposits of this group were selected for isotopic analysis. These are (from west to east) the Silver Spray, Panquay, Mt Babinda, Bloodwood, Mountain Maid (hereafter to be qualified by the name Omeo to distinguish it from the mine of the same name near the Tennyson Ring Dyke), Cosgrove, Lady Jane No. 2 (there is a mine of similar name in the Mungana area), Victoria Amalgamated, Great Adventure, Silver Lining and Great Western mines.

J) Herberton area

The tin and copper deposits of the Herberton area infrequently contain limited lead mineralisation. The quartz and quartz-chlorite lodes of these lead mines occur in thermally metamorphosed sediments of the Hodgkinson Formation. Two mines, the Isabel and the You and I, were sampled.

K) Silver Valley area

Rich silver-bearing copper and lead deposits have been mined in the Silver Valley area. The Lodes occur in steeply-dipping shear zones which strike between north and west in unmetamorphosed Hodgkinson sediments. In general the lead is not associated with tin. Galena was collected from the Battery, Target, and the Doc and Doris mines.

L) Mt Garnet area

Two copper - lead mines occur in this area. Both have been sampled. Oxidised copper - silver - lead ores were found in quartz and calc-silicate lodes at the Mt Garnet mine. The lodes occur in vertical north-south shears. Copper - lead mineralisation in a quartz bed at the Chinaman mine was of minor economic significance. The ore occurs as carbonate in an outcrop of unnamed granite. Lead deposits in granite are rare in the area.

M) Brownville area

A group of economically unimportant lead-bearing mines is situated in contact-metamorphosed Hodgkinson sediments around Brownville. The ore, which was localised in small steeply-dipping shears, was mostly won from the oxidised zone. Some of the mines also produced economic quantities of tin. Galena was collected from the Bolivia, Tuckers, Kohinoor and Excellent mines and from a small unnamed prospect three miles south-east of Brownville.

N) Isolated mines

A small unnamed lead mine occurring in the Robs Range (on the southern boundary of the study area) is unusual in that it lies in Elizabeth Creek Granite.

A previously collected sample of galena from Blackwell's mine in the Georgetown region (40 miles to the south-south-west of the study area) was analysed. No information is available on these mines.

ORIGIN OF THE LEAD MINERALISATION

Although it is unanimously agreed that the tin, tungsten, molybdenum mineralisation is genetically related to the Elizabeth Creek Granite, there is much controversy over the origin of the lead. Two schools of thought persist. Best (1962), de Keyser and Wolff (1964) and Branch (1966) believe that the copper, lead, silver and gold deposits have been introduced by the Almaden Granite. This theory has arisen from field studies in the Chillagoe - Almaden region where contact metamorphism and metasomatism has produced strong mineralogical changes in limestone. Marble, calc-silicate and skarn rocks, and magnetite and hematite - quartz lodes have been formed. The minerals wollastonite, tremolite, actinolite, epidote-zoisite diopside, scapolite and plagioclase commonly occur. Many of the most important Cu-Ag-Pb deposits of the Chillagoe district are associated with these contact rocks, in which they typically occur as irregular and unpredictable bodies. They are thus considered to represent contact metasomatic deposits formed from the nearby Almaden Granite.

Blake (1968), on the other hand, from his experience in the Mt Garnet - Herberton area contends that the Elizabeth Creek Granite is responsible for all mineralisation. This idea is based on two lines of evidence. Firstly, mineralisation is restricted to the Elizabeth Creek Granite and rocks intruded by it (not all of these, however, are mineralised). The second line of evidence is presented

by mineralogical zoning in the metamorphic aureole of a body of Elizabeth Creek Granite in the Emuford - Irvinebank - Stannary Hills area. Four zones have been distinguished (see figure 1). The innermost is restricted to the granite and contains wolframite (and some molybdenite) as the main ore mineral; quartz, mica, fluorite and topaz constitute the gangue. The second, or tin zone, occurs in granite and Hodgkinson sediments. Cassiterite is the dominant ore mineral. Gangue minerals are quartz, mica and fluorite in the granite, and quartz, chlorite, tourmaline and sericite in the sediments. Still further away from the granite is the copper zone in which chalcopyrite and secondary copper minerals are found in quartz gangue. Most of the deposits are in unmetamorphosed Hodgkinson sediments. Galena and sphalerite in quartz gangue characterise the outermost zone. The host rocks are unmetamorphosed Hodgkinson Formation and Featherbed Volcanics.

Blake notes that this district zoning is very similar to that in Cornwall, England and Bolivia, South America, where zoning is also attributed to a mineralising granitic body. He considers that the zonal sequence in the Atherton Sheet area is also largely controlled by decreasing temperature and pressure conditions away from the granite.

Although the specific origin of the silver - lead - copper ores is controversial, there is general agreement that the Upper Palaeozoic granites are responsible for all the mineralisation in the area.

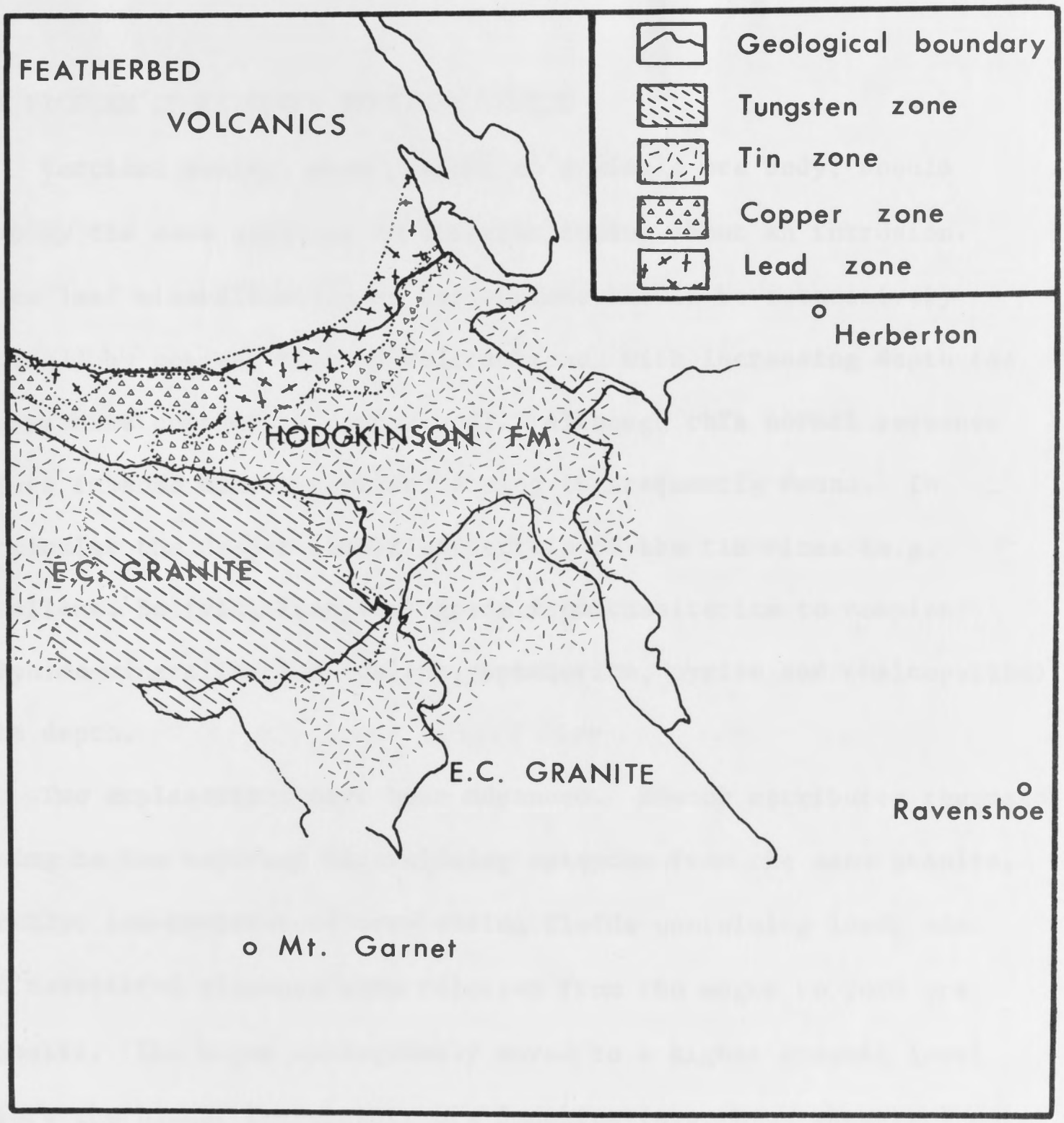

Figure 1. District mineral-zoning in the Herberton - Mt Garnet area.

THE PROBLEM OF REVERSED VERTICAL ZONING

Vertical zoning, when present in a single ore body, should display the same sequence as district zoning about an intrusion. Hence lead mineralisation at the surface should be successively replaced by copper, tin and wolfram zones with increasing depth (as the granite contact is approached). Although this normal sequence occurs in some mines, reversed zoning is frequently found. In particular the deeper levels of certain of the tin mines (e.g. Excellent, Bolivia, Tennyson) grade from cassiterite to complex sulphide mineralisation (galena, sphalerite, pyrite and chalcopyrite) with depth.

Two explanations have been advanced. Branch attributes reversed zoning to two separate mineralising episodes from the same granite. Firstly, low-temperature ore-bearing fluids containing lead, zinc and associated elements were released from the magma to form ore deposits. The magma subsequently moved to a higher crustal level before the higher temperature ore deposits (e.g. tin, tungsten) were formed. A. K. Denmead (in Blake, 1968) contends that the zoning is a secondary feature. He suggests that the primary mineralisation consisted of stannite and other sulphide minerals (including galena and sphalerite); no depth-zoning was originally present. Leaching and oxidation above the water table have converted the stannite to cassiterite and removed the other sulphides. The complex sulphides at depth would represent the unaltered ore and the zone of secondary sulphide enrichment.

CHAPTER 3

TECHNICAL ASPECTS

This chapter describes the various analytical techniques used. Isotopic analyses of Pb, Rb and Sr, and isotope dilution determinations of Rb, Sr, Pb, U and Th have been made using conventional mass-spectrometric procedures. The potential of the X-ray fluorescence technique for Pb, U and Th analyses has also been investigated. The attraction of this method is that it does not involve chemical processing, and thus reduces the possibility of contamination; it also obviates the use of the radioactive Th^{230} and U^{235} spikes. Rb, Sr, Y and Sn were also analysed by X-ray fluorescence. The γ-ray spectrometer was used for most K determinations, but a few flame-photometric measurements are included. Estimates of the U and Th content of the ore specimens were obtained by α-counting. The mass-spectrometric procedures involve extensive chemical treatment, and much of this chapter is devoted to the previous and current practices in this laboratory.

Ore Samples

Galena-rich ore (½ g.) was crushed in a steel percussion mortar to about one millimetre grain-size and converted to chloride in the manner described by Richards (1962), i.e. by HCl extraction followed by precipitating with ethanol. Approximately 10 mg. of the chloride was then dissolved in 2 ml. of hot water and centrifuged to remove insoluble material (sulphate?). Lead oxalate was then precipitated

from the clear solution with two drops of 10 per cent oxalic acid. The precipitate was washed six times with 70 per cent ethanol by repeated agitation and centrifuging, and then dissolved in 5 per cent HNO_3, reprecipitated with 20 per cent NH_4OH and washed twice with ethanol. It was finally redissolved in concentrated nitric acid, precipitated again with ammonia, and loaded on to a filament for mass-spectrometry (Cooper and Richards, 1966b).

A slightly modified procedure was used for 'spiked' runs. Five milligrams of stock chloride was dissolved in 50 ml. of water. A 0.5 ml. aliquot was taken, centrifuged to remove insolubles and sufficient spike was added to equalise the amounts of Pb^{208} and Pb^{207}. After precipitating as the oxalate the sample was washed six times with ethanol as before. It was then loaded in water onto a filament on which a small drop of three per cent ammonium nitrate solution had been dried. The much smaller quantities of lead used in the spiked analysis precluded the HNO_3 and NH_4OH steps as the oxalate is appreciably soluble in ammonium nitrate.

Rock Samples

SAMPLE PREPARATION

Initial preparation was much the same for all rock samples; subsequent chemical treatment was required only for the mass-spectrometric determinations. The approach to initial preparation was chiefly influenced by the geochemical behaviour of the elements most relevant to this study. Since much of the

uranium and thorium (and hence radiogenic lead) in a rock occurs in cracks and along grain boundaries (Catanzaro and Gast, 1960; Kleeman and Lovering, 1967) leaching is a particular hazard. Rock samples, therefore, must ideally be completely fresh. For this reason gelignite was routinely used for samples collected by the author.

About one kilogram of rock was progressively reduced to less than one centimetre grain-size in two steel jaw-crushers. Batches of approximately 150 g. were then ground for 15 seconds in a 'Sieb' tungsten-carbide high-speed mill, then thoroughly mixed before selection of 50 to 100 g. with a stainless-steel splitter. This fraction was further pulverised in the Sieb mill for 1.5 minutes. The grain-size distribution of two rocks crushed in this manner was determined by sieving and the pipette method of size analysis (Krumbein and Pettijohn, 1938) with the following results:-

Table 1

Grain-size Distribution (%)

Grain-size (mm.)	Adamellite	Rhyodacite
>.076 mm. (200 mesh)	9	3
.076 - .0312	35	29
.0312 - .0078	33	36
<.0078	23	32

LEAD BLANKS AND THE PURIFICATION OF REAGENTS

It is desirable to reduce the lead contamination level as far as possible so that only minor corrections have to be made to isotopic compositions and concentrations. Differential contamination between spiked and unspiked runs is particularly disturbing as it produces highly aberrant normalised results, as shown later in this chapter.

Normal analytical-grade reagents are not suitable for trace lead analysis as they contribute comparable amounts of lead to the 50 to 100 μg. in the sample; further purification is always necessary. Contamination from 'fallout' must also be minimised and closely monitored. Footware is changed in an antechamber, and residual dust is removed from the soles of laboratory shoes by standing on a mat coated with adhesive material. A filtered air supply maintains a positive pressure in the laboratory to minimise the entry of airborne material. Scrupulous attention is given to laboratory hygeine, even to the extent of fresh paper towelling placed frequently on the work-space.

Only borosilicate glassware is used (Pyrex, Duran 50 or Kimax) in lead extraction. The glassware is first treated with a cleaning mixture of 50 per cent water, 35 per cent concentrated nitric, 10 per cent hydrofluoric and 5 per cent Teepol to expose a fresh surface and to remove the brand names printed on the outside, as these contain lead (Swainbank, 1967). It is then thoroughly rinsed

in deionised water and left in mild detergent (a two per cent solution of R.B.S. 25) overnight. After thorough washing in cold water the glassware is 'stewed' in hot 50 per cent HNO_3 for approximately two hours. It is then washed in deionised water, immersed for one hour in hot deionised water, washed with distilled and deionised water, drained, and covered with Parafilm for storage. Teflon apparatus is cleaned similarly, except for the fluoride cleaning mixture.

All platinum vessels are alternately flamed at high temperature and boiled in concentrated hydrochloric acid about ten times before initial use. In between samples they are boiled first in concentrated HCl, then deionised water, and lastly concentrated HNO_3, before rinsing with distilled deionised water preparatory to use. The platinum crucible used in the fusion is flamed after the water-boiling stage.

A major problem has been the reduction of Pb contamination to an acceptable level. An initial 10 µg. blank has been reduced to about 0.8 micrograms, largely through purification of reagents. This value is still high when compared with that reported by Tatsumoto (1966a; 0.03 µg.). It is comparable, however, to the value reported by Doe et al (1967; 0.14 µg.) if the reagent quantities in their otherwise similar study are adjusted to the larger rock samples treated in this work.

Numerous reagents are used during trace lead analysis and the preparation and purification of these are discussed below; individual contamination levels are included where possible.

Water

As large quantities of water are used in the lead extraction, contamination from this material must be reduced as far as possible. The water in standard use at the beginning of this project was purified with an ion exchange resin, followed by treatment in an automatic still of 40 litre capacity. Two analyses made of this water in July 1967 and March 1968 yielded lead blank values of 0.04 and 0.003 µg./g. respectively. Not only were these results at least an order of magnitude higher than the tolerable limits but they were also disturbingly different. This probably results from a highly variable water supply which frequently saturates the deioniser. Subsequent to this, all water used in this study was redistilled in a separate small Pyrex still. P. H. Reynolds (of this laboratory) has determined the lead level of this water at 0.00025 µg./g. Pb.

Chloroform

A major contributor to the initial high blank was the chloroform. The original cleaning, by distillation of analytical grade reagent in Pyrex, yielded a blank value of 0.07 µg./g. Pb. This high value may have been due to the presence of volatile lead compounds. Shaking with 1 N HCl reduced the lead to an insignificant

level (not directly measured, only inferred from the difference in total blanks).

Dithizone (Diphenylthiocarbazone)

500 ml. of chloroform solution, containing 25 mg. of solid dithizone was prepared and shaken with dilute high-purity HCl before use.

Nitric Acid

This was purified from analytical-grade reagent by distillation in Pyrex. The lead level was inferred to be about 0.001 μg./g.

Hydrochloric Acid

This was purified in the same way as the nitric acid, for a comparable contamination level.

Hydrofluoric Acid

Table 2

HF Purity Levels

Name or Method	Stated Purity (μg./g.)	Actual Purity (μg./g.)	Comments
'Baker Analysed'	0.1	0.05	
'Ajax'		(0.03)	
'Aristar'	0.02	0.3 (0.3)	
Isothermal distillation			Too weak
Coprecipitation	0.002	0.01	
Gaseous condensation		0.006 (0.003)	

The preceding tabulation lists a series of tests on various brands of reagents, and purification methods. Determinations by Reynolds are parenthesized. The stated purity level for the coprecipitation treatment is that claimed by Rosenqvist (1942).

The most suitable product was made by passing HF gas (supplied by The Matheson Company Inc.) through a thick bed of Teflon shavings, and condensing it in twice-distilled water. In contrast to the NH_4OH procedure (see later) an intermediate aqueous cleaning stage could not be used as the gas is infinitely soluble in water below 19.4° and very soluble above this temperature (Hodgman, 1962). Teflon tubing was used in preference to the more flexible tygon, as the latter was decomposed by the HF, liberating water which condensed the gas prematurely. The two analyses were performed on separate batches.

The only attempt at the isothermal distillation of Kwestroo and Visser (1965) produced an unsatisfactorily weak product and, furthermore, was wasteful in time and material. The technique of Rosenqvist (1942) in which lead is coprecipitated by the dropwise addition of strontium chloride solution yielded a contamination level which contributed about 25 per cent of the total blank (0.8 µg.).

Perchloric Acid

A trial sample of $HClO_4$ supplied by Ajax Chemicals Ltd had a lead content of 0.01 µg./g. Distillation under vacuum in the

laboratory yielded a reasonably pure product (0.005 µg./g.) but the elaborate safety precautions seriously interfered with routine laboratory procedure.

'Aristar' perchloric acid purchased from The British Drug Houses Ltd (claimed purity of 0.005 µg./g.) was used in this project. Ten bottles, all from the same batch, were analysed, with the following results. (Determinations by Reynolds are parenthesized.)

Table 3

Aristar Perchloric Acid Assays

Perchloric Acid Bottle No.	Lead in µg./g.
A	0.030, 0.030
B	0.005
C	0.003
D	0.004
E	0.004
F	0.003
G	0.004, (0.005)
H	(0.006)
I	(0.110)
J	(0.005)

Bottles A and I have presumably been inadequately cleaned by the maker (cf. Aristar Hydrofluoric) and are clearly unsuitable for use. Fifty millilitres from any of the other bottles still yield about ten per cent of the total lead contaminant in each unspiked analysis.

Ammonium Hydroxide

This was prepared by passing ammonia gas (supplied by The Matheson Company Inc.) through two silica frits, scrubbing with a

concentrated ammonia solution, and condensing in water. The ammonium hydroxide obtained was the same purity as the ultrapure water from which it was made (0.00025 μg./g.).

Oxalic Acid

Oxalic acid was prepared and purified by J. A. Cooper (of this laboratory). Commercial reagent was eluted through a cation exchange column containing Dowex 50W-X8, 200 - 400 mesh resin.

Ethyl Alcohol

Analytical grade ethanol was distilled in Pyrex.

Ammonium Acetate

75 ml. of distilled glacial acetic acid was diluted to 1500 ml. with water. Ammonium hydroxide was added until the pH of this solution was 3.4.

10% Potassium Cyanide

A saturated solution (50 per cent) was prepared, filtered to remove laboratory dust, and shaken with successive portions of dithizone solution until the green colour persisted. Dithizone contained in the aqueous phase was then removed by repeated washings with high-purity chloroform and the solution was diluted to the desired concentration.

Other Reagents

(Sodium borofluoride, 25 per cent potassium oxalate, 30 per cent tribasic ammonium citrate, and eight per cent barium nitrate) Saturated solutions of these reagents (adjusted to pH 9 with NH_4OH

where necessary) were filtered to remove laboratory dust and shaken with successive aliquots of dithizone solution until there was no colour change. Excess dithizone was then extracted by repeated washings with acid-washed chloroform. The sodium borofluoride solution was next evaporated to dryness in a large platinum dish, and fused to remove all water. A blank determination on this reagent yielded a value of 0.1 μg./g. To test whether this was caused by free fluoride ions leaching lead from the glass, the procedure was repeated with about ten per cent boric acid to complex the fluoride ions. The result, confirmed independently by P. H. Reynolds, was the same (0.1 μg./g.). Hence it appears that this lead is present as a complex which will not react with dithizone. Only small quantities (about one g.) of this flux were used.

Composition of the Contaminant

The lead-206 spike used to determine blanks contained only minor quantities of Pb^{207} and Pb^{208}. After correcting for this the 208/207 ratio of the contaminant was found to be 2.28 and 2.32 in separate total-blank determinations. This agrees closely with a 208/207 ratio of 2.32 from Mount Isa-type lead, but is different from that of average North Pacific lead (2.49). Mount Isa lead composition is therefore assumed for contamination corrections.

Conclusions

Contamination must be continuously monitored in lead isotope work. It is imperative that the laboratory water be reliable.

Reagents supplied commercially should not be trusted and it is necessary to test the contents of each individual reagent bottle. Major portions of the total contamination are contributed by the following reagents which yield as much as 0.5 μg. of the total 0.8 μg. blank. H_2O, 0.05 μg.; HNO_3, 0.2 μg.; $HClO_4$, 0.1 μg.; HF solution, 0.1 μg.; $NaBF_4$, 0.05 μg. Most of the remaining 0.3 μg. is most probably contributed by the untested reagents, with accidental contamination being only a minor factor. Further purification of these reagents is thus required before blanks of less than 0.1 μg. will be achieved.

URANIUM AND THORIUM BLANKS AND THE PURIFICATION OF REAGENTS

In contrast to the preceding treatment for lead, contamination in the uranium - thorium chemistry is not a serious problem. With very little effort it was possible to reduce the uranium blank to 0.02 μg. As 20 μg. of the uranium-238 are handled in each analysis, this gives a comparative blank level of 0.1 per cent. This value is probably less than the fractionation uncertainties arising in the mass-spectrometry. With the single spike in current use no correction can be applied for this fractionation. No thorium contamination could be discerned at all. This may have been partly due to a fairly impure spike coupled with uncorrectable fractionation errors.

Only three new reagents needed to be prepared and purified. Methyl iso-butyl ketone (hexone): This was purified by distilling analytical grade reagent in Pyrex.

Aluminium nitrate: A saturated solution was made up of aluminium nitrate, water and nitric acid in the proportions 1,000 : 425 : 75. This was purified by shaking with two successive portions of purified hexone for five minutes each.

Ammonium nitrate: 800 gm. of ammonium nitrate were dissolved in 500 ml. of water (forming a saturated solution). This was purified in the same way as the aluminium nitrate.

WHOLE-ROCK LEAD METHOD

The details of the 'wet chemistry' lead method used in this laboratory until recently are given by Farquharson (1968). This method incorporated the dissolution technique of Tilton et al (1955), followed by a lead isolation and purification procedure based on the works of Sandell (1950), Patterson (1951), Tatsumoto (1966b) and Cooper and Richards (1966a). Replicate dissolutions, and comparison of isotope-dilution (I.D.) and X-ray fluorescence (X.R.F.) values, have revealed several inadequacies. The resulting modifications will now be discussed individually in some detail; the complete method is outlined in the appendix.

A) The Fusion

The insoluble residues after the HF - $HClO_4$ treatment are concentrated and fused in a platinum crucible to decompose the resistant U- and Th-bearing minerals such as zircon and monazite. Initially a borax (sodium tetraborate) flux was used but evidence of

variable lead-loss during fusion has necessitated the use of lower fusion temperatures and a new flux, sodium borofluoride, has been utilised.

Lead-loss was suggested by comparative studies and confirmed by direct monitoring of the fusion. Table 4 compares 17 isotope dilution analyses incorporating borax fusions with corresponding X-ray fluorescence results, each of which is the average of four measurements.

Table 4

Assessment of Borax Fusion

Sample No.	X.R.F. Concentration (µg./g.)	I.D. Concentration (µg./g.)	% 'Lead-loss'
2952	29.2	28.9	
2954	37.6	37.8	
2956	30.3	23.0, 26.8	24, 12
2957	28.5	26.5, 28.0	7, 2
2960	27.7	27.7	
2961	17.9	18.0	
2962	38.6	37.3, 37.0, 34.9	3, 4, 10
2964	24.1	25.8	-7
2969	37.4	33.8	10
2973	21.6	23.5	-9
2974	19.9	16.7,20.4	22, -3
2975	28.7	30.4	-6

Although most samples show a general correlation, two (2956 and 2974) are significantly lower by isotope dilution; only one of the five replicate isotope dilution runs shows reasonable internal agreement.

The fusion-loss hypothesis was directly tested by adding a known weight of 208-spike to the crucible and fusing for two hours at 1020°C

under oxidising conditions. This temperature was chosen since it has been found that zircons in these rocks are extremely resistant; even after ten hours, complete reaction has often not occurred. The range of fusion temperature from 990 to 1020°C was suggested by G. R. Tilton in a personal communication to J. R. Richards.

The sample was dissolved in HCl, the underside of the lid also being washed with acid, and mixed with a known amount of 206-spike. A 60 per cent loss of 208-spike was apparent. More flux and 206-spike was added to the crucible and fused at 1060°C in an effort to induce evaporation of lead from the platinum. Six micrograms of common lead was extracted; no trace of the 208-spike was found. This would suggest that the loss of the spike occurred by evaporation rather than absorption.

To test the effect of temperature on the lead-loss the first experiment was repeated at 990°C but allowed to proceed for three, rather than two hours. An 80 per cent lead-loss clearly indicated that even 990°C is too hot.

Reynolds has documented a 20 per cent lead-loss in a dissolution incorporating a borax fusion (at 970°C for one hour), by comparing the yield with a separate dissolution of the same sample with a $NaBF_4$ fusion.

Tilton et al (1957) have also recorded lead-loss during borax fusion in platinum but report proportions considerably lower than those obtained here (five to ten per cent for a fusion of an hour or

longer). Tilton ascribes the loss to diffusion into platinum (where it is strongly held) rather than loss to the atmosphere (advocated by C. C. Patterson in a personal communication to J. R. Richards).

Data from Hodgman (1962), indicate that of all measured lead compounds, lead metal has the lowest volatility (lead tetraborate was unfortunately not mentioned). The volatility of lead metal, one mm. vapour pressure at 970°C, exceeds that of iodine during heat-wave conditions (greater than 38°C). All other recorded compounds (except the oxide) are at least an order of magnitude more volatile. It is therefore entirely possible that lead will be lost to the atmosphere, in the absence of special precautions such as cooling coils around the side of the crucible and on the lid.

It is evident that the radiogenic lead residing in the resistant minerals cannot constitute the 20 per cent of the total lead lost from some samples (see Table 1). Hence in many instances lead other than this radiogenic component must be reaching the crucible for the fusion step. This could well be trapped in a white amorphous substance which formed to various degrees during the dissolution and which, because of its solid nature, was transferred with the resistates to the fusion vessel. (It is thought that a substantial part of the lead in the crucible has been lost during <u>each</u> fusion. Lead-loss is principally determined by the amount of this amorphous substance transferred to the fusion vessel.) This substance was subsequently concentrated and analysed by A. J. Graham on an MS7 spark-source

mass-spectrograph. It was found to consist dominantly of aluminium (oxide or hydroxide); both lead and thorium were present in quantity (about 100 μg./g. of Pb, 50 μg./g. of Th). Because of its resistance to acid attack this substance is assumed to be the oxide.

In an attempt to avoid the fusion loss problem further investigation was made of a new flux suggested some years ago by J. A. Cooper (of this laboratory). Sodium borofluoride is a compound which melts at only 384°C (Hodgman, 1962), with slight decomposition to sodium fluoride and boron trifluoride even at this temperature. It has the obvious advantage of allowing fusions 600°C below those using borax but must be used in a fume cupboard to remove the toxic BF_3. Preliminary tests showed that it attacked beach-sand zircons very readily, although the zircons from some rocks in this study proved resistant to attack by the $NaBF_4$, as well as by borax. Lead loss was tested with a 15 minute fusion of 51.5 μg. of Pb^{206} (two grams of beach-sand zircons completely dissolved in less than five); 51.6 micrograms were recovered. The small excess of Pb^{206} was common lead contamination from the flux itself.

Sodium borofluoride has therefore been adopted as the standard flux, even although further improvements in its purification are still required.

In view of these errors introduced by the fusion, it is pertinent to enquire whether this step may be dispensed with entirely. Some evidence is beginning to suggest that it may indeed not be necessary.

For example rock no. 2962 which has been analysed by the author frequently under different conditions (see section E of this chapter) yielded comparable isotopic ratios with and without the fusion. During the experiment already discussed, Reynolds (personal communication) has shown that even with 20 per cent lead-loss during fusion, isotopic compositions are not significantly altered (less than 0.1 per cent). Samples 2956 and 2974, analysed by the author and showing comparable lead-loss, were changed in isotopic composition by less than 0.5 per cent.

Table 5

Effect of Fusion Loss on Lead Isotopic Composition

Sample No.	206/204 with Fusion Loss	206/204 with Borofluoride Fusion
2956	19.527	19.507
2974	19.701	19.779

These small differences (0.1 and 0.4 per cent) are probably due to a random sampling error caused by inhomogeneous distribution of uranium and thorium (and hence radiogenic lead) within the rock powder (see next section).

Farquharson (1968) indirectly examined the amount of U, Th and Pb remaining in the insoluble residues of a single sample by duplicate dissolutions both with and without borax fusion. He found insignificantly different contents and concluded that effectively all

the U, Th and Pb originally in the insoluble residues had been removed by the acid treatment. Further work is plainly required to resolve the situation, but the tentative findings suggest that the residue-fusion step may not be necessary.

B) Aliquotting Procedures

Non-uniform sampling is a particularly acute problem in lead geochronology since uranium and thorium are in part concentrated in minor phases.

Previous practice in this laboratory (Farquharson, 1968) was based on the work of Tilton et al (1955). In this, a single sample of the powdered rock was treated with hydrofluoric and perchloric acids, the residue was fluxed, and then the combined solutions were divided into three separate aliquots. One of these was reserved for quantitative lead determination, another for quantitative uranium and thorium measurements, and the third was used for lead isotopic analysis. This procedure ensured that the lead, uranium and thorium were representative of the same rock fraction, provided that the aliquotted solution was completely homogeneous. It transpires that this condition is not always fulfilled.

Gross discrepancies have been documented on four occasions where the sample was fused in sodium borofluoride and aliquotted immediately after the dissolution. In each case the solution was vigorously stirred before aliquotting, even although it appeared to be completely

clear; the first fraction was used for quantitative lead determination. Two anomalous effects were noted.

a) Isotopic fractionation within the mass-spectrometer yields enrichment in the heavy isotope. This effect is removed by a joint normalisation of 'unspiked' and 'spiked' run to a known spike ratio (see mass-spectrometry chapter). In most cases this normalisation reduces the 207/204 ratios of the 'unspiked' run to about 15.7 or less. With one of the four samples some reduction occurred, but not as far as this value; the other three moved in the opposite direction.

Table 6

Aberrant Normalisation Effects (Isotopic Ratios)

Sample Number	Raw 7/4	Normalised 7/4
2962b	15.850	15.791
2973	15.882	16.010
2974	15.784	16.247
2975	15.733	15.940

b) The lead content determined by isotope dilution on these samples was radically different from that obtained by X-ray fluorescence.

Table 7

Aberrant Concentration Effects

Sample Number	Lead (X.R.F.) µg./g.	Lead (I.D.) µg./g.
2962b	46.5	61.8
2973	21.6	41.6
2974	19.9	46.6
2975	28.7	46.8

Farquharson (1968) has shown that the first anomalous effect occurs where, compared with the unspiked run, the spiked run is differentially contaminated with a lead of less radiogenic composition than the sample lead. The degree of discrepancy is proportional to the amount of contaminant. Contamination of the unspiked run (with less radiogenic lead) with respect to the spiked run produces the opposite effect - ie. normalised 208/204, 207/204 and 206/204 values become obviously too low.

Systematic fallout to the degree required to explain the results (5 µg. or more) is out of the question, as four blank determinations performed at this time were consistently low; furthermore, accidental contamination could hardly be as specific as this for the spiked analysis. Abnormal cycling has also been observed in a sample where the residue was not fused (see section E), and occasionally after borax fusions. Farquharson found the same effect to a much larger extent. At times he needed 20 µg. of differential contamination to

explain his results. The most plausible explanation seems the following.

The first leachings during dissolution are presumably the radiogenic lead along cracks and grain boundaries, and the composition of the leached lead will progressively change from radiogenic to the true total-rock value. Hence absorption of lead onto one or more relatively water-insoluble chemical species at any intermediate stage will yield a heterogeneous, aqueous system. Since in each case the combination of fusion products and main sample was strongly heated for an hour to form a completely clear solution, it is quite probable that the heterogeneity is caused by differential absorption onto a colloidal sol. The aluminium oxide mentioned in the previous section is considered a primary constituent in sol formation. Although the exact nature of the process is not understood it is clear that a vertical zonation must exist in the aqueous solution and the uppermost fraction is relatively enriched in lead which appears to be less radiogenic than average.

These observations and their consequent interpretations led to the abandonment of aqueous aliquotting in favour of a different approach. Three separate dissolutions are now performed for each total-rock analysis. Lead concentration is determined on one of these, and uranium-thorium concentration on the second. The third is used for lead-isotope determination. The fractions for the unspiked and spiked analyses (still needed to correct for fractionation) were

separated near the end of the dithizone treatment stage. It is felt that the lead is truly homogeneously distributed at this stage. 'Sensible' cycling characteristics of all subsequent qualitative samples strongly supports this.

C) Separate Dissolutions, Early Spiking, and the Platinum Problem

If separate portions of rock powder are to be used for each analysis, then these portions must be large enough to be representative of the powder as a whole. The data of Kleeman (1967), who discussed the problem of representative sampling, permit us to estimate the likely errors involved. The approximate zircon concentration (0.05 per cent) in five of the rocks, determined by mineral separation, may be taken as a measure of the abundance of uranium-thorium-bearing accessory minerals. For a grain-size of less than 150 mesh (see sample preparation section) the approximate two-sigma relative sampling errors amount to three per cent and two per cent respectively for two and three gram samples. The effect of uranium and thorium in other positions in the rock (e.g. grain boundaries and cracks) should reduce these limits by a further unknown quantity. Hence uranium-thorium analysis should be accurate to about one or two per cent. As almost all the lead is included in common minerals the uncertainty of the lead concentration determined by separate dissolutions will be quite low (of the order of 0.2 per cent). The expected reproducibility of lead composition is exceedingly difficult to analyse as it depends on a wide range of compositions and

concentrations in various phases, which themselves vary in abundance by orders of magnitude.

These calculations suggested that the separate dissolution procedure should be reasonably acceptable. All isotopic compositions, and a series of lead and uranium concentrations, were subsequently measured using this procedure.

Samples were weighed into a platinum dish and a known amount of spike immediately added where relevant, in an effort to give the spike maximum opportunity to mix with the rock lead. Platinum was used in preference to Teflon because of its heat-conducting properties which allow a lower hot-plate setting. The use of Teflon resulted in a larger degree of sample baking with increase in the yield of the aluminium oxide, an undesirable consequence.

A series of quantitative determinations gave the following results.

Table 8

Aberrant Concentration Estimates Caused by Pt Dissolution Vessel

Sample Number	Concentration (X.R.F.) (µg./g.)	Concentration (I.D.) (Pt dish - early spiking) (µg./g.)
2955	16.5	20.9
2956	30.3	34.8
2959	19.0	23.3
2960	30.2	39.4
2962	46.5	56.8
2967	24.4	35.4
2968	10.8	15.2
2969	40.8	40.4
2973	21.6	28.2
2974	19.9	32.4
2975	28.7	30.2
2976	14.8	24.2

It is immediately clear that these isotope dilution results are never significantly lower than, and often very much higher than the X-ray results. The normalisation routine produced abnormal 207/204 ratios similar to those noted in the last section. As all samples were processed with exactly the same batches of reagents, the highly variable results can not be due to reagent contamination. Frequent accidental contamination of this order is entirely inconsistent with the experience gained from the blank determinations. It is conceivable that the small amount of nitric acid in the spike (equivalent to one drop of concentrated acid) and the hydrofluoric acid combined to form acid similar to aqua regia, which dissolved the platinum dish. The dish lost one milligram in weight during each dissolution (a similar amount to that lost when no spike was present). However, in order to have supplied the contaminant the lead content of the platinum would need to be about 20,200 µg./g., a value which is unreasonably high.

The following is a more reasonable explanation. The presence of spike lead produced unusual conditions in the early stages of dissolution in that there was a high lead content (much spike plus a little radiogenic lead) relative to other ions. This caused some lead to be absorbed onto the platinum before there was time for dissolution of the rock to appreciably affect conditions in the solution. This loss of spike with respect to rock lead, and radiogenic with respect to common lead, respectively, would cause an

overestimation of the sample lead, and give a false impression of contamination of the spiked run (loss of radiogenic lead produces the same effect).

To test this argument the two samples showing the worst discrepancy were processed with the same reagents in a similar manner as before. The only difference was the use of Teflon rather than platinum dissolution vessels.

Table 9

Effectiveness of Teflon Dissolution Vessel
(Pb concentration in μg./g.)

Sample Number	(Lead) X.R.F.	(Lead) I.D.
2967	24.4	24.5
2976	14.8	16.4

Sample 2967 agrees very well but 2976 is a little outside the normal error limits of about 0.8 μg./g. Both spiked runs, however, when normalised with previous unspiked analyses, cycle to closely similar 207/204 values within the normal mass-spectrometer error limits of $\pm$ 0.2 per cent (see table 10). These results have a twofold significance. Firstly, they support the use of Teflon dissolution vessels. They also show that the unspiked lead analyses performed in platinum may be considered reliable, in that radiogenic lead (or any non-representative lead for that matter) was not lost

preferentially to the platinum. It appears that the presence of the lead spike is necessary for significant lead loss into platinum.

Table 10

Normalised Isotopic Compositions Resulting From Use of Pt and Teflon Dissolution Vessels

Sample No.	206/204	207/204	208/204
2967'	19.872	15.717	40.335
2967*	19.853	15.695	40.258
2976'	19.290	15.656	39.279
2976*	19.313	15.685	39.374

' - Single dissolution in platinum, late aliquotting.

* - Unspiked from above normalised with a spiked analysis from dissolution in Teflon.

D) Volatilisation Method

Lead may be isolated by the Volatilisation technique of Masuda (1962) instead of the acid dissolution and fusion. Several experiments were undertaken to investigate the suitability of the method, using apparatus borrowed from J. A. Cooper. However, despite some promising indications it was not pursued because of an unexpected difficulty.

In this procedure the rock powder, intimately mixed with ultra-pure graphite, is heated at 1,000°C under vacuum in a fused-quartz container. Lead volatilised from the sample condenses on a water-cooled

'cold finger' and is then washed off with nitric acid and treated with the standard dithizone procedures.

It is most desirable to achieve the maximum extraction efficiency; different minerals will generally contain lead of different isotopic composition, and any selective volatilisation is likely to give an erroneous answer. For this reason the volatilisation technique has been applied for the most part to very young volcanic rocks (these are the only very young rocks at the surface) as hopefully, the lead in each mineral phase will have been the same at the time of crystallisation and will have had insufficient time to be significantly changed since then. This approach neatly sidesteps the problem of incomplete lead extraction.

The rocks involved in this study are about three hundred million years old, however, and each mineral will have a unique, distinct isotopic composition. Hence high yields are imperative. As a yield-test two rocks were analysed by this technique. One was a relatively coarse-grained porphyritic adamellite, the other a fine-grained andesite. X-ray fluorescence analysis had been performed on both. The yields were estimated from a measure of the lead in the residue of the adamellite (determined by A. J. Graham and S. R. Taylor using an MS7 spark-source mass-spectrograph) and an isotope-dilution measurement of the lead extracted from the andesite. The yield estimate was 70 per cent for the adamellite, and 80 per cent for the andesite. These yields are a little lower than ideal, but

surprisingly the compositions obtained agreed very closely with those obtained by wet chemistry. Only a spiked run was processed for the andesite, but it normalised with an acid-dissolution unspiked analysis to the same value yielded by the full acid-dissolution calculation. The adamellite (2962) composition is very similar by both methods (see next section). Not only do these results suggest that the volatilisation technique is a useful tool in the analysis of these rocks, but they also show again that selective loss of radiogenic lead into platinum does not appear to occur in unspiked dissolutions.

The volatiliser was not brought into routine use, however, because a slightly more acid rock (a rhyolite) which melted during extraction was accompanied by disintegration of the apparatus on cooling. It was found that the inner part of the pot had metastably converted to the high temperature polymorph, cristobalite, either from chance nucleation alone or calalyzed by vapour from the sample.

E) Replicate Analysis

Many of the problems encountered and the effects they have had on the results can be seen in the replicate analyses of sample 2962 (see figure 2). In this figure only normalised isotopic values are plotted; the un-normalised points would plot at the end of lines of slope 51° (fractionation lines; Doe et al, 1966) towards the top of the diagram and above it.

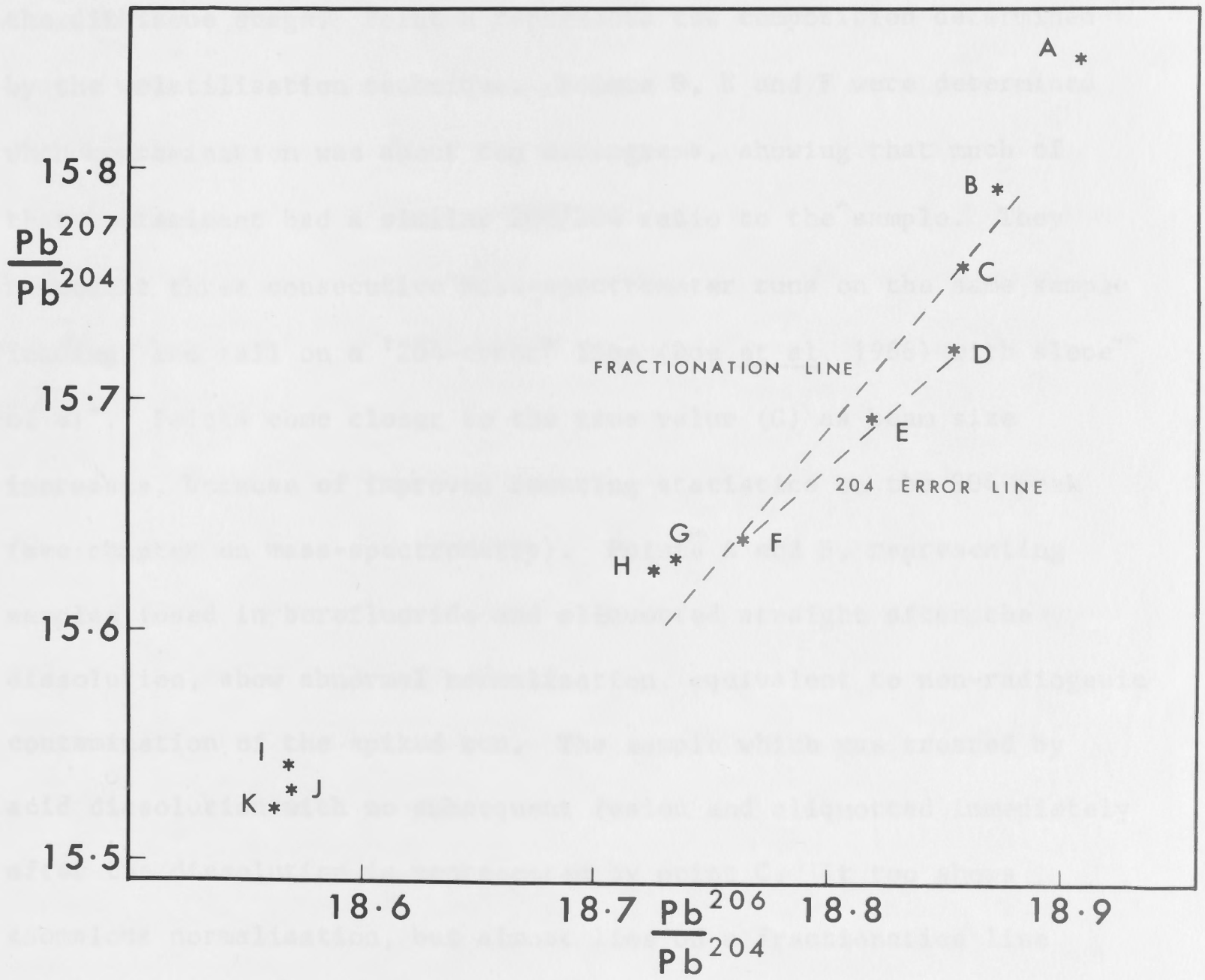

Figure 2. Replicate analyses of sample 2962.

The point G is believed to be close to the correct value. It is the result of a HF-$HClO_4$-$NaBF_4$ treatment followed by aliquotting at the dithizone stage. Point H represents the composition determined by the volatilisation technique. Points D, E and F were determined when contamination was about ten micrograms, showing that much of that contaminant had a similar 206/204 ratio to the sample. They represent three consecutive mass-spectrometer runs on the same sample loading, and fall on a '204-error' line (Doe et al, 1966) with slope of 41°. Points come closer to the true value (G) as beam size increases, because of improved counting statistics on the 204 peak (see chapter on mass-spectrometry). Points A and B, representing samples fused in borofluoride and aliquotted straight after the dissolution, show abnormal normalisation, equivalent to non-radiogenic contamination of the spiked run. The sample which was treated by acid dissolution with no subsequent fusion and aliquotted immediately after the dissolution is represented by point C. It too shows anomalous normalisation, but almost lies on a fractionation line passing through point G, suggesting that non-representative aliquotting rather than the fusion has produced the dominant compositional difference. If the latter applied, a horizontal difference component would also be expected.

A puzzling and somewhat disturbing feature is the cluster of points I, J, and K (fused in borax). These represent analyses on a different crushing of the same rock. Points J and K were determined

from one unspiked analysis, normalised with two separate spiked runs (one from the same dissolution as the unspiked). Point I represents a completely separate dissolution. If these points represent the true compositions of the lead in this crushing then the rock possessed most unusual characteristics with respect to the other rocks in the area (and also to the second crushing of the same rock). It is considered, in the light of past experience, that unusual cycling characteristics due to inhomogeneous aliquotting after the borax dissolution have produced this effect.

The anomalous normalisation shown on this diagram is comparatively mild. The scatter on the diagram still serves to show, however, that the results obtained are critically dependent on the techniques used.

WHOLE-ROCK URANIUM - THORIUM METHOD

The basic chemical procedure used in this laboratory was developed by Farquharson (1968) from the method outlined in Tilton et al (1957). Uranium and thorium are purified simultaneously as a single chemical sample. In this study it was possible by means of a well-type gamma scintillation counter to monitor the thorium spike partitioning at each extraction. This revealed some unusual results which have occasioned further changes to the method.

The dissolution procedure is identical to that for lead. Spiking in the Teflon dissolution vessel is recommended. After dissolution is complete the aqueous solution is heated strongly, but not boiled, for about an hour to remove dissolved carbon dioxide.

Filtered ammonia gas is added to the solution until the R_2O_3 group (iron, aluminium hydroxides etc.) precipitates. Both uranium and thorium are absorbed on the precipitate provided carbon dioxide is absent. As much as possible of the aqueous phase is separated by multiple centrifuging, and discarded. The residue is dissolved in about 2 ml. of concentrated nitric acid and made up to 40 ml. with aluminium nitrate solution. This is transferred to a separating funnel, and 40 ml. of hexone added. Vigorous shaking for five minutes is reputed (Tilton et al, 1957; Farquharson, 1968) to assist a 'salting-out' effect which causes uranium and thorium to be extracted into the hexone.

The somewhat different experience of the author is probably not typical. In every case a gel formed at this stage (Farquharson mentions occasional emulsions) and prolonged centrifuging was required to break it. The gel separated into layers of aluminium nitrate (lower) and hexone (upper) divided by a zone of gelatinous material considered to be the aluminium oxide discussed in the lead section, as it too was brought down in a nitrate environment. The partitioning of the thorium between the phases was found to be unfavourable and somewhat variable (50 per cent to virtually nothing in the hexone). Thorium was firmly held in the aluminium nitrate and gel and further shaking with fresh hexone did not induce further extraction (even when more nitric acid was added). As the thorium yield can be so

drastically reduced in this step, it is important that subsequent loss be reduced to an absolute minimum.

The hexone is collected in a beaker and the other phase (or phases) is discarded. After thorough cleaning of the funnel the hexone is returned together with ten ml. of water. Brief shaking causes the uranium and thorium to extract into the water. This is collected in a beaker and evaporated almost to dryness.

The sample is taken up in 20 ml. of saturated ammonium nitrate with swirling and slight heating, and transferred to the cleaned funnel, to which an equivalent volume of fresh hexone has been added. This is vigorously shaken for five minutes to extract the uranium and thorium once more into the hexone (any aluminium remains in the aqueous phase). As the thorium recovery is only 40 per cent in this step, it is repeated with a fresh aliquot of hexone. The hexone fractions are added together and shaken with ten ml. of water in a clean funnel, whereupon uranium and thorium are back-extracted into the water. The water is collected and evaporated to dryness in a small beaker. Two drops of nitric acid are added to decompose any organic material. After further evaporation to dryness the sample is taken up in one drop of N/10 HNO_3 and transferred to a two ml. centrifuge tube. A single drop of ammonia is added to precipitate the diuranate, which is in turn partially converted to the phosphate by adding a drop of phosphoric acid and swirling vigorously. The

precipitate is washed six times with 70 per cent ethanol and loaded in a small drop of water onto the side filaments of a mass-spectrometer bead.

Reasonably strong uranium and thorium ion beams were obtained from all samples. Even the sample in which virtually all the original 100 µg. of thorium was lost in the first extraction produced a strong ion beam. The scintillation counter, with 95 per cent precision limits of $\pm$10 µg., actually indicated - six µg. of thorium in this case. This indicates that a yield of a few micrograms of thorium is sufficient for satisfactory results.

Six isotope dilution analyses were performed. Identical crushings of the same samples were also analysed for comparison by X-ray fluorescence and γ-ray spectrometry (see table 11). Only uranium and thorium values determined by X-ray fluorescence are used in the geological interpretation; the other two methods were employed to validate the use of the X-ray results.

The uranium results are reasonably consistent, with the γ-ray results tending to be lowest, the isotope dilution highest. All X-ray results (excepting 2967) are about one µg./g. lower than the corresponding isotope dilution value, a significant difference (see X.R.F. and Uranium-Thorium Reproducibility sections).

Table 11

Comparison of Uranium - Thorium Determinations

Thorium

Sample No.	γ-ray	X.R.F.	I.D.
2960	59.3	53.7	56.8
2961	14.3	17.2	17.2
2964	19.6	21.1	20.8
2967	-	55.7	44.2
2969	46.9	47.1	47.3
2971	26.1	24.6	19.0

Uranium

Sample No.	γ-ray	X.R.F.	I.D.
2960	11.4	13.1	14.4
2961	3.2	3.6	4.8
2964	6.1	6.0	6.9
2967	-	6.7	6.7
2969	10.6	11.5	12.4
2971	3.7	2.6	3.4

Two of the isotope dilution thorium analyses (2967, 2971) are distinctly low. These two rocks were dissolved in a platinum dish; dissolution of the other four was in Teflon. It seems evident, therefore, that the platinum plays a significant role. Any explanation must invoke some mechanism which involves the platinum surface and at the same time a selective removal of sample thorium relative to spike. It seems almost impossible to envisage anything less than a two-stage process for this. As postulated for the lead spike some thorium spike must have been absorbed onto the platinum in the early stages of the dissolution. Certain of the remaining

thorium, with an anomalously high sample to spike ratio was then strongly absorbed onto some particulate matter.

The MS7 measurement (see the fusion in the whole-rock lead section) and counting (this section) have together shown that Al_2O_3 is the end product of this analytical step, and that it strongly traps thorium and lead. With changing conditions (possibly the oxidising environment of the perchloric acid) the spike migrated out of the dish and back into solution. The thorium absorbed on the particulate matter was not subsequently released, thus enriching the solution in spike with respect to sample thorium and giving an anomalously low value. The other four isotope dilution results are encouraging.

Although the isotope dilution method is potentially much more precise than the other two it has one definite disadvantage in that it requires extensive chemical processing. The implications of some of this may not yet be properly understood. For example hydrofluoric acid may cause some immediate generation of uranium hexafluoride (extremely volatile). This sort of mechanism could contribute to the general trend of uranium results observable in the previous table. The γ-ray and X-ray fluorescence methods do not require any chemical processing; unfortunately they suffer from inferior counting statistics.

WHOLE-ROCK RUBIDIUM - STRONTIUM METHOD

The standard techniques used in this department, based on the work of Aldrich et al (1956) were followed. These have been described in Compston et al (1965). 0.5 g. of sample is treated overnight with ten ml. of cold hydrofluoric acid in a platinum dish. This is then heated to dryness, and five ml. of HF solution and five ml. concentrated $HClO_4$ are added. After evaporation to dryness, the sample is dissolved in 30 ml. of 2.5 N HCl and completely transferred to a tared pyrex beaker. Appropriate amounts of the solution, to provide approximately 7.5 µg. of Sr and about 15 µg. of Rb, are separately aliquotted into pre-spiked beakers, containing 0.4 micrograms of Sr^{84} spike and ten micrograms of Rb^{87} spike respectively. After evaporation to dryness, the aliquots are taken up in five ml. of HCl (2.5 N for Sr; 1 N for Rb), and concentrated by elution with HCl of the same respective strengths through cation-exchange columns. The same resin, Dowex 50W-X8, 200-400 mesh, is used for both elements. The samples are evaporated to dryness, taken up in one drop of water, and loaded onto the side filaments of separate triple-filament assemblies.

Compston et al (1965) and Chappell et al (in press) claim a contamination level of 0.055 micrograms of strontium and 0.011 micrograms of rubidium per analysis.

X-RAY FLUORESCENCE ANALYSIS

All uranium, thorium and lead values used for geological interpretation in this thesis have been determined by X-ray flourescence analysis under the supervision of Dr B. W. Chappell, of the Geology Department of this University.

He has converted his instrument, a Philips model PW1220, to a fully automatic design, on which it is now possible to determine eight different elements on 108 samples without supervision.

The analytical procedure is discussed in Norrish and Chappell (1967). The finely-ground sample was pressed into pellets (about two grams of powder) backed by compressed boric acid; duplicates were made where possible. At the present level of uncertainty no significant difference (see following page) was detected in the uranium, thorium or lead content of the duplicate pellets.

Operating conditions were as follows;

Table 12

Operating Conditions of X.R.F. Spectrometer

	Lead	Uranium	Thorium
X-ray tube:	with molybdenum anode, operating at 100kV, 20mA.		
Primary collimator:	160 μ	160 μ	160 μ
Analysing crystal:	LiF(200)	LiF(200)	LiF(220)
Detector:	Scintillation detector operating with a 0.8 - 2.2 volt window.		
Analytical line:	$L\beta_1$	$L\alpha_1$	$L\alpha_1$

Various corrections were applied to the raw data. Drift in machine conditions was accounted for by normalisation to a standard at the beginning and end of each set of three samples. Corrections were made for interference from adjacent spectral lines which are very minor for these elements. Mass absorption corrections were determined by direct measurement. An automatic electronic device compensated for the 'dead time' of detector and following circuits.

Background measurements were made on both sides of the peak position. Counting times were, 100 seconds for background, 200 seconds for the peak. Each pellet was measured twice for lead and thorium, four times for uranium because of the proximity to the detection limit for these samples. The statistical lower limit of detection for these elements under these conditions may be estimated from the formula given in Chappell et al (in press)

$$\text{L.L.D. (2 sigma)} = 2.83/m\sqrt{(Cb/Tb)},$$

where m = counts per second per μg./g., Cb = average background counts per second, and Tb = time on background. This lower limit also corresponds to the error limits of each sample analysis, which are, at the 95 per cent confidence level

$$\text{Uranium} = \pm 0.5\ \mu g./g.$$

$$\text{Thorium} = \pm 0.6\ \mu g./g.$$

$$\text{Lead} = \pm 0.7\ \mu g./g.$$

A consequence of the above equation is that achievement of significant improvement in the precision of these results would demand much

longer counting times under these machine conditions. For example, to improve the uranium precision to ±0.125 μg./g., 128 standard 200 second counts would be needed for each sample. Thus parity with isotope dilution determinations (see uranium and thorium reproducibility section) will only be achieved by alteration of operating conditions to increase the count rate - concentration ratio.

Rubidium, strontium and yttrium were also determined by X-ray fluorescence on this equipment (Rubidium and strontium were subsequently analyzed by isotope dilution) using similar techniques and the following machine conditions.

Table 13

Operating Conditions for X.R.F. Spectrometer

	Rubidium	Strontium	Yttrium
X-ray tube:	with molybdenum anode, operating at 100 kV, 20 mA.		
Primary collimator:	160 μ	480 μ	480 μ
Analysing crystal:	LiF(200) in each case.		
Detector:	Scintillation detector operating with window between 0.8 and 2.2 volts.		
Analytical line:	Kα	Kα	Kα

Semi-quantitative determination of tin in the ore specimens was performed by placing the mounted polished sections themselves in a Philips model PW1540 spectrometer and measuring the resulting

fluorescence. Measurements were made simply by scaling peak and background and comparing the nett height to that of a cassiterite standard. It is estimated that this crude procedure can detect about 0.1 per cent Sn, and lower values are reported as not significant in the appendix. Operating conditions were as follows:

Table 14

Operating Conditions for Tin Determination on X.R.F. Spectrometer

X-ray tube:	chromium, operating at 50 kV, 32mA.
Primary collimator:	480 μ
Analysing crystal:	LiF(200)
Detector:	Measured under vacuum using a flow proportional counter operating with window between 0.15 and 0.4 volts.
Analytical line:	$L\beta_2$

γ-RAY SPECTROMETRY

The method followed was outlined by Heier et al (1965). The instrument consisted of a five inch x four inch Tl-activated NaI crystal, coupled with a 200-channel model 34 - 8 R.I.D.L. pulse-height analyser with typewriter readout. Uranium was determined by means of the 1.76 MeV Bi^{214} peak, thorium from the 2.62 MeV Tl^{208} peak and potassium the 1.47 MeV K^{40} peak. Error limits for replicate analyses of six standard rocks are given by Morgan and Heier (1966).

α-PARTICLE COUNTING

Selected galena samples were tested for α-activity using a scintillation counter described by Richards et al (1966c). All samples were finely ground by hand in an agate mortar and placed on a demountable stainless-steel tray. The detector involved was a Du Mont photomultiplier of diameter 33 mm., type 8EM, with a Zn(Ag)S phosphor. Background corrections were generally determined after every second run upon the empty tray. Individual measurements (both sample and background) were made for at least 24 hr.

Mass-Spectrometry

GENERAL PROCEDURES

Four (Sr, Pb, U, Th) of the five elements determined by mass-spectrometry were analysed with a twelve-inch radius, sixty-degree sector mass-spectrometer manufactured by Nuclide Analysis Associates. This instrument operates at 6kV accelerating voltage and has a series of vacuum locks to permit rapid sample introduction. Although the instrument incorporates an electron multiplier, this is not used for routine work. Rubidium analyses were performed on a Metropolitan-Vickers MS2-SG instrument, a six-inch radius, ninety-degree sector mass-spectrometer with 2KV accelerating voltage and an isolation valve between the analyser and ion chamber. All Rb measurements were made with a 10^{11} ohm leak resistor.

All elements were measured by solid-source thermal-ionisation techniques with rhenium filaments; single-filament procedures were

used for lead, triple-filament for the other four elements. The singly-changed metal ions were used in the analysis of all elements. Data, which were recorded both in graphical form and as digitised output, were collected from sets of alternate measurements on isotope pairs. Fast (five sec.) magnet-switching was used for Rb, voltage-switching for Sr (Arriens and Compston, 1968) and Pb was measured by magnet-switching. Because of the slow magnet response on the 12 inch machine a twelve-second delay was allowed between peaks one mass unit apart, and 20 seconds for peaks of two mass-units difference during lead analysis; integration time was four seconds in all cases. Furthermore, a ten-minute 'magnet-cycling' procedure was required before the beginning of a run to obtain a stable hysteresis loop. In the later stages of this study a field controller utilising a Hall-effect Probe was built into the mass-spectrometer. By specifying magnetic field rather than current, a much quicker response time was obtained and a delay time of eight seconds was adequate for all ratios, irrespective of mass separation. Automatic peak-switching is also incorporated with the field controller. All U and Th measurements were taken with fast magnet-switching, using the Hall-effect field controller.

Arriens and Compston (1968) have described the data-collection procedure for Sr. Ion beams of 6×10^{-11} amp. were generally obtained from side filament settings of 1.2 amp. and 4.0 amp. centre

filament current. Under normal conditions data was not taken until the Rb^{85} had fallen to less than three per cent of the Sr^{87} peak. This ensured that Rb^{87} was less than one per cent of Sr^{87}.

Rb measurements were made with a side filament current of about 0.8 amp. and a centre filament current of approximately 3.4 amp. The resultant ion beams were about 10^{-10} amp.

The procedures used for U and Th in this laboratory have been described by Farquharson (1968). For U the approximate filament temperatures were: centre filament, six amp.; side filament, uranium emission began at 2.5 amp., and the beam was measured at 3.5 amp. Thorium appeared at a slightly higher temperature than the initial uranium beam, and, in contrast to the results of Farquharson, was found to be compatible with reasonably big uranium ion intensities. For thorium measurement the side filaments were generally increased to about four amp. and the centre increased by 0.2 to 1.0 amp., but in two cases uranium was determined after thorium. Beam size varied from 0.2 to 1.5×10^{-11} amp. for uranium, and 0.3 to 3.0×10^{-12} amp. for thorium. It was thus not necessary to use the electron multiplier.

The procedures used for Pb were slightly more complex than the previous elements. After introducing the sample into the machine it is 'outgassed' slowly in the innermost vacuum lock. In this process water, ammonium nitrate, and oxalate breakdown products (water, CO and CO_2) are liberated sequentially. It is imperative that this

step be performed slowly to avoid mechanical loss of sample. The source-carriage is then removed from the mass-spectrometer, for replacement of the electrode box (to remove hydrocarbons - see section on hydrocarbon interference in the lead spectrum) before it is reinserted (in stages) into the ionisation chamber. The filament current is slowly increased until lead emission begins (about 1.6 amp.). Data are generally taken after a beam build-up period of about one hour (at about 1.8 amp. filament current). Total beam intensity generally varies between 3×10^{-11} and 1×10^{-10} of an amp. Alkali beams, provided they are of comparable size or smaller, apparently have little effect on beam size or stability.

DATA HANDLING

The raw machine data were treated in much the same manner for all elements since alternate isotope-pair measurements were incorporated in all procedures. Fewer corrections were applied to U, Th, and Rb data than to Pb and Sr data, however, as the former involve the measurement of only one isotopic ratio.

In the case of lead, 15 ratios are measured for each peak-pair set. Data is collected in the following order:

Twenty Zero measurements, to estimate the linear background under the peaks.

A set of 208/206 ratios, then the 206/204 ratio measurements, followed by another zero measurement.

Then 207/206 ratios, preceding the final set of 208/206 ratios, followed by the last linear zero measurement.

An estimate of the lag in electrometer response is obtained by making a 'Dynamic Zero' (Arriens and Compston, 1968) correction. This entails switching alternately from the 208 peak to background with the same time-sequence as used in the ratio measurements. The augmented background thus obtained is combined with the other 'linear zeros' in estimating a correction to the observed ratios. A spectrum of the peaks is then drawn by slow magnet-scanning. The 'tail' corrections inferred from this scan are also applied as corrections to the observed ratios.

This order of ratio measurement is based on the following considerations. Firstly, the normalisation procedure assumes that all ratios refer to the same degree of fractionation. If this is changing over the course of a run, all ratios need to be corrected to a 'common time' value. To achieve this, one of the ratios needs to be determined both in the beginning and at the end of the run. Under most circumstances the 208/206 ratio is associated with the biggest beam, and should provide relatively accurate data at the end in the event of significant within-run decay. Secondly, as the 204 peak is always the smallest, the 206/204 ratio is generally the least accurately determined of all sets. It is thus measured as soon as possible to utilise the maximum beam size. A correction is made to the raw data to compensate for curvilinear decay (or rise) of the

beam. Aberrant ratios are excluded by a procedure incorporating rejection limits of 2.2 S.D. and one per cent coefficient of variation. The treatment of raw Sr data, which is similar to that for Pb is described in Arriens and Compston (1968).

Only few corrections were applied to the Rb, U and Th data as the analysis of each of these elements involved the measurement of a single comparable-size isotope-pair. Corrections were made for background, beam curvature, and anomalous ratios.

DATA PROCESSING

The computer program for processing all machine output, as well as that for regressing the Rb - Sr results, was written by P. A. Arriens of this department. The Pb normalisation and the special Pb tail-correction subroutines were designed and written by J. R. Richards.

SPECIAL PROBLEMS

Uranium - Thorium Reproducibility

The contamination level for U and Th was shown, in the blank and purification section, to be negligible. Other errors, besides unusual chemical affects, are due to measurement error and fractionation uncertainties. The 95 per cent confidence limits for the internal mass-spectromectric precision of the mean ratios of six samples (15 individual ratios measured in each case) averaged 0.13 per cent for uranium and 0.11 per cent for thorium. These uncertainties probably result from measurement error alone as isotopic fractionation should

be negligible over the limited time of data collection (six minutes). It is not possible to make fractionation corrections with the U and Th spikes in current use; an additional isotope would need be incorporated in each spike solution before this could be done. Hence the uncertainty resulting from different degrees of isotopic fractionation is poorly understood. No replicate analyses were made in this study as the isotope dilution determinations of this study have been used solely as a check for the X-ray fluorescence results; the latter are used for all geochemical interpretations. P. H. Reynolds (this laboratory; personal communication) reports two per cent agreement for a duplicate U analysis on a single sample. Farquharson (1968) arrives at a figure of less than one per cent from only one duplicate U measurement (less than two per cent for Th) and the considerations of Crouch and Webster (1964). He says 'if the calibrators and the unknowns have similar isotopic compositions, then with standard machine conditions (providing similar expected fractionation), fractionation errors tend to cancel out'. It would appear, though, that standard machine conditions are unlikely to be attained for both calibration and normal runs. The latter would be expected to contain a higher level of interfering ions. In the case of Th, in particular, Farquharson states that calibration runs yielded strong beams, but only weak beams showing considerable variation in size were obtained for the sample rock

runs. Furthermore, oxide beams were observed in the Th calibration runs but never during routine Th analysis.

At this stage, then, the reproducibility of U and Th isotope-dilution analyses must remain somewhat speculative. The tentative value of Reynolds for U agreement is probably the most realistic appraisal at present.

Hydrocarbon Interference in the Lead Spectrum

During the first half of this study, anomalous peaks were often noticed in the region of the lead spectrum. These were represented by a dominant 215 peak, a smaller one at mass 205 and other minor peaks. When present in the unspiked run, fractionation corrections yielded absurdly low 206/204, 207/204 and 208/204 values; if in the spiked run, the opposite effect was obtained. This behaviour would be expected if the contaminating species were also represented by a peak at 204 under the least abundant lead isotope. The interfering compound is thought to be a hydrocarbon since the dominant odd-mass peaks are characteristic of this group (Beynon, 1960, p.330). It has a spectrum which is distinct from the silicone contaminant previously reported in gas-source studies (Slawson and Russell, 1963).

Evidence of the nature of the hydrocarbon contaminant was gleaned from three experiments. A tiny hydrocarbon spectrum which was observed immediately before lead emission in one run confirmed that a 204 component was present. In this instance it was only one quarter

the size of the 205 peak; comparable-size peaks were seen under the other lead mass units. The hydrocarbon peaks generally increased as the lead beam intensified. An effort was made to correct for the anomalous 204 component by using a constant proportion of the size of mass 205. However, the degree of anomalous normalisation was found not to be proportional to the peak-height. Moreover, the 215/205 ratio was monitored during several runs and was found to vary significantly. Thus two or more chemical species were probably present.

In the second experiment the first of two consecutive bead-loadings of the same sample was found to produce a hydrocarbon beam while the second did not. This means either that the hydrocarbons were heterogeneously distributed in the sample as very coarse particles or that they were not derived from the sample at all. In the latter case, the bead, electrode box or mass-spectrometer itself would be responsible.

Thirdly, it was found that the hydrocarbon beam is extremely insensitive to machine focussing, suggesting a source of emission other than the filament. As most of the focussing probably occurs between the filament and the electrode box (S. W. Clement - personal communication) it appears that the hydrocarbons were being emitted either from the box itself or a region beyond it. Every time hydrocarbons were subsequently encountered, the box was replaced with a freshly-cleaned one, invariably removing the hydrocarbons.

It is difficult to envisage how the second box was never contaminated when the first often was, especially when both were cleaned simultaneously. The only suitable explanation is that the hydrocarbons were transferred from the sample to the box in the early stages of a run. Secondary emission occurred with lead-ion bombardment yielding a beam which essentially could not be focussed. It would appear that the hydrocarbons are formed by incautious degassing in which some of the oxalate material itself, or an included organic impurity on the filament, is blasted onto the box, from which secondary emission begins with the onset of the lead beam. Certainly no hydrocarbon beams are encountered if the box is changed immediately after outgassing. The primary source is still uncertain, but the hydrocarbon problem has been eliminated by changing the electrode box for every sample. This procedure removed the possibility of obtaining an unobserved contamination during part of the data collection, and yielded an interference-free background for the lead spectrum.

Lead: Fractionation Effects and Data Reproducibility

One of the most important sources of error in mass-spectrometric analysis is isotopic fractionation. Until recently gas-source mass-spectrometry was producing results more consistent than those obtained by solid-source procedures (Richards, 1967), although it had been suggested that the combined effects of viscous flow to the ionisation chamber and molecular flow to the pumping system could

give rise to a systematic error (Whittles, 1964). The advantage of the solid-source technique, on the other hand, is that it can be applied to smaller samples and hence to a greater range of geological problems. Thus, during the last few years attempts have been made to increase the precision of the solid-source method.

Doe has shown that increased precision can be obtained by using a fixed filament material (Doe et al, 1965) and by maintaining on the filament a constant ratio of ammonium nitrate 'cement' to lead (Doe et al, 1967). Cooper and Richards (1966b) replaced the more traditional lead sulphide with lead oxalate, which breaks down on heating in vacuum to a mixture of relatively involatile lead metal and oxide. The increased ionisation to evaporation ratio gives rise to larger beams from which more precise data can be obtained (by reducing measuring errors). Even though the single filament approaches of both Doe, and Cooper and Richards, have yielded more precise results they are still susceptible to fractionation uncertainties. Two separate approaches have been devised to overcome this problem.

Catanzaro (1967, 1968, --- et al, 1968) uses a standardised triple-filament procedure coupled with a machine-bias normalisation. The bias correction is determined by running standards of known composition in an identical manner to routine samples. Catanzaro attributes the high precision of this method to the triple-filament method itself rather than to the fairly rigorous time and temperature

controls. Poor results are associated with small beams and high measurement errors.

An alternative approach has been outlined by Compston and Oversby (in press) in which variable fractionation effects are corrected by use of a lead 207/204 double spike (commonly referred to as 'the spike'). Two mass-spectrometer runs are required. Firstly the sample lead is measured alone. In the second run the sample is mixed with the spike (which is accurately calibrated and highly enriched in the 207 and 204 isotopes) and the composition of the mix is determined. By combining the two analyses it is possible to make corrections for isotopic fractionation in each by using an iterative method and assuming a mass dependency for fractionation errors. If the weight and concentration of added spike are also known it is possible to calculate the amount of sample lead in the mix. Compston has shown that results obtained by this method on the C.I.T. standard agree to within experimental uncertainty with those obtained by Catanzaro (1968) using the triple-filament technique.

In this study the double-spike technique has been used to remove the effects of mass-dependent fractionation from the unspiked analyses. All samples have been loaded as oxalate and run on a single rhenium filament.

Extended Analyses. The nature of the isotopic fractionation occurring in the mass-spectrometer was examined by measurement on a strongly emitting sample over an extended period. About 200 μg. of lead were loaded to ensure a strong ion beam for sufficient time, and

the thermal conditions were not changed from the first measurement to the last. This is similar to an experiment described by Doe et al (1967), in which no systematic change in ratios could be detected. The data now reported were collected over a much longer time interval; the experiment was performed in duplicate. The term 'run' in the text will refer to the results obtained from a single mass-spectrometer loading. Each run is composed of one or more data-sets; ie. run A comprises eight data-sets, whereas run B comprises ten.

It can be seen from figure 3 that both beams decayed by different amounts during the course of the measurements. Whereas run A decreased to less than three per cent of its original height, run B was still considerably over 30 per cent. Although neither line can be represented by a simple exponential function, they may well be treated as the sum of different exponentials.

Figures 4, 5 and 6 show the time-variation of 206/204, 207/206 and 208/206 in both runs. Vertical bars denote 95 per cent confidence limits. No fractionation effect is visible above the scatter in the 206/204 diagram, although the scatter is considerably greater than the precision within each data-set. The other two graphs show a general increase with time. A significance test, incorporating the residual sum of squares and the F distribution, indicates that the points of run A (both ratios) are best fitted by a curve, rather than a straight line; those in run B (both ratios again) are not significantly curved

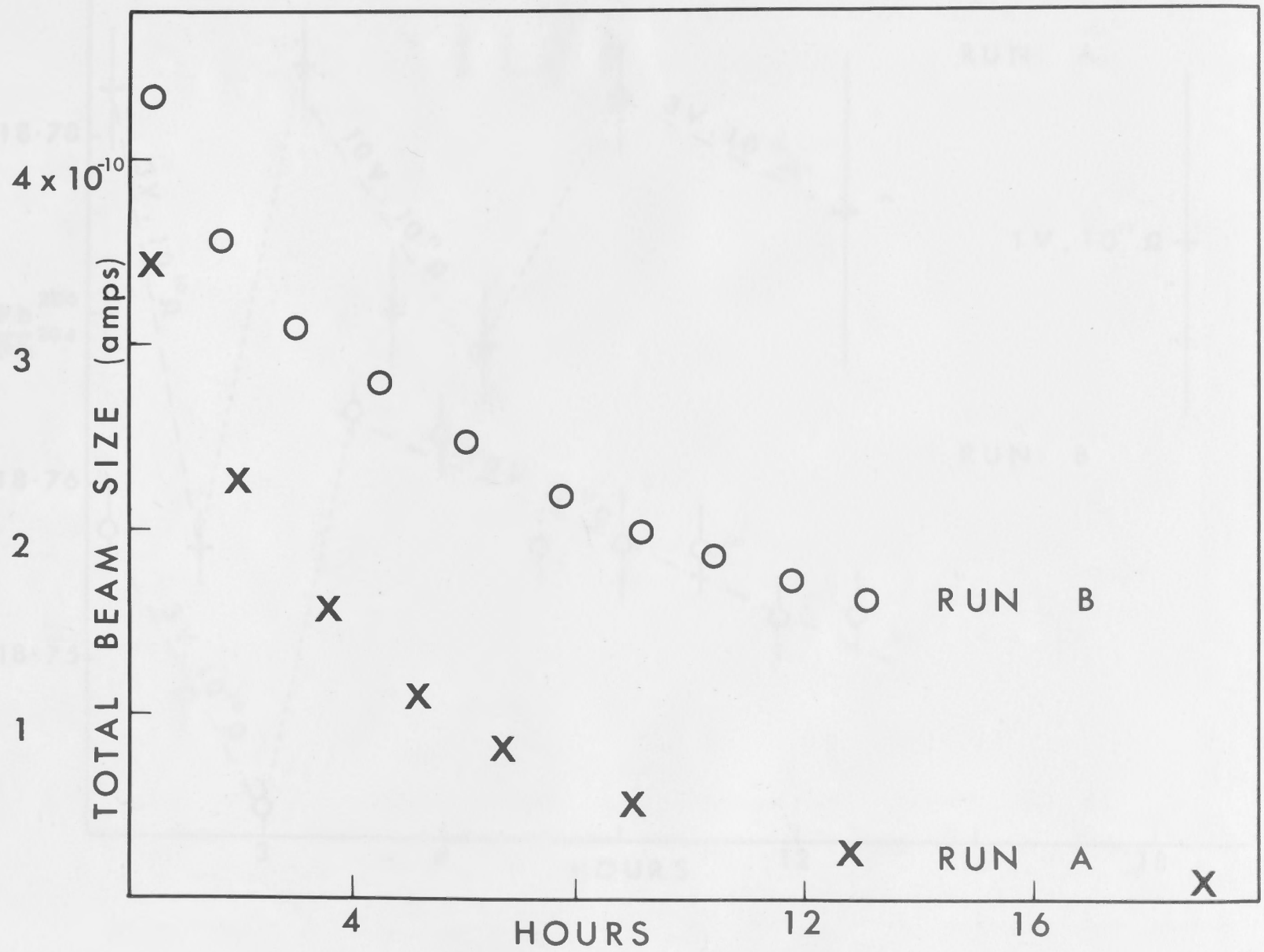

Figure 3. Time variation of total beam size in extended analyses.

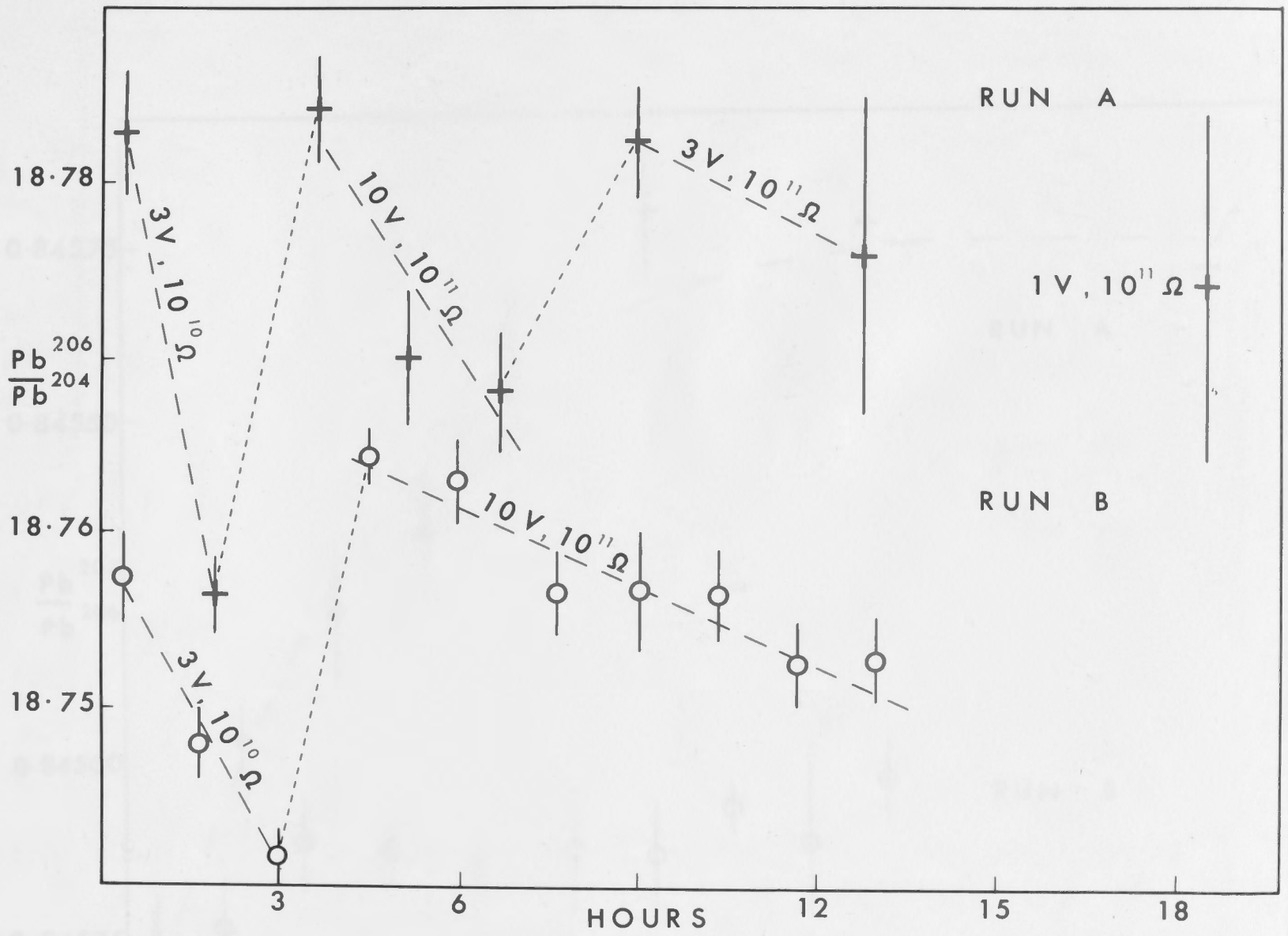

Figure 4. Time variation of Pb^{206}/Pb^{204} in extended analyses.

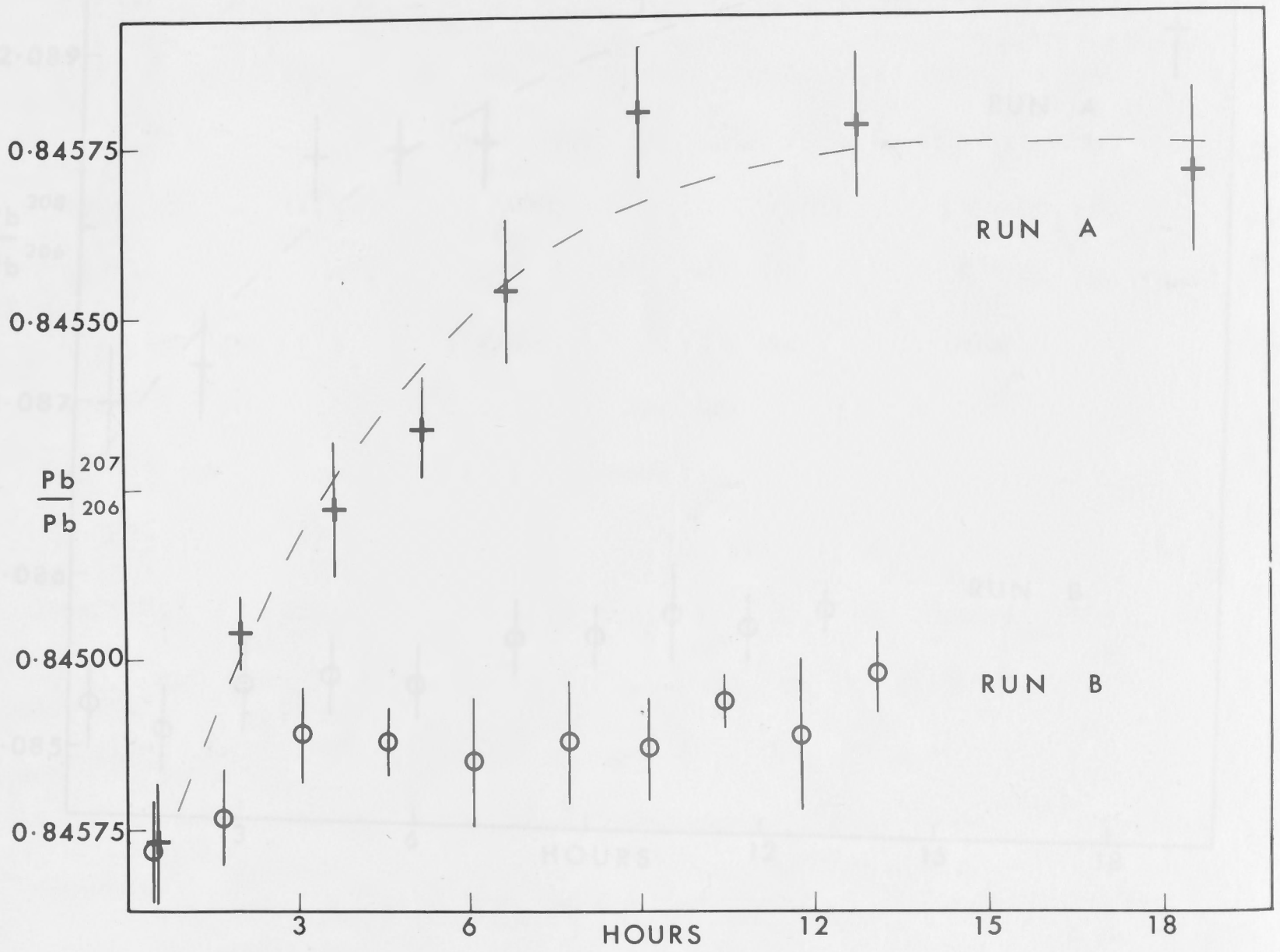

Figure 5. Time variation of Pb^{207}/Pb^{206} in extended analyses.

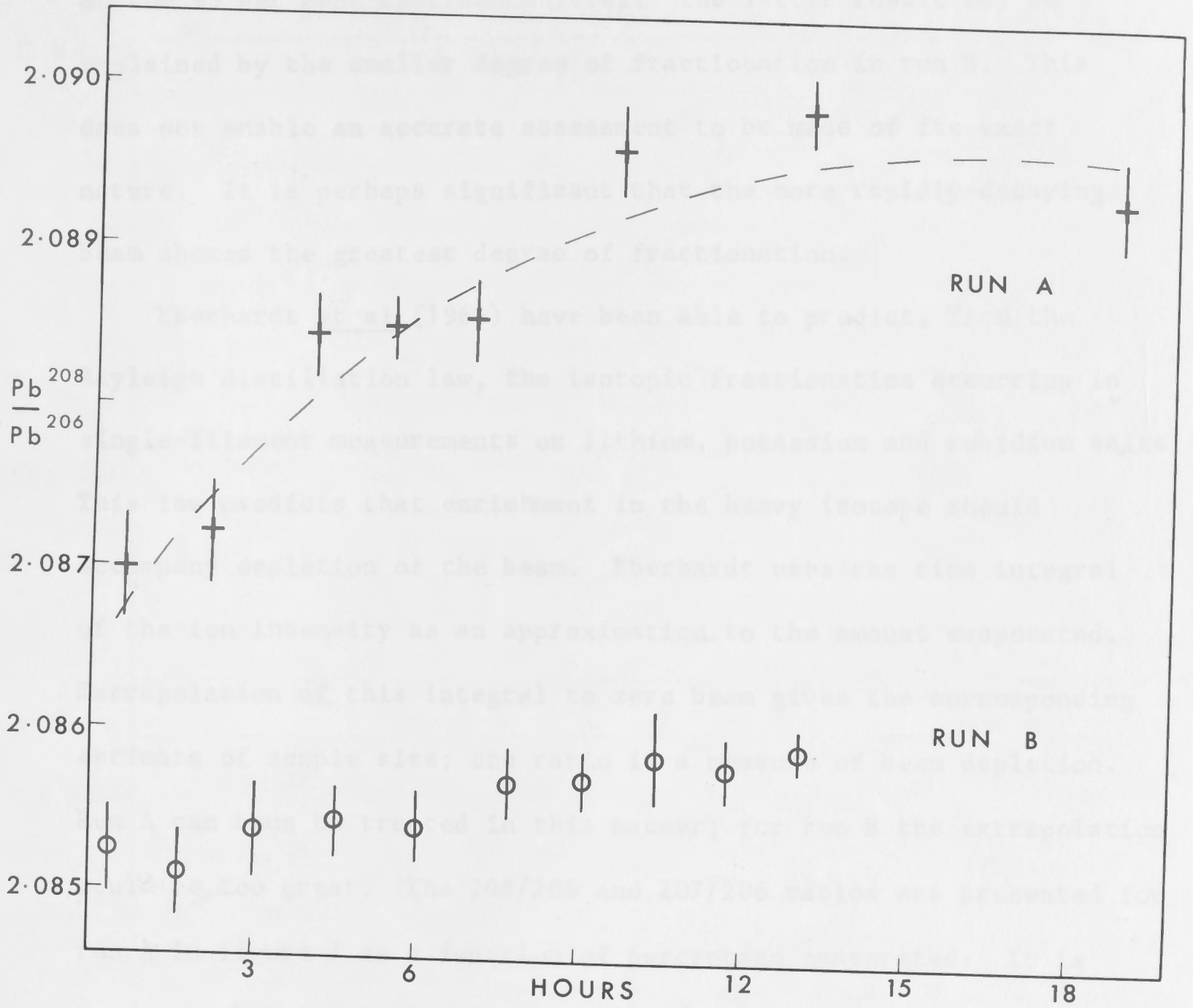

Figure 6. Time variation of Pb^{208}/Pb^{206} in extended analyses.

at the 95 per cent confidence level. The latter result may be explained by the smaller degree of fractionation in run B. This does not enable an accurate assessment to be made of its exact nature. It is perhaps significant that the more rapidly-decaying beam showed the greatest degree of fractionation.

Eberhardt et al (1964) have been able to predict, from the Rayleigh distillation law, the isotopic fractionation occurring in single-filament measurements on lithium, potassium and rubidium salts. This law predicts that enrichment in the heavy isotope should accompany depletion of the beam. Eberhardt uses the time integral of the ion intensity as an approximation to the amount evaporated. Extrapolation of this integral to zero beam gives the corresponding estimate of sample size; the ratio is a measure of beam depletion. Run A can thus be treated in this manner; for run B the extrapolation would be too great. The 208/206 and 207/206 ratios are presented for run A in figure 7 as a function of percentage evaporated. It is apparent that in the later stages the isotopic ratios, instead of progressively increasing, tend to level out, and perhaps even decrease. This representation is not particularly satisfactory, since it effectively compacts the scale and hence obscures the results at high evaporation percentages. It does, however, serve to show that the fractionation is not obeying the Rayleigh law. In figures 5 and 6, with abscissa linear in time, the representation of the fractionation is much more clear.

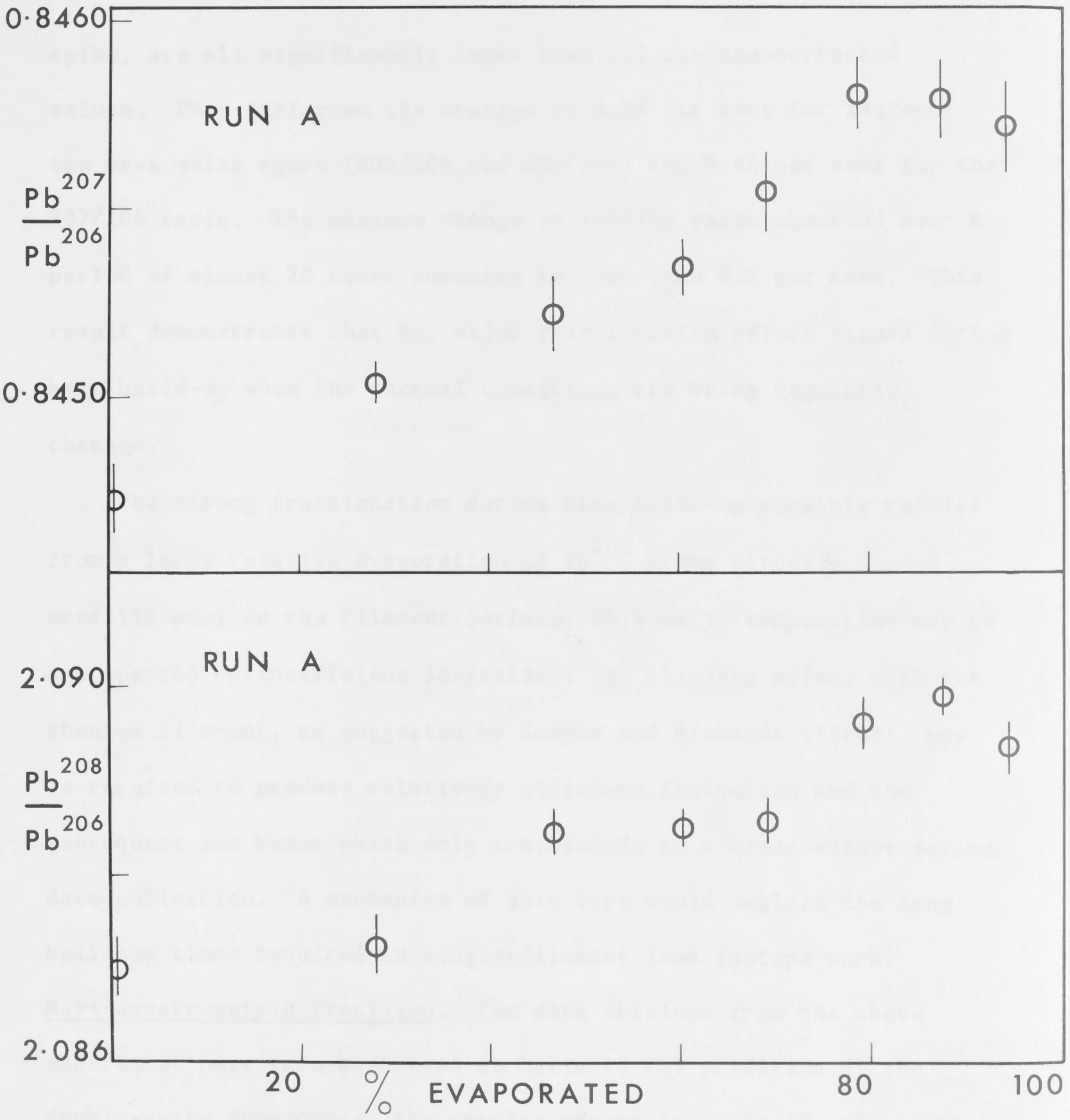

Figure 7. Pb^{208}/Pb^{206} and Pb^{207}/Pb^{206} ratios as a function of sample evaporated.

The absolute ratios, corrected for fractionation by the double spike, are all significantly lower than all the non-corrected values. They differ on the average by 0.88 per cent for isotopes two mass units apart (208/206 and 206/204) and 0.44 per cent for the 207/206 ratio. The maximum change in 208/206 ratio observed over a period of almost 20 hours amounted to less than 0.2 per cent. This result demonstrates that the major fractionation effect occurs during beam build-up when the thermal conditions are being regularly changed.

The strong fractionation during beam build-up possibly results from a large relative evaporation of Pb^{204} atoms directly from a metallic pool on the filament surface; this early evaporation may be accompanied by inefficient ionisation. An alloying effect with the rhenium filament, as suggested by Cooper and Richards (1966b), may be required to produce relatively efficient ionisation and the consequent ion beams which only fractionate to a minor extent during data collection. A mechanism of this type would explain the long build-up times required in single-filament lead isotope work.

Mass-spectrometric Precision. The data obtained from the above experiment have also been used to estimate the precision of the double-spike procedures; the results appear in table 15. Two extra unspiked analyses of the same sample on separate loadings of oxalate are included. Three completely distinct spiked runs were measured, and each of these has been used to normalise various combinations of

Table 15

Mass-spectrometric Precision

	206/204	208/206	207/206
RAW DATA			
Run A (n = 8)	18.773±.011	2.0886±.0011	.8450 ±.00038
Run B (n = 10)	18.756±.007	2.0856±.0004	.84487±.00008
All Runs (n = 20)	18.766±.015	2.0871±.0021	.84514±.00047
Run A & Run B (n = 18)	18.765±.013	2.0869±.0017	.84510±.00037
NORMALISED WITH N2942			
*Run A	18.599±.015	2.0689±.0003	.84140±.00015
*Run B	18.608±.010	2.0692±.0003	.84153±.00008
All Runs	18.605±.014	2.0691±.0003	.84148±.00013
*Run A & Run B	18.604±.013	2.0691±.0003	.84147±.00013
NORMALISED WITH N2609			
Run A	18.582±.016	2.0670±.0005	.84100±.00015
Run B	18.592±.011	2.0674±.0004	.84116±.00010
All Runs	18.588±.015	2.0672±.0005	.84110±.00014
Run A & Run B	18.587±.014	2.0672±.0005	.84109±.00014
NORMALISED WITH N2566			
Run A	18.604±.018	2.0695±.0007	.84151±.00014
Run B	18.616±.013	2.0701±.0006	.84171±.00014
All Runs	18.612±.017	2.0699±.0007	.84164±.00018
Run A & Run B	18.611±.016	2.0698±.0007	.84162±.00017

the raw data. All uncertainties quoted in the table are standard deviations of a single measurement.

The variation in the raw data from run to run is greater than the scatter of individual data-sets derived from a single filament load (A or B). This suggests that the major fractionation differences, which are corrected out by normalisation, occur during the initial build-up of the beam; subsequent processes, even over an extended 24 hours of emission, appear to be only of minor importance. Normalisation has not systematically affected the between-run variation in 206/204, and seems to increase the within-run uncertainty in the 206/204 ratio (ie. in runs A and B). The adverse effect of normalisation observed for the 206/204 ratio is not apparent in the 208/206 and 207/206 ratios, which are generally much improved by normalisation. The adverse 206/204 effect is probably due to a measurement error component, since 204 is the smallest peak and therefore most susceptible to error. The dominant perturbation in the other unspiked ratios results from fractionation. That the reproducibility of the results obtained from run B is greater for both the corrected and uncorrected ratios than run A, appears to be related to the lower relative drop in both beam intensity and fractionation change over the course of the experiment.

An uncertainty (one standard deviation) for a single measurement of 0.8 per cent is obtained for the 206/204 ratio when the data are normalised with run 2609. The relatively precise 208/206 and 207/206

ratios of 0.029 and 0.017 per cent respectively, contribute only a minor component to the 208/204 and 207/204 uncertainties, which are essentially the same as that for the 206/204 ratio. If run 2942 is used for normalisation a more optomistic figure is obtained whereas 2566 yields a larger uncertainty than run 2609. The relative uncertainties correlate with the relative beam-size of the spiked runs; the data of runs 2942, 2609 and 2566 were collected from ion-beams of 1×10^{-10} amp., 2×10^{-11} amp. and 6×10^{-12} amp., respectively. As lead ion-beams usually range from 3×10^{-11} to 1×10^{-10} amp. the normalised results obtained using run 2609 (see above) probably yield the most realistic precision estimates.

Although 0.17 per cent is a reasonable value for the 95 per cent confidence limits of the 206/204, 207/204 and 208/204 ratios it is still outside the limits obtained by some workers. The best gas-source work of Ostic et al (1967) and Stacey et al (1968), and the solid-source techniques of Catanzaro (1968) and Compston and Oversby (in press), produce results which are almost a factor of two more precise. In particular the results should be comparable with those of Compston. Perhaps part of the discrepancy results from differences in the two experiments. Compston's precision is based on only one unspiked analysis and 15 spiked runs. With a seven-times enrichment of 204 in the spiked runs, it is to be expected that the one unspiked analysis will be much more prone to 204 measuring error. This error would be repeated in each normalised result, yielding an

answer which is possibly inaccurate. The precision, however, would be controlled by the spiked analyses, in which the effect of 204-error is much reduced. An optimistic assessment of precision would thus be obtained.

Possible sources of the deduced imprecision may be inferred from further scrutinising of the results of these experiments. In theory all fractionation effects should be removed by the normalisation process. Hence the only likely remaining source of inaccuracy, apart from contamination, is 204-measurement error. This is demonstrated in figure 8, where the unspiked 206/204 - 207/204 results are plotted both before and after normalisation with one spiked run only. The raw data scatter about a fractionation line (slope 51°) whereas the corrected results fall on a 204-error line (slope 42°). Any 204-measurement error will obviously be manifested during the measurement of the 206/204 ratio. By referring back to figures 4 and 6 it can be seen that although on the fractionation hypothesis the raw 206/204 and 208/206 ratios should show identical behaviour, they are in fact distinctly different. Figure 4 exhibits an apparent random scatter pattern well outside the uncertainty limits calculated for the individual data-sets. An almost identical scatter pattern is obtained when normalised 206/204 points are plotted against time (not shown). Furthermore, normalised 208/206 and 207/204 ratios also show the same pattern. Hence it is clear that this is due to a 204-measurement error which has systematically perturbed all ratios on normalisation.

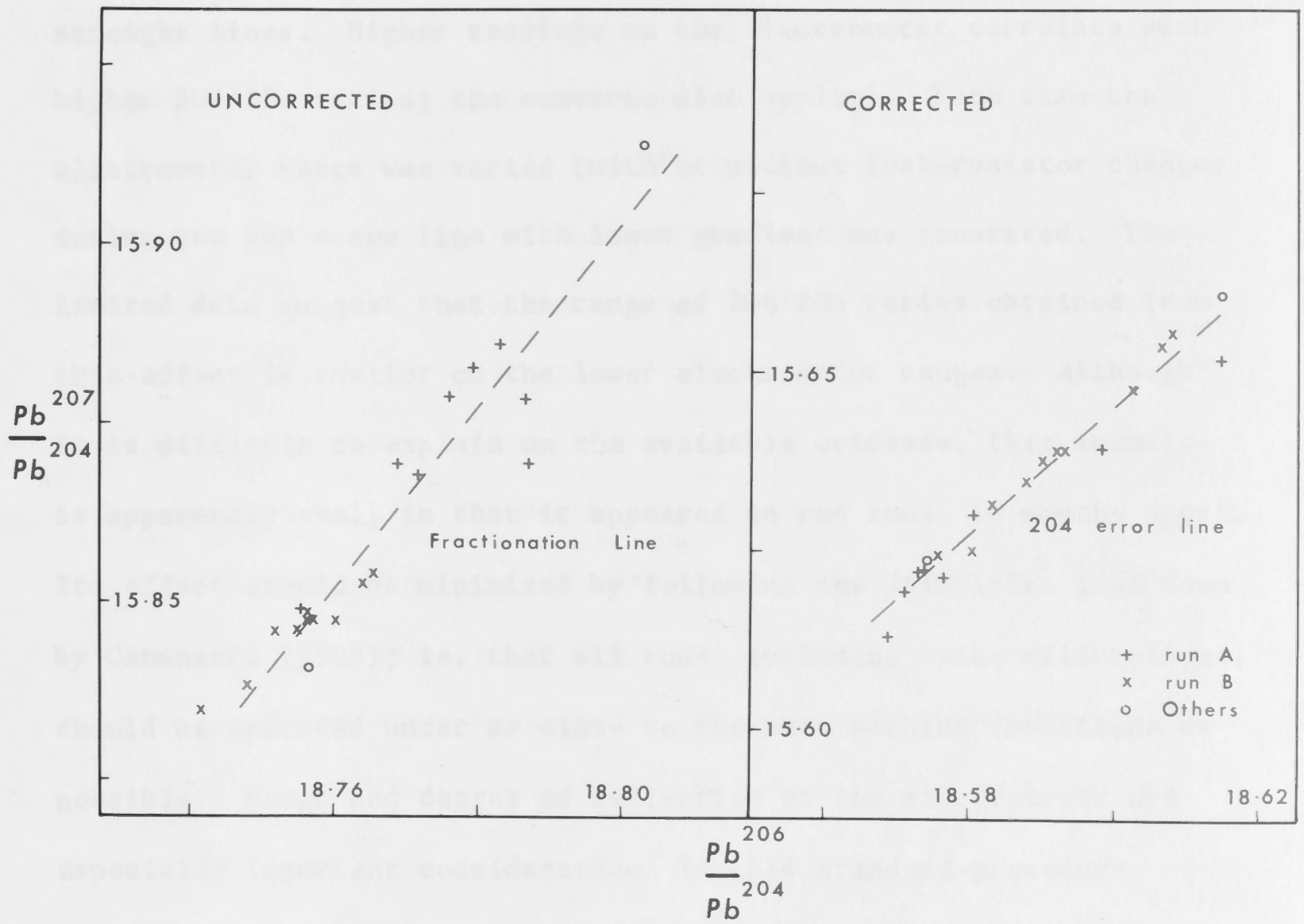

Figure 8. Unspiked Pb^{207}/Pb^{204} - Pb^{206}/Pb^{204} results before and after normalisation.

The probable reason for this perturbation can be gleaned from figure 4. All ratios which were measured on a constant range setting on the electrometer (Carey model 31) fall on approximate straight lines. Higher readings on the electrometer correlate with higher 206/204 ratios; the converse also applies. Each time the electrometer range was varied (with or without leak-resistor change) during the run a new line with lower gradient was generated. The limited data suggest that the range of 206/204 ratios obtained from this effect is smaller on the lower electrometer ranges. Although it is difficult to explain on the available evidence, this anomaly is apparently real, in that it appeared in two runs, 16 months apart. Its effect should be minimized by following the principles laid down by Catanzaro (1968); ie. that all runs, including spike calibrations, should be operated under as close to the same machine conditions as possible. Range and degree of deflection of the electrometer are especially important considerations in this standard-procedure technique. Data collected on the lower ranges are apparently less susceptible to the observed effect.

These two extended runs provide a means of eliminating this electrometer effect, and thereby estimating the limiting precision which is presently attainable. The method of doing this, suggested by M. J. Dallwitz, utilizes the time-variation of the 'raw' 207/206 and 208/206 ratios. For each run, treated separately, the time-curves for each ratio are brought to a common basis a) by expressing each

ratio-set as a fraction of the first of its kind and b) by adjustment of the reduced 207/206 ratios to compensate for the fact that they involve a single mass-unit difference, in contrast to the two mass-unit spread in the 208/206 and 206/204 ratios. This second adjustment is achieved by doubling the difference between the reduced 207/206 ratio and unity. The resulting 208/206 and 207/206 ratios should now furnish a common time-curve. Each set is plotted on a separate sheet of transparent paper; these are superposed and adjusted solely in the ordinate direction until the combined points show the least scatter. The resulting curve-of-best-fit is then transferred to a third graph, on which have been plotted the correspondingly-reduced 206/204 results. Corrected 206/204 ratios are deduced from the curve at the appropriate time-values, and are then re-presented as un-reduced 206/204 ratios by reference to the first 206/204 ratio-set value. The resulting data still, of course, incorporate fractionation error. This is removed in the normal way, in combination with the original raw 208/206 and 207/206 ratios, by normalisation against the spiked run 2942.

The eight results from run A and the ten from run B yield the mean values ($\pm$ one individual-result S.D.) summarized in table 16. These should be compared with the original values in those rows marked by an asterisk, in table 15.

Table 16

Reproducibility after Elimination of the 'Electrometer Effect'

	206/204	208/206	207/206
Run A	18.6100±.0085	2.0692±.0003	0.84146±.00025
Run B	18.6096±.0025	2.0692±.0001	0.84154±.00008
Runs A & B pooled	18.6098±.0057	2.0692±.0002	0.84150±.00018

The pooled results yield the following relative 95 per cent confidence limits of a single result:-

206/204 - 0.065 per cent

207/204 - 0.08 per cent

208/204 - 0.07 per cent.

This precision compares favourably with the best results of other workers.

Theoretical Limit of Precision. The ultimate precision limit for this measuring system is once again highly dependent on the least abundant, 204, isotope, and can be predicted from elementary statistical considerations. It is not the number of counts recorded that imposes the ultimate limit. If this were the case, 10,000 lead-204 counts would be required before one per cent precision is obtained. Most results are more than an order of magnitude better than this, with a smaller number of counts. The direct counts are not amenable to statistical analysis because they already represent averaged numbers which would not follow a normal distribution. This is because the

204 ions impinging on the collector are bundled together into discrete quanta before being digitally recorded. The precision is limited by the number of ions collected, a quantity which is amenable to valid statistical treatment. Table 17 compares the theoretical limit of precision and that currently being obtained within a single data-set. The effect of isotopic fractionation on the numbers is negligible over the small time interval (12 minutes). The number of 204 ions per counting period (four seconds) calculated from Coulomb's law is presented in the left-hand column. Column two contains the average number of 204 counts recorded during each of the 15 integration periods in the one ratio-set. The standard deviation in the next column is obtained from the following formula

$$\text{S.D.} = \text{av. counts}/\sqrt{\text{no. ions}}$$

and is represented in the next column as a percentage of the total number of counts. This is the maximum precision that could be expected from the various sized beams. These results are compared with the actual coefficients of variation for a single measurement of the 206/204 ratios within each data-set. The final column shows the percentage of the actual error that can be attributed to the number of lead ions collected. It is encouraging to note that over this short time interval machine conditions are so stable that additional imprecision is no more than comparable to that imposed by the fundamental counting statistics. The remaining problem to overcome in reaching these precision limits is the effect associated with different electrometer ranges and deflections.

Table 17

Comparison with Theoretical Precision Limits

Data-set	Number of ions	Av. counts	S.D. (in counts)	% S.D.	% S.D. 206/204	Proportion of error due to 204 ions (%)
A1	1.168×10^8_7	6231	0.58	.0093	.0404	23
A2	7.824×10^7_7	4173	0.47	.0113	.0246	46
A3	5.373×10^7_7	8597	1.17	.0136	.0341	40
A4	3.811×10^7_7	6097	0.99	.0162	.0421	38
A5	2.813×10^7_7	4501	0.85	.0189	.0373	51
A6	1.820×10^7_7	9707	2.28	.0234	.0363	64
A7	0.8942×10^7_7	4769	1.56	.0327	.0984	33
A8	0.3466×10^7_8	6026	3.11	.0515	.1086	47
B1	1.476×10^8_8	7871	0.65	.0083	.0290	29
B2	1.2077×10^8_8	6441	0.59	.0092	.0211	44
B3	1.0484×10^7_7	5591	0.55	.0098	.0194	51
B4	9.404×10^7_7	15064	1.55	.0103	.0182	57
B5	8.307×10^7_7	13291	1.46	.0110	.0277	40
B6	7.337×10^7_7	11739	1.37	.0117	.0261	45
B7	6.671×10^7_7	10674	1.31	.0123	.0380	32
B8	6.239×10^7_7	9983	1.26	.0126	.0285	44
B9	5.829×10^7_7	9326	1.22	.0131	.0270	49
B10	5.446×10^7_7	8713	1.18	.0135	.0374	36
					Average =	43

CHAPTER 4

AN INTRODUCTION TO LEAD ISOTOPIC STUDIES

Recently, the variation of lead isotopic composition in rocks and minerals has been extensively used as a geochemical tracer. Unlike the light elements such as carbon, oxygen and sulphur, no measurable chemical fractionation has been detected at the present levels of mass-spectrometric uncertainty. Rather, the observed isotopic variations result from the radioactive decay of the naturally-occurring elements, uranium and thorium. In their simplest form the decay schemes can be expressed as

$$U^{238} \longrightarrow Pb^{206} + 8He^{4} + \text{energy},$$

$$U^{235} \longrightarrow Pb^{207} + 7He^{4} + \text{energy},$$

$$\text{and } Th^{232} \longrightarrow Pb^{208} + 6He^{4} + \text{energy}.$$

These three lead isotopes are the stable end-products of their respective radioactive chains. A fourth stable isotope, Pb^{204}, which is not produced by radioactive decay, is used as a reference isotope to monitor changes in the absolute amounts of the other three. All naturally-occurring lead contains less than two per cent of lead-204. Generation of the three radiogenic isotopes is described by relationships of the form

$$N = N_o e^{\lambda t}.$$

In this equation N_o is the original number of parent atoms, N the number after time t, and λ is known as the decay constant. The decay constants used in this thesis for the parent atoms are

$\lambda = \lambda 238 = 1.537 \times 10^{-10} y^{-1}$ (Stieff et al, 1959),

$\lambda' = \lambda 235 = 9.722 \times 10^{-10} y^{-1}$ (Stieff et al, 1959),

and $\lambda'' = \lambda 232 = 4.99 \times 10^{-11} y^{-1}$ (Kulp et al, 1954).

The different decay rates for the uranium isotopes have resulted in a continuous change of abundance ratio, with progressive enrichment in the heavier isotope. No natural fractionation of uranium isotopes has ever been observed, so the ratio at any given time may be taken to be constant; the present-day proportion, designated α, is taken as 137.8 (Inghram, 1946).

Galena Studies and Lead Systematics

Galena ore was used as a starting point in the evaluation of lead isotope systematics because of the high lead concentrations which made it accessible to the comparatively primitive techniques of 10-15 years ago. Furthermore, the insignificant uranium and thorium relative abundances removed the added complication of post-crystallisation radiogenic lead addition which is always present in silicate systems. The principle isotopic trend in lead-ores was shown to be time-dependent. It has been taken to represent the result of adding radiogenic lead to a primeval parent lead of unique composition, the whole process occurring in a widespread region which has remained essentially closed with respect to uranium, thorium and lead since its formation. A condition of the model is that the intermittent removal of lead for ore-body formation has not significantly affected the unique properties of this source.

Russell and Reynolds (1965) have deduced the properties of this source region by fitting a curve on the 207/204 vs 206/204 diagram to samples from selected ore-bodies which they considered to represent most closely material derived from this source. Selection was based on geologic and isotopic criteria arising from the conviction that this primary source is both deep-seated, and highly uniform in its uranium-thorium-lead relationships. The conformable 'pyritic' deposits thought to have been derived from a deep source (Stanton and Russell, 1959) and lead of direct volcanic origin (White Island, New Zealand) are included. Russell and Reynolds point out that the calculation is relatively insensitive to contamination by non-primary lead and that large secondary additions are generally distinguishable. No assumptions are made about the age of any point. The shape of the resultant ore-body curve can be defined by the radioactive decay law and the assumption of a constant U/Pb ratio in the source region. The calculations permit estimation of the U/Pb ratio, and of the isotopic composition of the modern end of the 'growth curve'.

The troilite phase in iron meteorites contains such minute quantities of uranium and thorium that the isotopic composition of the enclosed lead has remained virtually constant since the time of formation of the troilite. This isotopic composition lies very close to the growth curve, which has been derived solely from terrestrial leads. The age of the troilite point deduced from the growth curve agrees remarkably well with that derived by Patterson from the

meteoritic system alone (Patterson, 1956). It thus seems likely that at a time 4.55×10^9 years ago, lead in the primary terrestrial system, and probably the earth as a whole, was similar in composition to that in the meteoritic system. The 206/204, 207/204 and 208/204 ratios of this primeval lead (time = t_o) are designated by x_o, y_o and z_o, respectively.

If this reasoning is accepted, a 'lead model age' may be calculated with the Holmes-Houtermans equation (Holmes, 1946; Houtermans, 1946) which is the result of combining two of the growth equations simply deduced from the laws of radioactive decay. This takes the form

$$(y-y_o)/(x-x_o) = 1/\alpha.(e^{\lambda' to}-e^{\lambda' t})/(e^{\lambda to}-e^{\lambda t}),$$

where x, y, and z are the observed 206/204, 207/204 and 208/204 ratios, and t is the time of separation of the ore-body from the primary source. All other terms are as previously defined. Assessment of the geological relevance of this model age must depend on the extent to which it is possible to believe a) that such a primary source, if it exists, is relevant as a source of the lead under consideration, and b) that contamination by lead from other sources is minimal.

The 'primary' ore-leads selected by Russell and Reynolds also closely fit a curve on the 208/204 vs 206/204 diagram; the shape of this curve is also defined by the radioactive decay law. The closeness of fit implies that the source region is characterised by a

constant thorium to uranium ratio, as well as a constant uranium to lead ratio. Because of the divergent behaviour of uranium and thorium under oxidising conditions, this remarkable uniformity of Th/U has been taken as suggesting a reducing environment in the source region which has been taken (eg. Wilson et al, 1956; Stanton and Russell, 1959) to be the upper mantle. Numerous ore-bodies have been found which conform closely to this model and some of these have been major producers. As many of these deposits were originally thought to be syngenetic sedimentary deposits the name 'conformable' was applied. The term 'ordinary', implying 'good fit to the isotopic criteria', has also been used. Australian examples include Broken Hill, Mount Isa, Captains Flat, Cobar and Hall's Peak.

Although many ore bodies were found to fit this simple model, many others clearly did not. Penecontemporaneous leads were found which possessed a wide range of model ages, scattered considerably about the 'conformable' lead growth curve, and often fell far to the right with consequent negative model ages. These were called 'anomalous' (see Russell and Farquhar, 1960) and were interpreted as leads which had developed in more than one uranium-thorium-lead system. All stages subsequent to the initial primary system were considered crustal. Within a single geological province it was found that anomalous isotopic ratios plotted linearly on both 207/204 vs 206/204, and 208/204 vs 206/204 diagrams. In one case the results fall along a chord on the 207/204 vs 206/204 plot, which intersects

the growth curve at two points but does not extend above it. This pattern has been interpreted by Kanasewich (1968) as resulting from the mixing in variable proportions of two single-stage leads. By using the Holmes-Houtermans formula one can calculate the age of mineralisation of each end member. The youngest age should also correspond to the time of mixing.

In general, however, the isotopic array extends beyond the younger intercept on the growth curve and different models are used. The most general was proposed by Russell and Farquhar (1960). In it a particular mass of lead is separated from the primary source at a time t_1 and introduced into a crustal environment in a disseminated form. Each lead sample is associated with a different U/Pb and Th/Pb environment and correspondingly incorporates a radiogenic component at different rates. The time of separation of the primary lead does not necessarily equal the onset of radiogenic accumulation. Mineralisation occurs at time t_2 when this radiogenically-contaminated lead is isolated from the uranium and thorium and concentrated into local ore-bodies. Providing each lead sub-system has remained closed during its growth a straight-line relationship is obtained. The slope of this line on the 207/204 vs 206/204 diagram represents the 207/206 ratio of the radiogenic component. Kanasewich (1962, 1968) has used a special case of this model to explain the Broken Hill deposits in which generation of the radiogenic lead begins at the same time that the ordinary lead was removed from its primary system.

The length of the anomalous lead line in variations of the model is controlled by the range of uranium to lead ratios, the time in the second environment, and the degree of homogenisation immediately prior to the mineralising episode.

Kanasewich (op. cit.) has also investigated theoretically the nature of the multistage growth systems in which two or more distinct phases of crustal history were involved. He found that, as the number of stages increased, the points formed a broader but shorter array about the original straight line. Although such systems might occur in nature Kanasewich feels that with the present level of analytical uncertainty they would remain undetected.

Whole Rocks and the Isochron Plot

Unlike the galena system, most rocks do not provide a uranium- or thorium-free environment and progressive isotopic changes occur after formation. To determine the initial isotopic composition allowance must be made for in situ radioactive decay. This may be done for a series of related samples with the isochron* plot of Nicolaysen, (1961), which was successfully applied to lead work by Ulrych and Reynolds (1966). This method in which, for example, Pb^{206}/Pb^{204} is plotted as a function of U^{238}/Pb^{204}, yields the original isotopic composition and

---

* Altogether there are three types of line called isochron: a) on the 207/204-208/204 plot (Holmes-Houtermans isochron) referred to in the literature at least by implication although their actual existence is doubtful. b) on the 206/204-U/Pb plot (Nicolaysen isochron) c) on the 'concordia' plot ie. 206/238-207/235.
Only isochron b) will be referred to in this thesis.

the time of emplacement of a rock, provided that it has remained a closed system. This method is based upon the following three equations, which describe the development of the respective radiogenic additions:

$$(Pb^{206}/Pb^{204})_p = (Pb^{206}/Pb^{204})_i + (U^{238}/Pb^{204})_p.(e^{\lambda t}-1)$$

$$(Pb^{207}/Pb^{204})_p = (Pb^{207}/Pb^{204})_i + (U^{235}/Pb^{204})_p.(e^{\lambda' t}-1)$$

$$\text{and } (Pb^{208}/Pb^{204})_p = (Pb^{208}/Pb^{204})_i + (Th^{232}/Pb^{204})_p.(e^{\lambda'' t}-1)$$

where subscript p represents the present ratio and subscript i the initial ratio. Each may be used to correct data from individual samples.

Furthermore, each of these expressions is the equation of a straight line with slope proportional to the age of the system and the ordinate intercept the initial ratio. Thus three independent ages should be available for related rock samples. Young rocks have low contents of U^{235}, however, and consequent enrichments in 207-lead are often negligible with respect to experimental errors. A more comprehensive treatment of the method is given in Ulrych and Reynolds (op.cit.). In this thesis the major interest lies in the initial ratio information.

The Crustal - Mantle Dilemma

A point of view referred to in the systematics section, suggests that ordinary leads are mantle derivatives and anomalous leads are crustal. However, it has now been established (e.g. Ostic et al, 1967; Kanasewich, 1968) that leads which were chosen on geological grounds

as derived from the mantle are not always ordinary; e.g. Rosebery, Tasmania. Also, a sample of lead incrustation from the vent of a modern andesite volcano (White Island, New Zealand) was found to have a composition beyond the end of the growth curve. Furthermore, some rock-lead studies have yielded results which are inconsistent with the ore-lead single-stage growth curve. Catanzaro and Gast (1960) analysed ten pegmatites which were considered to be of crustal origin and seven of these yielded model ages consistent with the true age; ie. they were essentially ordinary leads. In their study of the Atlantic islands, Ascension and Gough, Gast et al (1964) found both inter- and intra-island variations in lead isotopic composition. These volcanics, then, which almost certainly were derived from the mantle, did not fit the single-stage model. Further work by numerous authors (e.g. Tatsumoto, 1966a; Cooper and Richards, 1966a) has confirmed that oceanic volcanic magmas display a considerable range in isotopic composition. This evidence has led Kanasewich (1968) to allow that 'the mantle may have quite local heterogeneities of the U^{238}/Pb^{204} ratio, μ, and the Th^{232}/Pb^{204} ratio, W. It should be expected that local irregularities of μ and W also exist in the continental crust.' (my emphasis). The preceding evidence, however, is quite compelling that the irregularities under the ocean are other than 'local', and that the same conditions probably prevail under the continents. In fact, Cooper and Richards (1966a) have claimed that 'it seems that no clear distinction may yet be drawn on isotopic

grounds between volcanic rocks of oceanic or of continental environment.' Various suggestions have been made for a mantle source for the ordinary leads that is compatible with these observations. Cooper and Richards (op. cit.) have suggested that the mantle could be homogeneous on the larger scale of ore body formation. They preferred, however, the idea that ore concentration takes place at greater depths than magma formation. Richards (1968b) suggested a slightly modified alternative in which ore bodies are generated from the mantle before magma fractionation begins. The evidence suggests at this stage that it is more difficult to derive a single-stage lead ore from the mantle than originally thought. This has led to a re-examination of the crustal-source theory.

Shaw (1957) proposed that crustal-averaging processes such as gradation, diastrophism and vulcanism could combine on a scale large enough to produce 'single-stage' ore leads. This theory was refuted by Kanasewich (1962), who theoretically investigated isotope behaviour during multistage mixing. The assumptions used, however, excluded the one possibility that would allow such a process (ie. complete homogenisation on a grand scale). Richards (1968a) re-examined a number of ordinary leads and found that he could subdivide them on the basis of model age and μ-values. He states that those which plot nearest the growth curve (e.g. Broken Hill and Balmat) occur in high-grade metamorphic areas and are apparently not associated with volcanic rocks; they need have no direct connection with mantle processes.

Kanasewich (1968) presented a histogram showing the great similarity between the Th/U ratios of the source rocks for the anomalous galena components of many deposits, and the Th/U ratios of crustal rocks as directly measured. It is also possible to see on this diagram that the ordinary leads plot in a narrow band resembling the crustal rock distribution in mean value but not in width. Kanasewich uses the distribution width to refute a crustal origin; the mean value could well be used, however, in conjunction with large scale homogenisation processes to support crustal derivation. As no infallible geological criteria have been found for distinguishing ordinary leads (Ostic et al, 1964; Kanasewich, 1968), they must be ultimately discerned by their isotopic composition. Surely, choosing results in such a way as to fit the single-stage model is highly subjective; it is hardly surprising that the selected analyses conform so precisely to the model.

It thus appears that the crust may well be as acceptable as the mantle as a possible source for the ordinary ore leads; it is a little premature to make dogmatic statements. If a model similar to that proposed by Armstrong (1968) should prove to be correct, in which ore leads and magmas are derived from crustal material carried down into the mantle, such clear distinctions may not be relevant.

Previous Comparative Studies of Ores and Associated Rocks

The first study of this nature was made by Murthy and Patterson (1961) on the ores and associated granitic rocks at Butte, Montana.

The ore had been previously considered (Bateman, 1950) as a classical hydrothermal deposit, and as such was particularly suitable for initial study. The authors analysed lead from the ore body as well as from feldspar and quartz out of the associated adamellite. Although the feldspar and ore leads were identical, the one quartz sample yielded lead which was distinctly different. Murthy and Patterson preferred to believe that the feldspar had been contaminated with galena lead and that only the lead in the quartz was representative of the original rock. They thus came to the startling conclusion that the ore lead was not derived from the adamellite. However, in 1968, Doe et al presented new, basically very similar data, which were interpreted completely differently. The feldspar lead was considered to faithfully represent the initial rock composition, as evidence for large scale ore-lead contamination of granite could not be found. Furthermore, the single discrepant quartz result was considered to be due to laboratory contamination. It appears highly probable that Doe's suggestions are correct and that the ores are related to the granite magma.

In another study Doe (1962) found that ore from Balmat, New York, has a different composition from that in the associated synkinematic granites and pegmatites. Additional work by Reynolds (1967) has shown that although some of Doe's measurements were inaccurate, he did reach the correct conclusion. Reynolds also found that feldspar leads from the Nelson batholith, British Columbia, are identical in

composition with some of the closely associated ore leads. Stacey et al (1968) have also shown that many of the largest copper - lead - zinc deposits in Utah have lead of isotopic composition similar to that in the associated Tertiary intrusives. Thus, although in some studies positive correlations have been found between ores and adjacent igneous rocks, it has not always been the case.

All the studies cited were made on mineral grains separated from the igneous rocks, and only in one case was a mineral other than feldspar analysed. This procedure has been adopted because of the high lead content and consequent lack of technical problems associated with the feldspars. Also the small amounts of included uranium and thorium ensure that only minor additions of radiogenic lead are produced in situ decay. Catanzaro and Gast (1960) have shown, however, that feldspars can be contaminated with radiogenic lead after crystallisation. If such radiogenic additions are derived purely from an inter-mineral redistribution (ie. the rock as a whole has remained a closed system) then only an analysis of the whole rock itself (together with its lead, uranium and thorium contents) will yield a meaningful initial ratio. Hence, the isotopic investigation of rock-system leads in this thesis has been exclusively by means of the whole-rock method. A similar method was used by Farquharson (1968) in an isotopic study of ores and associated rocks from the Mt Isa region, Queensland.

CHAPTER 5

CHEMICAL ANALYSES

A small quantity of trace element data was obtained by X-ray fluorescence analysis (ref. chapter 3) during routine pre-isotopic investigation. Lead, uranium and thorium were analysed for the calculation of initial lead-isotope ratios, rubidium and strontium to determine the appropriate spiking proportions (independent rubidium and strontium abundances were later derived from these isotope dilution analyses). Because of the automatic design of the instrument and identical X-ray tube and pulse height selector conditions it was also possible to measure yttrium abundances. In order to co-ordinate the results a little, γ-ray spectrometric determinations of the major element, potassium, were made for many samples. The attendant uranium and thorium information is not included because these elements occur in minor mineral phases and a separate rock crushing was used for the γ-ray analyses; five duplicate potassium determinations agreed to within five per cent of each other. Major element data (from Branch, 1966, 1967 and J. C. Bailey - unpublished) are also included for comparative purposes (see table 6).

Major Elements

Perhaps the most pertinent feature of the major element data in table 18 is the lack of clear-cut division between the major rock types. For example, although it encompasses more basic varieties, the Herbert River Granite shows very considerable overlap in composition

Table 18

Major Element Chemistry of the Dominant Rock Types

	Rhyolites, rhyodacites of the Featherbed Volcanics (after J. C. Bailey)	Elizabeth Creek Granite (Branch, 1967)	
	Range (%)	Average (%)	Range (%)
SiO_2	70.8 - 77.6	76.3	71.3 - 78.4
TiO_2	0.3 - 0.1	0.08	0.0 - 0.4
Al_2O_3	14.3 - 11.4	12.8	11.9 - 14.8
Fe_2O_3	0.6 - 0.6	0.9	0.4 - 1.9
FeO	1.8 - 0.8	0.6	0.0 - 1.7
MnO	0.05 - 0.03	0.04	0.01 - 0.08
MgO	0.6 - 0.04	0.1	0.0 - 0.8
CaO	2.4 - 0.5	0.6	0.2 - 1.6
Na_2O	3.5 - 3.0	3.5	2.6 - 4.4
K_2O	4.1 - 4.7	4.6	2.4 - 5.3
P_2O_5	0.06 - 0.02	0.04	0.01 - 0.09

	Herbert River Granite (Branch, 1966)	Almaden Granite (Branch, 1966)	
	Range (%)	Typical (%)	Most Basic Member (Diorite)
SiO_2	65.4 - 77.4	66.8	59.8
TiO_2	0.1 - 0.1	0.3	0.7
Al_2O_3	16.7 - 11.5	15.3	16.5
Fe_2O_3	1.8 - 0.5	1.4	1.1
FeO	2.5 - 1.2	2.9	4.9
MnO	0.1 - 0.04	0.1	0.1
MgO	2.0 - 0.3	2.0	4.1
CaO	3.0 - 1.0	4.2	6.9
Na_2O	4.5 - 3.3	3.1	2.7
K_2O	3.3 - 4.1	3.2	2.2
P_2O_5	0.05 - 0.05	0.2	0.1

with the Elizabeth Creek Granite. It also closely resembles the Featherbed Volcanics; this similarity is greater when basic variants of the volcanics (such as the dacite) are included. The typical Almaden Granite analysis approximates the basic member of the Herbert River Granite, but the diorite is considerably more basic. The Mareeba Granite (not shown) covers a range of compositions similar to the more acid members of the Herbert River Granite.

A notable feature of the province as a whole is the common occurrence of very acidic rocks, which are not only confined to the Elizabeth Creek Granite type. Acid members of the Featherbed Volcanics, Herbert River and Mareeba Granites can all contain more than 76 per cent SiO_2. It is perhaps significant to note that the Herbert River Granite from the type area is thus far the most acidic example of this granite. The data also indicate that the volcanics tend to be slightly more basic than their assumed comagmatic plutonic equivalent, the Elizabeth Creek Granite. If there should be a fundamental genetic difference between the Elizabeth Creek Granite (and Featherbed Volcanics) on the one hand, and the Herbert River, Mareeba and Almaden Granites on the other, it is not reflected in the major element chemistry.

Trace Element Data

The trace element data which are presented in table 19 are subdivided into rock types according to Branch's classification (1966); the most controversial samples are referred to in the footnotes. The

Table 19

Trace Element Concentrations (µg./g.)

Sample	Rb	Sr	Y	Pb	Th	U	K (%)
			ELIZABETH CREEK GRANITE				
2952	231	48	36	29	24	6.5	3.92
2956	312	41	58	30	30	8.6	3.78
2957 a	305	61	53	29	34	8.4	4.02
2959	174	21	38	19	26	4.5	3.71
2960	490	16	100	30	54	13.1	4.12
2967	289	25	35	24	44	6.7	4.19
2969	443	25	74	41	47	11.5	4.26
2991	1210 g	15 g		44	43	21.4	
2992	518 g	16 g		25	53	22.5	
2995	486 g	24 g		29	44	12.8	
2996	344 g	30 g					
2997	553 g	20 g		24	66	10.6	
2998	558 g	17 g					
2999	504 g	15 g					
2962 b	201	141	18	47	21	3.1	3.13
			FEATHERBED VOLCANICS				
2961	100	204	32	18	18	4.3	1.73
2964	229	77	57	24	20	4.1	3.58
2970	223	115	44	24	29	6.9	3.68
2973	210	98	55	22	20	5.2	3.55
2974	270	49	29	20	33	8.2	4.30
2993	349	51		42	25	9.6	
2976 c	234	103	34	15	16	4.6	3.41
			HERBERT RIVER GRANITE				
2955	169	134	21	17	23	3.9	3.05
2965	218	163	36	14	20	5.1	3.34
2968 d	63	381	11	11	5	0.5	1.56
2977	238	119		19	29	6.3	3.67
2978	216	158					
2979	153	154					
2975 e	244	86	34	29	19	3.8	3.72

Table 19 (cont.)

Sample	Rb	Sr	Y	Pb	Th	U	K (%)
			concentrations in µg./g.				
			ALMADEN GRANITE				
2953	167	176	28	19	17	4.3	2.79
2963	139	219	27	19	15	3.7	1.79
2966	171	160	25	18	18	2.6	2.54
2971	175	174	29	18	19	2.5	2.65
2972	154	169	23	13	17	3.8	2.53
			GURRUMBA GABBRO				
2994	7	424	27 f				0.17 f
			NYCHUM VOLCANICS				
2951	236	36	67	43	26	6.7	4.21
2980	302	86					
2981	128	175					2.04 h
2982	54	213					0.59 h
2983	133	186		20	6	2.6	1.73 h
2984	254	115		31	12	5.7	
2985	184	139					
2986	388	118		41	26	6.7	
2987	136	179					
2988	14	222					
2989	138	202					
2990	205	145		23	12	3.4	
			PRECAMBRIAN				
2950L	14	208	5	19	5	0.4	0.63
2950M	102	230	10	22	10	1.1	1.81
2954	94	365	13	38	7	1.6	2.79
2958	76	356	17	27	8	1.4	2.09

a Branch has called this an Elizabeth Creek - Herbert River hybrid. Its dominant characteristics appear, however, to be of the former.

b Very controversial Elizabeth Creek Granite specimen; in the author's opinion it would be best classed on geochemical evidence as Featherbed Volcanics.

Table 19 (footnotes cont.)

c Slaughter Yard Creek Volcanics.

d J. C. Bailey contends that this is a member of a distinct Na-rich, K-poor magma series which has a restricted occurrence in the Claret Creek Ring Complex.

e On the basis of its K-Ar age I prefer this to be classified as Mareeba Granite.

f Analysis by J. C. Bailey.

g Isotope dilution determinations.

h Flame photometric determinations.

uranium and thorium contents of the various rock types are compared in figure 9 with the average ratio, 3.9, for acid and intermediate rocks (Kanasewich, 1968). It can be seen that although there is an approximate correlation, several of the samples show considerable scatter. From a study of the uranium - thorium - lead system (see chapter 7), it appears that in three of the four most widely divergent of these rocks (2991, 2992 and 2997) mass transfer of uranium has occurred since formation; thorium, however, appears to have been affected to only a minor extent. On this basis the pattern in figure 9 implies that samples 2991 and 2992 have gained uranium and 2997 lost it. From the isotopic evidence (not plotted) it also appears possible that 2967 has lost uranium; this too is compatible with its position on figure 9. It must be emphasised here that although the first three samples were not collected by the author, they were nervertheless blasted and carefully chosen; all three have remained completely closed with respect to rubidium and strontium. Hence it is apparent that uranium in particular is extremely susceptible to weathering. The greatest value of the uranium - thorium plot may well be in its ability to detect weathering in samples before lead isotopic analysis. It is clear that any primary geochemical conclusions based on such a diagram must be treated with the utmost caution.

Uranium and thorium behave similarly with respect to potassium; a Th-K plot is presented in figure 10. Thorium increases regularly to about 22 μg./g. (uranium about six μg./g.) for four per cent

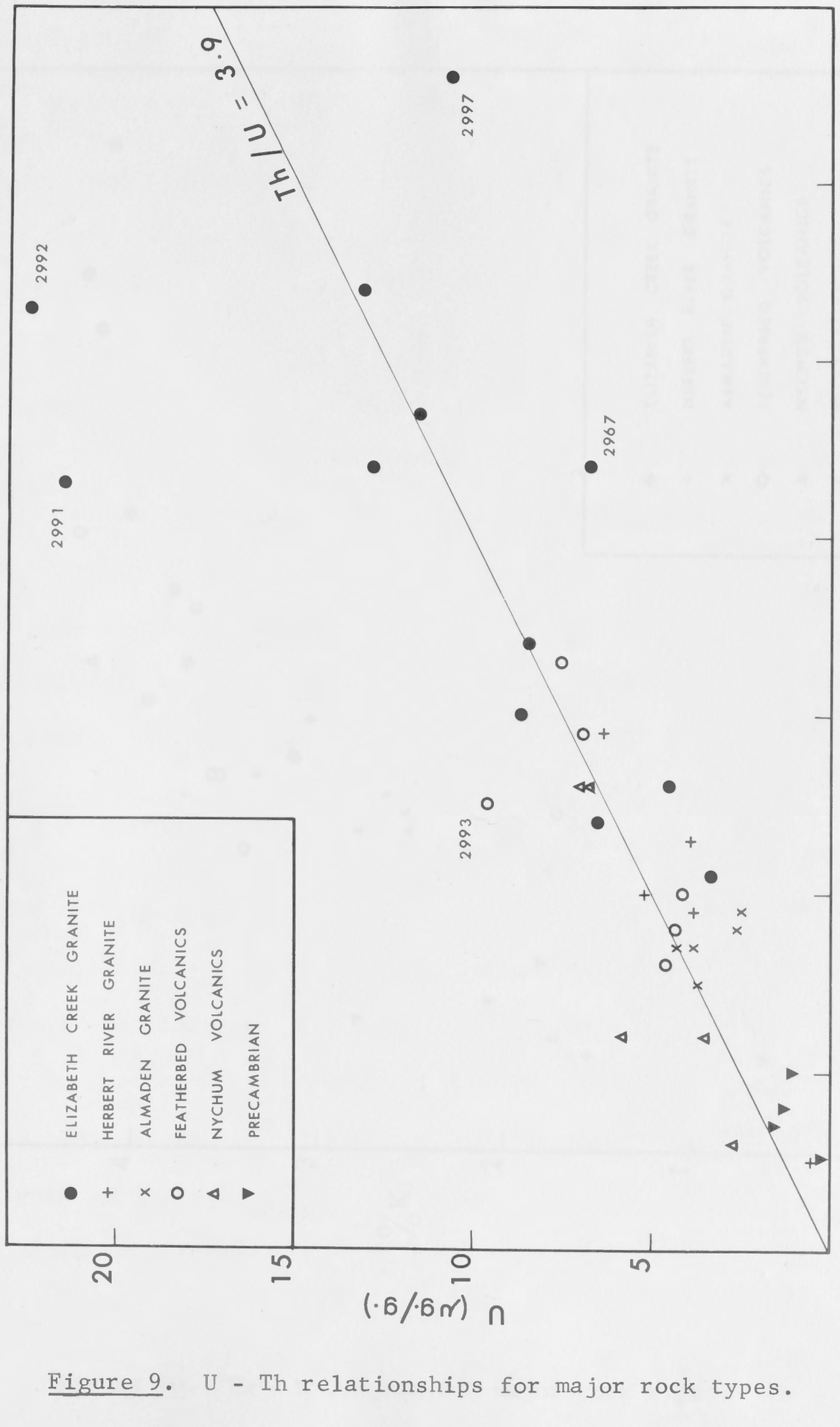

Figure 9. U - Th relationships for major rock types.

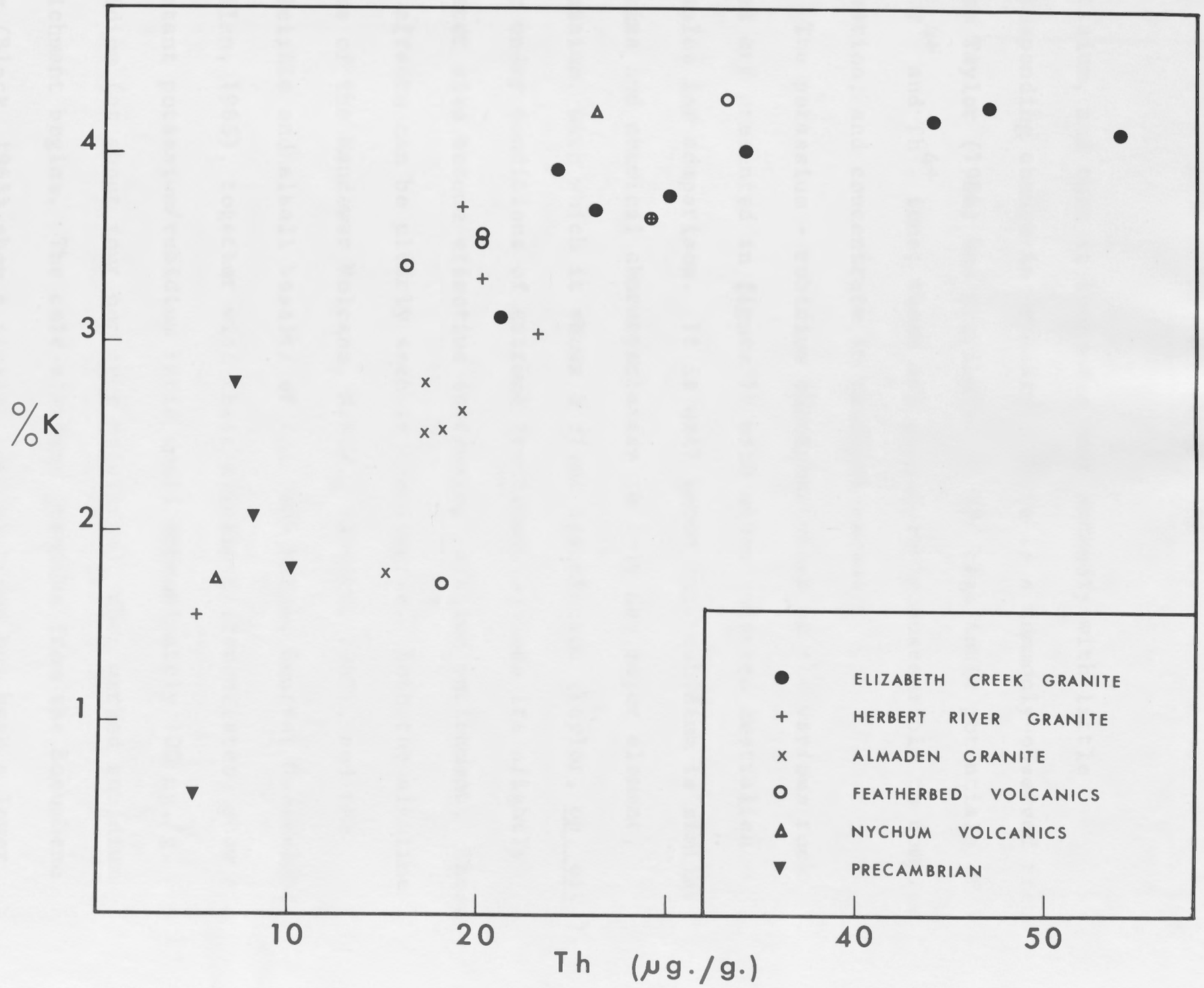

Figure 10. Th - K diagram for major rock types.

potassium, and then it increases most markedly with little corresponding change in potassium. This is a commonly-observed trend which Taylor (1966) has attributed to the high ionic potentials of the U^{4+} and Th^{4+} ions; these are particularly susceptible to complex formation, and concentrate in residual magmas.

The potassium - rubidium characteristics of the various rock types are presented in figure 11 with other selected Australian examples for comparison. It is well known that rubidium is similar in size and chemical characteristics to only one major element, potassium, with which it shows a close association (Taylor, op. cit.). Only under conditions of extreme fractionation does its slightly greater size become effective in causing relative enrichment. These two effects can be clearly seen in the diagram. Both the alkaline rocks of the Nandewar Volcano, N.S.W., (Abbott, 1965), and the tholeiitic and alkali basalts of the Peak Range, Central Queensland (Mollan, 1965), together with their alkalic differentiates, show a constant potassium/rubidium ratio until approximately 100 µg./g. rubidium (at about four per cent potassium), when marked rubidium enrichment begins. The calc-alkaline granites from the Eucumbene area (Black, 1965) show a similar initial trend but have a lower potassium/rubidium ratio; those from the Moonbi district (Chappell, 1966) plot over a limited range at the end of this line, and appear to show the first signs of enrichment. Most of the Atherton rocks possess similar relationships. The Featherbed trend is similar to

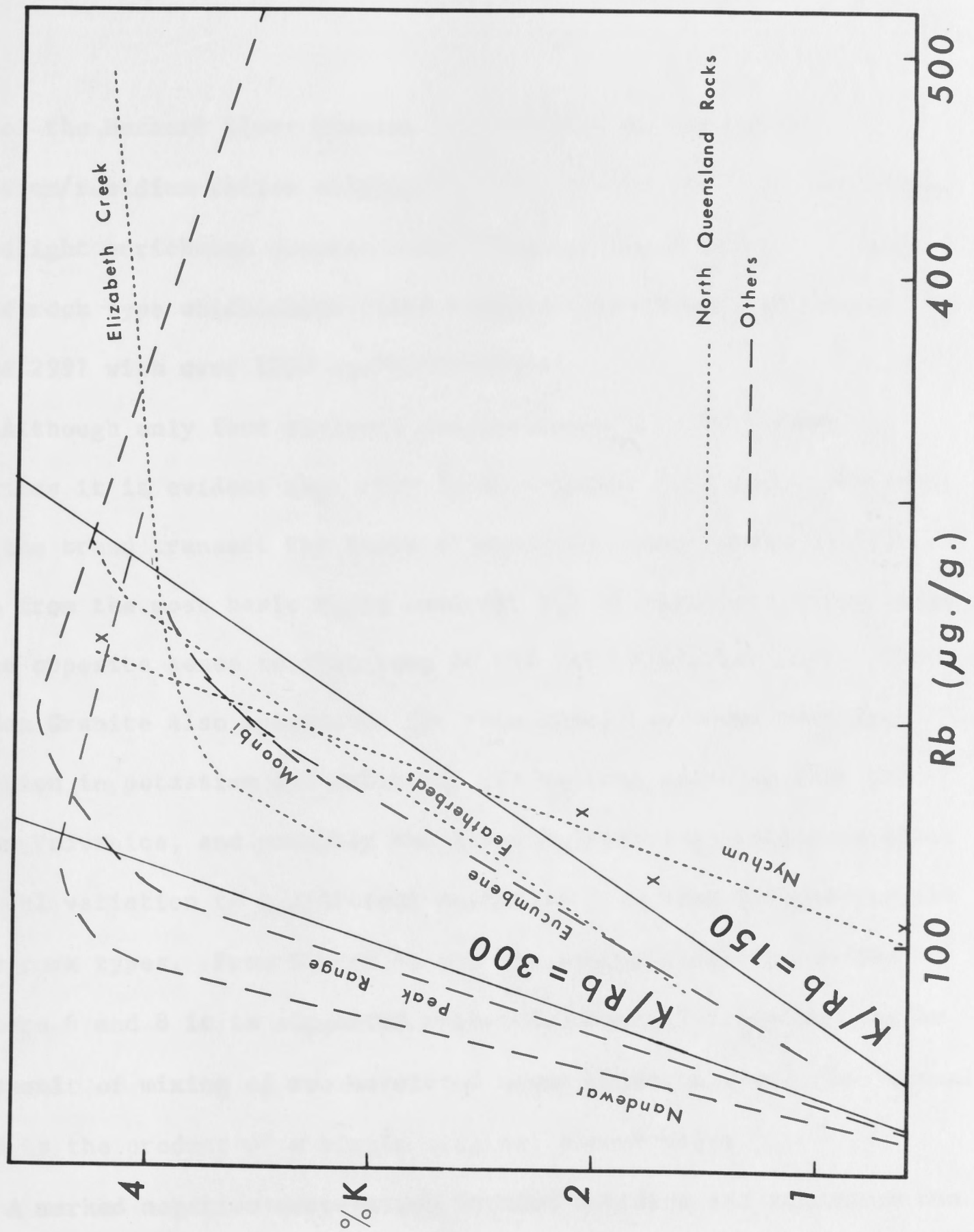

Figure 11. K-Rb relationships of the main rock types.

that of the Herbert River Granite (not shown), with constant potassium/rubidium ratios of about 200 until four per cent potassium, when slight enrichment occurs. The Elizabeth Creek Granite, a highly acidic rock type which shows clear signs of enrichment, culminates in sample 2991 with over 1200 µg./g. rubidium.

Although only four analyses are available for the Nychum Volcanics it is evident that they form an aberrant pattern. Not only does the trend transect the lines of equivalent potassium/rubidium ratio from the most basic rocks onwards, but it also cuts these lines in the opposite sense to that seen in the late differentiates. The Almaden Granite also appears to fit this line, but shows much less variation in potassium and rubidium. It is thus possible that the Nychum Volcanics, and possibly the Almaden Granite as well, owe their chemical variation to a different mechanism from that influencing the other rock types. From figure 11 and the isotopic data presented in chapters 6 and 8 it is suggested that this abnormal behaviour may be the result of mixing of two unrelated magma types, whereas the 'normal' trend is the product of a single original parent magma.

A marked negative correlation between rubidium and strontium can be seen from table 19. The Elizabeth Creek Granite, which is generally highly enriched in rubidium, contains very small quantities of strontium; the opposite extreme is seen in the Gurrumba Gabbro. The two Nychum basalts (nos 2982 and 2988) are interesting in that although their strontium content is similar to that of the Almaden

Granite (No. 2963 - dioritic phase), their rubidium content is more than a factor of two less. The Granodioritic phase of the Herbert River Granite (2968) has a remarkably high strontium content which is comparable to that of the Gurrumba Gabbro; the gabbro, however, has 23 per cent less SiO_2 than the granodiorite (SiO_2 analyses by J. C. Bailey - personal communication, and Branch, 1966). Although showing considerable variation, the rubidium content of the plutonic rocks is distinctly greater than the average values presented by Taylor and White in 1966 (average granite = 145 µg./g., granodiorite = 110 µg./g., basalt = 26 µg./g.); the strontium values are correspondingly lower (285, 440, 465 µg./g. respectively). The Precambrian metamorphics are characterised by high strontium and low rubidium contents.

Yttrium is a difficult trace element to assess fully because it concentrates in minor phases such as sphene and apatite. The data show that its abundance is proportional to the acidity of the igneous rock types; concentrations in the metamorphics are particularly low.

Lead concentrations also appear to be related to acidity in the igneous rocks; the lead and potassium relationships of the main rock types are shown in figure 12. The Almaden and Herbert River Granites (excluding the one sample that is possibly Mareeba type) are uniformly low in lead. The lead to potassium ratios of all rock types, however, vary over approximately the same ranges, showing that no magma was unduly enriched; the average lead contents agree well with those quoted in Taylor and White for granites and granodiorites

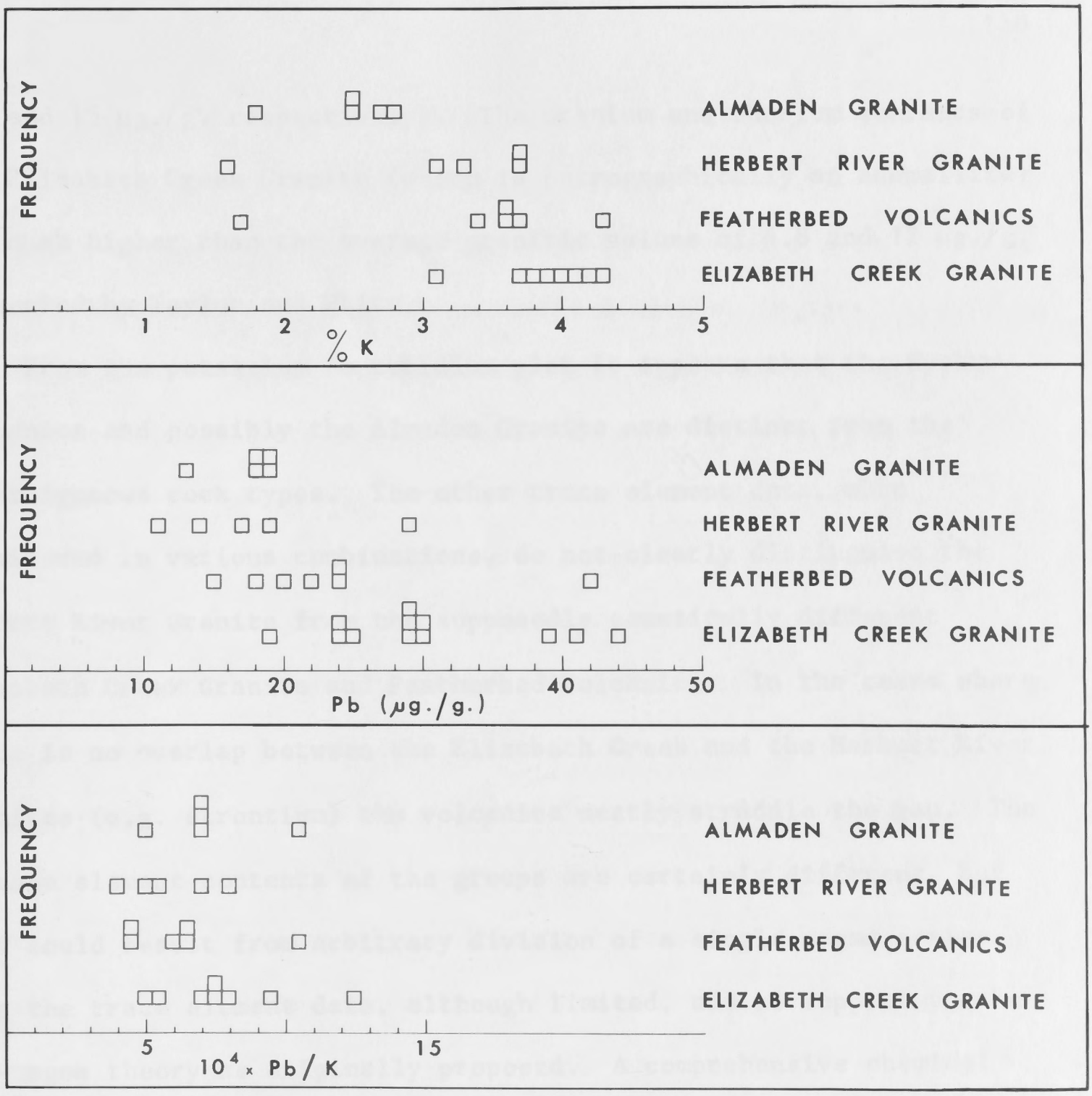

Figure 12. Pb and K relationships of the main rock types.

(30 and 15 μg./g. respectively). The uranium and thorium contents of the Elizabeth Creek Granite (which is petrographically an adamellite) are much higher than the average granitic values of 4.8 and 17 μg./g. presented by Taylor and White.

From the potassium to rubidium plot it appears that the Nychum Volcanics and possibly the Almaden Granite are distinct from the other igneous rock types. The other trace element data, when considered in various combinations, do not clearly distinguish the Herbert River Granite from the supposedly genetically different Elizabeth Creek Granite and Featherbed Volcanics. In the cases where there is no overlap between the Elizabeth Creek and the Herbert River Granites (e.g. strontium) the volcanics neatly straddle the gap. The average element contents of the groups are certainly different, but this could result from arbitrary division of a single magma series. Thus the trace element data, although limited, add no support to the two-magma theory as originally proposed. A comprehensive chemical study is being carried out on this area by J. C. Bailey in the Geology Department of this university. Bailey's results (personal communication) virtually demand that the Elizabeth Creek and Herbert River Granites are part of the same magma series.

The rocks as a whole are characterised by high uranium, thorium and rubidium contents, moderate lead and low strontium. This distinctive trace element pattern reflects the major element chemistry of these 'highly fractionated' rocks. In 1968, Taylor et al made a

comparative study of the small leucogranite intrusions in the Snowy Mountains N.S.W., and the widespread rhyolites and ignimbrites of the North Island, New Zealand. Although both showed similar major element distributions, they were clearly different in minor elements. The leucogranites were fractionated to the same degree as the Elizabeth Creek Granite and contained the same major element pattern. Taylor considered that the results indicated a partial melting origin for the New Zealand lavas and a fractional crystallisation history for the leucogranites. Only relatively minor volumes (hundreds of cubic miles) of parent magma were needed to derive the small leucogranite bodies. If this interpretation is applied to the North Queensland rocks, however, enormous quantities (the order of 50,000 cubic miles) of liquid parent magma must be involved. Although this is a difficult hypothesis to envisage it is not necessarily infeasible, for no more is needed than a one-mile-thick layer of liquid granodioritic magma under the entire Georgetown Inlier. Another alternative which could be considered is a partial melting process operating on already significantly fractionated source material. A selective 'incompatible element' enrichment from wall rocks in the manner invoked by Harris (1957) and Green and Ringwood (1967) could also explain the high concentrations of these trace elements. All these possibilities, however, must be no more than speculative at this stage.

CHAPTER 6

RUBIDIUM - STRONTIUM STUDIES

A brief Rb - Sr study was included to supplement the work of Richards et al (1966) in providing age information for the interpretation of the rock lead and galena results. The attendant initial ratio information should show whether or not the individual rock types are comagmatic.

The whole rock Rb - Sr method is based on models proposed by Schreiner (1958), Compston and Jeffery (1959), Compston, Jeffery and Riley (1960) and Nicolaysen (1961); it has been adequately summarised in Hamilton (1965, 1968). Treatment of the raw data generally involves the use of isochron plots (Nicolaysen, op. cit.) in which a line of best fit is statistically regressed through the experimental points. The method of regression followed here is based on the work of McIntyre et al (1968) in which allowance is made for known experimental error in both co-ordinates. Several models are used. A model I fit implies that all points fit the isochron within the limits of experimental uncertainty. This is the ideal case, where it is possible to be most confident about the interpretation. In other cases, where the mean square of weighted deviates is significantly greater than unity, different models are applied and confidence in the isochron interpretation is correspondingly diminished. For preference, other supporting lines of evidence should then be sought. As will be seen in succeeding

chapters, these sometimes do not support the model, but rather suggest an alternative explanation of the data. In model II, geological variation in Sr^{87}/Sr^{86} is proportional to that in Rb^{87}/Rb^{86}. This is thought to result either from samples which have the same initial ratio but slightly different ages, or from those which are cogenetic and co-eval but have subsequently suffered a slight internal redistribution of radiogenic strontium. Independent variation of Sr^{87}/Sr^{86} and Rb^{87}/Sr^{86} is covered by model III, in which samples of the same age are considered to have had slightly different initial ratios. Model IV combines the assumptions of models II and III. All uncertainties quoted for ages and initial ratios in the geochronology section are taken at the 95 per cent confidence level. Isotopic composition and Rb and Sr abundances for individual samples are presented in table 20.

A discussion of the controversy surrounding the Rb^{87} decay constant can be found in Hamilton (1965). Perhaps the most authoritative geological determination has been made by Aldrich et al (1956), who compared the radiogenic strontium to rubidium ratio of micas of various ages with concordant uranium ages from comagmatic accessory minerals. Their value, $1.39 \times 10^{-11} y.^{-1}$, is used throughout this thesis. The work of Kulp and Engels (1963), however, has shown that the $1.47 \times 10^{-11} y.^{-1}$ decay constant is more appropriate for comparing the Rb - Sr and K - Ar ages of micas. Goldich et al (1966) have also expressed a preference for this value in a study involving

Table 20

Rb - Sr Isotopic Analyses

Sample No.	Rb (μg./g.)	Sr (μg./g.)	Rb^{87}/Sr^{86}	Sr^{87}/Sr^{86}
		ELIZABETH CREEK GRANITE		
2952	232.1	47.91	14.08	0.7757
2956	316.5	41.20	22.39	0.8056
2957	309.9	60.61	14.87	0.7838
2959	173.1	21.44	23.53	0.8071
2960	494.1	16.30	90.93	1.1162
2967	298.1	24.77	34.19	0.8558
2969	446.9	25.31	52.18	0.9480
2991	1210.1	15.00	259.9	1.8911
2992	518.3	16.33	95.54	1.1444
2995	486.3	23.55	61.26	0.9898
2996	343.8	29.94	33.71	0.8683
2997	553.0	20.30	81.55	1.0826
2998	558.2	17.06	98.72	1.1655
2999	503.8	15.12	100.7	1.1800
		FEATHERBED VOLCANICS		
2961	100.1	202.5	1.428	0.7164
2962	144.2	200.3	2.081	0.7183
2964	231.7	77.02	8.720	0.7475
2973	211.5	97.14	6.303	0.7370
2974	260.7	47.07	16.10	0.7786
2993	348.5	51.14	19.84	0.7912
		GLEN GORDON VOLCANICS		
2976	232.5	103.3	6.511	0.7327
		HERBERT RIVER GRANITE		
2955	169.5	133.0	3.688	0.7281
2965	220.6	162.8	3.920	0.7264
2968	63.32	378.5	0.483	0.7123
2977	241.6	121.3	5.769	0.7346
2978	221.5	158.9	4.032	0.7259
2979	155.0	154.4	2.902	0.7249

Table 20 (cont.)

Sample No.	Rb (µg./g.)	Sr (µg./g.)	Rb^{87}/Sr^{86}	Sr^{87}/Sr^{86}
		MAREEBA GRANITE		
2975	244.9	86.40	8.232	0.7427
		ALMADEN GRANITE		
2953	169.9	175.0	2.812	0.7229
2963	142.9	217.9	1.895	0.7163
2966	171.9	159.6	3.114	0.7247
2971	178.0	172.3	2.989	0.7235
2972	156.4	166.3	2.720	0.7218
		GURRUMBA GABBRO		
2994	7.078	424.2	0.0482	0.7070
		PRECAMBRIAN		
2950L	13.77	204.2	0.1953	0.7394
2950M	105.6	238.4	1.2843	0.7461
2954	96.57	361.8	0.7727	0.7327
2958	77.90	352.5	0.6399	0.7293

both mineral and whole-rock Rb - Sr and K - Ar analyses. To maintain consistency between the ages determined from all three methods in the present study, the K - Ar ages reported hereafter will be adjusted upwards by a factor 1.058 to make them comparable with Rb - Sr ages based upon the 1.39×10^{-11} $y.^{-1}$ Rb^{87} decay constant. This factor, when applied to the widely-accepted Phanerozoic Time-scale (Harland et al, 1964), gives ages of 238, 296 and 365 for the bases of the Triassic, Permian and Carboniferous periods respectively.

The isochron method of presentation has been used to obtain independent age and initial ratio information as much as possible. In some instances, however, the complex geological relations and reconnaissance nature of the investigation have made it necessary to determine age information from one sample alone. This has been done by assuming an initial ratio for the rocks involved on the basis of previous experience. For this reason, and also because such a result is not amenable to statistical assessment, these age estimates are somewhat less certain. The Rb - Sr isotopic analyses of all rocks discussed in this chapter are presented in table 20.

The Featherbed Volcanics

Four whole-rock samples collected from the main cauldron and one from the Tennyson Ring Dyke were analysed (see sample locality map in pocket); these are supplemented by the single measurement published by Richards et al (1966). The age, 297±12 million years, obtained from a model II isochron (see figure 13), is in excellent

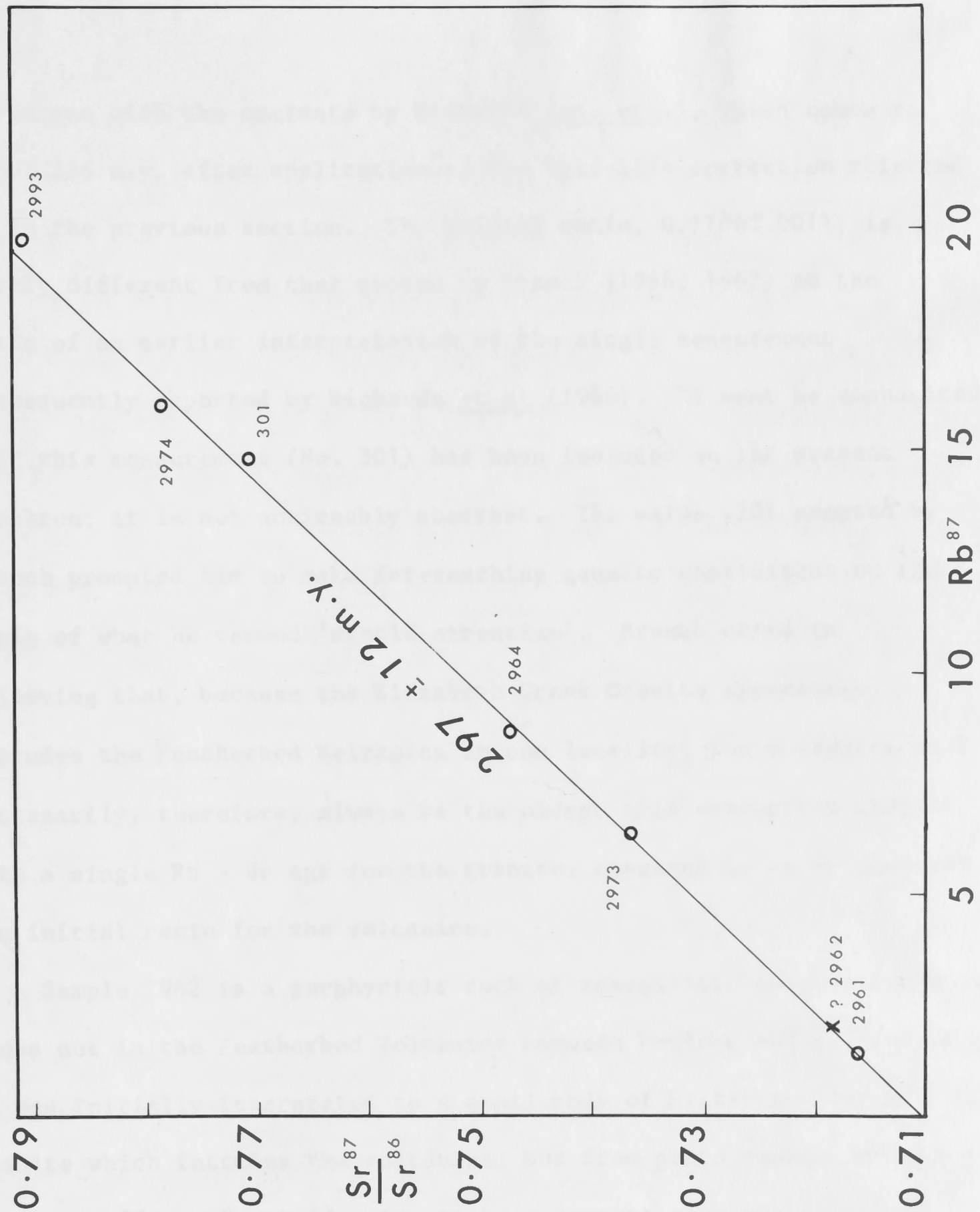

Figure 13. Isochron plot of Rb-Sr data for the Featherbed Volcanics.

agreement with the estimate by Richards (op. cit.), which comes to about 296 m.y. after application of the half-life correction referred to in the previous section. The initial ratio, 0.7106±.0011, is vastly different from that quoted by Branch (1966, 1967) on the basis of an earlier interpretation of the single measurement subsequently reported by Richards et al (1966). It must be emphasized that this measurement (No. 301) has been included on the present isochron; it is not noticeably aberrant. The value .701 adopted by Branch prompted him to make far-reaching genetic conclusions on the basis of what he termed 'mantle strontium'. Branch erred in believing that, because the Elizabeth Creek Granite apparently intrudes the Featherbed Volcanics in one locality, the volcanics must necessarily, therefore, always be the older; this assumption coupled with a single Rb - Sr age for the granite, resulted in an erroneously low initial ratio for the volcanics.

Sample 2962 is a porphyritic rock of adamellitic composition which crops out in the Featherbed Volcanics between Petford and Wolfram Camp. It was initially interpreted as a small body of Elizabeth Creek Granite which intrudes the volcanics, but from petrographic and trace element evidence I consider it may be a remnant of a coarsely recrystallised volcanic flow. Inclusion of this point on the isochron plot leaves the age (299±12 m.y.) and initial ratio (0.7102±.0010) virtually unaltered.

It may be permissible to sub-divide the data further according to one of the assumptions of a model II isochron (same initial ratio but different age). From the diagram it can be seen that five of the points fit a straight line with the limits of experimental uncertainty, and the line drawn through the other two (2964 and 2974) yields the same initial ratio. From this it might be inferred that the volcanics were extruded at two distinct times, 302 and 291 m.y. ago. If this is the case the Tennyson Ring Dyke was formed by the older event. The alternative explanation is that the rock has not remained a closed system with respect to Rb and Sr. Whatever the true explanation, the Featherbed Volcanics form a valuable marker horizon between the Carboniferous and Permian rocks of this area (see The Phanerozoic Time Scale - editor Harland, 1964).

The Elizabeth Creek Granite

As this granite (s.l.) is often highly enriched in Rb it is particularly amenable to accurate dating, but generally yields somewhat imprecise initial ratio information. Fourteen samples (including 2962) were collected from the study area. When regressed these yield an age of 327±5 m.y. and an initial ratio of 0.710±.005. Although the results fit a model III isochron in theory they obviously do not fulfil the geological implications. For example 2962 is either the same age as, or younger than the volcanics, hence clearly younger than 327 m.y. Thus the assumption of equivalent ages but different initial ratios obviously does not hold. Application

of model II yields an age of 330±9 m.y. and an initial ratio of 0.7090±.0012, which only disagrees significantly from the earlier result in initial ratio uncertainty. By neglecting the possibly volcanic 2962, which also controls the initial ratio to a large extent, the age becomes 327±5 m.y. and the initial ratio 0.710±.006 (see figure), once again with a model III fit. As before this model indication must not be taken too strictly at its face value, for the K - Ar results of Richards et al (1966) suggested a significant age spread for this granite. A model II interpretation yields the barely different parameters 323±12 m.y. and 0.712±.005. Thus it can be seen that model selection causes only minor age and initial ratio differences, but may be somewhat misleading as indication of the cause of geological variation; where possible it may well be better to select the appropriate model on the basis of geological criteria.

The mean square of weighted deviates (M.S.W.D.) amounts to 43 when all samples are considered together. This indication of a substantial geological effect could be taken as warning of incorrect classification - ie. that more than one granite, differing either in age or origin, has been included on the isochron. In an attempt to minimise such a possibility the nine samples from the large mass of tin-bearing granite in the Emuford - Mt Garnet - Ravenshoe area were regressed as a separate group. The resulting age, 326±7 m.y., and initial ratio, 0.713±.009, are indistinguishable from the other

results. Once again the scatter is geologically significant, showing that even in this relatively restricted area real age or initial ratio differences exist, or alternatively, completely closed systems were not attained.

The results have a twofold significance. The initial ratio, although somewhat uncertain, is indistinguishable from that obtained for the Featherbed Volcanics. This supports the conclusion of Branch (1961, 1966) that the two are in fact comagmatic. The indicated age of the granite is greater than any obtained by the K - Ar method (Richards et al, 1966), and clearly greater than that derived for the Featherbed Volcanics in this study. Thus the conclusions of Branch (1961, 1966, 1967) and Blake (1968) are incorrect and the definite example of the reverse relationship at Wolfram Camp (de Keyser and Wolff, 1964), and possibly also Bamford Hill (Branch, 1966) are probably atypical. Furthermore, Blake's argument (op. cit.) that the Elizabeth Creek Granite in the Emuford - Irvinebank area has caused extensive mineralisation in the volcanics and must therefore be younger, is apparently invalid on the basis of the nine samples from this area. In particular, interpretation of the zoned mineral distribution about this Elizabeth Creek Granite mass must be treated with some caution; that part,at least,of the lead zone occurring in the volcanics can not have been derived from the nearby outcropping granite (see figure 1).

From the relationship depicted for the Lappa area (see Atherton Sheet in back pocket) at least a partial justification of the isotopic analysis is possible. In this area the Tennyson Ring Dyke is thought to be continuous with at least part of the main mass of volcanics (Branch, 1966); isotopically it appears to be the same age or slightly older, and is shown as being faulted against the granite. In 1967 J. C. Bailey returned to examine this area and found that the granite is definitely sheared by the dyke and must therefore be older. On his 1966 map Branch shows that the marginal fault around the volcanics cuts the Elizabeth Creek Granite in a number of restricted locations: just north of Lappa Junction, also east of Petford, east of Orient Camp, at Wolfram Camp and at the northern end of the cauldron on the Mossman Sheet. Many of these, however, are not believed by other workers. A case in point is the commentary by de Keyser and Wolff (1964) on the Wolfram Camp locality (see also Atherton Sheet in back pocket) which is supported by J. C. Bailey (pers. comm.). It is difficult to reconcile this claim for marginal faults with the statement that the granite postdates the volcanics, if it is true that the cauldron subsidence and the extrusion of the volcanics were essentially coincident (Branch, 1966, 1967). J. C. Bailey (personal communication) has also found from field relations that there were two periods of Elizabeth Creek Granite intrusion in and around the Claret Creek Ring Complex.

The overall evidence, then, points to at least two periods of granite intrusion as was deduced by de Keyser and Wolff (1964) from field observations; most of the granite appears, however, to be older than the Featherbed Volcanics.

The Herbert River and Almaden Granites

The data are presented in figure 14 along with four analyses of Precambrian rocks; the latter are naturally not included in any of the following regressions. When all 11 points are included an age of 320±53 m.y. and an initial ratio of 0.710±.002 are obtained. The large age uncertainty derives from a significant geological scatter (M.S.W.D. = 19) and the low Rb/Sr ratio of most samples. A remarkable feature of this diagram is that all five Almaden points fit a discordant straight line within the limits of experimental uncertainty.

Two separate explanations could be invoked. a) The line may truly represent an isochron, with age 475±50 m.y., and initial ratio 0.704±.002. b) It may be an expression of the mixing of granite magma with material from other sources. Precambrian rocks and basic igneous rocks occur in the neighbourhood; either or both could be involved.

Alternative a) seems fairly easily eliminated. In this region Richards and co-authors found in one rock a biotite which corrects to 1100 m.y., and also two biotite-hornblende pairs which gave a fairly consistent age around 310 m.y. (again corrected). Taken together, these data furnish a reasonably convincing argument against a fairly extensive

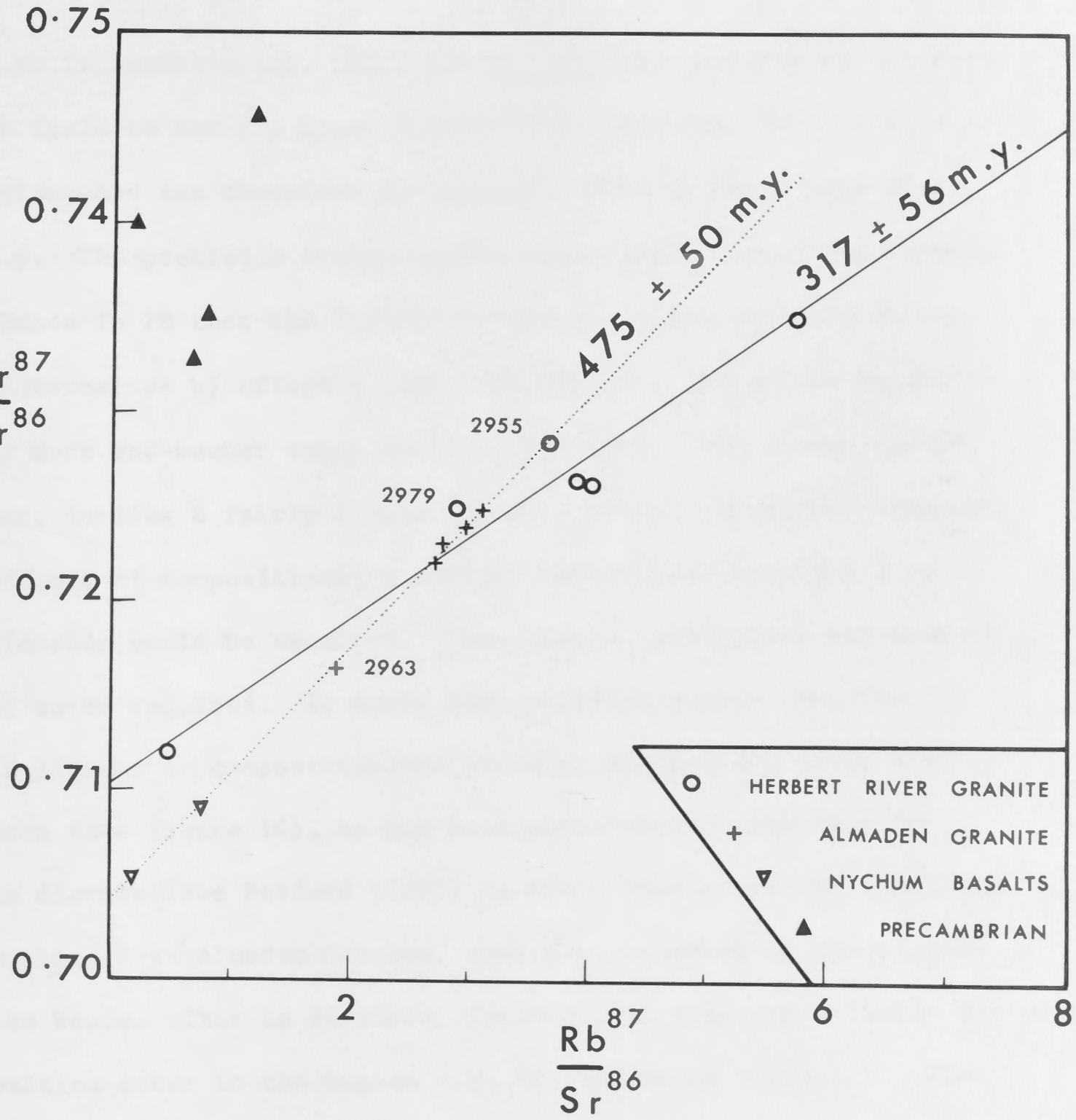

Figure 14. Isochron plot for Herbert River and Almaden Granites.

475 m.y. intrusive event. Moreover, the Almaden Granite can be seen in the field to cut the Upper Silurian - Lower Devonian Chillagoe Formation, and can therefore be expected to be no older than about 425 m.y. The precision limits quoted above imply that there is only one chance in 20 that the 'isochron' and the field evidence agree.

Alternative b) offers a number of possible mechanisms in which two or more end-member types could be involved. The linear spread, however, implies a fairly simple system. If any postulated component had a range of compositions, a scatter rather than straight-line relationship would be expected. Thus simple, well-mixed end-members appear to be required. It seems reasonable to assume that the original granitic composition was close to the Herbert River Granite isochron (see figure 14), as has been postulated by Branch (1966). If the diorite from Petford (2963) is truly related to the remaining rocks classed as Almaden Granite, then one component of the mixture must be basic. This is feasible, for basaltic rocks of suitable isotopic composition occur in the region e.g. in the Nychum Volcanics. The acidic member cannot, however, be pure Herbert River Granite type as most of the Almaden sample points lie above the Herbert River Isochron. Admixture with Precambrian material, on the other hand, is quite possible and would produce a magma with the right isotopic characteristics. As can be seen from figure 14 the Precambrian samples have high Sr^{87}/Sr^{86} and low Rb/Sr ratios; hence a small proportion of such material will shift a granitic composition upwards and to the left. Contamination

with such Precambrian material is advanced as the explanation of the two Herbert River Granite samples, 2955 and 2979, from the Dargalong and Ootann areas respectively.

The implication of this discussion is that contamination of the acid magma with Precambrian material should occur first, resulting in a reasonably homogeneous melt. This then is one end-member in a less well-stirred mixture with the basic end-member. This would yield a linear initial spread of points which could then grow over the succeeding time to the observed anomalously old 'isochron'. A fuller treatment of the mixing-line model will be given in the section on the Nychum Volcanics (chapter 8).

In principle there are other ways of generating such a line from a more complicated mixing, but these involve ratios of mixing proportional to Rb/Sr ratio and thus appear to be less likely. It is not possible to assess the role of the Palaeozoic sedimentary rocks in the postulated mixing process, or the overall magma generation, as no isotopic information relevant to this aspect is available.

Any interpretations of the age or origin of the Almaden Granite are handicapped by the general chemical uniformity of this rock type. However, an abnormal relationship was also observed on the K/Rb plot which is difficult to reconcile with 'normal' magmatic evolution. J. C. Bailey (pers. comm.) has also observed chemical relationships for many other elements which distinguish the Almaden Granite from

the Herbert River and Elizabeth Creek Granites. In particular a P_2O_5 vs MgO diagram clearly delineates two divergent linear trends, one of which involves the Elizabeth Creek and Herbert River Granites and the Featherbed Volcanics, and the other the Almaden Granite, included xenoliths, and the Nychum basalts. Thus mixing may well have been involved in the formation of the Almaden granite; more comprehensive evidence will be presented later to show that the spacially-associated Nychum Volcanics could also be the result of such a process.

By regressing the remaining Herbert River Granite points, after exclusion of the Almaden samples and the apparently contaminated 2955 and 2979, an age of 296±43 m.y. and initial ratio of 0.7102±.0016 is obtained. Inclusion of these two discrepant samples yields 317±56 m.y. and 0.7102±.0013. The results, then, confirm the observation reported by Richards et al (1966) that no significant age difference exists between the Herbert River and Elizabeth Creek Granites, even though, in restricted localities, the latter nearly always intrudes the former. Mineral isochrons will be needed for accurate resolution of the Rb - Sr age of the Almaden Granite, as each whole-rock sample may have been characterised by a unique initial ratio.

In all regressions the initial ratio, also, of the Herbert River Granite shows no detectable difference from that of the Elizabeth Creek Granite or the Featherbed Volcanics. Because of the low Rb/Sr

in most samples it is also relatively precise, and the statement of similarity to the volcanic value can be made with some confidence. Thus an interpretation which demands an anatectic origin for the Herbert River Granite and a simatic origin for the Elizabeth Creek Granite and Featherbed Volcanics seems most unlikely; all appear rather to have come from the same source at about the same time. As mentioned in Chapter 5, J. C. Bailey has also been unable to demonstrate a distinctive trace element pattern for this granite. On these grounds, then, the division between the two granites is an arbitrary one, based on mineralogy alone, which has no genetic significance. The new data justify rather the assertion by de Keyser et al (1959, 1964) that the granite varieties are numerous modifications of the same batholith with no major genetic differences. The line of thought typified by Branch (1966):- 'In this Bulletin the Upper Palaeozoic acid igneous rocks are divided into two groups on genetic grounds', must therefore be rejected.

Miscellaneous Results

A small number of isolated analyses yields further limited isotopic information.

Data on the four Precambrian samples indicate that assimilation by later magmas will yield rocks relatively enriched in radiogenic strontium.

The Gurrumba Gabbro (2994) is so depleted in rubidium with respect to strontium ($Rb^{87}/Sr^{86} = 0.05$) that its present day Sr^{87}/Sr^{86}

ratio is virtually unchanged from its initial value. This value, 0.7070, has not been found in any uncontaminated rocks in the area. It is also difficult to derive this value from a contamination process, as mixing with any of the known rock types should have significantly altered the low Rb content of seven μg./g. Thus, the gabbro appears to be unrelated to surrounding penecontemporaneous rocks.

The single measurement on the Slaughter Yard Creek Volcanics plots significantly below the Featherbed isochron. Thus either the sample is younger, or it possesses a lower initial ratio, or it is weathered, or perhaps the explanation involves some combination of the three, in a proportion difficult to assess.

A little more information can be extracted from the lone analysis on rock 2975. This rock has been classed by Branch as Herbert River Granite, by Blake as a separate unit which he calls Watsonville Granite, but is considered by the author to be Mareeba Granite. Except for a dearth of muscovite it is petrographically very close to the Mareeba Granite, and has a suitable chemical composition. De Keyser (pers. comm.) and Blake (pers. comm.) also admit to this possibility. A most cogent argument comes from the work of Richards et al (1966), who have demonstrated a K - Ar age for this intrusion of 279 m.y. (after normalisation by the factor 1.058 to enable direct comparison with the Rb - Sr result) a value indistinguishable from the sharply-defined event that produced the Mareeba Granite. It would appear that geologists have recognised this possibility before but have been

reluctant to categorise it because this intrusion is further south than the main batholith. If this K - Ar age is used to calculate the initial ratio of the granite, the result is 0.7109, a value indistinguishable from that of the Elizabeth Creek and Herbert River Granites and the Featherbed Volcanics. So, if this granite is indeed a member of the Mareeba batholith, and if it is a typical representative, the origin of this suite is probably the same as the Herbert River Granite (as was suggested by Branch, 1966), the Elizabeth Creek Granite, and the Featherbed Volcanics.

Individual Age Calculations

The significant scatter for all isochrons (ie. none of them is a model I fit) indicates a rather complex geological history, which may be partially or completely explained by the age differences demonstrated by Richards et al (1966). It is important that ages of individual intrusions should be known as accurately as possible for lead-isotope initial ratio calculations. These may be derived for individual samples by assuming a particular strontium initial ratio for samples which do not fall on a documented isochron. The accuracy of such an age estimate depends on the amount of Rb enrichment and the correctness of the assumed initial ratio. Most of the regressions have yielded an initial ratio indistinguishable from 0.710, which is therfore a reasonable tentative value for individual age calculations. Furthermore, if 2968 (see table 20) is representative, it is particularly useful for a more precise

estimate, since with a Rb^{87}/Sr^{86} ratio of only 0.483, its initial ratio is virtually unaffected by assumed age. A suitable age estimate may be obtained by first applying the half-life correction, discussed in the introduction of this chapter, to the estimate of Richards et al (1966). The resulting 296 m.y. is then further adjusted upwards to account for possible argon loss (see next page). From the resulting estimate of 310 m.y., an initial ratio of 0.7102 is calculated, a result which agrees remarkably well with the Featherbed regression using the other poorly-enriched sample, 2962.

We proceed, then, on the reasonable extension from the available observations, that the initial ratio 0.7102 applies to all igneous rocks of the region, apart from a few exceptions. These are the poorly-enriched rocks with consequently large uncertainties, and the Almaden Granite, which may be typified by a variable initial ratio; these rocks are excluded. The resulting ages are given in table 21 and are shown graphically in figure 15. 'Errors' quoted are the number of years by which each age will change for a change of 0.0010 in the initial ratio. The Elizabeth Creek Granite is seen to yield precise ages whilst the Herbert River ages are subject to greater uncertainty. Two of the three rocks apparently 350 m.y. or older, outcrop on the margins of intrusions immediately adjacent to Precambrian rocks, and are therfore interpreted as being contaminated with radiogenic strontium. The other (2979, near Almaden) is also believed to be contaminated. A K - Ar measurement on 2955 (near

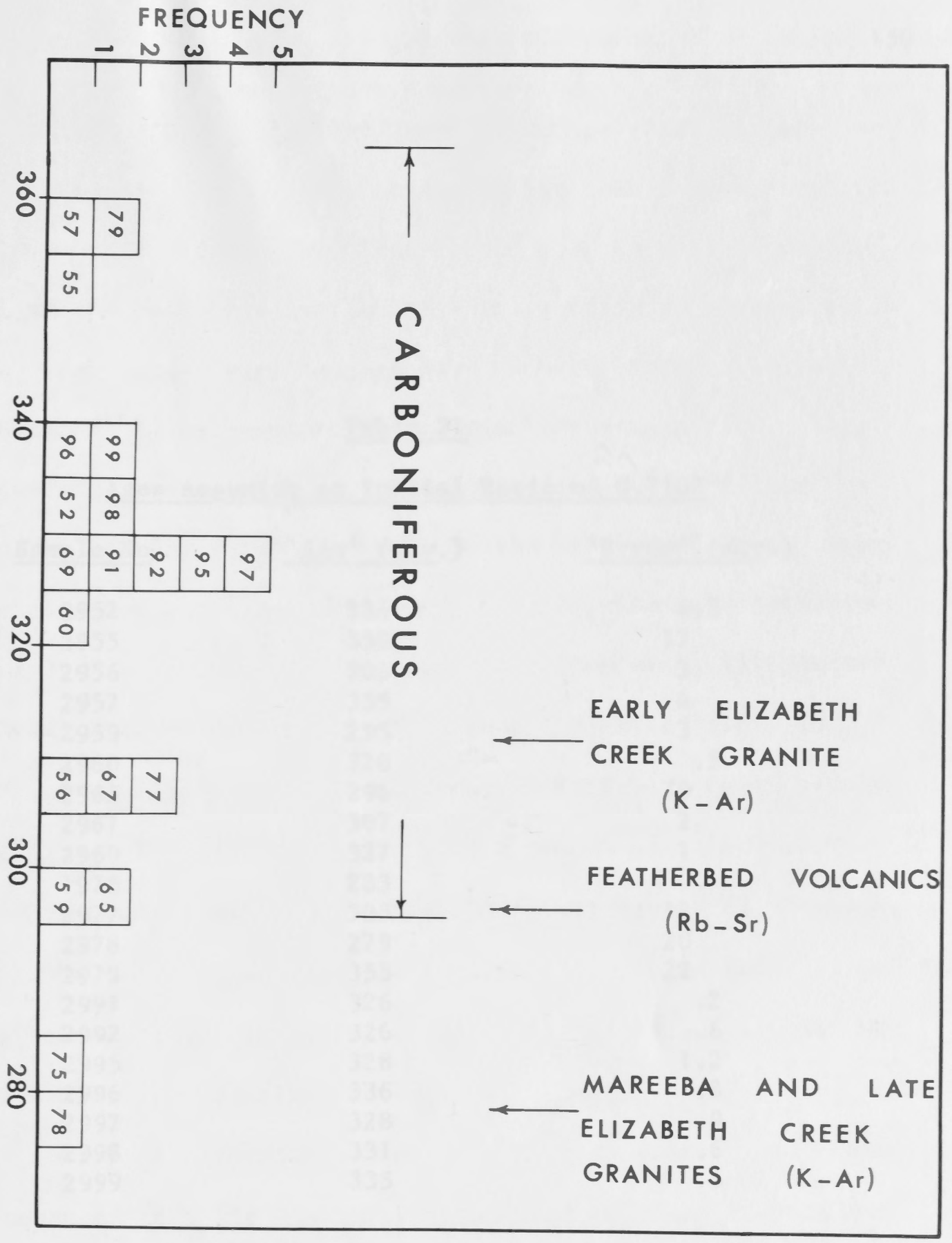

Figure 15. Ages calculated from assumed initial ratio.

Table 21

Ages Assuming an Initial Ratio of 0.7102

Sample No.	'Age' (m.y.)	'Error' (m.y.)
2952	334	4.5
2955	350	17
2956	306	3
2957	355	4
2959	295	3
2960	320	.5
2965	296	19
2967	307	2
2969	327	1
1975	283	9
2977	305	12
2978	279	20
2979	355	22
2991	326	.2
2992	326	.6
2995	328	1.2
2996	336	1.8
2997	328	.9
2998	331	.6
2999	335	.6

Dargalong; Richards et al, 1966) yielded an age which corrects to 301 m.y. These rocks possibly belong to the main intrusive period at 327 m.y. (see figure 15). This latter time is well documented, as most of the rocks are particularly insensitive to initial ratio errors. The younger ages can not have resulted from assimilation of Precambrian rocks by magma from the main intrusive period. This again could be taken to support the suggestion by the former K - Ar study of a definite range of ages. On the other hand, even though the K - Ar ages have been normalised to agree with ages determined from the 1.39×10^{-11} $y.^{-1}$ Rb decay constant they are still younger than those obtained by the Rb - Sr method (refer to figure 15). Richards et al (1966) also show a group of Elizabeth Creek samples of similar age to the Mareeba Granite, a result which was not observed in the present study. A sampling difference is unlikely; sample 2959, which comes from the area in which these young Elizabeth Creek ages were found (at latitude 18°00'S) indicates an older age by the Rb - Sr initial-ratio method.

As no K - Ar ages younger than the Mareeba Granite are recorded, it is inferred that the last well-documented Palaeozoic event is associated with the age discrepancies. Two explanations seem possible. The widespread magmatism may have persisted for a sufficient period in a temperature range where argon loss could continue after closing of the total-rock Rb - Sr system. After emplacement of the Mareeba Granite, the region cooled relatively quickly with no

subsequent argon loss. Alternatively, the terrain could have cooled after the first intrusion and the postulated resetting may have been entirely associated with the Mareeba event. The results of Goldich et al (1966), who have shown that the Rb - Sr total-rock system is less susceptible to open-system behaviour than the K - Ar system in biotite, would appear to support either alternative.

Except for No. 2978 all analysed Herbert River and Elizabeth Creek Granite samples appear to have been emplaced in the Carboniferous; it is naturally tempting to suggest that sample 2978 was formed by the Mareeba event, and is in fact a representative of this granite type.

The age assigned to the Almaden Granite for lead isotope calculations must be chosen somewhat arbitrarily, but the main period of intrusion at 327 m.y. appears most appropriate.

CHAPTER 7

WHOLE-ROCK LEAD RESULTS

U^{235}-Pb^{207} dating of relatively young systems, such as the 300 m.y. of this study, produces ages particularly prone to error. In this time period the 207 radiogenic addition from the small amounts of U^{235} is very small, of no greater magnitude than the experimental uncertainties. The 207/204 vs 206/204 plot, and associated equations which are also widely used for age information, are likewise affected by the same uncertainty. Relatively precise ages, then, can only be gained from the U^{238}-Pb^{206} and Th^{232}-Pb^{204} isochron methods, and only these will be considered. The two rock units for which precise Rb-Sr ages were derived are discussed separately. This is followed by a discussion of the initial ratios derived for all the rocks. The isotopic ratios of all rocks, and data derived therefrom, are presented in table 22. The U^{238}/Pb^{204} (μ) and Th^{232}/Pb^{204} (W) values for each sample are derived from the concentration data in table 19.

The Featherbed Volcanics

The U^{238}-Pb^{206} isochron diagram for this unit is presented in figure 16. Vertical bars represent the average 206/204 mass-spectrometric uncertainty based on a slightly pessimistic appraisal (0.2 per cent) of the repeated analyses of Pb245 (see chapter 2). Most of the uncertainty of these points is in the horizontal direction, however, and arises from the imprecision in

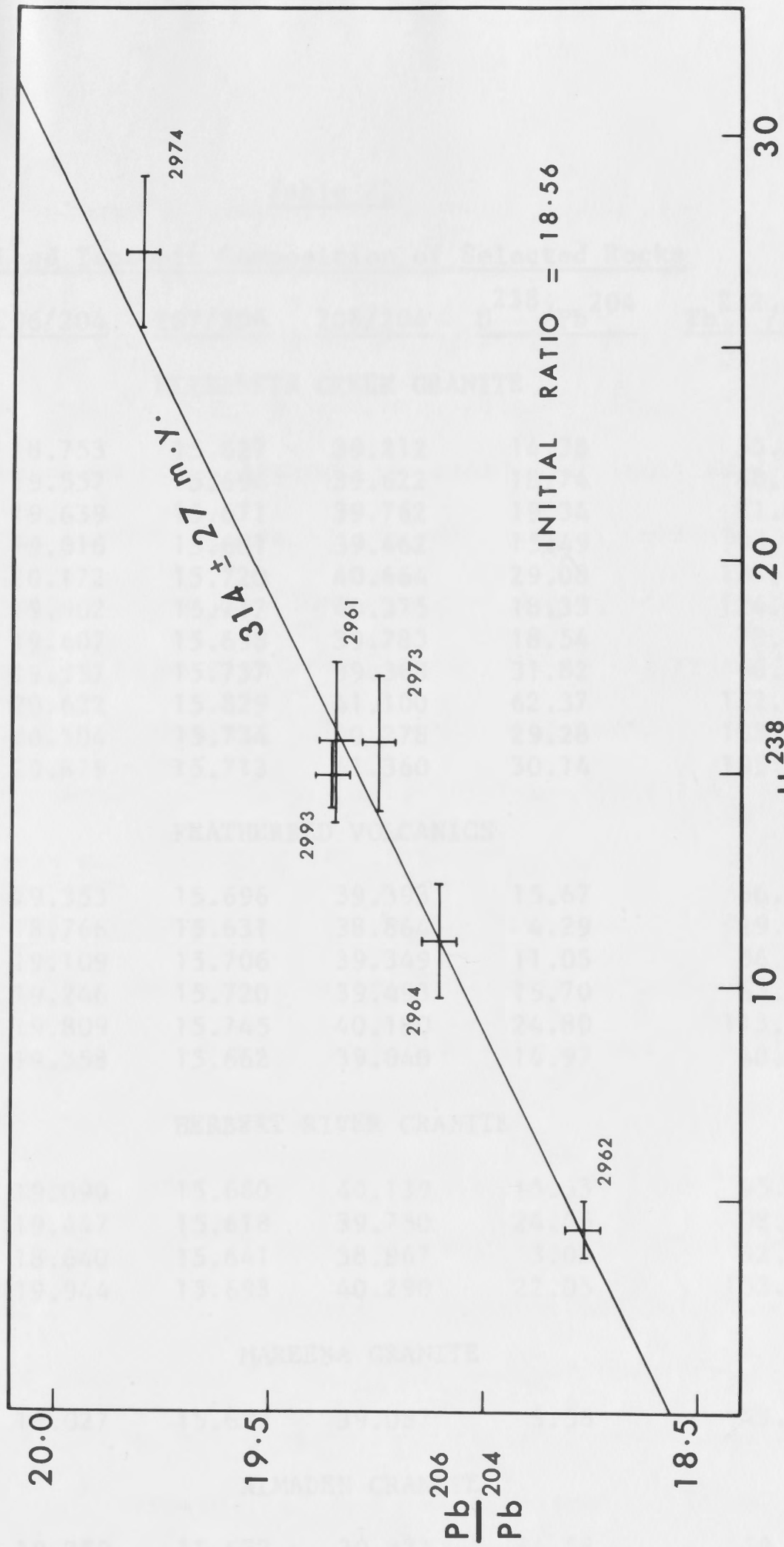

Figure 16. U^{238} - Pb^{206} isochron diagram for the Featherbed Volcanics.

Table 22

Lead Isotopic Composition of Selected Rocks

Sample No.	206/204	207/204	208/204	U^{238}/Pb^{204}	Th^{232}/Pb^{204}
			ELIZABETH CREEK GRANITE		
2952	18.753	15.627	39.212	14.38	55.23
2956	19.557	15.694	39.622	18.74	68.09
2957	19.639	15.671	39.762	19.34	81.06
2959	19.016	15.681	39.462	15.49	90.10
2960	20.172	15.720	40.664	29.08	123.18
2967	19.902	15.717	40.375	18.33	124.01
2969	19.607	15.698	39.783	18.54	78.45
2991	19.357	15.737	39.368	31.82	66.52
2992	20.622	15.829	41.100	62.37	152.07
2995	20.504	15.734	40.278	29.28	103.74
2997	20.879	15.713	41.360	30.14	195.10
			FEATHERBED VOLCANICS		
2961	19.353	15.696	39.393	15.67	66.27
2962	18.766	15.631	38.864	4.29	29.24
2964	19.109	15.706	39.349	11.05	56.84
2973	19.246	15.720	39.493	15.70	63.66
2974	19.809	15.745	40.180	24.80	113.30
2993	19.358	15.662	39.040	14.97	40.77
			HERBERT RIVER GRANITE		
2955	19.090	15.680	40.139	15.55	95.77
2965	19.447	15.618	39.750	24.45	98.87
2986	18.640	15.641	38.967	3.03	32.17
2977	19.944	15.693	40.290	22.05	103.06
			MAREEBA GRANITE		
2975	19.027	15.637	39.087	9.56	43.05
			ALMADEN GRANITE		
2953	19.289	15.672	39.321	14.58	59.54
2963	19.323	15.627	39.255	12.79	55.00
2971	19.155	15.657	39.298	9.27	73.12
2972	19.427	15.670	39.696	18.96	88.73
			PRECAMBRIAN		
2954	17.453	15.555	38.768	2.64	12.97

the X-ray fluorescence determinations of uranium and lead concentrations. Both errors are taken at the 95 per cent confidence level. The points are regressed according to the method of York (1969) using a computer program made available by him. This assumes errors in both co-ordinates and weights each point individually, according to the inverse square of the experimental uncertainties referred to above. Large lead loss occurred during the treatment of sample 2973, making it particularly susceptible to contamination; it has consequently been allotted only one third the weight of the other points in the regressions. Sample 301, which was included on the Rb - Sr plot, was not available for this analysis.

The regression through the six points, which include the controversial 2962 (see the Featherbed Volcanics section of the previous chapter), yields an age of 314±27 m.y., compared with the 299±12 m.y. of the corresponding Rb - Sr isochron; the initial ratio is 18.56. An age of 312±37 m.y. and initial ratio of 38.42 is derived from the Th^{232}/Pb^{208} system (figure 17). Although these ages are not as precise as that determined from the Rb - Sr method they nevertheless demonstrate consistency between the three techniques. This in turn indicates that the Rb - Sr results can be treated with some confidence, as it is most unlikely that all systems would be perturbed to the same degree (contrast Nychum Volcanics of chapter 8).

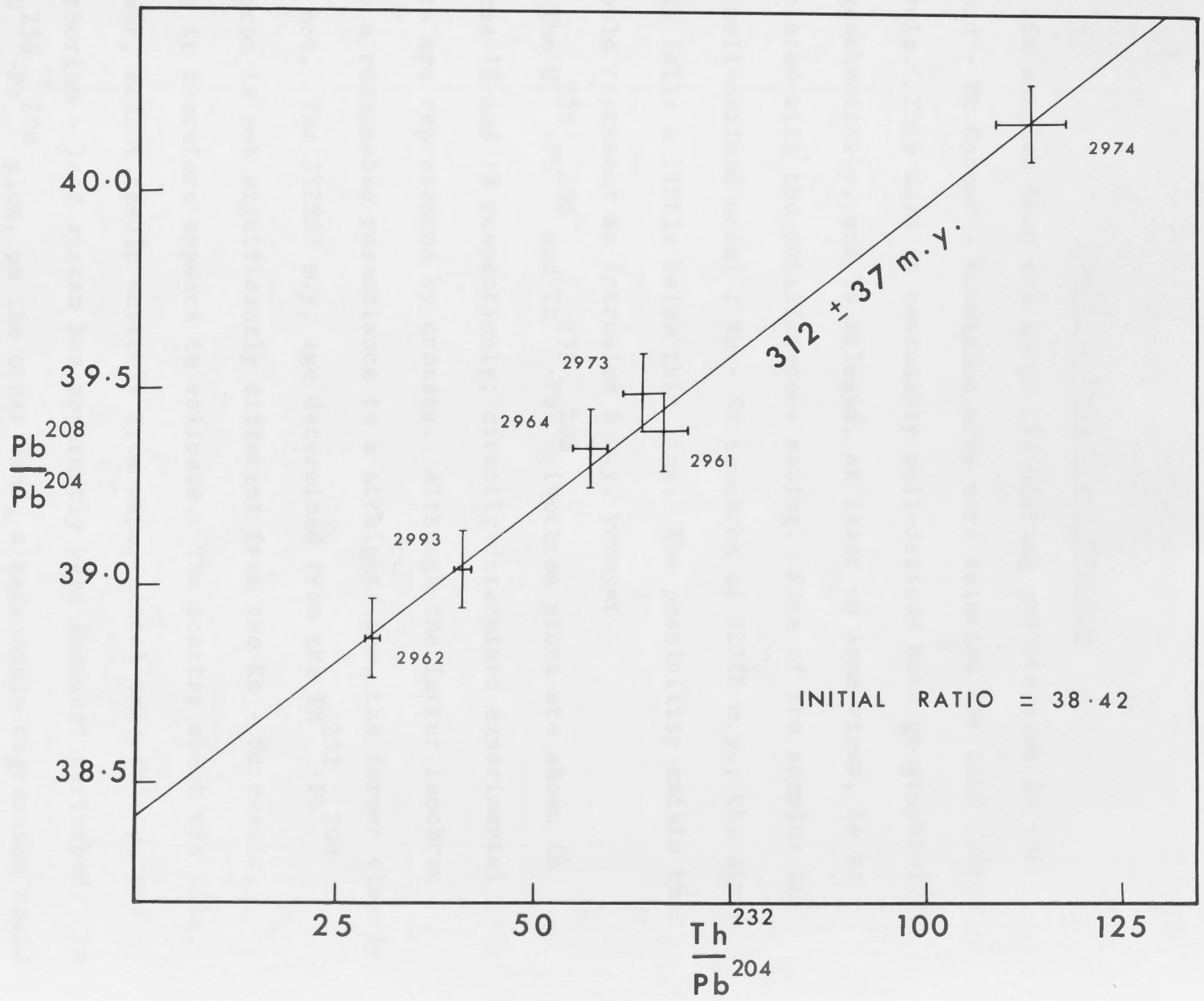

Figure 17. Th^{232} - Pb^{208} isochron diagram for the Featherbed Volcanics.

The Elizabeth Creek Granite

Six samples from the large tin-bearing granite mass in the Emuford - Mt Garnet - Ravenshoe area were selected for lead isotopic analysis. This mass is reasonably well-defined both geographically and geochemically, and is alleged, at least on some views, to be associated with the metalliferous zoning. Five of the samples lie on a well-defined model I Rb - Sr isochron of 327±6 m.y.; the sixth (2960) falls a little below this line. The possibility exists that it could represent an intrusion 6 m.y. younger.

The U^{238}-Pb^{206} and Th^{232}-Pb^{208} isochron plots are shown in figures 18 and 19 respectively; directly-determined experimental points are represented by crosses. Although the latter isochron bears a reasonable resemblance to a straight line, the former clearly does not. The 332±27 m.y. age determined from the Th^{232}-Pb^{208} isochron is not significantly different from the Rb - Sr result, which it therefore appears to validate. The scatter about the line, however, cannot result entirely from experimental uncertainty, and the thorium - lead system has apparently been somewhat perturbed. In the U^{238}-Pb^{206} plot, on the other hand, a reasonable regression could not even be attempted. It is proposed that the scatter in this diagram is the result of relatively recent open-system behaviour of uranium. On the other hand, since the Th^{232}-Pb^{208} plot is reasonably concordant, it appears that neither lead-208 nor thorium have migrated in or out of the rock to any marked extent. Tilton et al

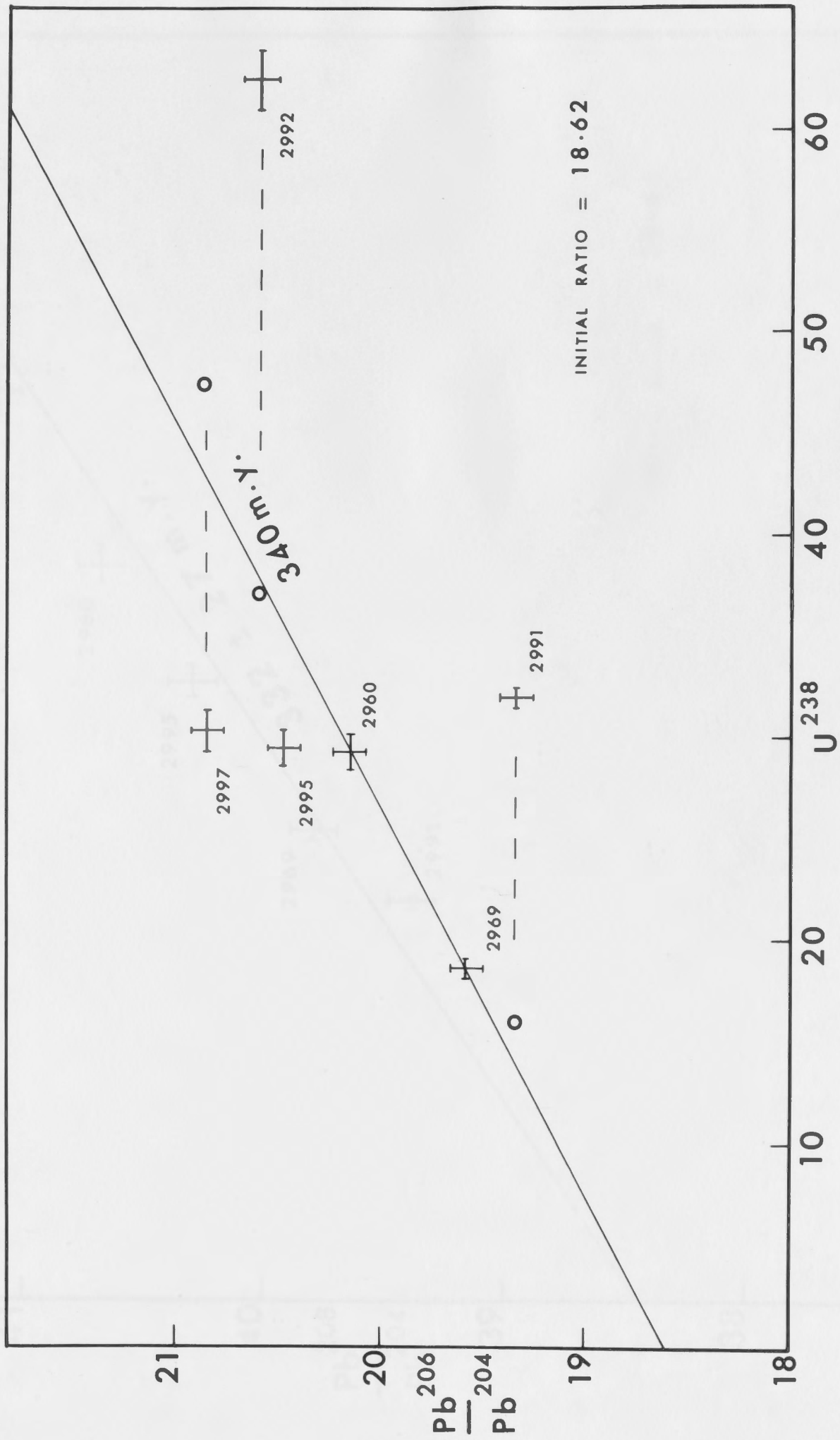

Figure 18. U^{238} - Pb^{206} isochron diagram for the Elizabeth Creek Granite.

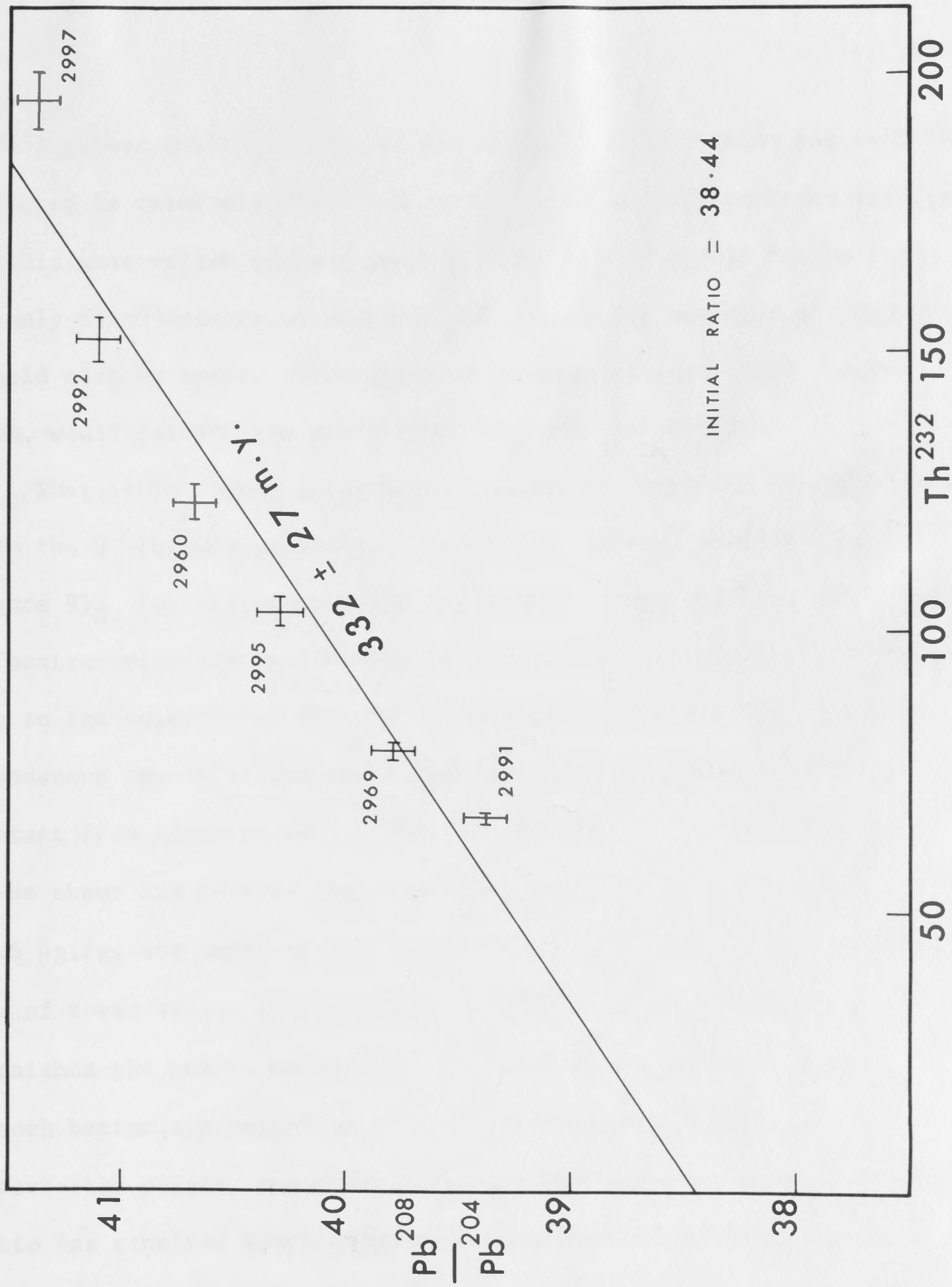

Figure 19. Th^{232} - Pb^{208} isochron diagram for the Elizabeth Creek Granite.

(1955) showed that more thorium and lead-208 than uranium and lead-206 occurred in chemically unstable environments in a Precambrian granite. If this observation were of general relevance it should follow that if only minor amounts of lead-208 were lost, the movement of lead-206 should also be small. Discrepancies in the uranium - lead system, then, would result from preferential movement of uranium.

That it is indeed uranium which moves is supported by deductions from the U -Th plot presented in the trace element section (ref. to figure 9). In this diagram the points 2991, 2992 and 2997 were found to scatter widely from the typical rock trend. If this is principally due to the movement of uranium as postulated, the original uranium abundances can be estimated by drawing lines of constant thorium content from these points to the average Th/U ratio, which appears to be about 3.9 in this region of the graph. Values of 10.7, 13.3 and 16.6 μg./g. are obtained for samples 2991, 2992 and 2997 respectively. Use of these values to calculate new U^{238}/Pb^{204} co-ordinates furnishes the points marked by circles in figure 18. These give a much better approximation to a feasible isochron than the uncorrected points, and provide further confirmation that the Th/Pb ratio has remained comparatively un-affected. Thus it appears that the U - Th diagram provides a useful guide to rocks in which uranium has recently migrated. If this is so, this test should be used as a routine geochemical tool before lead isotopic analysis to facilitate rejection of clearly unsuitable samples.

Confirmation of the extreme susceptibility of uranium to weathering has come from the work of Barbier and Ranchin (1969) who have shown that uranium movement begins when alteration is virtually restricted to partial oxidation of ferrous iron. It is now commonly accepted that much of this mobility is controlled by the high solubility of hexavalent uranium in carbonate-bearing solutions (e.g. Naumov, 1959); thorium, which cannot exist in this higher oxidation state, is relatively immobile.

The reliability of the remaining granite analyses which cannot be tested with precise Rb - Sr comparisons may well be much greater than would appear from these data. The argument for this rests on the rigour of the sample selection criteria. Only two of the samples considered on this diagram (2960, 2969) were collected by the author; the other four, although blasted, were not primarily selected with lead isotopic analysis in view, and cannot therefore be guaranteed to be of the same standard of freshness. The two rocks collected by myself could be interpreted as falling on a 340 m.y. U - Pb isochron, a value in reasonable agreement with the Th - Pb isochron and the Rb - Sr result. Thin sections were examined, but no objective selection criteria could be detected. If the U - Th diagram (figure 9) can indeed be taken as a weathering guide, then 2967 is the only other sample which might be markedly weathered. Although Featherbed sample 2993 plots a little away from the normal trend it

does fall close to the Featherbed isochron, and most probably indicates the extent of the primary scatter of the U/Th ratio.

From the isochrons shown in figures 18 and 19, and the 207/204 content of samples 2960 and 2969, the initial ratio of the large tin-bearing mass of Elizabeth Creek Granite is estimated to be 204 : 206 : 207 : 208 = 1 : 18.62 : 15.64 : 38.44. This result agrees in essence with that for the Featherbeds (1 : 18.56 : 15.64 : 38.41). The initial ratios, then, present further evidence for the comagmatic origin of these two units suggested by Branch (1966, 1967). However, whereas the rocks appear to have been derived from a common source region, the trend of the lead results adds support to the Rb - Sr age in suggesting different generation times, with the volcanics being distinctly younger than this granite mass (see table 23).

Table 23

Summary of Age Determinations for the

Elizabeth Creek Granite and Featherbed Volcanics (in m.y.)

	Rb^{87}/Sr^{87}	U^{238}/Pb^{206}	Th^{232}/Pb^{208}
Elizabeth Creek Granite	326±7	?340	332±27
Featherbed Volcanics	298±12	314±27	312±37

Other Rock Types

The initial compositions of all rocks, excluding the Nychum Volcanics (discussed in the next chapter) and the samples of Elizabeth Creek Granite not collected by the author (which are probably weathered), are presented in table 24 and on the conventional 207/204 vs 206/204 plot in figure 20. Ages used in the calculation are derived from the Rb - Sr results of table 21, the previous K - Ar dating, and inferred geological relationships; these ages are also shown in table 24. The average initial ratios, derived by assumption of the Featherbed Volcanics Rb - Sr age are also presented. Uncertainties associated with concentration estimates amount to about ±0.1 in the 206/204 ratio; mass-spectrometric precision is indicated by the oval field. All errors are expressed at the 95 per cent confidence level. A ten million year error in age estimate will, in most cases, affect the 206/204 ratio by less than .03. The curve shown for reference is a recalculation of the single-stage growth curve by Cooper, Reynolds and Richards (in preparation) in which allowance has been made for systematic isotopic fractionation of the gas-source data. The position of sample 2967 must be treated with extreme caution, as the U - Th plot suggests that it has lost uranium; correction for this would bring its initial ratio back to within the main group of points to the left.

Most of the results fall to the right of the growth curve with consequent future model ages; they appear to fall on an extension of

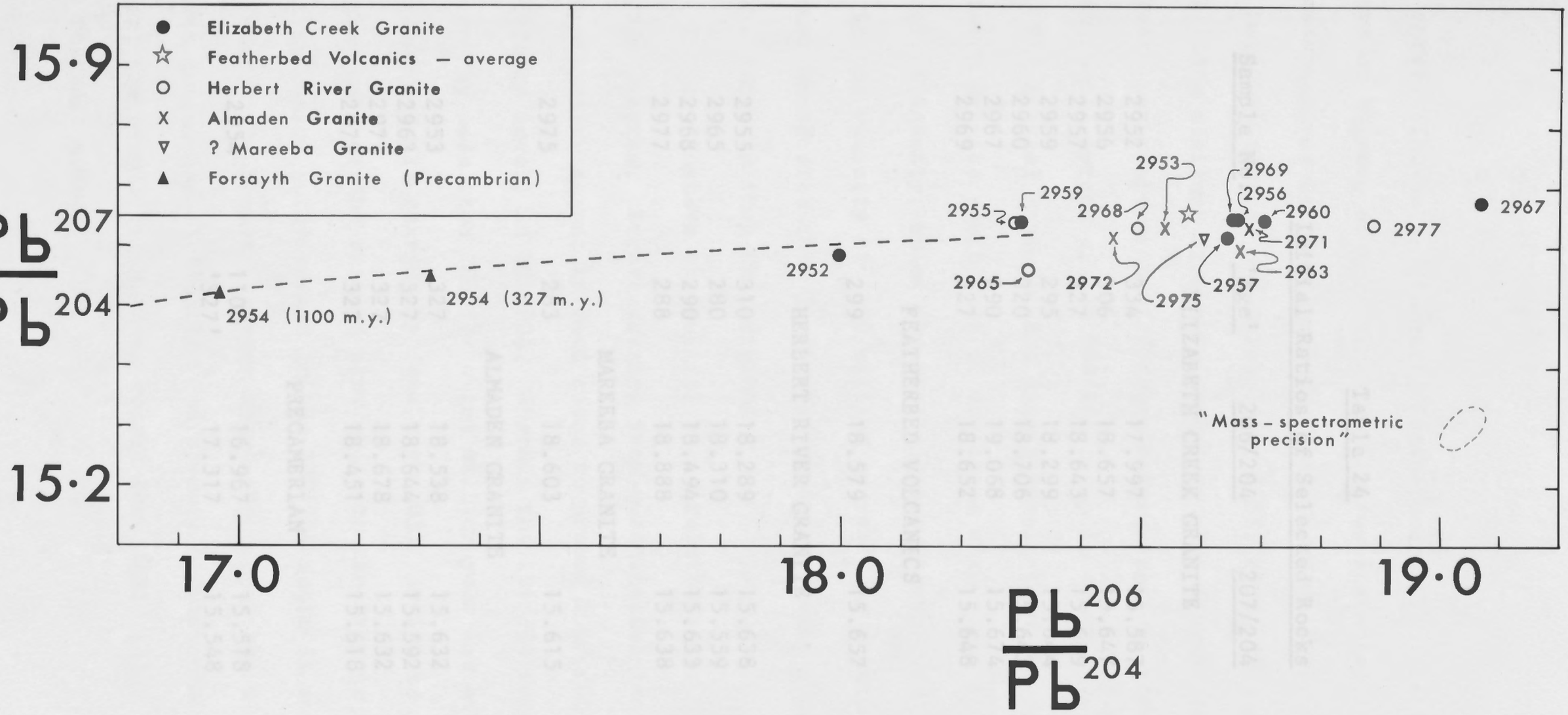

Figure 20. Initial Pb^{207}/Pb^{204} - Pb^{206}/Pb^{204} relationships of all rocks.

Figure 20. Initial Pb^{207}/Pb^{204} - Pb^{206}/Pb^{204} relationships of all rocks.

Table 24

Initial Ratios of Selected Rocks

Sample No.	'Age'	206/204	207/204	208/204
		ELIZABETH CREEK GRANITE		
2952	334	17.997	15.587	38.284
2956	306	18.657	15.647	38.580
2957	327	18.643	15.619	38.433
2959	295	18.299	15.644	38.138
2960	320	18.706	15.643	38.693
2967	290	19.068	15.674	38.577
2969	327	18.652	15.648	38.496
		FEATHERBED VOLCANICS		
	299	18.579	15.657	38.470
		HERBERT RIVER GRANITE		
2955	310	18.289	15.638	38.568
2965	280	18.310	15.559	38.287
2968	290	18.494	15.633	38.475
2977	288	18.888	15.638	38.723
		MAREEBA GRANITE		
2975	283	18.603	15.615	38.480
		ALMADEN GRANITE		
2953	327	18.538	15.632	39.345
2963	327	18.644	15.592	39.353
2971	327	18.678	15.632	38.099
2972	327	18.451	15.618	38.241
		PRECAMBRIAN		
2954	1100	16.967	15.518	38.080
	'327'	17.317	15.548	38.568

the curve. The well-documented Featherbed initial ratio lies in the centre of a group of indistinguishable results which includes representatives of the Elizabeth Creek, Herbert River, Almaden and (?) Mareeba Granites. Samples 2952, 2955, 2959, 2965 and 2977 (and 2967?) are distinct from this grouping. The diagram fails to indicate any systematic difference between the upper Palaeozoic rock types; total spread of the 206/204 ratio is about five per cent.

The initial ratio of the single sample from the Precambrian Forsayth Granite south-west of Chillagoe also plots a little, but not significantly, below the single-stage growth curve, with a model age in the vicinity of 1000 million years. Any contamination of the Permian rocks with this lead would clearly produce a composition less radiogenic than the original.

Figure 21 shows the initial ratio relationships on a 208/204 vs 206/204 diagram. Errors arising from quantitative lead and thorium determinations amount in most cases to around $\pm$.07 (95 per cent confidence level) in 208/204. Whereas the 206/204 ratio is mostly altered by less than .03 for a ten million year age error, the 208/204 ratio is changed by less than .05. As in the previous diagram many of the results plot close to the average Featherbed initial ratio; total spread in the 208/204 ratio is approximately 1.5 per cent. The results scatter about the end of the single-stage growth curve. No distinction can be made between the various rock types; the single (?) Mareeba result once again falls very close to the volcanic point.

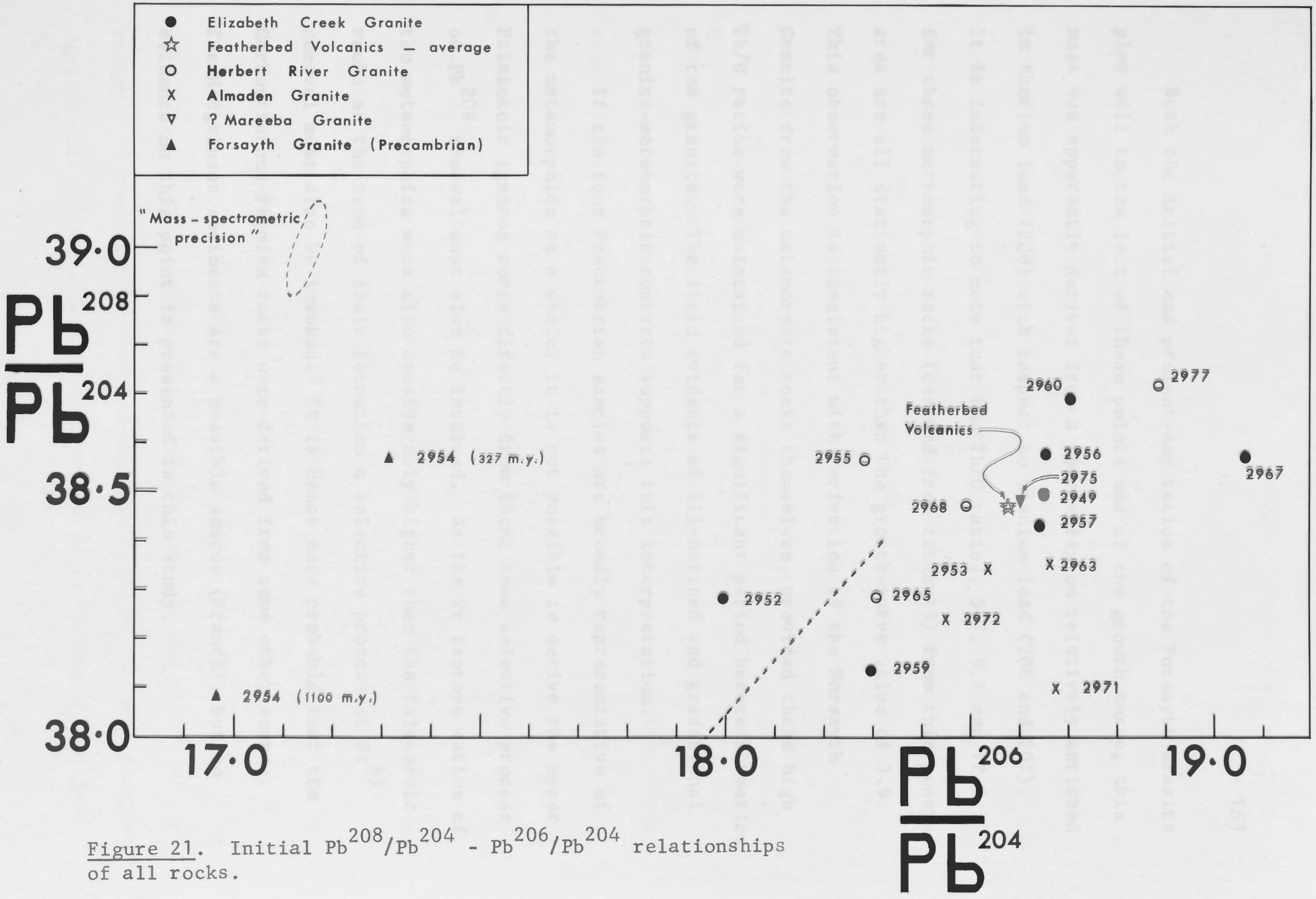

Figure 21. Initial Pb^{208}/Pb^{204} - Pb^{206}/Pb^{204} relationships of all rocks.

Figure 21. Initial Pb^{208}/Pb^{204} - Pb^{206}/Pb^{204} relationships of all rocks.

Both the initial and present-day ratios of the Forsayth Granite plot well to the left of these points and of the growth curve; this mass was apparently derived from a source region relatively enriched in thorium lead (208) with respect to uranium lead (206 and 207). It is interesting to note that the Th/U ratios, 5.7, 9.1 and 12.5, for three metamorphic rocks (derived from table 19) from this general area are all distinctly higher than the growth-curve value of 3.9. This observation is consistent with derivation of the Forsayth Granite from the metamorphic rocks themselves, provided these high Th/U ratios were maintained for a significant period before formation of the granite. The field evidence of ill-defined and gradational granite-metamorphic contacts supports this interpretation.

If the four Precambrian samples are broadly representative of the metamorphics as a whole, it is not possible to derive the upper Palaeozoic igneous rocks directly from them; some selective process of Pb^{208} removal must also be involved. As the Sr isotope ratios of the metamorphics were also considerably higher than the Palaeozoic rocks at the time of their formation a selective process of Sr^{87} removal must also be invoked. It is hence more probable that the Carboniferous-Permian rocks were derived from some other source. The Hodgkinson sediments are a possible source (Branch), but no evidence on this point is presented in this study.

CHAPTER 8

THE NYCHUM VOLCANICS

The Nychum Volcanics are discussed separately as their age has been in doubt for some time, with contradictory stratigraphical and palaeobotanical relations. Even now, no simple solution can be advanced which explains all the features of these enigmatical rocks.

The following descriptions are mainly taken from the work of Morgan (1961 and personal communications), but also from Amos and de Keyser (1964), de Keyser and Wolff (1964), and Branch (1966).

The volcanics cover an area of approximately 240 square miles and occur in four areally distinct outcrops to the north and north-west of the Featherbed cauldron on the adjoining Mossman Sheet area (see figure 22).

These occur:-

a) On the Mitchell River to the west of the Palmerville Fault.

b) Further south, on the Walsh River immediately west of the Palmerville Fault.

c) East of the Palmerville Fault in the area around Nychum Homestead, and

d) Further east near Mount Mulligan.

Branch (1966) considers that these volcanics, which have a maximum thickness of 500 feet and are gently folded, do not occupy a cauldron subsidence area. Lateral variation in rock type has given

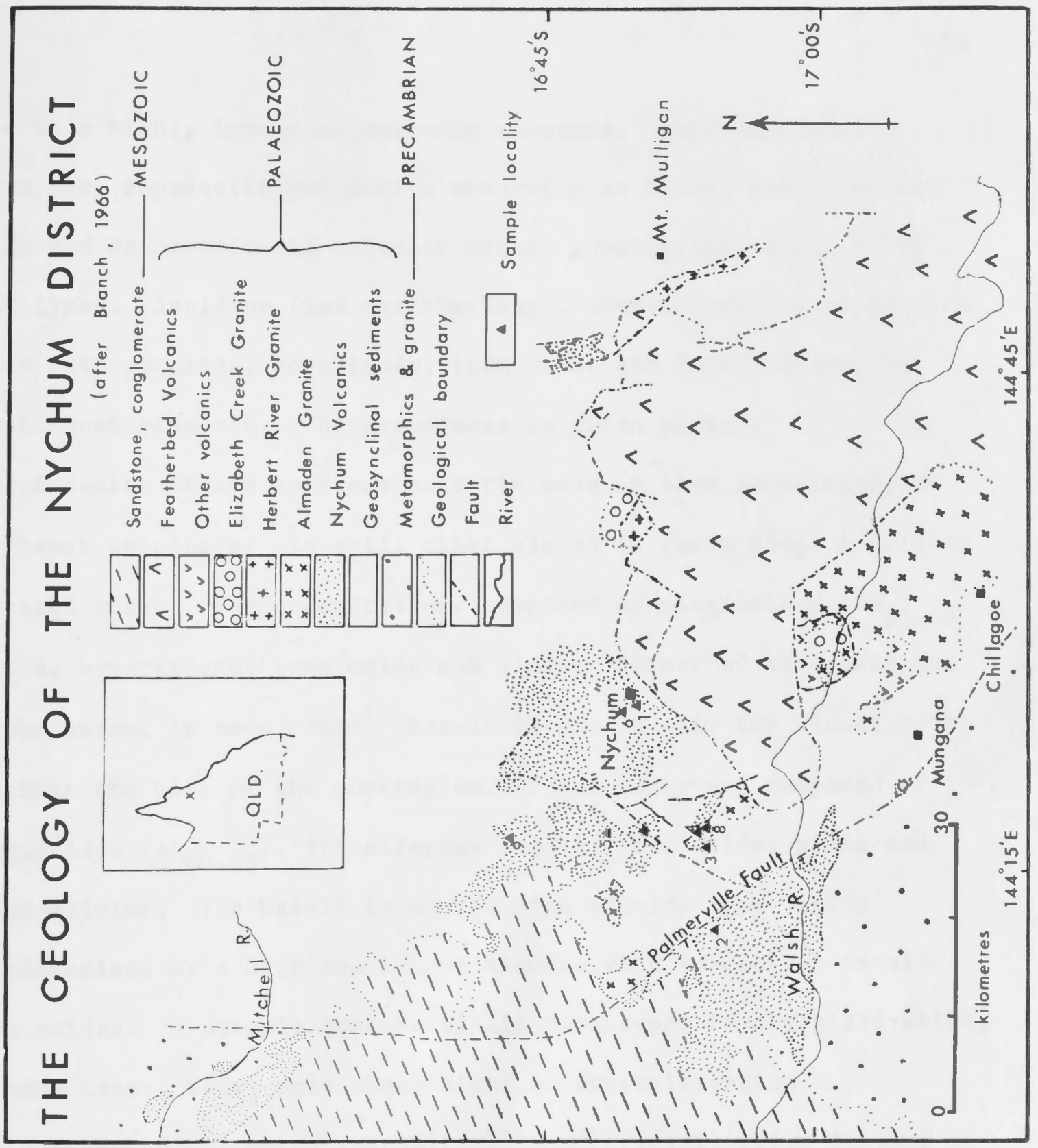

Figure 22. Location of the Nychum Volcanics.

rise to a highly irregular volcanic sequence. Acid volcanics (rhyolite, rhyodacite and dacite occurring as flows, tuffs, welded tuffs and as breccias in volcanic necks) greatly exceed all other rock types. Sanidine (and anorthoclase), somewhat calcic plagioclase, green clinopyroxene, hornblende, iron oxide and fayalite are the constituent minerals. The groundmass is often glassy.

Andesite occurs as flows near the base in some localities; it is absent in others. In still other places it forms plugs intruding the acid rocks. The andesites are composed of plagioclase (An_{55-65}), augite, hypersthene, iron oxide and glass. Either of the pyroxenes may be absent in some rocks. Basalt occurs in only two flows; both are near the base of the succession. These rocks are composed of plagioclase (An_{60-65}), titaniferous augite, iron oxide, glass and minor olivine. The basalt is of the high alumina type, being characterised by a high content of alumina with respect to total iron oxides. A notable feature of all rock types is the glass which, in many cases, shows only minor signs of devitrification.

Morgan (1961) noted sporadic signs of disequilibrium in some of the rocks. He has found rare strongly-embayed xenocrysts of quartz and plagioclase, and xenoliths of basalt and andesite in the intermediate rocks; plagioclase phenocrysts have basified margins in hypersthene-free varieties. Xenoliths of basalt and of palaeozoic sediments have been found in the acidic volcanics.

Field Relations

The various areas of rock classed as Nychum Volcanics unconformably overlie Precambrian metamorphics on the western side of the Palmerville Fault, and steeply-dipping Palaeozoic formations on the eastern side. The fossils in these Palaeozoic rocks are Silurian to Devonian and possibly extend into the Lower Carboniferous. Flat-lying Cretaceous sandstone overlies the Nychum Volcanics with a small angular unconformity.

In 1961 Morgan found evidence suggesting that the Almaden Granite intruded the southern mass of the Nychum Volcanics to the west of the Palmerville Fault. At this location the granite appears to have a chilled margin against these volcanics and contains rounded xenoliths of them. There is doubt about this contact, however, as it may be obscured by the Palmerville Fault. The Almaden Granite is overlain by the Featherbed Volcanics (Best, 1962) and hence the Nychums should be older than both the Almaden Granite and Featherbed Volcanics. Furthermore, the south-east boundary of the Nychum Volcanics near Nychum Homestead is cut by the marginal fault around the Featherbed Volcanics; a north-north-westerly trending dyke swarm in the Nychum Volcanics is abruptly terminated against this fault.

Stratigraphic evidence, then, points to a Palaeozoic age for the Nychum Volcanics, not earlier than Carboniferous and not later than Cretaceous. The Nychums should be older than both the Almaden Granite and the Featherbed Volcanics.

Previous Palaeobotanical Observations

De Keyser (1961) found plant fossils in the Mitchell River outcrops of the Nychum Volcanics near Mount Mulgrave Homestead. These fossils were identified by M. E. White as Glossopteris indica Sch., Glossopteris angustifolia Brong., Taeniopteris cf. T. elongata Walk., Taeniopteris cf. T. wianamattae, small herbaceous Equisetalean and small seeds associated with Glossopteris indica which resemble the nucule of Samaropsis barcellosa White. This glossopterid assemblage was considered as Upper Permian, because of the presence of Taeniopterids which are absent in the Lower Permian Glossopteris flora. De Keyser (1961) also Amos and de Keyser (1964), and de Keyser and Wolff (1964) report that B. E. Balme identified the associated spores and pollen grains as Lunatisporites, Pityosporites, Striatopodocarpidites and Marsupipollenites triradiatus Balme and Hennelly. On the basis of this microflora Balme placed the rocks in the Upper Permian. De Keyser (1961) also states that P. R. Evans, after examining the microflora, came to the same conclusion.

The Palaeobotanical evidence, then, suggests that the Nychum Volcanics are Upper Permian. This result was consistent with the broad stratigraphical evidence already discussed.

Previous Radiometric Dating

The results of a series of predominantly K - Ar ages (Richards et al, 1966), considered in conjunction with the stratigraphical relations, did not directly date the Nychum Volcanics, but placed limits on their age which were incompatible with the palaeobotanical age. From the field evidence it has been concluded above that the Nychum Volcanics should be older than both the Almaden Granite and the Featherbed Volcanics. Two samples from the main mass of Almaden Granite were dated by the K - Ar method. One yielded a biotite age (all ages are adjusted to conform to the greater Rb half-life; see chapter 6) of 307 m.y. and a hornblende age of 317 m.y.; biotite from the other sample indicated an age of 301 m.y. Some uncertainty exists, however, as the Almaden Granite purportedly intruding the volcanics occurs as a small, isolated mass and could possibly differ in age. On the other hand, a series of ages obtained on granites of both Elizabeth Creek and Herbert River type yielded an average age only slightly younger than this result, showing that it is not an unreasonable age to expect for a granite mass in the area. From considerations involving the relationship of the Featherbed Volcanics and associated areas of Elizabeth Creek Granite, and also a single Rb - Sr measurement, Richards deduced that the Featherbed Volcanics must be about 296 million years old. Field relations suggest that the Nychum Volcanics must be older than this and, thus, not younger than Carboniferous (ref. normalised time scale of chapter 6).

This evidence compelled both Richards et al (1966) and Branch (1966, 1967) to dissociate the rocks designated Nychum Volcanics on the Mitchell River from the outcrops in the Nychum Homestead area. The former were considered Upper Permian on the basis of the fossil evidence, the latter considerably older.

New Palaeobotanical Observations

In 1965 W. R. Morgan and I. H. Perrott found well-preserved plant fossils in a new locality, a tuff near the base of the Nychum Volcanics near Nychum homestead. On preliminary examination, these were classed as Upper Permian forms similar to those in the volcanics on the Mitchell River (in Branch, 1966), a result which appeared to invalidate the conclusions of Richards et al (1966) and Branch (1966, 1967). The results of a Rb - Sr study by the author precipitated a thorough re-examination of the fossils from this locality, and the following species have now been identified (M. E. White, pers. comm.).

Glossopteris indica Sch.

Glossopteris communis Feist.

Glossopteris fructification - Scutum sp.

Cardiopteris polymorpha Goepp.

Noeggerathiopsis hislopi (Bunb.)

Palaeovittaria kurzi Feist.

Gangamopteris cyclopteroides Feist.

Walkomiella australis (Feist.) Florin

Sphenopteris polymorpha Feist.

Annularia sp.

All elements of the flora occur in various combinations in individual samples; Glossopteris indica and Cardiopteris polymorpha have been found within the same hand-specimen. The overall assemblage, then, contains elements of both the Glossopteris and the Rhacopteris floral associations. The former is generally thought to have replaced the more primitive Rhacopteris flora at the beginning of the Permian and to have continued to the Triassic. Thus Dickins (1961) contends that, in Australia, at least, Glossopteris first appeared in the Lower Permian or less probably in the very uppermost Carboniferous. If this is correct the highly unusual mixed flora should indicate an age close to the Carboniferous-Permian boundary for the volcanics around Nychum Homestead. P. R. Evans, who has examined the associated microflora, is generally in accord with this conclusion (personal communication to J. R. Richards).

New Radiometric Age Study

A Rb - Sr age study was commenced when the palaeobotanical evidence suggested an Upper Permian age, in an attempt to resolve the discrepancy between the stratigraphical and palaeobotanical methods. W. R. Morgan supplied nine rocks for analysis. One of these came from the western side of the Palmerville Fault, the other eight from the eastern side. The occurrence on the Mitchell River, often correlated with the Nychum Volcanics, and the small mass north-west of Mt Mulligan, were not sampled.

The line shown in figure 23, giving a model II age of 344±16 m.y., is regressed through the points representing the eight rocks from the eastern side of the Palmerville Fault. By including the western sample (2981) a slightly older age of 351±15 m.y. is obtained from a model IV isochron. All whole-rock analyses, which are represented by circles on this diagram, are presented in table 25.

Table 25

Rb - Sr Isotopic Analyses of the Nychum Volcanics

Rock No.	Locality (fig. 22)	Rb (µg./g.)	Sr (µg./g.)	Rb^{87}/Sr^{86}	Sr^{87}/Sr^{86}
2990	9	204.6	145.2	4.076	0.7234
2989	8	137.9	202.1	1.972	0.7135
2988	7	14.23	222.1	0.1850	0.7055
2986	6	387.5	117.6	9.550	0.7511
2984	5	253.6	115.3	6.366	0.7346
2983	4	132.9	185.8	2.066	0.7138
2982	3	53.79	212.5	0.7307	0.7082
2981	2	128.1	175.2	2.112	0.7158
2980	1	301.6	86.21	10.149	0.7551
2980An	1	117.7	123.4	2.758	0.7232
2980Py	1	49.23	46.43	3.067	0.7242

The Sr^{87}/Sr^{86} ratios of the two most discrepant samples (2980 and 2981) have been calculated from both spiked and unspiked analyses; these agree to within .0002 in both cases. X-ray fluorescence determinations by Mrs T. R. Martin on these two rocks also agreed with the previous isotope-dilution results. Hence the isochron appears to be a valid representation of the samples as collected.

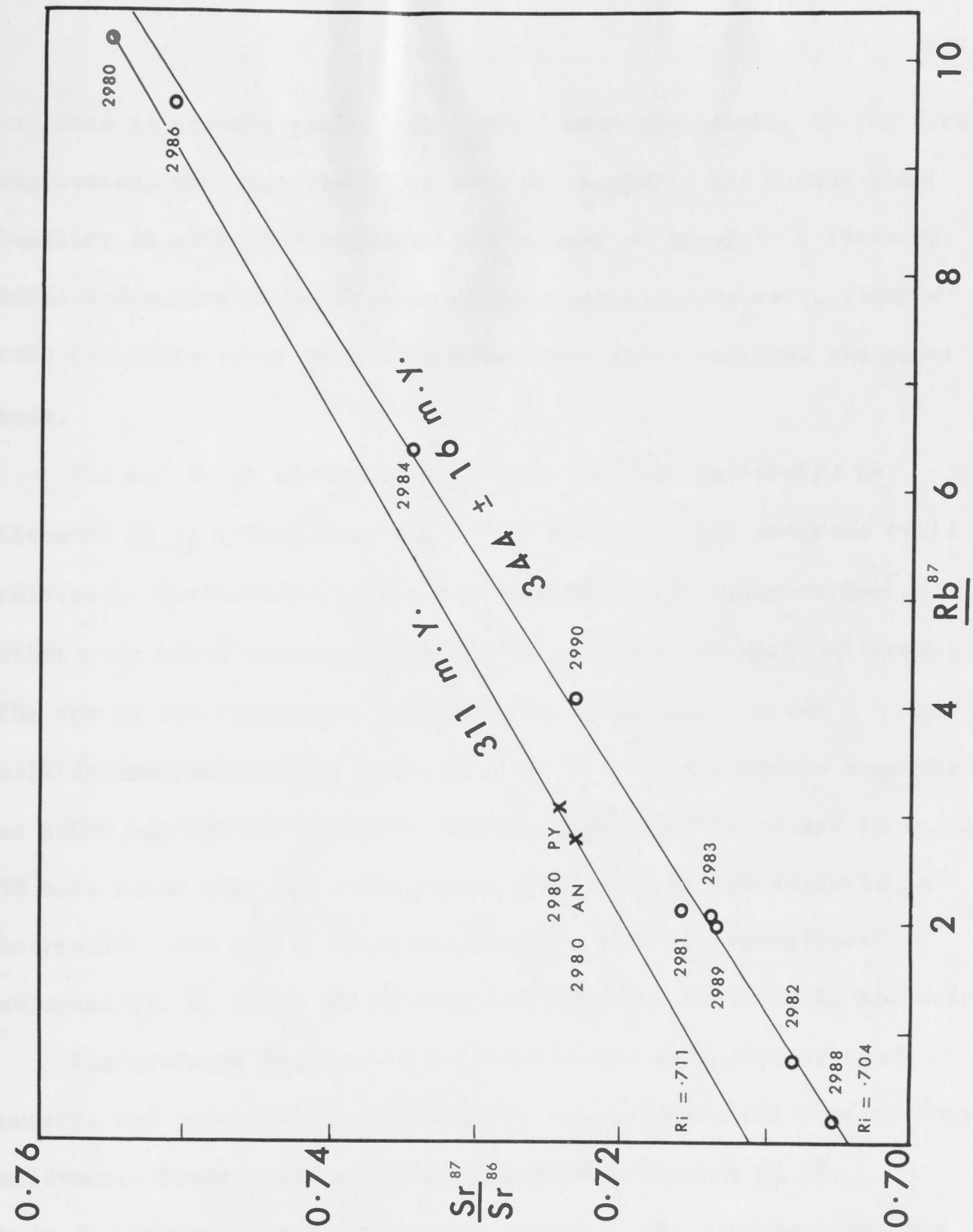

Figure 23. Rb - Sr isochron diagram for the Nychum Volcanics.

As there is greater geological control over the samples in the first regression, that age should be more meaningful. The fossil plant locality is about one kilometer north-west of locality 6 (Rock No. 2986) and occurs about 50 feet stratigraphically below it. Sample 2980 (locality 1) is part of a dyke swarm which intrudes the plant beds.

The age is in agreement with that obtained indirectly by Richards et al (1966) from the K - Ar study and the observed field relations. Furthermore, the new geochronological observations on other rock units in this study are also consistent with this result. The age of the Featherbed Volcanics in particular, is now well-documented at about 298 m.y., and the field evidence suggests an older age for the Nychums. On the other hand, this age is about 50 m.y. older than any other known occurrence of Glossopteris in Australia. The age is also incompatible with the microfloral evidence (P. R. Evans in a personal communication to J. R. Richards).

The profound implication of this result made further study urgent, and other dating systems were investigated for confirmatory evidence. Fission-track dating proved unsuccessful as the hydrofluoric acid strongly etched the whole glass rather than the fission tracks alone. J. D. Kleeman (pers. comm.) considers that the glass must be devitrified on a submicroscopic scale for this behaviour to occur. Two andesites and a basalt were analysed by the K - Ar method under the guidance and with the help of I. McDougall.

The basalt (2982) yielded an age of 95 m.y. and the two andesites (2981 and 2983) ages of 143 and 131 m.y. respectively. There seems little doubt that these low variable ages are due to argon loss, which is presumably aided by the submicroscopic devitrification of the glass. An anorthoclase separate from sample 2980 (an obsidian) produced an age of 269 m.y., with experimental scatter not greater than ± 7 m.y. at the 95 per cent confidence level. This result, too, is incompatible with the observed field relationship between the Nychum and Featherbed Volcanics, and the well-documented age of the latter. It would appear that the anorthoclase has also been affected by argon loss.

WHOLE-ROCK LEAD RESULTS

Lead isotopic studies have also been performed and these analyses are presented in table 26. The Th^{232}-Pb^{208} isochron plot (figure 24) gives an age of 198 ± 116 m.y. and a 38.42 ± 0.19 initial ratio (using the York regression of chapter 7). The large age uncertainty is controlled by measurement imprecision and the small number of analyses rather than actual scatter of the points, as these appear to fit the regression to within the normal error limits. The error limits yielded by the regression program indicate that there is only slightly more than one chance in 20 that this age could be as old as that predicted from the palaeobotanical and stratigraphical evidence (about 296 m.y.).

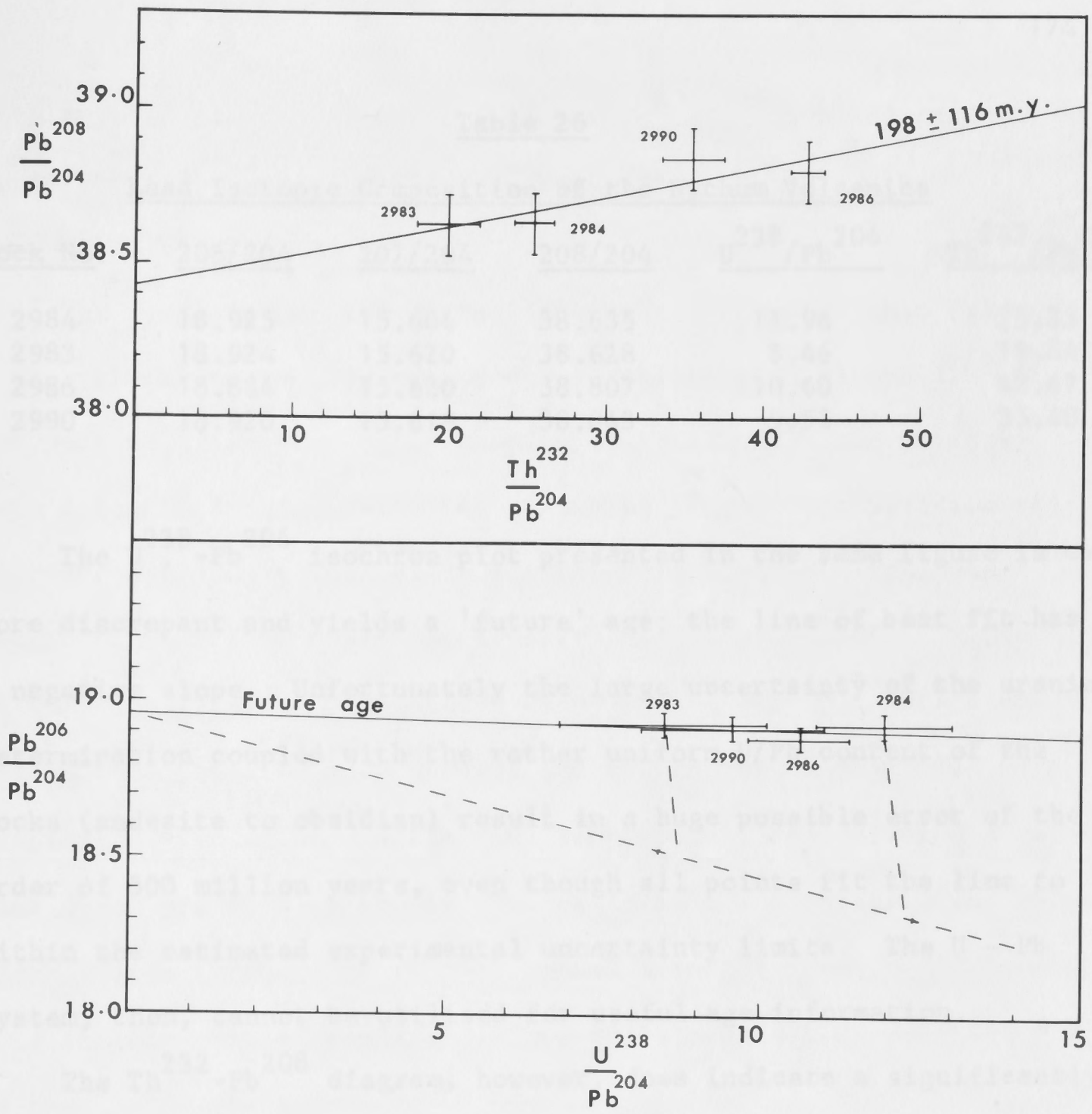

Figure 24. Th^{232} - Pb^{208} and U^{238} - Pb^{206} isochron diagrams for the Nychum Volcanics.

Table 26

Lead Isotopic Composition of the Nychum Volcanics

Rock No.	206/204	207/204	208/204	U^{238}/Pb^{204}	Th^{232}/Pb^{204}
2984	18.925	15.604	38.635	11.94	25.33
2983	18.924	15.620	38.628	8.46	19.84
2986	18.884	15.620	38.807	10.60	42.67
2990	18.920	15.619	38.843	9.55	35.40

The U^{238}-Pb^{206} isochron plot presented in the same figure is even more discrepant and yields a 'future' age; the line of best fit has a negative slope. Unfortunately the large uncertainty of the uranium determination coupled with the rather uniform U/Pb content of the rocks (andesite to obsidian) result in a huge possible error of the order of 500 million years, even though all points fit the line to within the estimated experimental uncertainty limits. The U - Pb system, then, cannot be utilised for useful age information.

The Th^{232}-Pb^{208} diagram, however, does indicate a significantly different age from the Rb - Sr result at the 95 per cent confidence level. This is unlikely to be due to a general unsuitability of volcanic rocks for dating by the U - Pb and Th - Pb methods, for the similar rock types of the approximately contemporaneous Featherbed Volcanics, occurring immediately to the south-east, show quite good agreement between all three methods.

These discrepant Nychum Volcanic results may be explained as the result of mixing two unrelated magma types, say a basic component

with an acid magma possessing a higher Sr^{87}/Sr^{86} initial ratio and lower Pb^{206}/Pb^{204} and Pb^{208}/Pb^{204} ratios.

THE MIXING HYPOTHESIS

The evolution of the 'normal' Rb - Sr system and that resulting from such mixing is illustrated diagramatically in figure 25. In the more familiar case (a), in which comagmatic and coeval rocks have a common initial ratio their initial isotopic composition can be represented by points along a straight horizontal line. The length of this line depends only on the range of Rb^{87}/Sr^{86} ratios of the samples. The radioactive decay of Rb^{87} to Sr^{87} with time causes each point to move upwards and to the left along lines with gradient = -1. At any instant all samples will fall along a straight line which projects to the initial ratio at the ordinate. The slope of this line is equal to $(e^{\lambda t}-1)$, where λ is the decay constant and t is the time since formation. Thus the slope is a direct measure of the age of the system.

Let us now suppose two magmas each relatively homogeneous and with a different initial ratio. These are mixed in various proportions to form a related group of rocks. We shall also assume that the acid member has a more radiogenic composition (ie. higher Sr^{87}/Sr^{86}) than the basic end member. Incomplete mixing of these will produce a magma series in which the Rb^{87}/Sr^{86} ratio, which is dependent on the acidity of the rock, and thus the proportion of each end member, is directly correlated with the Sr^{87}/Sr^{86} ratio. In other words,

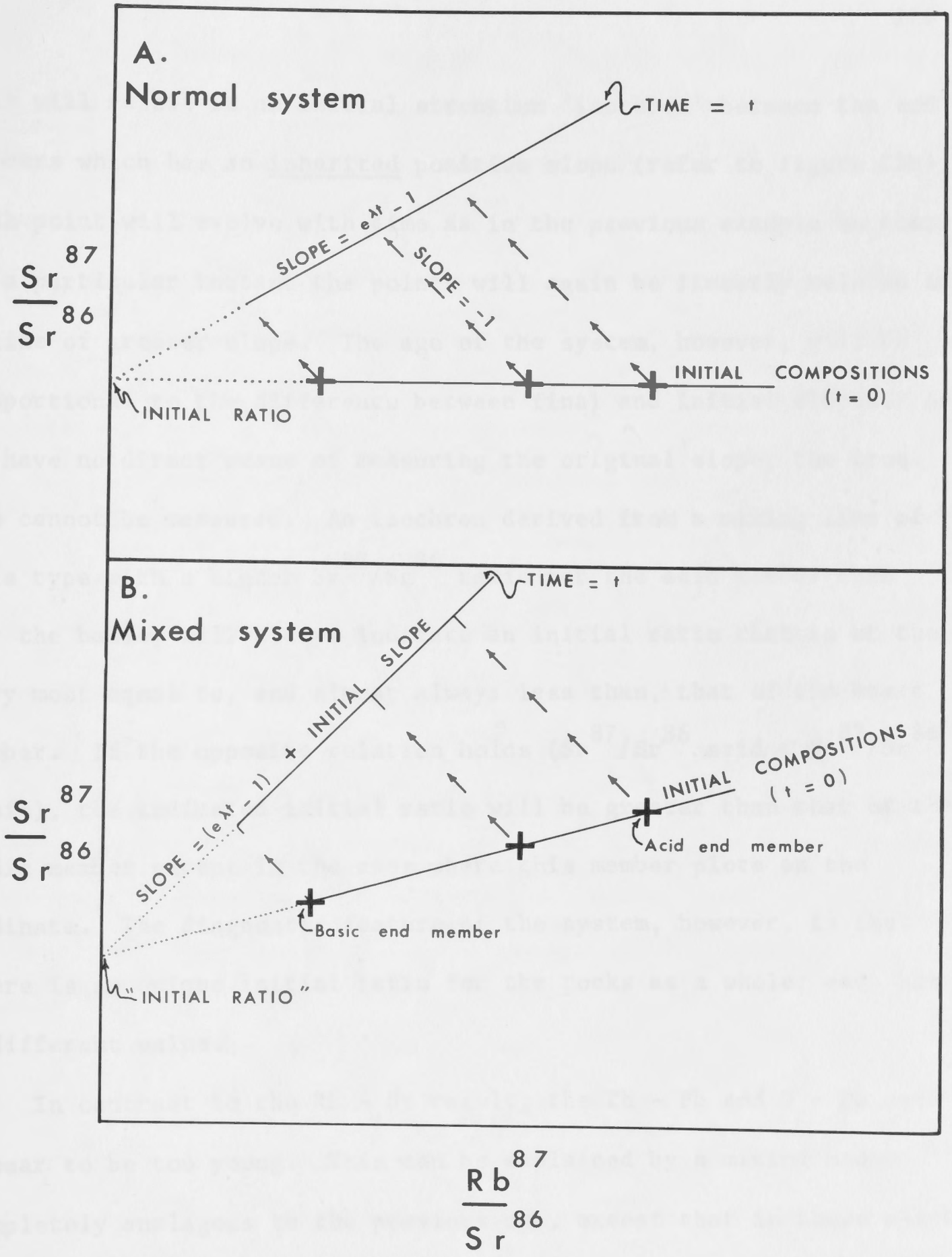

Figure 25. The 'normal' and mixed Rb - Sr systems.

this will result in an initial strontium 'isochron' between the end members which has an inherited positive slope (refer to figure 25b). Each point will evolve with time as in the previous example so that at a particular instant the points will again be linearly related in a line of greater slope. The age of the system, however, will be proportional to the difference between final and initial slopes. As we have no direct means of measuring the original slope, the true age cannot be measured. An isochron derived from a mixing line of this type with a higher Sr^{87}/Sr^{86} ratio for the acid member than for the basic, will always indicate an initial ratio that is at the very most equal to, and almost always less than, that of the basic member. If the opposite relation holds (Sr^{87}/Sr^{86} acid < Sr^{87}/Sr^{86} basic), the indicated initial ratio will be greater than that of the basic member except in the case where this member plots on the ordinate. The diagnostic feature of the system, however, is that there is no unique initial ratio for the rocks as a whole; each has a different value.

In contrast to the Rb - Sr result, the Th - Pb and U - Pb ages appear to be too young. This can be explained by a mixing model completely analagous to the previous one, except that in these cases the acid end member has a less-radiogenic initial isotopic composition than the basic parent. A distribution of this type results in an 'isochron' with initial negative slope. The initial slope of the U^{238}-Pb^{206} line may have been such that only now is it approaching the horizontal.

It is possible to estimate the initial isotopic composition of the two end members if their age and approximate Rb^{87}/Sr^{86} contents are known (see the Pb^{206}/Pb^{204} vs U^{238}/Pb^{204} plot of figure 24). This is done by subtending a line from the indicated initial ratio below the 'isochron' at an angle which is proportional to the age of the system [slope = $(e^{\lambda t}-1)$]. In this case the approximate age of 300 m.y. suggested by the fossil evidence will be used. The present compositions of the two extreme members are then joined to this line along lines of slope = -1 to yield their initial isotopic composition. We can then place limits on the most acid and basic end members, which have not necessarily been sampled. For example, if the line in figure 24 were precisely determined we could say that the initial 206/204 ratio of the acid parent was 18.3 or less, whereas the basic member composition was in the range 18.5 to 18.9. Similar treatments can be applied to the other plots.

RB - SR MINERAL AGE

If a mixing-line model applies each whole-rock sample could have a different initial ratio. If, however, all the minerals present in a particular rock crystallised in situ, or alternatively equilibrated with the magma before total crystallisation, the mineral isochron should reflect both the true age and initial ratio of each particular rock. To test this hypothesis the two minerals listed in table 25 were separated by R. Rudowski and chemically treated by M. J. Vernon; W. Compston and D. J. Millar performed the

mass-spectrometric analyses for Rb and Sr. Because of the scarcity of discrete minerals (phenocrysts form about one per cent of the rock, the rest is glass) it was not possible to obtain a sufficient quantity of pure clinopyroxene, so a concentrate containing about 20 per cent fayalite had to be utilised. It is interesting to note that the Rb/Sr ratio of both the anorthoclase and the pale green clinopyroxene (diopsidic augite?) are similar. The Rb content of the pyroxene is about 60 μg./g., if the reasonable assumption is made that the fayalite contains insignificant amounts of this element. This value is remarkably high when one considers the small amounts of K that are normally reported for this mineral (see Deer et al, 1963) and the low Rb content obtained from the few analyses (e.g. Griffin and Murthy, preprint; Chappell et al, in press). Perhaps the unexpectedly high Rb content is due to the acidic nature of the rock (an obsidian); previous analyses appear to be confined to basic and ultrabasic varieties. The only alternative would appear to be contamination by glass-pyroxene composites. However, microscopic examination has shown that although these contribute to the high value, the 20 per cent glass required to fully explain the results is certainly not present.

The line joining the total rock result to the two mineral points yields an age of 311±57 m.y. Although the three points are not significantly different from a straight line within the limits of experimental uncertainty, the small number of points results in

large error limits. However, the result does support the mixing hypothesis and yields an age which can be reconciled with the palaeobotanical evidence. In this connection recent work by Fitch, Miller and Williams on the Carboniferous of England should be noted. They present K - Ar data on a variety of igneous rocks which they assign to the Variscan arogeny, which occurred in the lower Stephanian. Their mean age (295 m.y. ≡ 312 m.y. on the conventions adopted in chapter 6 of this thesis) agrees remarkably closely with the mineral age deduced here. This implies that the Nychum Volcanics may also have formed within the Stephanian. This would be compatible with all the available evidence.

CONSEQUENCES OF THE MIXING HYPOTHESIS

There still remains one puzzling feature. It is a natural consequence of the model that mixing of two end members results in rocks of intermediate composition which must maintain a constant ordering-sequence no matter which system is considered. Figures 23 and 24 show that this relationship does not hold. It is difficult to envisage any other explanation which is even as satisfactory as the model already proposed.

Perhaps the observations of Gunn and Watkins on the Stretishorn composite dyke, eastern Iceland, are relevant to this question. The rhyolitic core of the Stretishorn dyke is separated from basaltic flanks by narrow transitional zones of andesitic, dacitic and rhyolitic composition. Gunn and Watkins have invoked a mixing origin

for the rocks of the transition zone. Trace element data are compatible with the major element analyses in most cases, and show a regular trend in concentration between the two postulated end members. The relatively volatile lead, however, is strongly enriched in the hybrid zones, a feature which Gunn and Watkins tentatively attribute to hydrothermal redistribution at a late stage in the cooling history.

This mechanism might also alter the original uranium distribution because of its mobility in the hexavalent state (Gunn and Watkins did not measure uranium). Combination of the two redistributions could effectively change the immediate post-mixing relationships for the U - Pb and Th - Pb systems, and yield ordering sequences which differ from each other and from the Rb - Sr diagram.

It thus seems credible that the discrepant total-rock isochrons may result from a mixing process and yield anomalous ages. The concordancy of the Rb - Sr mineral isochron, the field relations and the palaeobotanical evidence, then, point to an uppermost Carboniferous age only slightly older than the Featherbed Volcanics.

RELATION TO THE ALMADEN GRANITE

Morgan (1961) postulated that the Nychum Volcanics were comagmatic with the Almaden Granite on the basis of the close spacial association and the dominantly acid nature of the volcanics. He also noted that the petrographical evidence of xenocrysts and xenoliths suggested 'contamination by assimilation, or else mixing

of basic and acid magmas.' Both the K - Rb plot of figure 11 and Rb - Sr isochron diagrams (figures 14 and 23) suggest an "abnormal' origin for these two rock types, although the limited compositional range for the Almaden Granite makes confident interpretation difficult. The Rb - Sr whole-rock data appear to indicate anomalously old ages in both cases and could be explained by the contamination or mixing advocated by Morgan. A basic parent indistinguishable from the Nychum basalt would explain both trends (see chapter 6). Different acid members, however, would be needed, as the two lines have divergent slopes. Hence, although both rock series may well result from mixing, the Rb - Sr data would suggest that the acid parent-magmas had different Rb/Sr ratios and the rocks are not strictly comagmatic.

CHAPTER 9

ISOTOPIC COMPOSITION AND GENESIS OF THE ORES

Where possible the discussion will be in terms of the mining centres (A to N) defined in chapter 2 rather than of individual results. As the isotopic composition of over 50 ore-samples has been determined, this approach will simplify presentation and lead to the minimum of repetition. In almost all cases the analyses were performed on galena ore; the exceptions are noted in the appendix. The mineralogy of the various ores and gangue minerals as determined by the author from thin section and reflected light studies are also given in the appendix.

Ore-Lead Results

The 207/204 and 206/204 relationships, presented graphically in figure 26 (to be hereafter called the x-y plot for brevity), indicate that most of the ore bodies lie beyond the growth curve and possess future 'model ages'. The total model-age spread, however, ranges from 578 million years in the past to 373 in the future. Only the ore deposits of mining centre D have a model age (267 m.y.) that is at all comparable with the time of Upper Palaeozoic igneous events. It would be customary to regress a line through the analyses to obtain age information from the equations listed by Russell and Farquhar (1960), but the data indicate that a simple interpretation does not apply. Although many of the points would fit such a regression within the

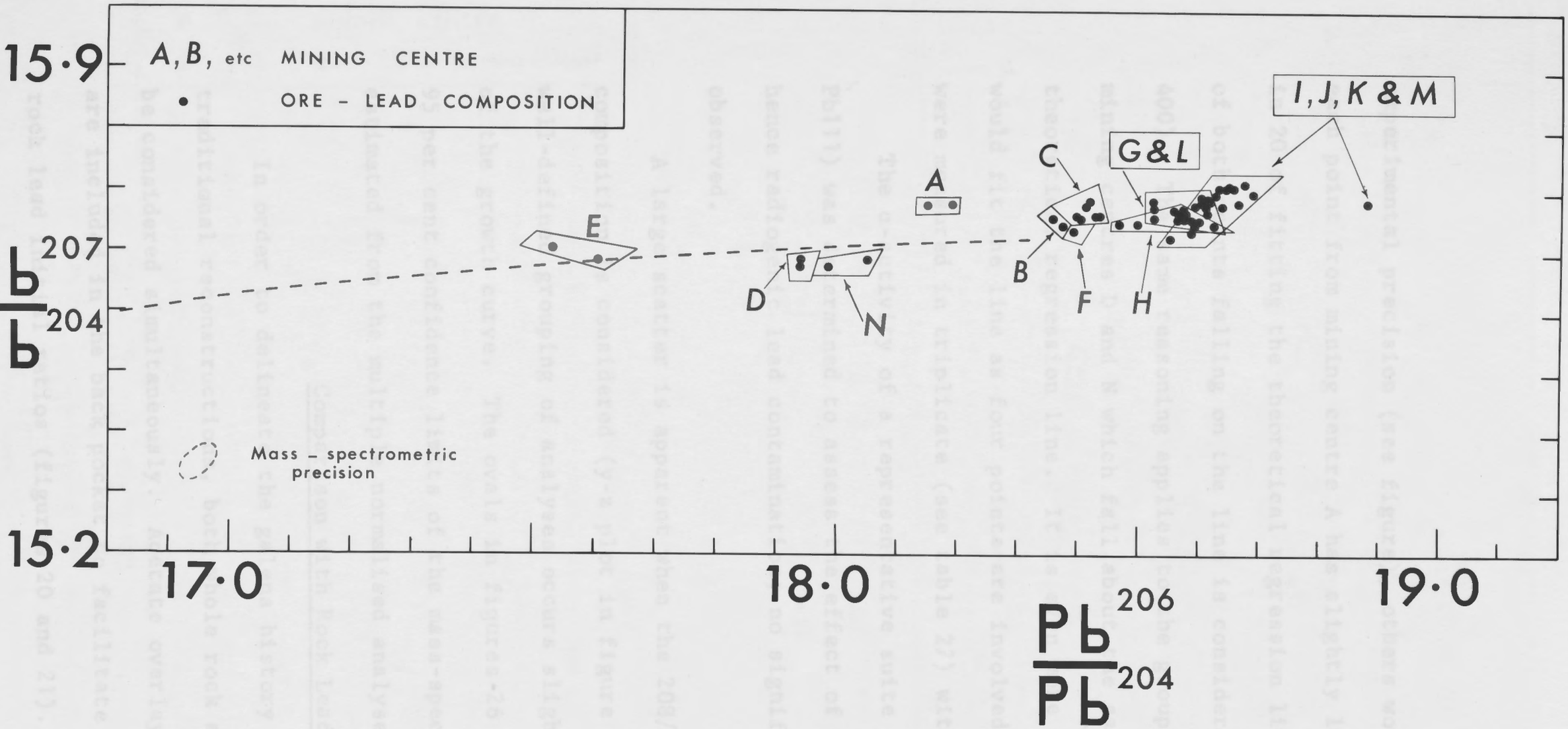

Figure 26. The Pb^{207}/Pb^{204} - Pb^{206}/Pb^{204} relationships of the ore leads.

Figure 26. The Pb^{207}/Pb^{204} - Pb^{206}/Pb^{204} relationships of the ore leads.

experimental precision (see figure), others would not. For example each point from mining centre A has slightly less than one chance in 20 of fitting the theoretical regression line; the possibility of both points falling on the line is considerably less (one in 400). The same reasoning applies to the group of analyses from mining centres D and N which fall about the same distance below the theoretical regression line. It is even more unlikely that these would fit the line as four points are involved and two of these were measured in triplicate (see table 27) with good reproducibility.

The α-activity of a representative suite of the ores (Pb96 to Pb111) was determined to assess the effect of possible uranium and hence radiogenic lead contamination; no significant radiation was observed.

A large scatter is apparent when the 208/204 vs 206/204 isotopic composition is considered (y-z plot in figure 27); however, a well-defined grouping of analyses occurs slightly beyond the end of the growth curve. The ovals in figures 26 and 27 represent the 95 per cent confidence limits of the mass-spectrometric precision as estimated from the multiple normalised analyses of Pb245.

Comparison with Rock Leads

In order to delineate the galena history without the aid of the traditional reconstructions, both whole rock and galena systems will be considered simultaneously. Acetate overlays of figures 26 and 27 are included in the back pocket to facilitate comparison with the rock lead initial ratios (figures 20 and 21).

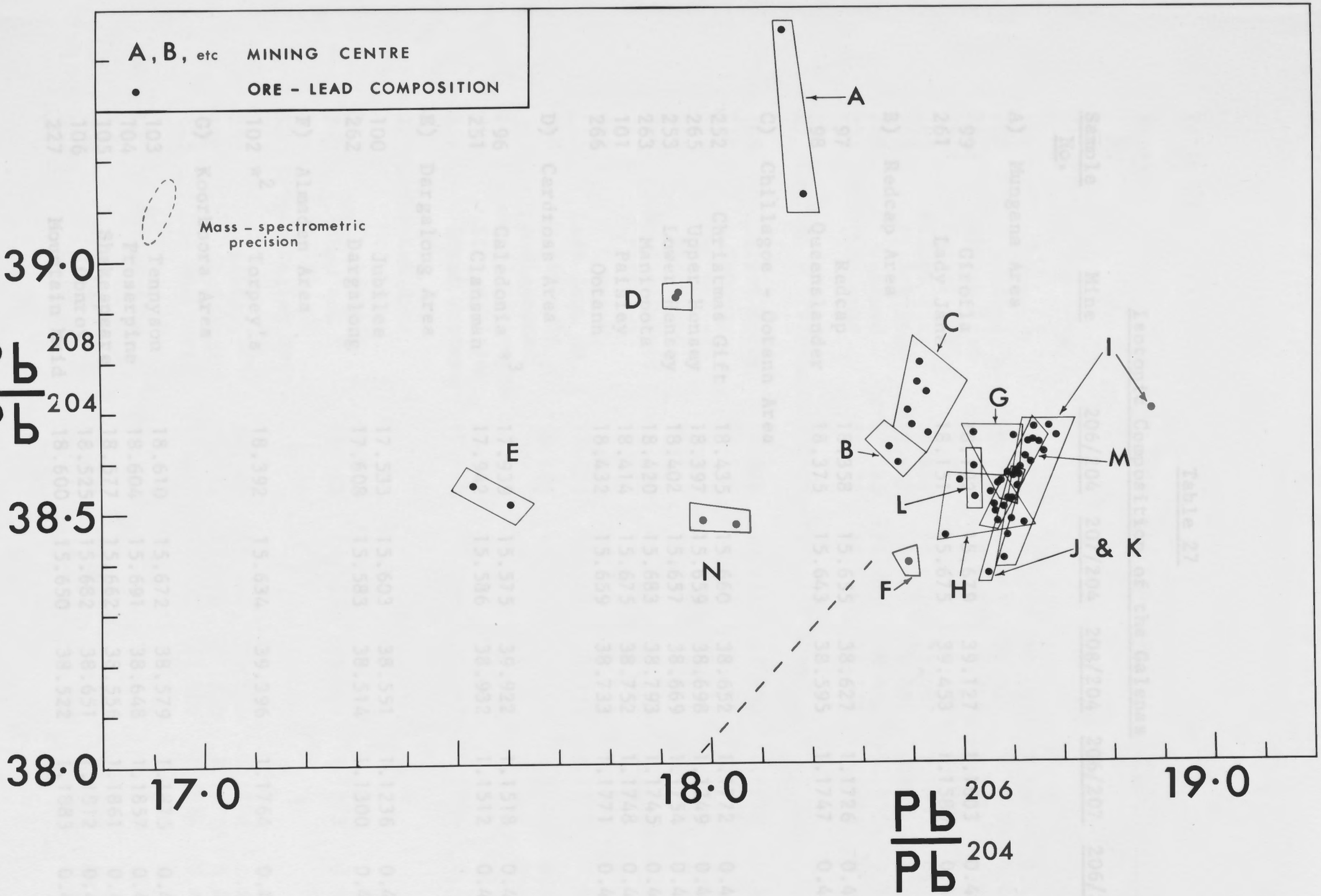

Figure 27. The Pb^{208}/Pb^{204} - Pb^{206}/Pb^{204} relationships of the ore leads.

Figure 27. The Pb^{208}/Pb^{204} - Pb^{206}/Pb^{204} relationships of the ore leads.

Table 27

Isotopic Composition of the Galenas

Sample No.	Mine	206/204	207/204	208/204	206/207	206/208
A) Mungana Area						
99	Girofla	18.192	15.679	39.127	1.1603	0.4650
261	Lady Jane	18.151	15.675	39.453	1.1580	0.4601
B) Redcap Area						
97	Redcap	18.358	15.655	38.627	1.1726	0.4753
98	Queenslander	18.375	15.643	38.595	1.1747	0.4761
C) Chillagoe - Ootann Area						
252	Christmas Gift	18.435	15.660	38.652	1.1772	0.4770
265	Upper Hensey	18.397	15.659	38.698	1.1749	0.4754
253	Lower Hensey	18.402	15.657	38.669	1.1754	0.4759
263	Maniopota	18.420	15.683	38.793	1.1745	0.4748
101	Paisley	18.414	15.675	38.752	1.1748	0.4752
266	Ootann	18.432	15.659	38.733	1.1771	0.4759
D) Cardross Area						
96	Caledonia *[3]	17.939	15.575	39.922	1.1518	0.4609
251	Clansman	17.942	15.586	38.932	1.1512	0.4609
E) Dargalong Area						
100	Jubilee	17.533	15.603	38.551	1.1236	0.4548
262	Dargalong	17.608	15.583	38.514	1.1300	0.4572
F) Almaden Area						
102 *[2]	Torpey's	18.392	15.634	39.396	1.1764	0.4790
G) Koorboora Area						
103	Tennyson	18.610	15.672	38.579	1.1875	0.4824
104	Proserpine	18.604	15.691	38.648	1.1857	0.4814
105	Shakespeare	18.577	15.662	38.556	1.1861	0.4818
106	Conroy	18.525	15.682	38.651	1.1812	0.4793
227	Mountain Maid	18.600	15.650	38.522	1.1883	0.4827

Table 27 (cont.)

Sample No.	Mine	206/204	207/204	208/204	206/207	206/208
H) Featherbed Area						
107	Comstock	18.565	15.654	38.487	1.1860	0.4823
108	Unnamed	18.558	15.669	38.533	1.1844	0.4816
254A	Silver Bead	18.565	15.658	38.509	1.1856	0.4821
254B	Silver Bead	18.573	15.671	38.552	1.1852	0.4818
245	Silver Star +	18.601	15.651	38.481	1.1885	0.4834
259	Nightflower	18.467	15.647	38.450	1.1802	0.48028
239	Unnamed	18.625	15.645	38.472	1.1905	0.4841
255	Unnamed	18.498	15.646	38.557	1.1823	0.4798
I) Emuford - Irvinebank - Stannary Hills Area						
109	Silver Spray	18.878	15.681	38.700	1.2039	0.4878
228	Panquay	18.586	15.631	38.404	1.1890	0.4840
229	Mt Babinda	18.666	15.681	38.616	1.1903	0.4834
238	Bloodwood	18.675	15.713	38.668	1.1886	0.4830
244	Mountain Maid (Omeo)	18.632	15.706	38.673	1.1863	0.4822
243	Cosgrove	18.643	15.707	38.639	1.1870	0.4825
241	Lady Jane No. 2	18.639	15.678	38.594	1.1889	0.4830
240	Victoria Amalgamated	18.618	15.684	38.582	1.1870	0.4826
242	Great Adventure	18.591	15.645	38.449	1.1883	0.4835
246	Silver Lining	18.628	15.697	38.605	1.1867	0.4825
247	Great Western	18.690	15.698	38.647	1.1906	0.4836
J) Herberton Area						
111	Isabel	18.615	15.687	38.560	1.1867	0.4828
248	You and I	18.552	15.623	38.374	1.1875	0.4835
K) Silver Valley Area						
250	Battery	18.612	15.667	38.546	1.1880	0.4829
110	Target	18.612	15.678	38.570	1.1872	0.4826
249	Doc and Doris	18.585	15.652	38.505	1.1874	0.4827
L) Mt Garnet Area						
267	Mt Garnet	18.527	15.657	38.526	1.1833	0.4809
237	Chinaman	18.527	15.674	38.588	1.1820	0.4801

Table 27 (cont.)

Sample No.	Mine	206/204	207/204	208/204	206/207	206/208
M) Brownville Area						
260	Bolivia	18.572	15.656	38.478	1.1862	0.4827
257	Tuchers	18.592	15.677	38.572	1.1859	0.4820
256	Kohinoor	18.646	15.709	38.663	1.1870	0.4823
264	Excellent	18.603	15.682	38.569	1.1863	0.4823
258	Unnamed	18.656	15.706	38.635	1.1879	0.4829
N) Isolated Mines						
273	Unnamed	18.051	15.587	38.471	1.1581	0.4692
112 *[3]	Blackwell's	17.987	15.575	38.480	1.1549	0.4674
96		17.927	15.564	38.887	1.1518	0.4610
		17.953	15.590	38.962	1.1516	0.4608
		17.938	15.572	38.916	1.1520	0.4609
112		17.984	15.572	38.471	1.1549	0.4675
		17.995	15.586	38.503	1.1546	0.4674
		17.983	15.568	38.467	1.1551	0.4675
102		18.410	15.666	38.483	1.1752	0.4784
		18.374	15.602	38.309	1.1759	0.4796

*[3] denotes a mean value with the numeral referring to the number of analyses. The individual analyses are

+ average of 60 results obtained from three spiked and 20 unspiked data sets.

The most noticeable feature of the two systems is the close correspondence of many of the rock and ore leads slightly beyond the end of the growth curves on the x-y and y-z plots. The 206/204 ratios of both are exceedingly similar but the 207/204 and 208/204 rock-lead ratios are often less than those of the ores. In particular, the 208/204 ratios of all four Almaden Granite samples are less than any of the galena values; for three of these, however, when considered individually, the displacement below the ore values is not significant. On the other hand, the ore composition which most closely resembles the Almaden initial ratios is not that of those spacially associated with the granite; the ores from the Mungana, Redcap, Chillagoe - Ootann and Almaden areas are quite distinct from the granite composition. This would suggest that the contact metasomatic theory widely advocated for the bulk of these ore bodies (see economic geology section) is not strictly applicable.

The inferred initial ratios of the Nychum Volcanics, which are not represented on these diagrams, fall close to the Almaden Granite samples 2953 and 2972 on the x-z plot. As all four Nychums also plot well below the galenas on the x-y diagram (207/204 less than 15.600) these also appear not to have been associated with ore formation in the Atherton Sheet area.

The Elizabeth Creek Granite (2959) from the extreme south of the area also apparently has no galena analogue. The possibility of uranium-loss from the aplitic Elizabeth Creek specimen (2967) from

Lappa Junction must lead to an indefinite conclusion; its present composition is not duplicated in any of the galenas measured.

Rock 2965 (Herbert River Granite near Almaden) does not have an initial ratio comparable with any ore sample unless its low 207/204 and 208/204 ratios result from an aberrant fractionation correction. If this were the case it would correlate best with the mines from the Redcap area (B).

Unless the age allotted to the small Elizabeth Creek intrusion (2952) on the Palmerville Fault near Mungana is 20 to 30 million years too old it has no galena analogue. Its location and size, however, would make it particularly susceptible to contamination by radiogenic strontium from the metamorphics. This condition would result in an anomalously old Rb - Sr age from the .7102 initial ratio assumption. Although the specimen used for analyses shows no obvious signs of contamination, an exposure one half mile to the north-west revealed numerous schistose xenoliths. By changing the age within the limits of the complete intrusive episode it is only possible to correlate this granite specimen with the galena sample from Robs Range, 60 miles to the south. If this theoretical Sr^{87} contamination occurred after an assumed ore-body formation, and was accompanied by lead contamination, it would obscure any original cogenesis. The isotopic ratios of this granite mass, however, are clearly different from either of the two closest mining centres,

for the Mungana mines are typified by a much higher 208/204 content, and those from the Redcap area are relatively enriched in lead 206.

The Herbert River Granite (2955) which is possibly the acid end-member for the Almaden Granite type, has an initial isotopic composition comparable to that of the ore from the Redcap area, 12 miles to the north; it is thus feasible that the two are cogenetic.

The isolated composition of galena Pb109 is closely matched by the initial ratio calculated for a Herbert River Granite (2977) sample from the Almaden area, 20 miles further west. Although it is difficult to envisage lateral migration of ore-bearing fluids on this scale at a high crustal level, the result nevertheless attests to the formation of a suitable magma type in the general vicinity.

The six remaining Palaeozoic granite data points on figures 26 and 27 are indistinguishable from the Featherbed Volcanic averages and the main mass of galena analyses beyond the end of the growth curves; the isotopic composition of these rocks is considered fundamentally important in the interpretation of the galena results. One of these rocks (2957), which appears to be contaminated with radiogenic Sr, comes from the Bullock Creek region on the western side of the Palmerville Fault. Another (2956, Elizabeth Creek Granite) comes from the same general area. The remainder were collected from the main tin-bearing area around Mt Garnet, Emuford and Herberton. The latter group includes representatives of the Elizabeth Creek, Herbert River and (?) Mareeba Granites, and the

Featherbed Volcanics. As all of these igneous rock types have lead of composition range similar to the spacially-associated lead ores from the Koorboora, Featherbed, Emuford - Irvinebank - Stannary Hills, Herberton, Silver Valley, Mt Garnet and Brownville areas, each must be considered as a possible source for these deposits.

Multiple Provenance

When we come to examine in greater detail the group of points beyond the end of the growth curve (figures 26 and 27), it can be seen that the samples from Koorboora (G) and Mt Garnet (L) possess 206/204 ratios significantly lower than those from other centres (I, J, K and M). It is proposed that this relationship derives dominantly from variable admixture of two end-member leads. The first is derived from the igneous rocks now being considered, and is of composition about 1 : 18.6 : 15.6 : 38.5; the second is similar to the leads found in the Mungana lodes (A). Each of these end-members possesses unique features of importance for the lead mines of the area. The former is isotopically similar to the spacially-associated igneous rocks, and occurs in the rich tin-field to the east of the area. Here this prolific igneous activity is associated with numerous small mines in which lead is generally not the main economic product. The Mungana lodes on the other hand, are characterised by high 208 content and occur in limestone in the north-west of the study area, close to the Palmerville Fault. Since almost one half of the economic lead

recovery from the whole area has come from these two mines, this lead type is particularly suitable as a fundamental end-member. However, the two results indicate that whereas this postulated end-member is characterised by high 208/204 and 208/206 ratios, it has by no means a constant composition; the Lady Jane and Girofla are both big mines, and are only one half mile apart, but have quite distinct isotopic compositions.

The mines associated with the granite-limestone contact along the Chillagoe - Ootann belt (C) also yield points falling between the two end-members, and thus appear to fit the mixing model. It seems relevant that these mines occur closer to Mungana than do the Mt Garnet and Koorboora mines; they also show evidence of a greater 'Mungana' component.

The Redcap group (B) is a little more difficult to interpret in this way, as the results fall slightly below the theoretical mixing line on both the x-y and x-z plots. In this case a suitable 206-deficient component could be a lead similar either to the lead from the Cardross district, or to a mixture of this and Mungana-type lead.

Both these 206-poor end members thus far advocated are represented by ores which occur either in or very close to the Precambrian rocks to the west of the area. This raises the question whether these end-members are both representatives of a possible range of leads derived from the Precambrian terrain. There are two other lines of evidence which support this.

a) The first is illustrated in figures 28 and 29 which are acetate overlays in the back pocket to be used in conjunction with the reduced area map in figure 30. These demonstrate the areal control of ore-lead composition by means of the 206/207 and 206/208 isotopic ratios. It can be seen that the contours on both diagrams closely follow the well-defined edge of the Palmerville Fault in the north-west corner. As the fault is approached from the east, both the 206/207 and 206/208 ratios decrease; this suggests very strongly that these parameters are controlled by the Precambrian rocks.

b) The remaining line of evidence for Precambrian derivation of the 206-poor lead component comes from the whole-rock lead results presented previously. Only one isotopic analysis is available for Precambrian material; this was collected from the small intrusion of Forsayth Granite south-west of Chillagoe. It was hoped that this would provide information on the origin of the closely-related Dargalong ores. As the present composition of the granite is less radiogenic than that of the ores, however, they can not have been directly derived therefrom at any time in the past, for the compositional difference between the two is accentuated as earlier periods of time are considered. The linearity between the Dargalong ores, the Forsayth Granite composition 327 m.y. ago, and the numerous results from the tin-bearing region in the east, on both x-y and x-z plots, on the other hand, suggest that the whole three are

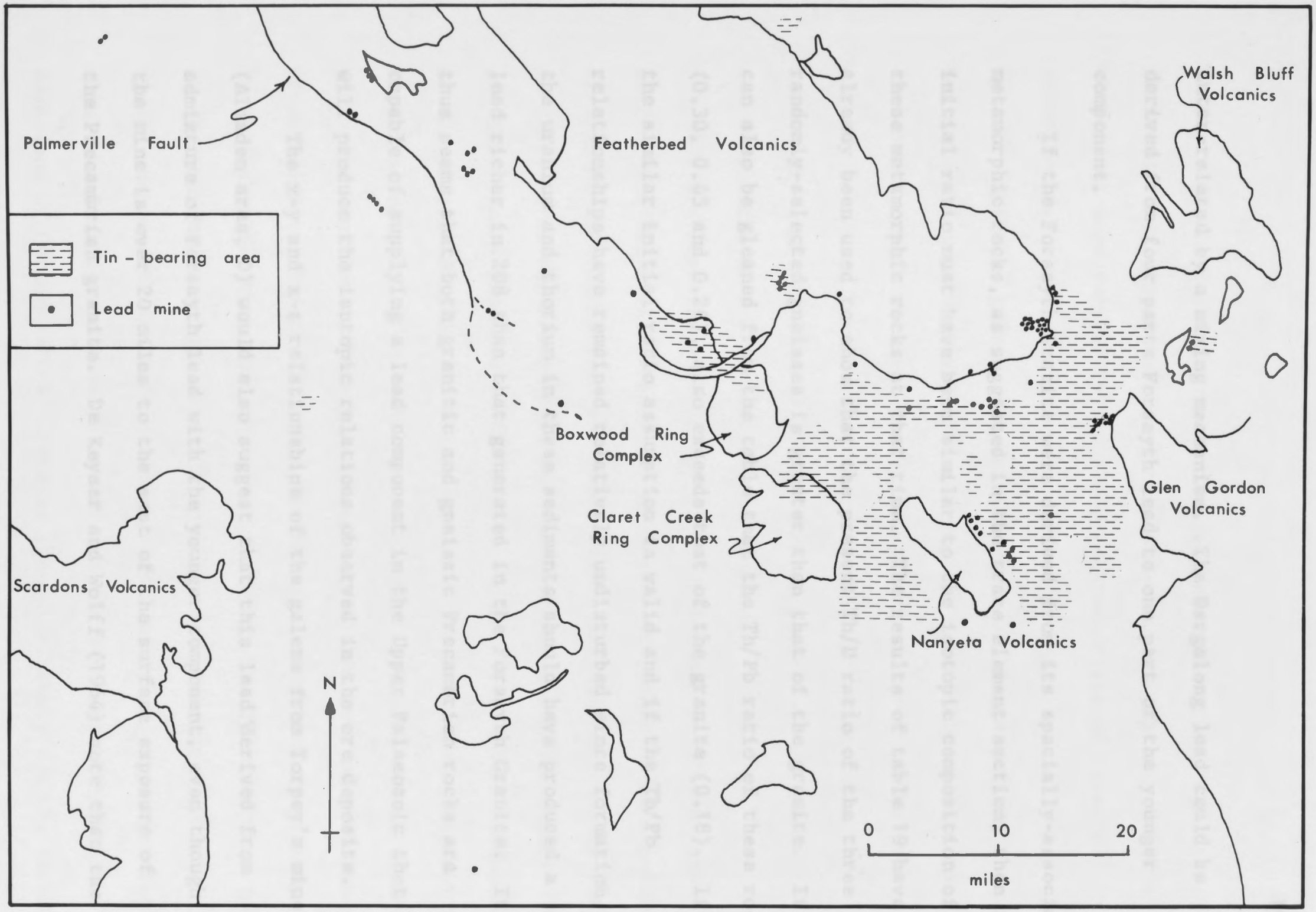

Figure 30. Geographical relationship between lead mines and tin-bearing areas.

Figure 30. Geographical relationship between lead mines and tin-bearing areas.

inter-related by a mixing mechanism. The Dargalong lead could be derived from four parts Forsayth lead to one part of the younger component.

If the Forsayth Granite were derived from its spacially-associated metamorphic rocks, as suggested in the trace element section, then its initial ratio must have been similar to the isotopic composition of these metamorphic rocks at that time. The results of table 19 have already been used to show that the present Th/U ratio of the three randomly-selected gneisses is greater than that of the granite. It can also be gleaned from the table that the Th/Pb ratio of these rocks (0.30, 0.45 and 0.26), also exceeds that of the granite (0.18). If the similar initial ratio assumption is valid and if the Th/Pb relationships have remained relatively undisturbed since formation, the uranium and thorium in these sediments should have produced a lead richer in 208 than that generated in the Forsayth Granite. It thus seems that both granitic and gneissic Precambrian rocks are capable of supplying a lead component in the Upper Palaeozoic that will produce the isotopic relations observed in the ore deposits.

The x-y and x-z relationships of the galena from Torpey's mine (Almaden area, D) would also suggest that this lead derived from admixture of Forsayth lead with the younger component, even though the mine is over 20 miles to the east of the surface exposure of the Precambrian granite. De Keyser and Wolff (1964) note that the

Torpey's ore is distinguished by its copper-free nature, and that the Dargalong ores also contain negligible amounts of copper. Perhaps this lends some support to a closely-related origin of these two occurrences.

The isolated galena analyses from the Robs Range and the Georgetown area, 70 miles further west, are remarkably similar to each other. Both fall too far below the growth curve on the x-y diagram to relate to the Forsayth-type lead, but possess the relatively high 208/206 and 207/206 ratios deduced to be generally characteristic of a Precambrian lead component.

All ore deposits which occur in the Precambrian rocks to the west of the Palmerville Fault are naturally difficult to date because of minimal stratigraphical and geochronological control. In as far as the ores in the Precambrian possess isotopic characteristics similar to many deposits in the Palaeozoic rocks, it seems rational on the present evidence to associate the two classes chronologically. The ores collected from the Palaeozoic rocks, however, can be treated with more confidence; thus the Mungana deposits cannot be older than Upper Silurian, and those in the Featherbed Volcanics are unlikely to be much older than Lower Permian. Although the isotopic data for the Mungana deposits could be interpreted as indicating a Devonian age in accordance with this stratigraphic limitation, a younger age cannot be excluded. Hence it seems reasonable to argue that the dominance of Carboniferous - Permian igneous activity and the current

absence of Devonian ages in the area indicate the younger igneous episode as primarily responsible for the mineralisation; it may be solely so.

Virtually all the variation in ore-lead isotopic composition, then, can be attributed to mixing of a rather uniform lead derived directly from the Palaeozoic igneous rocks in the east of the area with variable amounts of a non-uniform Precambrian component. It is difficult to generate the Silver Spray lead (Pb109) by this mechanism, but it may have been derived from a somewhat unusual Carboniferous or Permian magma of composition similar to rock 2977. However, the origin of the unusual isotopic composition of the lead in this magma is not known.

Examination of the vertical scatter on the x-y diagram for mining centres G to M reveals a slightly more complex relationship than has been so far presented. The ores in the Featherbed Volcanics (H), which show a considerable variation in 206/204 content, have relatively constant 207/204 ratios which tend to be lower than spacially-associated ores in the Hodgkinson Formation. Student's t test demonstrates that these two populations are significantly different at the 99.8 per cent confidence level, even although the total scatter is comparable to the estimated experimental uncertainty. No systematic error could apply to one group and not the other as the samples were analysed randomly. The composition of the galena in the Featherbeds also corresponds closely with the volcanic rock lead.

Thus the direct correlation of galena composition with rock type may well reflect contamination with Palaeozoic sedimentary lead. This hypothesis must for the present remain untested, however, since no representatives of this sedimentary suite were collected for analysis

Association with Tin

The composition of the lead occurring with tin mineralisation generally shows little variation, the 206/204, 207/204 and 208/204 ratios falling between the limits 18.52 - 18.69; 15.62 - 15.71; 38.37 - 38.67. These deposits occur east of the Koorboora area and encompass mining camps G to M. Microscope studies with reflected light (see appendix) showed that the great majority of the tin occurs as the oxide, cassiterite. Semi-quantitative studies (also reported in appendix), using the X-ray fluorescence technique (chapter 3) on the polished sections of ore, revealed that the isotopically distinct Girofla (Mungana) and Dargalong lead ores also contain some tin. Microscopic examination showed this to be present as the mixed-sulphide, stannite. The controlling mechanism correlating mode of tin occurrence with lead isotopic composition remains purely speculative.

Mechanism for Lead Concentration

It is imperative that the nature of the ore-forming process is condusive to the advocated widespread contamination. Previous workers, e.g. de Keyser and Wolff (1964) and Blake (1968), have regarded the ores as the products of residual mineralising fluids

emanating from the igneous rocks. Direct observations of such fluids during vulcanism and fumarolic activity have shown that they consist of water (80-90 per cent), CO_2, H_2S, S, CO, H_2, N, Cl, F, B and other substances besides the metals themselves (Bateman, 1950). Enormous quantities of hydrochloric and hydrofluoric acids and H_2S have been generated from the fumaroles of the Valley of Ten Thousand Smokes, Alaska (Zies, 1929). Evidence for similarly corrosive fluids in the Atherton area is found in the widespread hydrothermal alteration of sedimentary wall-rocks (de Keyser and Wolff, 1964), and the common occurrence of greisen in the more acidic intrusive rocks (Blake, 1968). The frequent occurrence of fluorite in the igneous rocks and mineral deposits throughout the area (especially in the fluorite lodes in the Precambrian) further attests to a corrosive acidic fluid. A fluid of this composition should efficiently leach rock-lead during its migration. In their study of the Utah mining districts, Stacey et al (1968) had to invoke a mineralising fluid which was able to leach excessive amounts of lead from upper crustal rocks. An earlier study by Doe et al (1966) on geothermal brine from the Salton Sea area, California, also demonstrated the leaching power of possible ore-bearing fluids. The limestone of the Chillagoe Formation would be expected to react strongly with those acidic fluids and thus provide favourable depositional environments. A chemical control of ore localisation is not so obvious in other rock types, where temperature and pressure differences may be primarily involved.

Origin and Time of Mineralisation

The isotopic data do not allow a specific decision on the source rock for the ore-bearing solutions, as the assumed original composition correlates with the initial ratio of representatives of the Herbert River, Mareeba and Elizabeth Creek Granites, and also the Featherbed Volcanics. However, the similarity of lead and strontium isotopic compositions for these rocks and their gradational geochemical relationship has shown them to belong to a single magma series. The more acidic rocks of this area, irrespective of designated rock type, are considered responsible for ore-body formation because the chalcophile elements such as lead, copper, tin and zinc (e.g. Taylor, 1966), and more importantly the hydrothermal fluids, with associated volatile constituents, are widely believed to concentrate in the residual melts.

Figure 30 is an attempt to show the areal relationship between all lead mines (dots) and the tin-bearing areas (hatched). The diagram has been compiled from information in de Keyser and Wolff (1964) and Blake (1968). Several interesting observations can be made, although the relationships are somewhat tentative in that detailed mapping has been confined to the areas of greatest economic importance.

There is a strong tendency for lead-bearing mines to occur close to the margins of volcanic rocks, and in particular, near the cauldron subsidence areas; the volcanics of the ring complexes do

not appear to be related to ore formation. The association may result either from a genetic relation in which the volcanics have supplied the ore-bearing fluids or alternatively, from a structural control of mineralisation. As the mineralisation is generally confined to the southern side of the large Featherbed Cauldron nearest the inferred Palmerville Fault, it is believed that the latter control is dominant. Indeed, the lead mines in the west may chiefly relate to the Palmerville Fault itself. The distribution of the lead mines then, appears to be related to faulted areas which have presumably acted as favourable channelways for ore-bearing solutions.

In the east the lead mines occur around the margins of tin-bearing areas, and are generally localised in sedimentary rocks between granites and volcanic rocks; some lead, however, occurs in the volcanics. Westwards, in the Koorboora and Bamford Hill areas, lead and tin occur together, and both are often found in the volcanic rocks. Further west, lead mineralisation occurs alone. This sequence could correlate with progressively shallower intrusions from west to east, which were either a primary feature or the result of differential erosion. The eastern area would be generally slightly below the granite roof zone, and the lead ores the result of lateral migration. In the Koorboora - Bamford area the granite is sufficiently below the present surface to expose the overlapping tin and lead zones, which were mineralised by ascending fluids. West of this the granite is still deeper, so that the tin zone is still not exposed, and only the lead zone can be seen.

Although this could explain the broad areal trends, as it correlates well with the amount of associated intrusion, it cannot be applied without qualification. For example, the Featherbed Volcanics have been shown to be younger than much of the Elizabeth Creek Granite outcropping in the east, and the lead mineralisation in the volcanics is most unlikely to have been derived from this granite. Furthermore, the tin deposits in the volcanics around Bamford Hill must also be younger than the dated Elizabeth Creek Granite to the south-east. During this study a grab sample (Pb239) was collected from a small mine west of Montalbion in the Featherbeds, and was found by X-ray fluorescence and reflected light microscopic techniques to contain about 40 per cent Pb. Not only does this point to another instance of post-granite tin, but it also directly weakens the reality of the district zoning around the granite, in that this mine occurs on the outermost edge of the lead zone.

Hence an unknown but definite proportion of the mineralisation is either the same age as, or younger than, the Featherbed Volcanics, and is probably Permian. Some representatives of the Elizabeth Creek (e.g. Wolfram Camp, Bamford Hill and sample 2959) and Herbert River (e.g. 2965) Granites which appear to be younger than the volcanics could have produced these ores. The Mareeba Granite which crops out mainly on the Mossman Sheet area must also be considered, as the isotopic composition of a possible representative of this granite is

indistinguishable from the lead in the tin mines in the central east of the study area. Amos and de Keyser (1964) show that this granite is associated with widespread tin mineralisation in the northern half of the Mossman area. Its association with lead mineralisation has not been reported but this may reflect stronger erosion, and hence a deeper level of exposure in the Hodgkinson Basin.

The precise mineralisation time is difficult to delineate, and more than one period of ore formation seems likely; this may be the explanation for the reversed zoning found in many of the mines. However, although the Precambrian rocks and Palaeozoic sediments are thought to supply a considerable portion of the lead in some deposits, it is not necessary to invoke a source other than the extensive Upper Carboniferous and Lower Permian acid igneous rocks for the primary mineralising fluid.

CHAPTER 10

SUMMARY

This thesis has been directed towards elucidating the magmatic relationships and origin of the mineral deposits in the Chillagoe - Herberton area, north Queensland. The major conclusions, which are derived essentially from studies of the Rb - Sr, U - Pb and Th - Pb systems, are listed hereafter.

1) Geological sampling for lead isotopic analysis must be undertaken with extreme care to avoid weathering effects. The U - Th diagram may be useful to reject samples unsuitable for isotopic analysis. Weathering appears to upset the U - Pb system before the Th - Pb system; this is attributed to the mobility of uranium in the hexavalent state.

2) The limited trace element data show no clear-cut division between the Elizabeth Creek and Herbert River Granites which were previously separated on 'genetic' grounds. High U, Th, Rb, and low Sr contents are characteristic of this petrographic province.

3) The Featherbed Volcanics were formed at a time very close to the Carboniferous - Permian boundary, and hence form a useful marker horizon. Most of the intrusion, except for the Mareeba Granite which crops out mainly to the north of the area, was confined to the Carboniferous period. A definite spread of ages appears probable.

4) No age difference could be found for the Herbert River and Elizabeth Creek Granite types, but the former yields a relatively imprecise value.

5) It is not possible to distinguish the Herbert River, Mareeba and Elizabeth Creek Granites on the basis of strontium or lead initial ratios.

6) The Nychum Volcanics and Almaden Granite possibly result from mixing of a basic end-member with two magma types, conceivably not directly related, and yield spuriously-old total rock Rb - Sr ages. The correct age of the volcanics is probably uppermost Carboniferous, a result which is consistent with the Rb - Sr mineral age. Aberrant results of this type may be detected on a K - Rb diagram.

7) Concordant U^{238}-Pb^{206}, Th^{232}-Pb^{208} and Rb^{87}-Sr^{87} ages for the Featherbed Volcanics demonstrate that the former systems can be utilised for geochronological studies.

8) The Elizabeth Creek Granite, which has been ascribed an important role in ore formation by Blake (1968) is isotopically similar to the spacially-associated ore-deposits in the east of the area. On the other hand, the sampled Almaden Granite has a quite different composition from its closest ores.

9) Extensive mixing of a fairly uniform lead component from Carboniferous - Permian magmas with readily-leachable country rock lead could produce the isotopic patterns observed in the galena ores.

It is not necessary to derive a mineralising fluid from any other but the Carboniferous - Permian igneous rocks.

10) The chief source of the ore-bearing fluids is attributed to the more siliceous rocks on mainly geochemical grounds.

11) The large Elizabeth Creek intrusion in the Emuford - Mt Garnet - Ravenshoe area can not have produced all the lead or tin deposits the near vicinity. It is probable that mineralisation was not confined to a well-defined episode but occurred at various times in the Upper Carboniferous and Lower Permian.

BIBLIOGRAPHY

Abbott, M. J., 1965. A petrological study of the Nandewar Volcano. Unpublished Ph.D. Thesis, Australian National University.

Aldrich, L. T., Davis, G. L., Tilton, G. R. and Wetherill, G. W., 1956. Radioactive ages of minerals from the Brown Derby mine and the Quartz Creek Granite near Gunnison, Colorado. J. Geophys. Res., 61, pp. 215-232.

Aldrich, L. T., Wetherill, G. W., Tilton, G. R. and Davis, G. L., 1956. Half-life of Rb^{87}. Phys. Rev., 103, pp. 1045-1047.

Amos, B. J. and Deyser, F. de, 1964. Mossman, Qld. - 1 : 250,000 Geological Series. Bur. Min. Resour. Aust. explan Notes SE/55 - 1

Arriens, P. A. and Compston, W., 1968. A method for isotopic ratio measurement by voltage peak switching and its application with digital output. Int. J Mass Spect. and Ion Phys., 1, pp. 471-481.

Barbier, J. and Ranchin, G., 1969. Influence de l'alteration meteorique sur l'uranium a l'etat de traces dans le granite a deux micas de St-Sylvestre. Geochim. et Cosmochim. Acta, 33, pp. 39-47.

Bateman, A. M., 1950. Economic mineral deposits. 2nd Ed. John Wiley and Sons, New York.

Best, J. G., 1962. Atherton, Qld. - 1 : 250,000 Geological Series. Bur. Min. Resour. Aust. explan Notes E155 - 5

Beynon, J. H., 1960. Mass spectrometry and its applications to organic chemistry. Elsevier, Amsterdam.

Black, L. P., 1965. The geology of the Eucumbene area. Unpublished B.Sc.(Hons.) Thesis, Australian National University.

Blake, D. H., 1968. Regional and economic geology of the Herberton - Mount Garnet area, Herberton tinfield, north Queensland. Bur. Min. Resour. Aust. Rec. 1968/79, (unpubl.)

Branch, C. D., 1960. Geology of the Ruddygore and Zillmanton copper mine areas, near Chillagoe, north Queensland. Bur. Min. Resour. Aust. Rec. 1960/51, (unpubl.)

Branch, C. D., 1961. The emplacement of acid magma in the epizone, and the relationship with ignimbrites, north Queensland, Australia. Bur. Min. Resour. Aust. Rec. 1961/143, (unpubl.).

Branch, C. D., 1962. The structural and magmatic relationship between acid lavas, pyroclastic flows and granite of the Georgetown Inlier, north Queensland. Unpublished Ph.D. Thesis, University of Sydney.

Branch, C. D., 1966. Volcanic cauldrons, ring complexes, and associated granites of the Georgetown Inlier, Queensland. Bur. Min. Resour. Aust. Bull./76

Branch, C. D., 1967. Genesis of magma for acid calc-alkaline volcano - plutonic formations. Tectonophysics, 4, pp. 83-100.

Catanzaro, E. J., 1967. Triple filament method for solid-sample lead isotopic analysis. J. Geophys. Res., 72, pp. 1325-1327.

Catanzaro, E. J., 1968. Absolute isotopic abundance ratios of three common lead reference samples. Earth and Planet. Sci. Letters, 3, pp. 343-346

Catanzaro, E. J. and Gast, P. W., 1960. Isotopic composition of lead in pegmatitic feldspars. Geochim. et Cosmochim. Acta, 19, pp. 113-126

Catanzaro, E. J., Murphy, T. J., Shields, W. R. and Garner, E. L., 1968. Absolute isotopic abundance ratios of common equal-atom and radiogenic lead isotopic standards. J. Res. Nat'l. Bureau Standards. A. Physics and Chemistry, 72A, No. 3, pp. 261-267.

Chappell, B. W., 1966. Petrogenesis of the granites at Moonbi, New South Wales. Unpublished Ph.D. Thesis, Australian National University.

Chappell, B. W., Arriens, P. A., Compston, W. and Vernon, M. J., in press. Rubidium and strontium determination by X-ray fluorescence spectrometry and isotope dilution below the part per million level.

Chow, T. J. and McKinney, C. R., 1958: Mass spectrometric determination of lead in manganese nodules. Anal. Chem., 30, pp. 1499-1503

Compston, W. and Jeffery, P. M., 1959. Anomalous "common strontium" in granite. Nature, 184, p. 1792.

Compston, W., Jeffery, P. M. and Riley, G. A., 1960. Age of emplacement of granites. Nature, 186, pp. 702-703.

Compston, W., Lovering, J. F. and Vernon, M. J., 1965. The rubidium - strontium age of the Bishopville aubrite and its component enstatite and feldspar. Geochim. et Cosmochim. Acta, 29, pp. 1085-1099.

Compston, W. and Oversby, V. M., in press. Lead isotope analysis using a double spike. J. Geophys. Res.

Cooper, J. A., Reynolds, P. H. and Richards, J. R., in preparation. Some consequences of lead isotope intercomparisons and a new terrestrial growth curve.

Cooper, J. A. and Richards, J. R., 1966a. Lead isotopes and volcanic magmas. Earth and Planet. Sci. Letters, 1, pp. 259-269.

Cooper, J. A. and Richards, J. R., 1966b. Solid-source lead isotope measurements and isotopic fractionation. Earth and Planet. Sci. Letters, 1, pp. 58-64.

Crouch, E. A. C. and Webster, R. K., 1963. Choice of the optimum quantity and constitution of the tracer used for isotopic dilution analyses. Journ. Chem. Soc., 18, pp. 118-131.

Deer, W. A., Howie, R. A. and Zussman, J., 1963. Rock forming minerals. Vol. 2. Chain silicates. Longmans, London.

Dickins, J. M., 1961. Eurydesma and Peruviopira from the Dwyka beds of South Africa. Palaeontology, 4, pp. 138-148.

Doe, B. R., 1962. Relationships of lead isotopes among granites, pegmatites, and sulfide ores near Balmat, New York. J. Geophys. Res., 67, pp. 2895-2906.

Doe, B. R., Hedge, C. E. and White, D. E., 1966. Preliminary investigation of the source of lead and strontium in deep geothermal brines underlying the Salton Sea geothermal area. Econ. Geol., 61, pp. 462-483.

Doe, B. R., Tatsumoto, M., Delevaux, M. H. and Peterman, Z. E., 1967. Isotope-dilution determination of five elements in G-2 (granite), with a discussion of the analysis of lead. U.S. Geol. Survey Prof. Paper, 575-B, pp. 170-177.

Doe, B. R., Tilling, R. I., Hedge, C. E. and Klepper, M. R., 1968. Lead and strontium isotopic studies of the Boulder batholith, south-western Montana. Econ. Geol., 63, pp. 884-906.

Doe, B. R., Tilton, G. R. and Hopson, C. A., 1965. Lead isotopes in feldspars from selected granitic rocks associated with regional metamorphism. J. Geophys. Res., 70, pp. 1947-1968.

Eberhardt, A., Delwiche, R. and Geiss, G., 1964. Isotopic effects in single filament thermal ion sources. Z. f. Naturforsch., 19, pp. 736-740.

Farquharson, R. B., 1968. Whole rock isotopic studies in the region of Mount Isa, Queensland. Unpublished Ph.D. Thesis, Australian National University.

Fitch, F. J., Miller, J. A. and Williams, S. C., in press. Isotopic ages of British Carboniferous rocks. C. R. 6th Int. Congr. Carb. Strat. Geol. (Sheffield 1967).

Gast, P. W., Tilton, G. R. and Hedge, C., 1964. Isotopic composition of lead and strontium from Ascension and Gough Islands. Science, 145, pp. 1181-1185.

Goldich, S. S., Muehlberger, W. R., Lidiak, E. G. and Hedge, C. E., 1966. Geochronology of the midcontinental region, United States. 1. Scope, methods and principles. J. Geophys. Res., 71, pp. 5375-5388.

Green, D. H. and Ringwood, A. E. 1967. The genesis of basaltic magmas. Contr. Mineral. and Petrol., 15, pp. 103-190.

Griffin, W. L. and Murthy, V. R., preprint. Distribution of K, Rb, Sr and Ba in some minerals relevant to basalt genesis.

Gunn, B. M. and Watkins, N. D., 1969. The Petrochemical effect of the simultaneous cooling of adjoining basaltic and rhyolitic magmas. Geochim. et Cosmochim. Acta, 33, pp. 341-356.

Hamilton, E. I., 1965. Applied Geochronology. Academic Press, London.

Hamilton, E. I., 1968. The isotopic composition of strontium applied to problems of the origin of the alkaline rocks. In "Radiometric Dating for Geologists", eds. Hamilton E. I. and Farquhar, R. M., Interscience Publishers, London.

Harker, A., 1954. Petrology for Students. Cambridge University Press.

Harland, W. B., Smith, A. G. and Wilcock, B., eds., 1964. The phanerozoic time scale. Geological Society of London.

Harris, P. G., 1957. Zone refining and the origin of potassic basalts. Geochim. et Cosmochim. Acta, 12, pp. 195-208.

Hatch, F. H., Wells, A. K. and Wells, M. K., 1961. Petrology of the Igneous Rocks. 12th Ed. Thomas Murby and Co., London.

Heier, K. S., Compston, W. and McDougall, I., 1965. Thorium and uranium concentrations and the isotopic composition of strontium in the differentiated Tasmanian dolerites. Geochim. et Cosmochim. Acta, 29, pp. 643-659.

Hodgman, C. D., eds, 1962. Handbook of Chemistry and Physics 43rd Ed. Chemical Rubber Publishing Company.

Holmes, A., 1946. A estimate of the age of the earth. Nature, 157, pp. 680-684.

Houtermans, F. G., 1946. The isotope ratios in natural lead and the age of uranium. Naturwiss., 33, pp. 185-186.

Inghram, M. G., 1946. Manhatten Project, tech. ser., Nat. nuclear energy ser., div II, vol. 14, chap. 5, p. 35. New York; McGraw-Hill.

Kanasewich, E. R., 1962. Quantitative interpretations of anomalous lead isotope abundances. Unpublished Ph.D. Thesis, University of British Columbia.

Kanasewich, E. R., 1968. Radiometric dating for Geologists. Ed., Hamilton, E. I., and Farquhar, R. M. Interscience Publishers, London. pp. 147-223.

Kanasewich, E. R. and Farquhar, R. M., 1965. Lead isotope ratios from the Cobalt - Noranda area, Canada. Can. J. Earth Sci., 2, pp. 361-384.

Keyser, F. de, 1961. Geology and mineral deposits of the Mossman 1 : 250,000 sheet area, north Queensland. Bur. Min. Resour. Aust. Rec. 1961/110, (unpubl.).

Keyser, F. de, 1963. The Palmerville Fault - a "fundamental" structure in north Queensland. J. Geol. Soc. Aust., 10, pp. 273-278.

Keyser, F. de, Bayly, M. B. and Wolff, K., 1959. The geology and mineral deposits of the Mungana, Chillagoe and Almaden 1 - mile sheets. Bur. Min. Resour. Aust. Rec. 1959/108, (unpubl.)

Keyser, F. de and Wolff, K. W., 1964. The geology and mineral resources of the Chillagoe area, Queensland. Bur. Min. Resour. Aust. Bull./70.

Kleeman, A. W., 1967. Sampling error in the chemical analysis of rocks. J. Geol. Soc. Aust., 14, pp. 43-47.

Kleeman, J. D. and Lovering, J. F., 1967. Uranium distribution in rocks by fission-track registration in lexan plastic. Science, 156, pp. 512-513.

Krumbein, W. C. and Pettijohn, F. J., 1938. Manual of sedimentary petrography. Appleton - Century - Crofts.

Kulp, J. L., Bate, G. L. and Broecker, W. S., 1954. Present status of the lead method of age determination. Amer. J. Sci., 252, pp. 345-365.

Kulp, J. L. and Engels, J., 1963. Discordances in K-Ar and Rb-Sr isotopic ages. Radiometric Dating. International Atomic Energy Agency, Vienna.

Kwestroo, W. and Visser, J., 1965. The ultrapurification of hydrofluoric acid. The Analyst, 90, pp. 297-298.

McIntyre, G. A., Brooks, C., Compston, W. and Turek, A., 1966. The statistical assessment of Rb-Sr isochrons. J. Geophys. Res., 71, pp. 5459-5468.

Masuda, A., 1962. Experimental method for determination of isotopic composition of lead in volcanic rock. Earth Sci. Nagoya Univ., 10, pp. 117-124.

Mollan, R. G., 1965. Tertiary volcanics in the Peak Range, central Queensland. Unpublished M.Sc. Thesis, Australian National University.

Morgan, J. W. and Heier, K. S., 1966. Uranium, thorium and potassium in six U.S.G.S. standard rocks. Earth and Planet. Sci. Letters, 1, pp. 158-160.

Morgan, W. R., 1961. The Carboniferous and Permo-Triassic igneous rocks of the Mossman four-mile sheet area, north Queensland. Bur. Min. Resour. Aust. Rec., 1961/125, (unpubl.).

Moroney, M. J., 1964. Facts from Figures. London Penguin.

Murthy, V. R. and Patterson, C. C., 1961. Lead isotopes in ores and rocks of Butte, Montana. Econ. Geol., 56, pp. 59-67.

Naumov, G. B., 1959. Transportation of uranium in hydrothermal solution as a carbonate. Geochemistry, 1, pp. 5-20.

Nicolaysen, L. O., 1961. Graphic interpretation of discordant age measurements on metamorphic rocks. Ann. N.Y. Acad. Sci., 91, pp. 198-206.

Nockolds, S. R., 1954. Average chemical compositions of some igneous rocks. Bull. Geol. Soc. Amer., 65, pp. 1007-1032.

Norrish, K. and Chappell, B. W., 1967. X-ray fluorescence spectrography. In "Physical methods in determinative mineralogy", Ed., Zussman, J. pp. 161-214. Academic Press.

Ostic, R. G., Russell, R. D. and Stanton, R. L., 1967. Additional measurements of the isotopic composition of lead from stratiform deposits. Can. J. Earth Sci., 4, pp. 245-269.

Patterson, C. C., 1951. The isotopic composition of trace quantities of lead and calcium. Atomic Energy Comm., Rept AECD 3180.

Patterson, C. C., 1956. Age of meteorites and the earth. Geochim. et Cosmochim. Acta, 10, pp. 230-237.

Reynolds, P. H., 1967. A lead isotope study of ores and adjacent rocks. Unpublished Ph.D. Thesis, University of British Columbia.

Richards, J. R., 1962. Isotopic composition of Australian leads I. Preparation of tetramethyl lead samples. Mikrochimica Acta, 4, pp. 620-627.

Richards, J. R., 1966. Some Rb-Sr measurements on granites near Mt Isa. Proc. Aust. Inst. Min. Met., No 218, pp. 19-23.

Richards, J. R., 1967. Lead isotopes at Dugald River and Mount Isa, Australia. Geochim. et Cosmochim. Acta, 31, pp. 51-62.

Richards, J. R., 1968a. "Primary" leads. Nature, 219, pp. 258,259.

Richards, J. R., 1968b. Lead isotopes and geochronology in western Tasmania. Aust. J. Sci., 31, pp. 129-137.

Richards, J. R., Berry, H. and Rhodes, J. M., 1966c. Isotopic and lead-alpha ages of some Australian zircons. J. Geol. Soc. Aust., 14, pp. 69-96.

Richards, J. R., White, D. A., Webb, A. W. and Branch, C. D., 1966. Isotopic ages of acid igneous rocks in the Cairns hinterland, north Queensland. Bur. Min. Resour. Aust. Bull./88.

Rosenqvist, I. T., 1942. Determination of lead in silicate rocks. Amer. J. Sci., 240, pp. 356-362.

Russell, R. D. and Farquhar, R. M., 1960. Lead isotopes in geology. Interscience Publishers, New York.

Russell, R. D. and Reynolds, P. H., 1965. The age of the earth. U.S.S.R. Academy of Sciences, Geochemical Institute. Translation from russian by F. Kousal and J. R. Richards, revised by P. H. Reynolds.

Sandell, E. B., 1950. Colorimetric determination of traces of metals. 2nd Ed. Interscience Publishers Inc., New York.

Schreiner, G. D. L., 1958. Comparison of the $^{87}Rb \longrightarrow {}^{87}Sr$ ages of the red granite of the Bushveld complex from measurements of the total rock and separated mineral fractions. Proc. Roy. Soc., A, pp. 112-117.

Shaw, D. M., 1957. Comments on the geochemical implications of lead-isotope dating of galena deposits. Econ. Geol., 52, pp. 570-573.

Slawson, W. F. and Russell, R. D., 1963. Concerning the occasional presence of a contaminant in tetramethyl lead. Mikrochimica Acta, 1, pp. 165-168.

Stacey, J. S., Zartman, R. E. and Nkomo, I. T., 1968. A lead isotope study of galenas and selected feldspars from mining districts in Utah. Econ. Geol., 63, pp. 796-814.

Stanton, R. L. and Russell, R. D., 1959. Anomalous leads and the emplacement of lead sulphide ores. Econ. Geol., 54, pp. 588-607.

Stieff, L. R., Stern, T. W., Oshiro, S. and Senftle, F. E., 1959. Tables for the calculation of lead isotope ages. U. S. Geol. Survey Prof. Paper 334-A, pp. 1-40.

Swainbank, I. G., 1967. The isotopic composition of lead and strontium from the volcanic rocks of the islands of the south Pacific. Unpublished Ph.D. Thesis, Columbia University.

Tatsumoto, M., 1966a. Genetic relations of oceanic basalts as indicated by lead isotopes. Science, 153, pp. 1094-1101.

Tatsumoto, M., 1966b. Isotopic composition of lead in volcanic rocks from Hawaii, Iwo Jima and Japan. J. Geophys. Res., 71, pp. 1721-1733.

Taylor, S. R., 1966. The application of trace element data to problems in petrology, in: Physics and Chemistry of the Earth, 6, pp. 133-213.

Taylor, S. R., Ewart, A. and Capp, A. C., 1968. Leucogranites and rhyolites: Trace element evidence for fractional crystallisation and partial melting. Lithos, 1, pp. 179-186.

Taylor, S. R. and White, A. J. R., 1966. Trace element abundances in andesites. Bull. Volcanol., 29, pp. 177-194.

Tilton, G. R., Davis, G. L., Wetherill, G. W. and Aldrich, L. T., 1957. Isotopic ages of zircon from granites and pegmatites. Trans. Amer. Geophys. Union, 38, pp. 360-371.

Tilton, G. R., Patterson, C., Brown, H., Inghram, M., Hayden, R., Hess, D. and Larsen, E., jr., 1955. Isotopic composition of lead, uranium, and thorium in a Precambrian granite. Bull. Geol. Soc. Amer., 66, pp. 1131-1148.

Ulrych, T. J. and Reynolds, P. H., 1966. Whole rock and mineral leads from the Llano Uplift, Texas. J. Geophys. Res., 71, pp. 3089-3094.

White, D. A., 1965. The geology of the Georgetown/Clarke River area, Queensland. Bur. Min. Resour. Aust. Bull./71.

White, M. E., 1961. Plant Fossils from the Hodgkinson Formation, north Queensland. Bur. Min. Resour. Aust. Rec. 1961/17. (unpubl.).

Whittles, A. B. L., 1964. Trace lead isotopic studies with gas source mass spectrometry. Unpublished Ph.D. Thesis University of British Columbia.

Wilson, J. T., Russell, R. D. and Farquhar, R. M., 1956. Economic significance of basement subdivision and structures in Canada. Canad. Min. Met. Bull., 59, pp. 310-318.

York, D., 1969. Least-squares fitting of a straight line with correlated errors. Earth and Planet. Sci. Letters, 5, pp. 320-324.

Zies, E. G., 1929. The Valley of Ten Thousand Smokes: Natl. Geog. Soc. Contr. Tech. Papers, Katmai ser., 1, No.4.

Zimmerman, D. O., Yates, K. R. and Amos, B. J., 1963. The geology and mineral deposits of the Mount Garnet area, north Queensland. Bur. Min. Resour. Aust. Rec. 1963/77, (unpubl.).

APPENDIX A

PETROGRAPHIC DESCRIPTIONS OF THE MAIN ROCK TYPES

The Featherbed Volcanics

a) RHYODACITE WELDED TUFFS (after Branch, 1966; the author, this study)

One of the most noticeable features of the rhyodacite welded tuffs is the high proportion of phenocrysts. These generally range between 20 and 80 per cent of the rock, and are commonly fragmented. The β-quartz phenocrysts are deeply embayed, range from one to four ml. in size, and show undulose extinction. Alkali feldspar consists of sanidine, anorthoclase and orthoclase. Fine perthite often occurs in intensely welded zones. Plagioclase phenocrysts are zoned from andesine to oligoclase and possess transitional to high-temperature optical properties. Antiperthite occurs locally. Biotite is generally altered to, or completely pseudomorphed by chlorite, calcite and iron oxide; unaltered biotite does occur locally. It is pleochroic from straw yellow to deep brown, and contains inclusions of apatite and zircon. Other ferromagnesian minerals are also commonly altered, but may be completely fresh. Hornblende is often found as olive-brown skeletal crystals and needles of arfvedsonite have been reported by Branch. Augite has been identified in some sections; Branch considers this to be a sub-calcic variety.

The fine-grained quartzofeldspathic groundmass is mostly devitrified glass. Very fine-grained pale green amphibole occurs sporadically in the groundmass. Devitrified glass shards occur in non- and poorly-welded varieties. Zircon, apatite, epidote, monazite and iron oxide are the accessory minerals. Pumice fragments and xenoliths are rare. The complete range of textures from incipiently to densely welded tuff can be seen in thin section.

b) RHYOLITE (the author, this study)

A rock of rhyolitic composition was collected from the Featherbed Volcanics five miles south of Wolfram Camp. It is porphyritic with about 45 per cent phenocrysts which average two mm. in size. β-quartz phenocrysts are common. These are highly embayed, often angular, but sometimes rounded. Potash feldspar occurs as irregularly shaped grains, some of which show Carlsbad twinning; others are more complexly twinned. Microperthite is occasionally present. Plagioclase is of albite to oligoclase composition and is subordinate to potash feldspar in both amount and grain size. The plagioclase grains are strongly sericitised and approximately lath-shaped. Aggregates of chlorite and carbonate with inclusions of iron ore, zircon and apatite appear to be pseudomorphing biotite.

The structureless quartzofeldspathic groundmass contains fine-grained iron oxide.

c) DACITES (the author, this study)

Two dacites were collected for this study. These outcrop five miles north of and six miles south-east of Petford. The first contains essentially no potash feldspar phenocrysts. Plagioclase grains are generally tabular and average .5 millimetres in size. Albite and albite-Carlsbad twins are common; pericline twins are rare. Most of the plagioclase is andesine; strong oscillatory zoning is abundant. Quartz grains are rounded and very deeply embayed. A fine-grained amphibole with the pleochroic scheme α = yellow green, γ = blue green, (actinolite ?) is associated with patches of chlorite, epidote and iron oxide. These aggregates probably represent the alteration products of an ancestral ferromagnesian mineral. The groundmass is very fine-grained and consists of greenish mica, quartz, plagioclase and potash feldspar. Accessory minerals include zircon, monazite, apatite and irregular grains of sphene.

The dacite south-east of Petford contains perthitic potash feldspar phenocrysts which are subordinate to the zoned plagioclase grains. Quartz and feldspar grains are generally angular. Mafic minerals include red brown biotite and both ortho- and clinopyroxene. The pyroxenes are sometimes surrounded by a rim of chlorite; iron oxides are generally associated with this alteration. The groundmass of this dacite is siliceous and very fine-grained.

The Herbert River Granite

(after de Keyser and Wolff, 1964; Branch, 1966; Blake, 1968; the author, this study)

This rock which is predominantly a biotite adamellite, locally grades into hornblende biotite granodiorite. Plagioclase forms from ten to 50 per cent of the Herbert River Granite and shows both oscillatory and normal zoning (from andesine in the centre to oligoclase at grain boundaries). Fluorite and hornblende inclusions have been found. Myrmekitic structures sometimes occur. Albite and albite-Carlsbad twins are most common; some pericline twinning occurs. The plagioclase occurs as the low temperature modification (Branch, 1966). The potash feldspar (ten to 45 per cent of the rock) is generally orthoclase which occurs as string or film perthite, although microcline perthite is also present in some samples. It occurs as phenocrysts, poikilitic plates enclosing plagioclase and biotite, and as interstitial grains. Potash feldspar is also intergrown with quartz in graphic intergrowth. Quartz varies between 25 and 50 per cent and is generally anhedral. Biotite (five to ten per cent) is pleochroic from straw yellow to dark brown. Muscovite is only rarely present. Anhedral hornblende is less abundant than biotite; it is partly replaced by epidote, chlorite, iron oxide and calcite. Accessory minerals are apatite, tourmaline, sphene, allanite, garnet, zircon and magnetite.

The Almaden Granite

(after de Keyser and Wolff, 1964; Branch, 1966; Blake, 1968; the author, this study)

The Almaden granite is a biotite-bearing hornblende granodiorite. Plagioclase grains are seen in thin section to possess both normal and oscillatory zoning. Marked normal zoning is restricted to grain margins. Most grains have a central composition of An_{34}. One grain with a highly irregular-shaped calcic core was found to have a compostition of An_{75}. Results quoted by Branch (1966), however, claim that the composition of calcic cores ranges from 60 to 92 per cent anorthite. This discrepancy and the measured range in composition may be best explained by my observations on granites from the Eucumbene area, southern New South Wales (Black, 1965)*.

Plagioclase grains in the Almaden Granite occasionally contain inclusions of fluorite, clinopyroxene, biotite and hornblende; cores of grains are often heavily sericitised. Myrmekitic structures are not common. Potash feldspar is subordinate to plagioclase; it is

---

*

In the Eucumbene area there appears to be three generations of plagioclase cores with characteristic compositions. The most basic were considered to be residual grains from the partial melt which generated the granite. These are rare, and show a marked optical break against the rest of the grain. The most common cores possess the most acid composition of the group, commonly show oscillatory zoning, and were interpreted as direct crystyllates from the melt. The intermediate cores possess the same composition as the plagioclase in the basic xenoliths, and may have been mechanically rafted off these xenoliths. This interpretation would suggest that the composition of plagioclase grains within a granite is somewhat complex.

often microperthitic but generally untwinned and occurs as interstitial grains. Quartz is present as small anhedral grains. Biotite and hornblende occur in approximately equal proportions and generally form about 20 per cent of the rock. Grains of augite occur rarely. Siderite, zircon, apatite, tourmaline, yellow pleochroic epidote, allanite and iron oxide occur as accessory minerals.

The following summary of the dioritic phase from Petford is derived from the work of de Keyser and Wolff (1964) and the author (this study). This rock contains lath-shaped plagioclase grains which are strongly zoned from labradorite to andesine and often even to oligoclase composition. Potash feldspar, which is one third as abundant as plagioclase, is generally interstitial; some grains may poikilitically enclose plagioclase grains. Quartz is also interstitial and forms ten per cent of the rock. Mafic minerals include red brown biotite, both ortho- and clinopyroxene (the former predominates) and pale-coloured hornblende which appears to be secondary after pyroxene. The colour index of the rock is about 35 per cent.

The Elizabeth Creek Granite

(after de Keyser and Wolff, 1964; Branch, 1966; Blake, 1968; the author, this study)

This rock is generally classed as an adamellite, but granitic varients do occur. Plagioclase occurs as euhedral to subhedral grains which show prolific twinning. Albite twins dominate;

albite-Carlsbad and pericline twinning are also present. Normal zoning is weakly developed and is generally confined to the margins of grains. Most grains are composed of oligoclase, although acid andesine does occur; albite is present in the granitic varieties. The plagioclase possesses low to transitional optical properties (Branch, 1966). Branch also reports rare xenocrysts of labradorite-bytownite composition. In porphyritic varieties the groundmass plagioclase is richer in albite than the phenocrysts. Fluorite inclusions are common; rarely a plagioclase grain is seived with rounded quartz blebs. Incipient sericitisation is frequent. Myrmekitic intergrowths with quartz are common in some varieties. The plagioclase content varies from ten to 40 per cent.

Potash feldspar (25-55 per cent of the rock) is generally more abundant than plagioclase. It appears to be dominantly orthoclase perthite in the western part of the area (Branch) and microcline perthite in the east (Blake). Perthite lamellae are composed of albite or acid oligoclase and range up to .2 ml. Carlsbad twinning occurs locally but is not general. The potash feldspar occurs either as interstitial anhedral grains (which may become poikilitic) or subhedral phenocrysts which commonly display graphic texture around their margin.

Quartz forms from 35 to 50 per cent of the granite and is generally anhedral and interstitial. Rounded phenocrysts occurring in porphyritic modifications are commonly composite.

Biotite is the only major primary ferromagnesian mineral; it comprises from one to five per cent of the granite. Both red brown and green brown varieties are present and in places these are partly altered to chlorite and iron oxide. Large tabular grains which may have ragged boundaries, and finer grains in distinct aggregates, occur. Inclusions of monazite are surrounded by intense pleochroic haloes. Fluorite is the most characteristic accessory mineral. Zircon, apatite, sphene, monazite, epidote, piedmontite, calcite, tourmaline, allanite (which is strongly zoned and often has strongly metamict margins), muscovite, iron oxide and cassiterite are the other common accessories.

APPENDIX B

ROCK CATALOGUE

The exact locations of samples listed in this catalogue will be found plotted on the Atherton 1 : 250,000 sheet in the back pocket.

G.A.2950. Lat. 17°02'S, Long. 144°12'E; Gneiss of the Dargalong Metamorphics. 2950L refers to a leucrocratic band of the gneiss, whereas 2950M refers to an adjoining biotite-bearing band. Collected by L. P. Black and E. H. Pedersen.

G.A.2951. Lat. 17°02'S, Long. 144°17'E; Rhyodacite phase of the Nychum Volcanics. Collected by L. P. Black and E. H. Pedersen.

G.A.2952. Lat. 17°05'S, Long. 144°21'E; Adamellite phase of the Elizabeth Creek Granite. Collected by L. P. Black and E. H. Pedersen.

G.A.2953. Lat. 17°08'S, Long. 144°33'E; Granodiorite phase of the Almaden Granite. Collected by L. P. Black and E. H. Pedersen.

G.A.2954. Lat. 17°13'S, Long. 144°27'E; Two mica granodiorite of the Forsayth Granite. Collected by L. P. Black and E. H. Pedersen.

G.A.2955. Lat. 17°15'S, Long. 144°23'E; Granodiorite phase of the Herbert River Granite. Collected by L. P. Black and E. H. Pedersen.

G.A.2956. Lat. 17°37'S, Long. 144°31'E; Adamellite phase of the Elizabeth Creek Granite. Collected by L. P. Black and E. H. Pedersen.

G.A.2957. Lat. 17°41'S, Long. 144°31'E; Adamellite. According to Branch (pers. comm.) this is a hybrid Elizabeth Creek - Herbert River Granite sample. Its dominant characteristics, however, appear to be of the former. Collected by L. P. Black and E. H. Pedersen.

G.A.2958. Lat. 17°44'S, Long. 144°34'E; Precambrian gneiss. Collected by L. P. Black and E. H. Pedersen.

G.A.2959. Lat. 17°58'S, Long. 144°50'E; Adamellite phase of the Elizabeth Creek Granite. Collected by L. P. Black and E. H. Pedersen.

G.A.2960. Lat. 17°29'S, Long. 145°01'E; Granite, Elizabeth Creek Granite. Collected by L. P. Black and E. H. Pedersen.

G.A.2961. Lat. 17°17'S, Long. 144°57'E; Dacite, Featherbed Volcanics. Collected by L. P. Black and E. H. Pedersen.

G.A.2962. Lat. 17°14'S, Long. 144°56'E; Previously interpreted as a porphyritic-adamellite phase of the Elizabeth Creek Granite. The trace element content, and the isotopic and petrographic features, however, would suggest that it may be a recrystallised rhyodacite flow of the Featherbed Volcanics. Collected by L. P. Black and E. H. Pedersen.

G.A.2963. Lat. 17°21'S, Long. 144°57'E; Orthoclase diorite of the Almaden Granite. Collected by L. P. Black and E. H. Pedersen.

G.A.2964. Lat. 17°24'S, Long. 144°51'E; Rhyodacite from the Tennyson Ring Dyke. Collected by L. P. Black and E. H. Pedersen.

G.A.2965. Lat. 17°22'S, Long. 144°43'E; Adamellite phase of the Herbert River Granite. Collected by L. P. Black and E. H. Pedersen.

G.A.2966. Lat. 17°21'S, Long. 144°42'E; Granodiorite phase of the Almaden Granite. Collected by L. P. Black and E. H. Pedersen.

G.A.2967. Lat. 17°22'S, Long. 144°54'E; Aplite phase of the Elizabeth Creek Granite. Collected by L. P. Black and E. H. Pedersen.

G.A.2968. Lat. 17°38'S, Long. 144°57'E; Micro-granodiorite phase of the Herbert River Granite. Collected by L. P. Black and E. H. Pedersen.

G.A.2969. Lat. 17°39'S, Long. 145°01'E; Porphyritic adamellite (grey) of the Elizabeth Creek Granite. Collected by L. P. Black and E. H. Pedersen.

G.A.2970. Lat. 17°18'S, Long. 145°12'E; Rhyodacite welded tuff of the Featherbed Volcanics. Collected by L. P. Black and J. R. Richards.

G.A.2971. Lat. 17°21'S, Long. 144°41'E; Granodiorite phase of the Almaden Granite. Collected by J. C. Bailey.

G.A.2972. Lat. 17°21'S, Long. 144°42'E; Granodiorite phase of the Almaden Granite. Collected by J. C. Bailey.

G.A.2973. Lat. 17°19'S, Long. 144°53'E; Rhyodacite from the Featherbed Volcanics. Collected by J. C. Bailey.

G.A.2974. Lat. 17°09'S, Long. 144°56'E; Porphyritic rhyolite from the Featherbed Volcanics. Collected by J. C. Bailey.

G.A.2975. Lat. 17°23'S, Long. 145°18'E; Interpreted here as an adamellite phase of the Mareeba Granite. Previously regarded as Herbert River Granite. Collected by D. H. Blake.

G.A.2976. Lat. 17°24'S, Long. 145°21'E; Blake (1968) classes this rhyodacite as Slaughter Yard Creek Volcanics. Collected by D. H. Blake.

G.A.2977. Lat. 17°21'S, Long. 145°43'E; Adamellite phase of the Herbert River Granite. Collected by J. C. Bailey.

G.A.2978. Lat. 17°22'S, Long. 145°42'E; Adamellite phase of the Herbert River Granite. Collected by J. C. Bailey.

G.A.2979. Lat. 17°23'S, Long. 145°38'E; Adamellite to Granodiorite composition. Herbert River Granite. Collected by J. C. Bailey.

G.A.2980. Lat. 16°51'S, Long. 144°24'E; Obsidian from the Nychum Volcanics. Collected by W. R. Morgan.

G.A.2981. Lat. 16°55'S, Long. 144°10'E; Andesite from the Nychum Volcanics. Collected by W. R. Morgan.

G.A.2982. Lat. 16°53'S, Long. 144°16'E; Basalt from the Nychum Volcanics. Collected by W. R. Morgan.

G.A.2983. Lat. 16°52'S, Long. 144°18'E; Andesite from the Nychum Volcanics. Collected by W. R. Morgan.

G.A.2984. Lat. 16°48'S, Long. 144°17'E; Obsidian from the Nychum Volcanics. Collected by W. R. Morgan.

G.A.2986. Lat. 16°50'S, Long. 144°23'E; Vitric welded tuff from the Nychum Volcanics. Collected by W. R. Morgan.

G.A.2988. Lat. 16°51'S, Long. 144°18'E; Basalt from the Nychum Volcanics. Collected by W. R. Morgan.

G.A.2989. Lat. 16°53'S, Long. 144°18'E; Andesite from the Nychum Volcanics. Collected by W. R. Morgan.

G.A.2990. Lat. 16°43'S, Long. 144°18'E; 'Acid' andesite from the Nychum Volcanics. Collected by W. R. Morgan.

G.A.2991. Lat. 17°30'S, Long. 145°16'E; Aplite phase of the Elizabeth Creek Granite. Collected by D. H. Blake.

G.A.2992. Lat. 17°27'S, Long 145°01'E; Granitic phase of the Elizabeth Creek Granite. Collected by D. H. Blake.

G.A.2993. Lat. 17°24'S, Long. 145°00'E; Dacite from the Featherbed Volcanics. Collected by D. H. Blake.

G.A.2994. Lat. 17°32'S, Long. 145°00'E; Gabbro from the Gurrumba Ring Complex. Collected by D. H. Blake.

G.A.2995. Lat. 17°36'S, Long. 145°02'E; Adamellite phase of the Elizabeth Creek Granite. Collected by D. H. Blake.

G.A.2996. Lat. 17°39'S, Long. 145°01'E; Elizabeth Creek Granite of granite-adamellite composition. Collected by D. H. Blake.

G.A.2997. Lat. 17°31'S, Long. 145°07'E; Adamellite phase of the Elizabeth Creek Granite. Collected by D. H. Blake.

G.A.2998. Lat. 17°30'S, Long. 145°12'E; Elizabeth Creek Granite of granite-adamellite composition. Collected by D. H. Blake.

G.A.2999. Lat. 17°36'S, Long. 145°14'E; Elizabeth Creek Granite of granite-adamellite composition. Collected by D. H. Blake.

APPENDIX C

MINERALOGY AND LOCATION OF THE ORE SPECIMENS

The following lists are chiefly drawn from the work of the author. Microscopic studies have been made using both reflected and transmitted light. Minerals referred to in the literature, but not seen by the author, are also included. The order of presentation does not relate to mineral abundance. The percentage of tin quoted was determined by X-ray fluorescence (see chapter 3) on a random sample from each deposit. Mines which are known to have been worked for tin are marked by an asterisk.

Pb96, Caledonia mine. Lat. 17°02'S, Long. 144°07'E. Pyrite, galena, chalcopyrite, quartz, iron-staining. (de Keyser and Wolff, 1964 - also sphalerite). No tin found.

Pb97, Redcap mine. Lat. 17°04'S, Long. 144°25'E. Siliceous, ferruginous and manganiferous lode; also tourmaline; in oxidised breccia with no primary lead mineral. No tin found.

Pb98, Queenslander mine. Lat. 17°05'S, Long. 144°25'E. Galena, pyrite (some intergrown with pyrrhotite), sphalerite, chalcopyrite, johannsenite, fluorite, quartz, witherite?, limonite (de K. and W. - cerussite, copper carbonates). No tin found.

Pb99, Girofla mine. Lat. 17°06'S, Long 144°23'E. Pyrite, galena, sphalerite (with chalcopyrite and pyrrhotite inclusions), chalcopyrite, stannite, tetrahedrite, carbonate (siderite?), quartz, limonite, epidote (de K. and W. - marcasite, jamesonite, arsenopyrite. Cerussite, covellite, chalcocite, cuprite, native copper). About 1% tin.

Pb100, Jubilee mine. Lat. 17°13'S, Long. 144°26'E. Galena with inclusions of pyrite; sphalerite with chalcopyrite and stannite inclusions (de K. and W. - cerussite, anglesite, massicot, bismuth, stibnite). About 1% tin.

Pb101, Paisley mine. Lat. 17°21'S, Long. 144°34'E. Galena, sphalerite, quartz, muscovite (de K. and W. - pyrite, garnet, calcite, bismuth). No tin found.

Pb102, Torpey's mine. Lat. 17°19'S, Long. 144°43'E. Galena, sphalerite, pyrargyrite?, quartz, apatite (de K. and W. - pyrite and fluorite). No tin found.

Pb103, Tennyson mine*. Lat. 17°24'S, Long. 144°48'E. Galena, sphalerite (with chalcopyrite inclusions), chlorite, epidote, sphene (de K. and W. - pyrite). About 6% cassiterite.

Pb104, Proserpine mine*. Lat. 17°23'S, Long. 144°48'E. Galena with minor chalcopyrite inclusions. About 0.5% cassiterite.

Pb105, Shakespeare mine*. Lat. 17°22'S, Long. 144°48'E. Galena, chalcopyrite, sphalerite, arsenopyrite, pyrite, chlorite, limonite, sericite. About 0.8% cassiterite.

Pb106, Conroy mine. Lat. 17°21'S, Long. 144°49'E. Arsenopyrite, sphalerite (with inclusions of chalcopyrite), galena, quartz, muscovite, limonite (de K and W. - kaolinite, cerussite, malachite, manganese oxides). About 2.6% cassiterite.

Pb107, Comstock mine. Lat. 17°19'S, Long. 144°53'E. Galena, sphalerite, arsenopyrite, limonite, carbonate, quartz. No tin found.

Pb108, Unnamed. Lat. 17°19'S, Long. 144°54'E. Cerussite, pyromorphite, anglesite, quartz, sericite, chlorite. No tin found.

Pb109, Silver Spray mine. Lat. 17°24'S, Long. 144°59'E. Galena, sphalerite, chalcopyrite, quartz, sericite, limonite, pyrite. No tin found.

Pb110, Target mine. Lat. 17°28'S, Long. 145°17'E. Arsenopyrite, galena, wolframite, chalcopyrite, quartz. No tin found.

Pb111, Isabel mine. Lat. 17°23'S, Long 145°22'E. Galena, marcasite, sphalerite (with chalcopyrite inclusions), sericite, limonite. About 0.8% cassiterite.

Pb112, Blackwell's mine. Lat. 18°17'S, Long. 143°27'E. Galena, sphalerite (with chalcopyrite inclusions), arsenopyrite, limonite, quartz, sericite. No tin found.

Pb227, Mountain Maid mine*. Lat. 17°23'S, Long. 144°52'E. Sphalerite (with chalcopyrite and pyrrhotite inclusions), galena, pyrite, quartz, limonite. About 0.6% cassiterite.

Pb228, Panquay mine*. Lat. 17°27'S, Long. 145°02'E. Arsenopyrite, sphalerite, galena, pyrite, marcasite, chalcopyrite, stannite, carbonate, chlorite, sericite, quartz, tourmaline. About 0.5% tin.

Pb229, Mt Babinda mine. Lat. 17°25'S, Long. 145°02'E. Galena, sphalerite, chalcopyrite, malachite, quartz. About 0.8% cassiterite.

Pb237, Chinaman mine. Lat. 17°42'S, Long. 145°09'E. Covellite, chalcocite, bornite, anglesite, pyrolusite. No tin found.

Pb238, Bloodwood mine*. Lat. 17°27'S, Long. 145°05'E. Sphalerite, chalcopyrite, arsenopyrite, galena, pyrite, sericite, siderite. About 1.0% cassiterite.

Pb239, Unnamed. Lat. 17°24'S, Long. 145°07'E. Galena, quartz. About 40% cassiterite.

Pb240, Victoria Amalgamated mine. Lat. 17°25'S, Long. 145°09'E. Galena, sphalerite, pyrite, quartz, limonite. About 1% cassiterite.

Pb241, Lady Jane No.2 mine. Lat. 17°24'S, Long. 145°08'E. Chalcopyrite, galena, pyrite, sphalerite, arsenopyrite, magnetite?, fine-grained mica.

Pb242, Great Adventure mine*. Lat. 17°26'S, Long. 145°09'E. Galena, chalcopyrite, covellite, bornite, sphalerite, pyrrhotite, quartz, carbonate.

Pb243, Cosgrove mine. Lat. 17°25'S, Long. 145°08'E. Sphalerite, galena, pyrite, quartz, limonite. About 5% cassiterite.

Pb244, Mountain Maid (Omeo) mine. Lat. 17°26'S, Long. 148°08'E. Anglesite, limonite, topaz. About 3% cassiterite.

Pb245, Silver Star mine. Lat. 17°21'S, Long. 145°11'E. Galena, pyrite, fine-grained mica, kaolinite, limonite, topaz. A little cassiterite.

Pb246, Silver Lining mine*. Lat. 17°20'S, Long. 145°13'E. Sphalerite (with pyrrhotite inclusions), pyrite, boulangerite, galena (with inclusions of tetrahedrite). About 6% tin; most is cassiterite, a little stannite.

Pb247, Great Western mine*. Lat. 17°19'S, Long. 145°13'E. Galena, chalcopyrite, sphalerite, quartz, fine-grained mica, limonite.

Pb248, You and I mine. Lat. 17°22'S, Long. 145°22'E. Galena, arsenopyrite, chalcopyrite, pyrite, sphalerite, fine-grained mica, quartz, limonite, fluorite. About 9% of cassiterite.

Pb249, Doc and Doris mine. Lat. 17°27'S, Long.145°16'E. Arsenopyrite, azurite, malachite, galena, anglesite, epidote, topaz. About 0.1% cassiterite.

Pb250, Battery mine. Lat. 17°27'S, Long. 145°17'E. Galena, sphalerite (with chalcopyrite inclusions), pyrite, arsenopyrite, quartz, limonite. About 0.1% cassiterite.

Pb251, Clansman mine. Lat. 17°03'S, Long. 144°06'E. Galena, arsenopyrite, chalcopyrite, covellite, bornite, sphalerite, malachite, azurite, chlorite, garnet. No tin found.

Pb252, Christmas Gift mine. Lat. 17°09'S, Long. 144°32'E. Galena, cerrusite, anglesite, quartz, calcite?, epidote. No tin found.

Pb253, Lower Hensey mine. Lat. 17°11'S, Long. 144°33'E. Galena, sphalerite, chalcopyrite, limonite, garnet, quartz, calcite? No tin found.

Pb254, Silver Bead mine. Lat. 17°19'S, Long. 144°53'E. Galena, sphalerite, pyrite, chalcopyrite, fine-grained mica. About 17% cassiterite.

Pb255, Unnamed. Lat. 17°19'S, Long. 144°58'E. Galena, chalcopyrite, pyrite, quartz, fine-grained mica, limonite. No tin found.

Pb256, Kohinoor mine. Lat. 17°36'S, Long. 145°07'E. Galena, anglesite, chalcocite, quartz, kaolinite? (Zimmerman et al, 1963 - cerussite, pyromorphite). No tin found.

Pb257, Tuckers mine. Lat. 17°37'S, Long. 145°08'E. Galena, sphalerite, chalcopyrite, quartz, limonite, chlorite. No tin found.

Pb258, Unnamed. Lat. 17°37'S, Long. 145°11'E. Pyromorphite, cerussite. No tin found.

Pb259, Nightflower mine. Lat. 16°51'S, Long. 144°32'E. Galena, pyrite, arsenopyrite, chalcopyrite, sphalerite, quartz, limonite. No tin found.

Pb260, Bolivia mine*. Lat. 17°34'S, Long. 145°12'E. Marcasite, galena, sphalerite (with chalcopyrite inclusions), quartz, limonite, fine-grained mica. A little tin found.

Pb261, Lady Jane mine. Lat. 17°06'S, Long. 144°24'E. Galena, chalcopyrite, sphalerite, limonite (de K. and W., 1964 - copper and lead carbonates). No tin found.

Pb262, Unnamed. Lat. 17°13'S, Long. 144°26'E. Galena, anglesite, cerussite, quartz, fine-grained mica, clinozoisite. No tin found.

Pb263, Maniopota mine. Lat. 17°18'S, Long. 144°38'E. Galena, garnet, quartz, limonite, much carbonate, some of which is cerussite. No tin found.

Pb264, Excellent mine. Lat. 17°35'S, Long. 145°08'E. Chalcopyrite, pyrite, galena, sphalerite, limonite, pyrrhotite, magnetite, quartz, chlorite. About 0.7% cassiterite.

Pb265, Upper Hensey mine. Lat. 17°11'S, Long. 144°32'E. Anglesite, cerussite, quartz, carbonate gangue, garnet, limonite, green fine-grained phyllosilicate, jasper. No tin found.

Pb266, Ootann mine. Lat. 17°27'S, Long. 144°38'E. Magnetite, galena, cerrusite, malachite, chalcedonic silica, limonite. No tin found.

Pb267, Mt Garnet mine. Lat. 17°41'S, Long. 145°07'E. Anglesite, cerussite, galena (Zimmerman et al, 1963 - chalcopyrite, sphalerite, pyrrhotite, pyrite). No tin found.

Pb273, Unnamed. Lat. 17°57'S, Long. 144°33'E. Galena, sphalerite, chalcopyrite, pyrite. No tin found.

APPENDIX D

CHEMICAL PROCEDURES USED FOR EXTRACTION AND PURIFICATION OF LEAD

The techniques used for measurement of isotopic composition are described first. The purification procedure is based on the differential behaviour of lead and other ions under variable pH conditions in the dithizone-aqueous system.

a) The Dissolution:

Sufficient rock powder to contribute 150 µg. of lead is placed in one or two dishes with up to eight grams of powder in each dish; Teflon-ware is preferable to platinum. After wetting with a little water the sample is allowed to stand overnight in 50 per cent hydrofluoric acid (50 ml. for 8.0 g.) During all stages of the acid dissolution the sample is enclosed in a Teflon box with stainless steel base (Chow and McKinney, 1958) connected to a supply of filtered dry nitrogen. The temperature is raised, with a hot-plate, for the slow evaporation of the hydrofluoric acid. The residue is slightly wetted, and 35 ml. of perchloric acid is added for each 50 ml. of hydrofluoric acid, the solution is thoroughly stirred and evaporated just to dryness. Multiple acid treatment has been found to be ineffective for breaking down any aluminium oxide which formed. The amount of oxide formation seems to depend on the temperature of evaporation and the amount of baking. For these reasons, only a single dose of each acid is used.

The sample is then taken up in water, transferred to a one litre beaker, and the volume is increased to about 500 ml. It is then heated strongly (but not boiled) under cover for about one hour to induce solution. By careful decantation the liquid may be transferred to another beaker, leaving the residuals behind. These are washed into a platinum crucible, evaporated to dryness, and fused for about 15 minutes in sodium borofluoride at about 400°C - slightly over the melting point. After cooling the readily-soluble fusion products are dissolved in hot water, and are then transferred back to the original dissolution vessel. Any free fluoride is removed by adding about three millilitres of perchloric acid, and evaporating to dryness. The perchlorate residue is then dissolved in hot water and added to the main solution. The dissolution should now be complete.

b) Purification Procedure:

The sample is now evaporated almost to dryness under cover (do not overheat). Concentrated nitric acid (40 ml. per g. of sample; Tatsumoto, 1966) is added and thoroughly stirred to dissolve as much of the sample as possible. The insolubles at this stage are predominantly the amorphous aluminium compound which at times can trap up to 70 per cent of the lead. Heating does not appear to release extra lead and may indeed accentuate the problem. The insolubles are then discarded by centrifuging as the aluminium oxide traps iron and nitric acid which interfere at a later stage.

Approximately four ml. of saturated barium nitrate solution is added (Tatsumoto, 1966) with vigorous stirring; lead coprecipitates on the barium nitrate. This is then centrifuged, and as much acid removed as possible by means of a small syringe-operated pipette. After dissolving in the minimum of water, four ml. of saturated KCOOH solution is added. Lead is again coprecipitated. The centrifuge tube is almost filled with ethanol which is mixed with the oxalate solution and centrifuged again. The main object of the nitrate and oxalate steps is to remove iron. After discarding the liquid phase, 30 ml. of ammonium citrate is added and the mixture is heated in a water bath until all the oxalate dissolves.

This solution is added to a separating funnel with ten ml. of potassium cyanide solution and 20 ml. of dithizone solution. After shaking, the resulting lead dithizonate is run off into a beaker; the aqueous phase is discarded. After carefully washing the funnel, the dithizone is poured back in, together with ten ml. of 0.05 per cent potassium cyanide solution (to remove any thallium), and shaken. The lead, which remains in the dithizone, is collected in another beaker and the aqueous phase is again discarded. The funnel is carefully washed once more and the sample returned to it with ten ml. of ammonium acetate. On shaking, the lead moves into the aqueous phase but bismuth remains in the dithizone solution. After rejecting the latter, the aqueous phase is successively washed with two more

aliquots of dithizone followed by three washings with chloroform. It is then taken back into dithizone (ammonia added to the acetate until the pH reaches approximately nine) and collected in two separate beakers in the ratio 2 : 1. The smaller aliquot is then spiked. Both samples are treated separately but similarly for the remainder of the procedure. The acetate is rejected and the funnel thoroughly washed. The lead is then successively taken into one per cent HCl and back into dithizone and this step is repeated after the funnel has been cleaned. After cleaning the funnel once more the lead dithizonate solution is again shaken with ten ml. of one per cent HCl which is drained off into a ten ml. beaker and evaporated to dryness.

Four drops of concentrated nitric acid are added to convert to nitrates and to destroy any organic material, and evaporated. Ammonium chloride is then removed by sublimation, at 200°C for 30 minutes. After cooling the sample is taken up in one drop of 0.1N HNO_3 and transferred to a two ml. centrifuge tube. Five drops of 100 per cent ethanol and one drop of oxalic acid are added and mixed thoroughly. Insoluble lead oxalate is formed. This is centrifuged and washed six times with 70 per cent ethanol. The solid oxalate is finally transferred in a small drop of water to a mass-spectrometer centre filament, to which it is fixed by means of an ammonium nitrate 'cement', and analysed. The procedures of this paragraph were taken from Cooper and Richards (1966b).

Quantitative lead determination is treated similarly. The rock powder must be accurately weighed, however, as must the spike which is added directly to the Teflon dissolution dish before the acids are added. There is no aliquotting or further spiking.

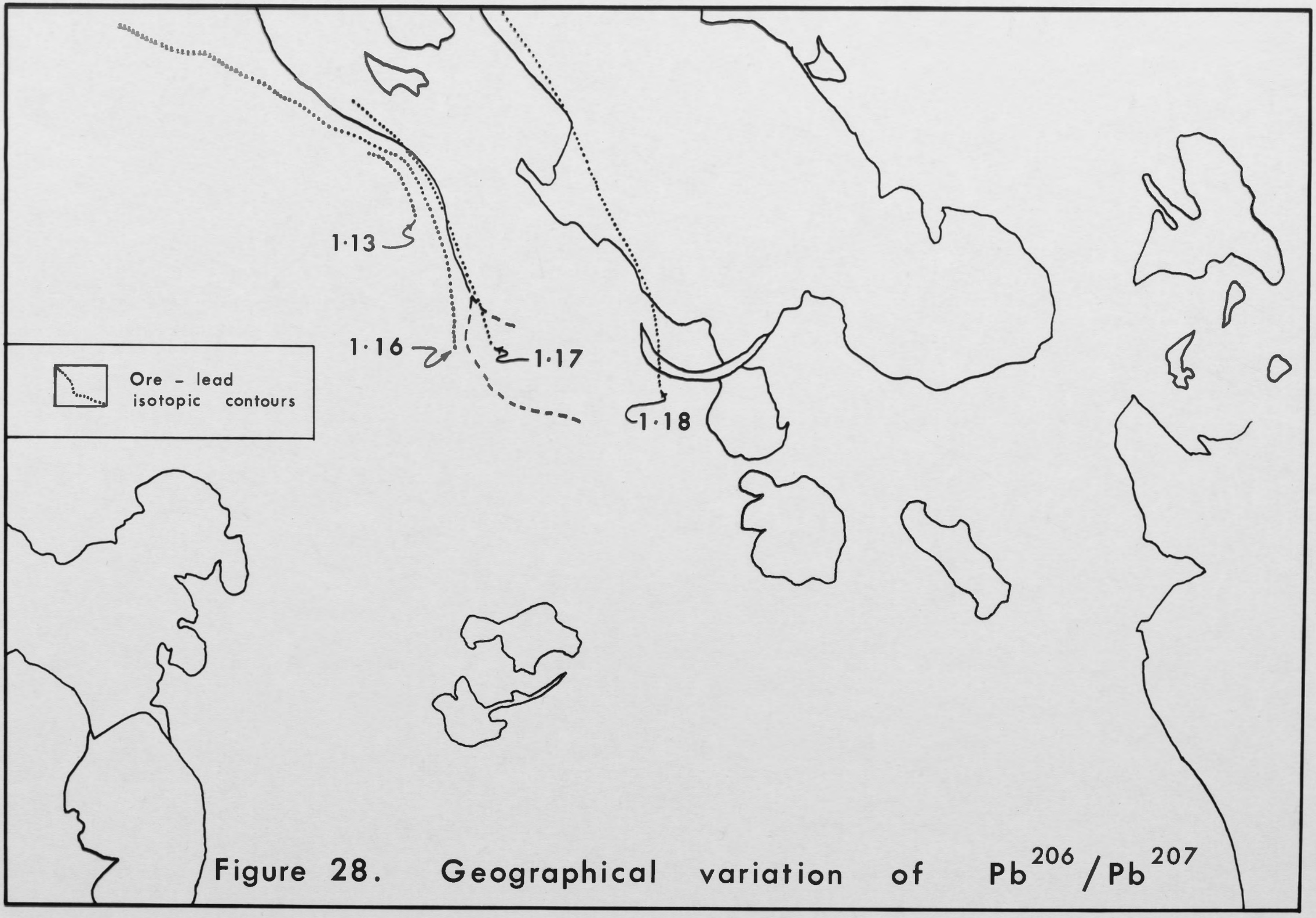

Figure 28. Geographical variation of Pb^{206}/Pb^{207}

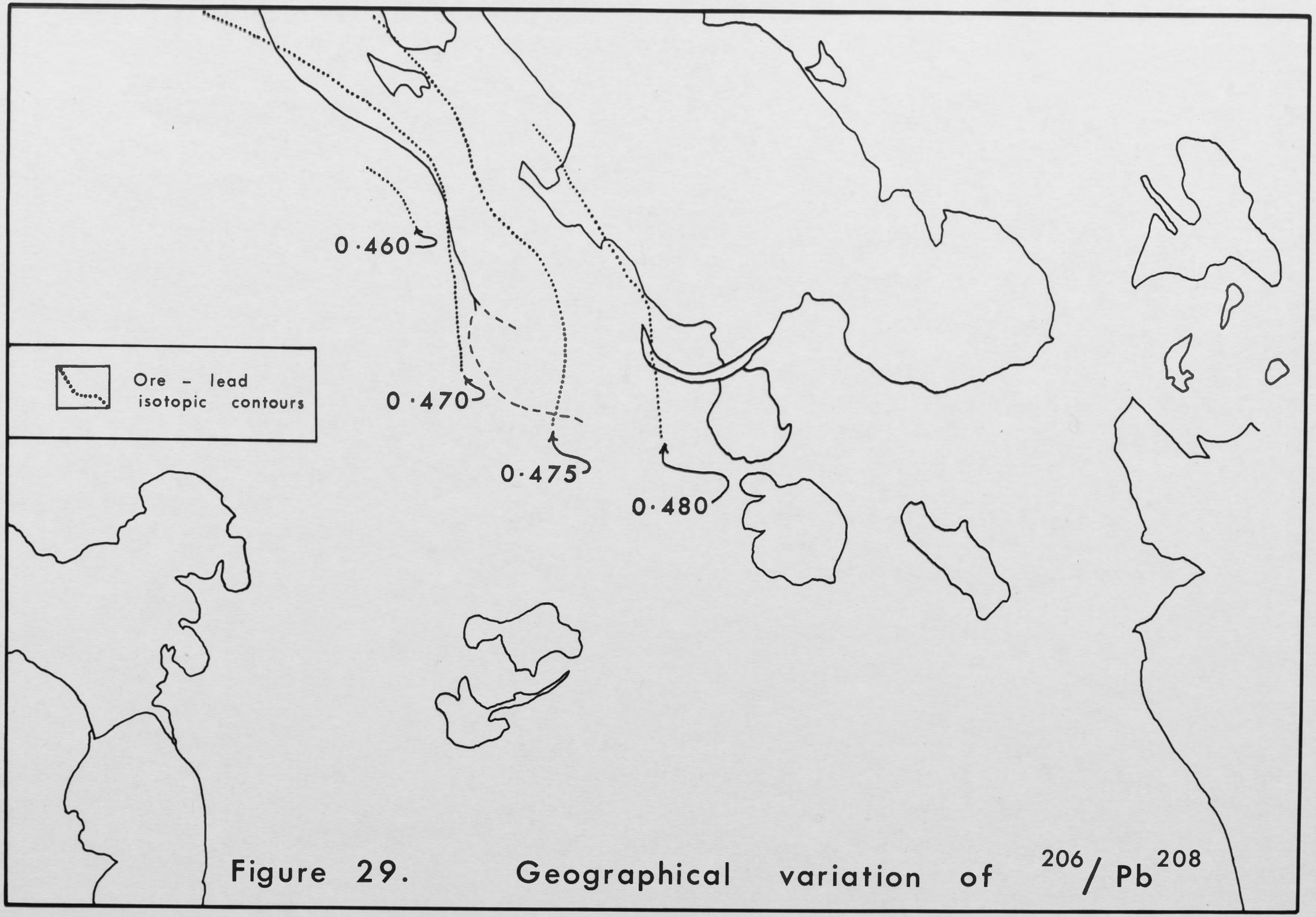

Figure 29. Geographical variation of $^{206}/Pb^{208}$

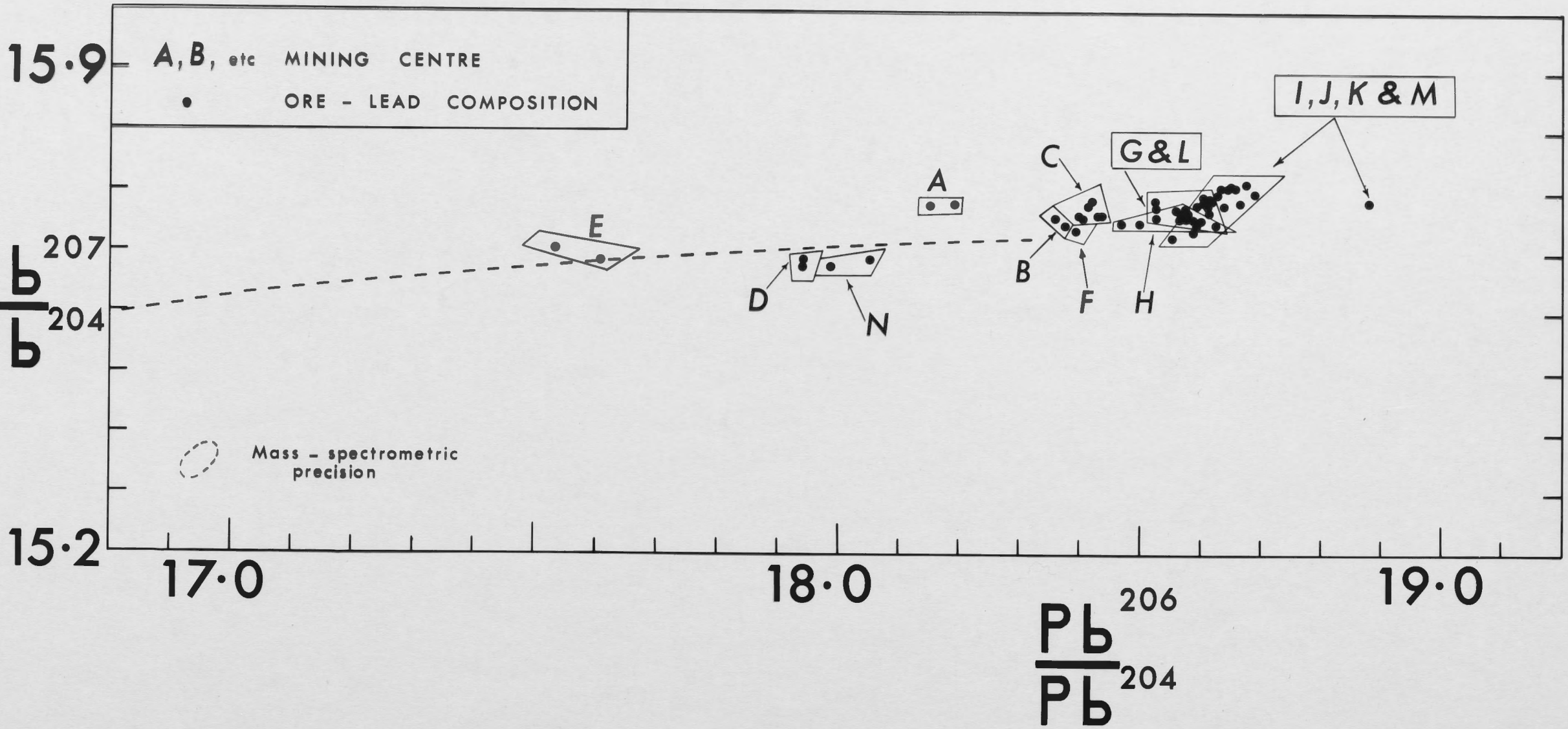
A, B, etc MINING CENTRE
ORE - LEAD COMPOSITION
Mass - spectrometric precision
A
B
C
D
E
F
G&L
H
I, J, K & M
N
15·9
15·2
17·0
18·0
19·0
Pb207/Pb204
Pb206/Pb204

A, B, etc MINING CENTRE

• ORE - LEAD COMPOSITION

Mass - spectrometric precision

A

D

C

I

G

B

M

L

J & K

F

H

E

N

$\frac{Pb^{208}}{Pb^{204}}$

39·0

38·5

38·0

17·0

18·0

19·0

$\frac{Pb^{206}}{Pb^{204}}$

SCALE 1:1,000,000

MILES

10 0 10 20 30 40 50 60 70 80 90 100

KILOMETRES

10 0 10 20 30 40 50 60 70 80 90 100

REFERENCE

Railways
Roads
State boundaries
County boundaries
County names

DENHAM

REFERENCE

CAINOZOIC	QUATERNARY	Q	Alluvial gravel, sand, silt, clay; beach and aeolian sand, gypseous and calcareous clays, travertine.
	TERTIARY	Tb	Volcanics, mainly basalt. Includes acid and alkaline lavas, dolerite and trachytic plugs.
		T	Undifferentiated sediments, mainly continental. Sand, clay, gravel, sandstone, shale, conglomerate, "greybilly", lignite.
		Tm	Sandstone and shale. Marine sediments of Murray Basin.
		Te	Sandstone, clay shale, conglomerate, quartzite ("billy"). Continental beds of "Eyrian Series".
MESOZOIC	CRETACEOUS	K	Undifferentiated. Sandstone, claystone, mudstone, shale, impure limestone and marl. Includes Blythesdale and Rolling Downs Group (Roma, Tambo and Winton Formations). Overlain superficially by unmapped thin Tertiary laterites. Marine and continental.
	CRETACEOUS-JURASSIC	K-J	Sandstone, shale and coal. Kangaroo Creek Sandstone and Grafton Formation. Continental.
	JURASSIC	Jw	Walloon Coal Measures. Sandstone, shale and coal. Continental.
		J	Conglomerate, shale, sandstone, siltstone. Includes Upper Merrygoen, Gowen, Purlawaugh, Pillaga and Munmurra Beds (includes Talbragar Fish Beds); Comials "Series". Continental.
		Jg	Garrawilla Lavas. Mainly basalt.
	JURASSIC-TRIASSIC	RM	Sandstone, siltstone, conglomerate, coal and fossil wood. Marburg Formation; Bundamba Group; Digby, Napperby, Pottinger and Ballimore Beds; Dubbo Sandstone. Continental.
	TRIASSIC	Rw	Wianamatta Group. Shale, mudstone and sandstone. Continental; local marine incursions.
		Rh	Hawkesbury Sandstone. Massive quartz sandstone with pebbly or shaly lenses. Continental.
		Rn	Narrabeen Group. Shale, claystone, sandstone, fine conglomerate. Continental.
		Rc	Conglomerate, sandstone, shale, coal, tuff and rhyolite. Nymboida, Evan's Head and Red Cliff Coal Measures; Chillingham Volcanics; Camden Haven Group. Continental.
		R	Undifferentiated continental sediments. Includes Gunnee and Lower Merrygoen Beds.
PALAEOZOIC	PERMIAN	Pcu	Former "Upper Coal Measures". Conglomerate, sandstone, shale, mudstone, tuff with coal and torbanite seams. Includes Newcastle, Tomago, Illawarra, Wollondilly and Lithgow Coal Measures; Black Jack Formation. Continental.
		Pmu	Former "Upper Marine Series". Conglomerate, sandstone, shale, mudstone, tuff, lava and glacial erratics. Includes Maitland, Capertee, Shoalhaven Groups; Gerringong Volcanics; Gladstone and Porpoise Formations. Marine
		Pcl	Former "Lower Coal Measures". Conglomerate, sandstone, shale with coal seams. Includes Greta, Werris Creek, Craven, Clyde, Muswellbrook and Ashford Coal Measures Nandewar Group. Continental.
		Pml	Former "Lower Marine Series". Sandstone, conglomerate tuff, basalt, shale, limestone and coal. Includes Dalwood and Temi Groups; Werrie Basalts; Avon Coal Measures. Chiefly marine, partly continental.
		P	Undifferentiated; mainly marine sediments. Includes Macleay Group.
	CARBONIFEROUS	C	Acid to basic lavas, conglomerate, sandstone, shale, mudstone, limestone, tuff, agglomerate, breccia, tillite, varved shale. Includes Burindi and Kuttung Groups. Continental and marine.
	DEVONIAN	Dl	Upper Devonian. Conglomerate, arkose, quartzite, sandstone, clayshale, mudstone, limestone, lavas, breccia, tuff. Includes Mulga Downs, Manilla, Lambie and Tylwal Groups; Merrimbula, Catombal, Baldwin Formations; Barraba Mudstone and Black Rock Sandstone. Continental and marine.
		Dm	Middle to Lower Devonian. Quartzite, lavas, tuff, greywacke, shale, conglomerate, limestone, chert, andesite, claystone, spilite, keratophyre. Includes Murrumbidgee, Kandos and Black Range "Series"; Tamworth, Amphitheatre, Burrags and Cunningham Groups; Siluma, Garra, Lob's Hole and Trundle Beds; Bulls' Camp Rhyolite, Merrions Tuff and Ainslie Volcanics. Marine.
		Dv	Quartz felspar porphyry, rhyolite, felsite, agglomerate, breccia and associated sediments. Includes Snowy River Volcanics, Eden Rhyolite, Culcairn Porphyry and Manar Porphyry.
		D	Undifferentiated strata, mainly marine.
	SILURIAN	S	Slate, quartzite, shale, mudstone, sandstone, limestone, tuff, conglomerate and lavas. Includes Cobar, Kildrummie, Campbell's, Crudine, Red Hill, Fairbairn and Canberra Groups; Manildra, Chesleigh, Cookman, Newbridge, Nanima, Mumbil, Gamboola, Panuara and Black Spring Formations; Jerrara, Hume, Yass and Bango "Series". Also Fitzroy Beds, Woolomin Group and Brisbane Metamorphics.
		Sp	Quartz felspar porphyry, lavas, felsite and ignimbrite with associated silicified and indurated sediments.
	ORDOVICIAN	O	Slate, shale, greywacke, sandstone, quartzite, chert, siltstone, tuff, andesite and limestone. Includes Tallebung Group; Nambucca Beds; Pittman, Maloneilli, Oakdale, Malachi's Hill, Walli, Muriarra and Millambri Formations; Black Mountain Sandstone and Sofala Volcanics; pre-Silurian Girilambone Group. Marine.
	CAMBRIAN	C	Conglomerate, shale, limestone, sandstone, lavas of Gnalta Beds west of White Cliffs. Includes Wagonga Beds and unnamed beds west of Stuart Town. Marine
PRECAMBRIAN	PROTEROZOIC	Pt	"Torrowangee Series" (equivalent of "Sturtian Series" in South Australia). Slate, quartzite, limestone, shale, flaggy sandstone, tillite with erratics, conglomerate with stretched pebbles.
	ARCHAEAN	Aw	Willyama Complex. High grade metamorphics; garnet-cordierite-sillimanite-schist and gneiss, mica schist with staurolite and cyanite, amphibolite. Intruded by Precambrian granite, pegmatite, gabbro and epidiorite.
	IGNEOUS	g	Mainly granite, granodiorite and granite porphyry. Includes Cooma Gneiss.
		sr	Serpentine and ultrabasics.
		b	Basic intrusives. Amphibolite.

Drawn and printed by Mercury Press Pty. Ltd., Hobart.
Cartographer: W. J. Bucknridge, M.A.I.C.